INFORMATION TO USERS

This manuscript has been reproduced from the microfilm master. UMI films the text directly from the original or copy submitted. Thus, some thesis and dissertation copies are in typewriter face, while others may be from any type of computer printer.

The quality of this reproduction is dependent upon the quality of the copy submitted. Broken or indistinct print, colored or poor quality illustrations and photographs, print bleedthrough, substandard margins, and improper alignment can adversely affect reproduction.

In the unlikely event that the author did not send UMI a complete manuscript and there are missing pages, these will be noted. Also, if unauthorized copyright material had to be removed, a note will indicate the deletion.

Oversize materials (e.g., maps, drawings, charts) are reproduced by sectioning the original, beginning at the upper left-hand corner and continuing from left to right in equal sections with small overlaps. Each original is also photographed in one exposure and is included in reduced form at the back of the book.

Photographs included in the original manuscript have been reproduced xerographically in this copy. Higher quality 6" x 9" black and white photographic prints are available for any photographs or illustrations appearing in this copy for an additional charge. Contact UMI directly to order.

UMI®

Bell & Howell Information and Learning
300 North Zeeb Road, Ann Arbor, MI 48106-1346 USA
800-521-0600

UNIVERSITÉ DE MONTRÉAL

NUMERICAL MODELING OF PETROLEUM CONTAMINATION IN THE SUBSURFACE SOIL LAYER

KOUROSH MOHAMMADI
DÉPARTEMENT DES GÉNIES CIVIL, GÉOLOGIQUE ET DES MINES
ÉCOLE POLYTECHNIQUE DE MONTRÉAL

THÈSE PRÉSENTÉE EN VUE DE L'OBTENTION
DU DIPLÔME DE PHILOSOPHIAE DOCTOR (Ph.D.)
(GÉNIE CIVIL)
SEPTEMBRE 1998

UNIVERSITÉ DE MONTRÉAL

ÉCOLE POLYTECHNIQUE DE MONTRÉL

Cette thése intitulée:

NUMERICAL MODELING OF PETROLEUM CONTAMINATION IN THE SUBSURFACE SOIL LAYER

présentée par: **MOHAMMADI Kourosh**

en vue de l'obtention du diplôme de : Philosophiae Doctor

a été dûment acceptée par jury d'examen constitué de:

M. **PRUD'HOMME Michel**, Ph. D., président

M. **KAHAWITA René**, Ph.D., membre et directeur du recherche

M. **ROUSSELLE Jean**, Ph.D., membre

M. **LEFEBVRE René**, Ph. D., membre

DEDICATION

To my wife Zahra Yazdankia

and my beloved daughters Mariam and Hoda

AKNOWLEGEMENTS

First and foremost, thanks go to Allah for his mercy and guidance.

I would like to express my sincere thanks and appreciation to my supervisor Professor Rene Kahawita for his assistance, inspiration, support and friendship throughout my study and research at the École Polytechnique de Montréal.

I would also like to thank the members of my committee, Dr. Jean Rousselle, Dr. Michel Prud'homme, and especially Dr. René Lefebvre for his valuable comments which improved the quality of this work.

I am grateful to the Ministry of Culture and Higher Education of Iran and its representative in Canada, Dr. Reza Hosseini, which provided financial support for my living and studying in Canada.

Thanks also go to Mr. André Ducharme in the Geotechnical Lab who was a great help in doing part of my experiments.

I would also like to thank office mates and friends who made my life away from home not only bearable but also enjoyable including Min Yan, A. Fredj, M. H. Mosuavi_Zadeh, M.K. Mesbah and J. Darehshiri.

I thank my parents for their continued encouragement and understanding and also my wife for her patience and support.

RÉSUMÉ

Les liquides qui ne se dissolvent pas dans l'eau et qui peuvent exister comme une phase fluide séparée sont connus comme étant des liquides en phase non-aqueuse (NAPL). Il y a deux groupes de NAPLs: ceux qui sont plus légers que l'eau (LNAPLs) et ceux avec une densité plus grande que celle de l'eau (DNAPLs).

Le but de cette recherche est de développé un modèle numérique pour simuler la migration des liquides de la phase non-aqueuse dans le système de sous-surface non-saturé qui utilise la méthode de support-opérateurs. Bien que cette méthode ait une longue histoire dans la science des mathématiques elle n'a pas été utilisée dans le monde de l'eau. Un modèle en deux dimensions a été développé afin de décrire l'écoulement de l'eau, du NAPL et l'air dans une région transversale et verticale. Les échanges de masse du NAPL à une phase du gazeuse par volatilisation et à la phase aqueuse par dissolution sont tenus en compte.

Le modèle considéré aura les caractéristiques et les capacités suivantes:

- Simuler l'écoulement de l'eau, du NAPL et de l'air simultanément. Aussi, la phase gazeuse et/ou la phase non-aqueuse peuvent être absentes durant la simulation.
- La phase gazeuse peut être considérée comme un fluide compressible ou non-compressible.

- Ce modèle peut être utilisé dans un milieu poreux hétérogène.
- La méthode utilisée de support-opérateurs sera capable de faire face à des domaines avec des frontières irrégulières. La méthode est basée sur une formulation intégrale ce qui assure la conservation des quantités variables.
- Les relations étendues de Van Genuchten sont utilisées pour définir la pression-saturation capillaire et les relations de la conductivité-saturation.
- Un pas du temps variable est utilisé pour augmenter l'efficacité de la solution.

Puisque quelques expériences seulement comportant un écoulement LNAPL étaient disponibles et aucune d'elles n'avait été faite dans un milieu poreux hétérogène, une expérience a été conduite pour obtenir une meilleure compréhension du comportement physique de l'écoulement multi-phase dans la zone non saturée et pour vérifier le modèle numérique par rapport à un cas hétérogène. Les travaux en laboratoire sont consisté en deux types d'essai.

En utilisant les résultats expérimentaux et aussi les travaux analytiques et expérimentaux d'autres chercheurs, le modèle numérique a été calibré et vérifié. Le modèle a été validé avec trois solutions analytiques et a été vérifié avec trois travaux expérimentaux. Dans tous les cas, les résultats numériques ont montré un bon accord avec les données observées.

ABSTRACT

Liquids that are insoluble in water and can exist as a separate fluid phase are known as non-aqueous phase liquids (NAPLs). There are two groups of NAPLs: those that are lighter than water (LNAPLs) and those with a density greater than water (DNAPLs). Most LNAPLs are hydrocarbon fuels such as gasoline and most DNAPLs are chlorinated hydrocarbons such as TCE.

The purpose of this research is to develop a numerical model to simulate the migration of non-aqueous phase liquids in the unsaturated subsurface system. A two dimensional model has been considered to describe the flow of water, NAPL, and air in a vertical cross sectional area. Mass exchange from the NAPL to the gas phase due to volatilization and to the water phase due to dissolution are taken into account. The model is verified against available analytical and experimental results.

In this thesis, the method of *support-operators* has been used to formulate a discrete model of the continuum physical system. Many of the standard finite difference methods and also the finite volume method are special cases of the method of support-operators. Unlike elementary finite difference methods, the method of support-operators may be used to construct finite difference schemes on grids of arbitrary structure.

Discrete methods usually give rise to a system of algebraic equations. A fully coupled Newton-Raphson technique is chosen to handle the nonlinearity and solve the equations sequentially in an iterative fashion. The nonlinearities inherent in the governing equations are the relative permeability $K_{r\alpha} = K_{r\alpha}(h_\alpha)$, saturation, $S_\alpha = S_\alpha(h_\alpha)$, and gas phase density $\rho_a = \rho_a(h_a)$. The equations are coupled because in all equations more than one primary variable appear concurrently.

For each grid there are (NPHASE) unknowns, where NPHASE is the number of phases considered in the simulation. The unknowns are the hydraulic head of water, h_w , NAPL, h_n , and air, h_a .

The model developed here has the following characteristics and capabilities:

- Simulating the flow of water, NAPL and air simultaneously. Also, gas phase and/or nonaqueous phase can be absent in the simulation.
- The gas phase may be considered as a compressible or an incompressible fluid.
- The model may be used in a heterogeneous porous media.
- The method of support-operators allows the model to handle irregular boundaries. The method is based on an integral formulation and conservation of variable quantities is assured.

- Extended Van Genuchten relationships are used to define the capillary pressure-saturation and the conductivity-saturation relationships.
- A variable time step is used to increase the efficiency of solution.

Since very few experiments containing a LNAPL flow have been published and none of them was done in a heterogeneous porous medium, a laboratory experiment was conducted to provide a better understanding of the physical behavior of multi-phase flow in the unsaturated zone and verify the model against a heterogeneous case.

Two analytical solutions for water flow and one for NAPL flow were used to compare the results of the numerical solution. Solutions were also compared with several available experimental results of NAPL movement in one and two dimensional domains and also with the results from the laboratory experiment. In all cases, the model showed good agreement with analytical and experimental data.

CONDENSÉ EN FRANÇAIS

MODÉLISATION NUMÉRIQUE DE LA CONTAMINATION PAR DU PÉTROLE DE LA COUCHE DE SOUS-SURFACE

Les liquides qui ne se dissolvent pas dans l'eau et qui peuvent exister comme une phase fluide séparée sont connus comme étant des liquides en phase non-aqueuse (NAPL). Il y a deux groupes de NAPLs:

- ceux qui sont plus légers que l'eau (LNAPLs)
- et ceux avec une densité plus grande que celle de l'eau (DNAPLs).

La plupart des LNAPLs sont des combustibles comme l'essence et la plupart des DNAPLs sont des hydrocarbures chlorés comme le trichloroethane et le tétrachlorure de carbone.

Un NAPL peut déplacer tout l'eau et l'air présents quand il entre dans la zone non-saturée. À l'exception des couches en dessus, qui sèchent par évaporation, le sol dans cette zone contient habituellement de l'eau près de la saturation résiduelle.

Puisque l'eau est présente, la pression du NAPL doit être plus grand que la pression capillaire d'entrée du NAPL dans l'eau afin que la pénétration puisse se produire. Puisque l'eau est la phase mouillante relative à l'air et au NAPL, elle a tendance à aligner les bords

des pores et le NAPL ne déplacera pas l'eau de la surface du grain du sol. Le polluant émigrera vers le bas à travers de la zone non saturée sous l'influence de gravité.

Le NAPL mobile pourra migrer horizontalement sous l'effet des forces capillaires. Une enveloppe gazeuse de vapeur chimique due à volatilisation peut s'étendre au-delà du corps principal de contamination.

Si le déversement est de dimension suffisante, une partie du contaminant pourrait atteindre la nappe phréatique. Bien que les produits du pétrole sont considérés immiscibles, cela ne veut pas dire que ces divers composants sont absolument insolubles dans l'eau. Les composants solubles se dissolvent et forment un panache d'eau contaminée qui s'étend à l'extérieur de la zone contaminée principale. Donc, ce panache émigre comme une partie du système de l'eau souterraine.

Cette portion du contaminant qui reste comme une phase distincte peut voyager sous sa propre inclinaison. Les fractions dissoutes des hydrocarbures toxiques peuvent entrer dans la nappe aquifère avec recharge à travers le sol contaminé et sont transportées sur les grandes distances horizontales vers des puits d'eau loin de la source originale. Même les très petites concentrations de ces composants peuvent rendre l'eau impropre pour l'usage domestique. De plus, les vapeurs de l'essence peuvent émigrer dans les sous-sols, les égouts et les tunnels ce qui peut causer des incendies et des risque d'explosion.

Une prise de conscience de la part des gouvernements, de l'industrie, et de la communauté professionnelle de l'eau souterraine au sujet des risques exceptionnels de contamination sévère et persistante de la nappe phréatique par les NAPL ne s'est produite qu'après que les problèmes actuels soient apparus.

Les modèles présents de transport de contaminants pour les composants miscibles sont inadéquats pour décrire la migration d'un contaminant immiscible. L'écoulement d'un contaminant immiscible est contrôlé par son propre potentiel qui dépend de la pression, de la gravité et des forces de surface ce qui n'est pas nécessairement semblable au potentiel d'écoulement de l'eau.

La compréhension et la prévision du transport des produits du pétrole dans les sols et l'eau souterraine sont d'importance fondamentale dans le développement de procédures de d'atténuation qui aideraient la récupération efficace et le nettoyage de ces contaminants. Elles aideraient également à évaluer le risque d'accidents qui pourraient interrompre l'approvisionnement en eau.

Les équations qui gouvernent l'écoulement aux phases multiples de contaminants dans un milieu poreux sont des équations non-linéaire de grand ordre . En règle générale, les solutions analytiques sont non-disponibles, sauf pour des cas restrictifs. Pour obtenir des solutions utiles, on doit recourir aux méthodes numériques. Dans la solution numérique de ces équations, la stabilité et les restrictions de la convergence limitent la taille des

noeuds et le pas de temps ce qui demande une grande capacité d'emmagasinement et beaucoup de temps de calcul pour l'ordinateur. Les modèles numériques pour la migration de NAPL dans la zone vadose et dans l'eau souterraine ont récemment été présentés par plusieurs chercheurs qui utilisent les méthodes des différences finies et celles des éléments finies. La majorité de ces modèles ont été développés pour une dimension peu de modèles bidimensionnels ont été présentés.

Le but de cette recherche est de développé un modèle numérique pour simuler la migration des liquides de la phase non-aqueuse dans le système de sous-surface non-saturé qui utilise la méthode de support-opérateurs. Bien que cette méthode ait une longue histoire dans la science des mathématiques elle n'a pas été utilisée dans le monde de l'eau. Un modèle en deux dimensions a été développé afin de décrire l'écoulement de l'eau, du NAPL et l'air dans une région transversale et verticale. Les échanges de masse du NAPL à une phase du gazeuse par volatilisation et à la phase aqueuse par dissolution sont tenus en compte. Le modèle sera vérifié avec les résultats analytiques et expérimentaux disponibles.

Les objectifs à long terme de cette thèse permettra une meilleure connaissance des mécanismes du système en fournissant un outil utile pour l'évaluation de la migration de NAPL dans la région de sous-surface.

Le modèle considéré aura les caractéristiques et les capacités suivantes:

- Simuler l'écoulement de l'eau, du NAPL et de l'air simultanément. Aussi, la phase gazeuse et/ou la phase non-aqueuse peuvent être absentes durant la simulation.
- La phase gazeuse peut être considérée comme un fluide compressible ou non-compressible.
- Ce modèle peut être utilisé dans un milieu poreux hétérogène.
- La méthode utilisée de support-opérateurs sera capable de faire face à des domaines avec des frontières irrégulières. La méthode est basée sur une formulation intégrale ce qui assure la conservation des quantités variables.
- Les relations étendues de Van Genuchten sont utilisées pour définir la pression-saturation capillaire et les relations de la conductivité-saturation.
- Le schème implicite du premier ordre est utilisé pour évaluer la dérivée par rapport au temps.
- Un pas du temps variable est utilisé pour augmenter l'efficacité de la solution.
- Le compilateur Microsoft Powerstation® 4.0, un compilateur FORTRAN 90 est utilisé pour compiler le programme.
- Pour les productions graphiques, Microsoft Excel® et SURFER® sont utilisés respectivement pour créer des graphiques et les lignes des contour.

Les limitations du modèle sont des souivants:

- Le transport du soluté par la convection, la dispersion et la diffusion n'est pas considéré ni dans l'eau ni dans la phase gazeuse.
- L'hystérèse dans les relations constitutives n'est pas prise en considération.
- Le NAPL est un fluide constitué d'un seul composant.
- On considère que les échanges de masse pour le NAPL ne se font qu'avec l'eau et la phase gazeuse. Elles sont calculée dans le terme puits.
- Le modèle ne considère pas la biodégradation, désintégration et l'adsorption/ la désorption.

Puisqu'il n'y avait aucune expérience disponible pour montrer le comportement du LNAPL dans un média poreux hétérogène, une telle expérience a été réalisée dans le Laboratoire Hydrodynamique de l'École Polytechnique de Montréal.

RECHERCHES BIBLIOGRAPHIQUES

L'écoulement de NAPL a intéressé premièrement les ingénieurs pétroliers. La première reconnaissance de mouvement de NAPL dans l'eau souterraine comme un phénomène d'écoulement biphasé est attribuée à Van Dam (1967). Par la suite, plusieurs modèles ont été développés pour décrire mathématiquement l'écoulement de NAPL immiscibles plus légers que l'eau dans les sous-surfaces.

Les travaux antérieurs peuvent être divisés en deux catégories majeures:

- travaux expérimentaux
- analytique et numérique

Le Tableau (1) donne un résumé des travaux expérimentaux qui ont été identifiés pendant la recherche bibliographique de ce travail. Il peut être conclu que:

- La dissolution d'hydrocarbures provenant d'une zone contaminée par de l'huile vers la nappe phréatique pourrait être déterminée par le coefficient de la partition des composés et par le rapport eau/huile.
- Le transport des vapeurs de NAPL peut être modélisé par une loi de diffusion Fickienne.
- l'enlèvement du NAPL peut être simulé en utilisant une approche basée sur un équilibre chimique.
- La saturation de l'eau résiduelle était indépendante du taux d'écoulement quand l'huile de faible viscosité déplaçait l'eau.

Un résumé des modèles analytiques et numériques est présenté dans le Tableau (2)

Tableau (1) résumé des modèles expérimentaux

Van der Waarden et al. (1971)	Dissolution des hydrocarbures d'une zone de l'huile résiduelle par de l'eau tombant goutte à goutte.
Hunt et al. (1988)	Dissolution de NAPL dans l'eau et propagation de la vapeur
Swallow & Gschwend (1983)	Les mécanismes du transport gazeux
Johnson, R.L. (1988)	Les mécanismes du transport VOCs
Johnson & Kreamer (1994)	Le modèle physique 2D pour déterminer les caractéristiques de la migration de vapeur et du liquide
Geller (1990)	Dissolution d'un mélange de toluène pur et du benzène - toluène dans un milieu de billes de verres saturé en eau.
Annable (1991)	Expérience avec une colonne du sol contenant trois phases fluides: air. eau, et essence qui a été conçue pour simuler les conditions dans la zone non saturée.
Alfossail (1986)	L'effet des forces visqueuses et des forces capillaires sur la saturation de l'eau résiduelle.
Abu-El-Sha'r (1993)	Évaluer l'application de trois modèles de transport par diffusion: La loi de Fick, les équations Stefan-Maxwell. et le Modèle du « Dusty Gas » (DGM)
Zhou (1994)	Évaluer la migration du gaz-huile et de l'essence JP-5 dans un milieu de sable et de sol en trois dimensions
Van Geel and Sykes (1994)	2D, expérience du l'écoulement à phases multiples avec LNAPL

Tableau (2) modèles Analytiques et numériques

Modèles Analytiques	Modèles de la Différence finis	Modèles de l'Élément Finis
Mull (1971)	Faust (1985)	Osborne & Sykes (1986)
Holzer (1976)	Abriola & Pinder (1985b)	Sheng (1986)
Dracos (1978)	Baehr & Corapcioglu (1987)	Kuppusamy et al. (1987)
Hochmuth & Sunada (1985)	Chang (1991)	Rajapaksa (1988)
Corapcioglu & Baehr (1985)	Van Geel & Sykes (1994b)	Kaluarachchi&Parker (1989)
Baehr (1987)	Munoz & Irarrazaval (1998)	Sleep & Sykes (1989)
Reible & Illangasekare (1989)		Katyal, et al. (1991)
Ryan & Cohen (1991)		Al-Sheriadeh (1993)
McWhorter & Sunda (1991)		Binning (1994)
El-Kadi (1994)		Guarnaccia & Pinder (1997)
Wu et al. (1994)		

Le but de cette revue de littérature est de donner une ideé sur les travaux antérieurs des autres chercheurs dans les domaines analytiques, expérimentaux et numériques. En conséquence, les modèles analytiques sont convenables seulement pour des problèmes simples, en général il ne sont pas applicables pour l'analyse des problèmes réels plus complexes.

Les modèles physiques et expérimentaux peuvent être utilisés pour mieux comprendre les phénomènes mais ils ne peuvent pas être utilisés comme outils de prévision. La seule

option qui reste, l'utilisation des modèles numériques. Durant les trente dernières années, des efforts considérables ont été faits dans ce domaine. Cependant, la plupart des modèles dans ce groupe se concentre sur un aspect particulier du problème, soit la partie du transport. Les autres sont beaucoup plus compliqués et souffrent même d'instabilité et de restrictions de la convergence ce qui les rendent difficiles à utiliser pour les applications pratiques. Dans les chapitres suivants, un modèle numérique de l'écoulement multi phase dans la zone du vadose est présenté. Il est basé sur un plan de différences finies conservateur connu comme la méthode de support-opérateurs. Les avantages les plus importants de cette méthode sont sa simplicité relative et aussi le fait qu'il peut être utilisé sur un grille de géométrie arbitraire.

LE MODÈLE NUMÉRIQUE

Dans cette thèse, la méthode des support-opérateurs a été utilisée pour formuler un modèle discret du continuum système physique. Beaucoup de méthodes de différences finies standards et aussi des méthodes de volumes finis sont des cas spéciaux de la méthode des support-opérateurs. Contrairement aux méthodes de différences finies élémentaires, la méthode des support-opérateurs peut être utilisée sur une grille de structure arbitraire.

La méthode des support-opérateurs a été choisie plutôt la méthode que les éléments finies pour sa simplicité relative et le fait qu'il n'y avait aucune raison a priori pour que les méthodes des élément finis fournissent des meilleurs résultats. Un argument courant à l'appui des méthodes des éléments finis est sa prétendue plus grande souplesse pour faire face aux frontières irrégulières. Un tel argument ne peut pas être appliqué ici, puis qu'une maille irrégulière peut aussi être considérée par la méthode des support-opérateurs.

Les méthodes discrètes engendrent habituellement un système d'équations algébriques. Une technique de Newton-Raphson entièrement couplée est choisie pour gérer le non-linéarité et résoudre les équations séquentiellement dans une mode itératif. Les non-linéarités inhérentes aux équations principales sont la perméabilité relative $K_r = K_r(h)$, la saturation, $S = S(h)$, et la densité de la phase du gazeuse $\rho_a = \rho_a (h_a)$. Les équations sont couplées parce que dans toutes les équations plus qu'une variable fondamentale apparaît.

Pour chaque grille il y a (NPHASE) inconnus où NPHASE est le nombre de phases considérées dans la simulation. Les inconnus sont les charges hydraulique, h_w, de NAPL, h_n, et de l'air, h_a. L'algorithme de la solution est esquissé dans le Tableau (3).

Le modèle peut être utilisé pour simuler le mouvement complet de NAPLs à partir de réservoirs souterrains ou provenant d'un déversement d'huile dans un milieu poreux véritablement saturé. Il peut aussi être utilisé pour analyser l'écoulement biphasé de l'eau et du NAPL dans un système où le gaz est absent ou présent mais à pression constante.

Les données nécessaires pour analyse du l'écoulement comprennent les conditions initiales, les propriétés hydrauliques du sol, les propriétés du fluide, les paramètres de l'intégration du temps, les données de la condition de la frontière et géométrie du maillage. La Volatilisation et la dissolution du NAPL sont supposées se produire sous des conditions d'équilibre. Le modèle prédira la charge hydraulique et la saturation des trois phases à chaque noeud pour des intervalles spécifiés.

Tableau (3) Algorithme de la solution

1)	Fournir une estimation initiale h_w , h_n , et h_a pour chaque noeud
2)	Substituer les estimations dans les équations discretisées et trouver $F(x^{(k-1)})$
3)	Évaluer les termes dans la matrice Jacobienne
4)	Résoudre pour Δh_w, Δh_n , Δh_a
5)	Remettre à jour les estimations pour les variables fondamentales: $h_w^{\,1} = h_w^{\,0} + \Delta h_w$, $h_n^{\,1} = h_n^{\,0} + \Delta h_n$, $h_a^{\,1} = h_a^{\,0} + \Delta h_a$
6)	si $\Delta h_w > \varepsilon_w$ or $\Delta h_n > \varepsilon_n$ or $\Delta h_a > \varepsilon_a$ aller ensuite à l'étape 2

L'EXPÉRIENCE DU LABORATOIRE

Puisque quelques expériences seulement comportaient un écoulement LNAPL étaient disponibles et aucune d'elles n'avait été faite dans un milieu poreux hétérogène, une expérience a été conduite pour obtenir une meilleure compréhension du comportement

physique de l'écoulement multi-phase dans la zone non saturée et pour vérifier le modèle numérique par rapport à un cas hétérogène. Les travaux en laboratoire sont constitués ou deux types d'essai

1. quelques expériences indépendantes pour trouver les caractéristiques physiques du sol comme la conductivité hydraulique saturée, la courbe de rétention de l'humidité du sol et la densité sèche;
2. L'écoulement de LNAPL.

Les résultats de l'expérience ont que le NAPL qui s'écoule vers le bas à partir d'une région composée de matériau grossier rencontrera une pression d'entrée supérieur quand il touchera une région composé de grains fins. Ce comportement a causé la dispersion d'heptane au-dessus du sable fin à l'interface du sable grossier vers fin dans l'expérience du laboratoire. Le NAPL a émigré durant la passage de la couche à gros grain préférentiellement, et n'a pas pénétré dans la couche à grain fin substantiellement.

VALIDATION ET VÉRIFICATION DU MODÈLE

En utilisant les résultats expérimentaux et aussi les travaux analytiques et expérimentaux d'autres chercheurs, le modèle numérique a été calibré et vérifié. Le modèle a été validé avec trois solutions analytiques et a été vérifié avec trois travaux expérimentaux. Dans

tous les cas, les résultats numériques ont montré un bon accord avec les données observées.

L'ANALYSE DE LA SENSIBILITÉ

L'analyse de la sensibilité des paramètres du modèle a montré que la conductivité a l'influence la plus considérable sur le courant de NAPL comparativement aux autres caractéristiques du sol. La haute porosité du milieu peut limiter la région de sol contaminé grâce à sa haute capacité de retenir le polluant.

LA CONCLUSION

Dans cette thèse une tentative a été faite pour simuler numériquement la propagation d'un écoulement multi-phase dans la zone non saturée. Le modèle opère sur une section à deux dimensions et pour un milieu poreux hétérogène. Le processus du transfert de masse, comprenant la dissolution du NAPL dans la phase aqueuse et la volatilisation du NAPL vers la phase gazeuse, est représenté par une mécanisme simple du transfert de masse dans un terme puits.

Le modèle peut être utilisé pour simuler le mouvement complet du NAPLs provenant d'un réservoir souterrain ou d'un déversement dans un milieu poreux variablement saturé. Il

peut aussi être utilisé pour analyser l'écoulement biphasé de l'eau et du NAPL dans un système dans où gaz est absent ou présent mais à pression constante. Le programme établira des prévisions pour la charge hydraulique et la saturation des trois phases à chaque noeud pour des intervalles spécifiés. Son schèma numérique, la méthode de support-opérateurs, permet au modèle d'être appliqué sur une frontière irrégulière sans ajouter à la complexité de la solution.

TABLE OF CONTENTS

LIST OF TABLES

LIST OF FIGURES

LIST OF APPENDICES

NOMENCLATURE

a	Air entry value in Brooks and Corey relationship
C	concentration of organic compound [M/L^3]
C_{am}	equilibrium concentration in gas phase [M/L^3]
C_{wm}	equilibrium concentration in water phase [M/L^3]
D_0	molecular diffusion [L^2/T]
D_m	mechanical dispersion [L^2/T]
e_a	absolute convergence error
e_r	relative convergence error
g	gravitational acceleration [L/T^2]
h	pressure head [L]
K	hydraulic conductivity [L/T]
k	intrinsic permeability [L^{-2}]
k	relative permeability
P	pressure [M/LT^2]
$P_{\alpha\beta}$	capillary pressure between phase α and β [M/LT^2]
R	mass transfer between phases as source/sink per unit volume[L/T]
n	empirical constant of retention curve
S_α	saturation of phase α
$S_{r\alpha}$	residual saturation of phase α
$\bar{S}_\alpha$	effective degree of saturation of phase α
S_t	total liquid saturation
$\bar{S}_t$	effective total liquid saturation
t	time [T]
V	velocity [L/T]
x	horizontal direction [L]

z	vertical direction [L]

Greek Letters

α	empirical constant of retention curve
β_{an}	ratio of water surface tension to oil surface tension
β_{nw}	ratio of water surface tension to oil-water interfacial tension
ε_α	fraction of bulk volume occupied by the α phase
ϕ	porosity
γ	specific weight
λ	pore size distribution parameters in B&C relationships
λ_D	dissolution rate constant
λ_V	mass transfer coefficient for volatilization
μ	dynamic viscosity
ν	kinematic viscosity
θ_α	fraction of bulk volume occupied by the α phase
θ_r	residual water content
θ_s	saturated water content
ρ	mass density
σ_{nw}	interfacial surface tension between the organic liquid phase and the aqueous phase;
Ω	cell area
ω_k^α	mass fraction of component k in the α phase

CHAPTER I

INTRODUCTION

Liquids that do not dissolve in water and can exist as a separate fluid phase are known as non-aqueous phase liquids (NAPLs). There are two groups of NAPLs: those that are lighter than water (LNAPLs) and those with a density greater than that of water (DNAPLs). Most LNAPLs are hydrocarbon fuels such as gasoline and most DNAPLs are chlorinated hydrocarbons such as 1,1,1-trichloroethane and carbon tetrachloride.

When NAPL enters the unsaturated zone, it may displace any water and air already present. Except for the uppermost layer, which dries out due to evaporation, the soil in this zone usually contains water near residual saturation. Since water is present, the NAPL pressure must be larger than the entry capillary pressure of NAPL into a partially water-saturated porous media before penetration can occur. Since water is the wetting phase relative to both air and the NAPL, it tends to line the edges of the pores and NAPLs will not displace the water from the surface of the soil grain. The pollutant will migrate downwards through the unsaturated zone under the influence of gravity. Some horizontal migration of the mobile NAPL will also occur due to capillary forces. Finally, a gaseous envelope of chemical vapor due to volatilization may extend beyond the main body of contamination.

If the spill is of sufficient volume, some of the contaminant could reach the groundwater level. Although petroleum products are termed "immiscible", this does not mean that various

constituents are absolutely insoluble in water. The most soluble components dissolve, forming a plume of contaminated water, which extends outward from the main contamination zone. This plume then migrates as part of the groundwater system. The immiscible portion of the contaminant that remains as a distinct phase may travel under its own gradient.

Dissolved fractions of these hazardous hydrocarbons can enter the aquifer with water recharge through the contaminated soil and then be transported over large horizontal distances toward water wells away from the original source. Even very small concentrations of these constituents can render water unfit for domestic use. In addition, gasoline vapors can migrate into basements, sewers, and tunnels causing fire and explosion hazards.

Traditional contaminant transport models for miscible components are inadequate in describing the migration of an immiscible contaminant. The flow of an immiscible contaminant is controlled by its own flow potential, which depends on pressure, gravity, and surface forces, and is not necessarily similar to groundwater flow potential.

The understanding and prediction of petroleum product transport in soils and groundwater is of primary importance in the development of mitigation procedures that would aid effective recovery and cleanup of these contaminants as well as help to assess the risk of potential accidents that could disrupt water supplies.

The equations governing the multiphase flow of contaminants in a porous medium are highly nonlinear. As a general rule, analytical solutions are unavailable except under highly restrictive assumptions. To obtain useful solutions, resort must be made to numerical methods. In the numerical solution of these equations, stability and convergence restrictions limit the size of nodal spacing and time steps, which results in a large demand for computer storage and CPU time. Numerical models for NAPL migration in the vadose zone and in the groundwater has recently been presented by various researchers using finite difference and finite element methods. Most of them have been developed for one dimension although a few two dimensional models are available.

1.1 OBJECTIVES

The purpose of this research is to develop a numerical model to simulate the migration of non-aqueous phase liquids in the unsaturated subsurface system using the method of support-operators. Although this method has a long history in discrete mathematics, it has not been used in computational hydraulics. A two dimensional model is developed to describe the flow of water, NAPL and air in a vertical cross sectional area. Mass exchange from the NAPL to a gas phase due to volatilization and to the water phase due to dissolution are taken into account. The model has been verified against available analytical and experimental results. It is hoped that the model will provide further insight into the mechanics of the system while providing a useful assessment tool for the evaluation of NAPL contaminant migration in the subsurface region.

The model developed here has the following characteristics and capabilities:

- Simultaneous simulation of the flow of water, NAPL and air. The gaseous phase and/or nonaqueous phase may be absent in the simulation.
- The gas phase may be considered as a compressible or an incompressible fluid.
- The model may be used in heterogeneous porous media.
- Using the method of support-operators allows treatment of irregular boundaries. The method is based on an integral formulation and conservation of variable quantities is thus assured.
- Extended Van Genuchten relationships are used to define the capillary pressure-saturation and the conductivity-saturation relationships.
- A variable time step is used to increase the efficiency of solution.
- A FORTRAN 90 compiler which is Microsoft Powerstation® 4.0 is used to compile the program.
- For graphical outputs, Microsoft Excel® and SURFER® are used to create graphs and contour lines, respectively.

The limitations of the model are as follows:

- Solute transport due to convection, dispersion and diffusion is not considered either in water or the gas phase.

- Hysteresis in the constitutive relationships is not taken into account.
- NAPL is a single component fluid.
- Dissolution and volatilization are only considered from the NAPL to the water and to the gas phase, respectively and is calculated in the sink term.
- The model does not consider biodegradation, decay and adsorption/desorption

A laboratory experiment was conducted in the Hydrodynamic Laboratory of the École Polytechnique de Montréal for further validation of model in a multi-layered soil.

CHAPTER II

LITERATURE REVIEW

The flow of NAPL has primarily been of interest to petroleum engineers. The first recognition of NAPL movement in groundwater as a two-phase flow phenomenon is attributed to Van Dam (1967). Several models were subsequently developed to mathematically describe the immiscible flow of lighter than water NAPL in the subsurface.

2.1 Experimental models

Van der Waarden et al. (1971) studied the transfer of hydrocarbons from a residual oil zone to trickling water with an experimental model. They used a pack of non-adsorbing glass as a soil model. Experiments were carried out with very small amounts of a gas oil raffinate, 2-isopropylphenol as a model for transferable components and with actual mineral oil products: gasoline, kerosene, and gas oil. They found that extractable components are leached out from the oil zone by trickling water at a rate which is determined by the partition coefficient of the components and by the water/oil ratio. When the glass particles were replaced by natural dune sand, the transfer of oil components was delayed by adsorption and their concentration in the drain water decreased correspondingly.

A series of laboratory sand column experiments was conducted by Hunt et al. (1988) to evaluate the NAPL mobilization by water flooding, the dissolution behavior in a multi component separate phase, and the displacement of residuals by steam propagation through the sand pack. Experiments with trichloroethylene, a benzene-toluene mixture, and a commercial gasoline, showed that water flow at rates as high as 15 m/day could not displace the separate phase liquids. These experiments demonstrated the feasibility of steam injection for effective recovery of separate phase liquid contaminants.

To determine the relative importance of gaseous transport mechanisms, Swallow & Gschwend (1983) completed laboratory experiments using volatile organic compounds (VOCs). They concluded that vapor transport could be modeled by Fickian diffusion.

Johnson (1988) used a large scale, three-dimensional physical model to study transport mechanisms of VOCs. He discovered significant advective flow due to density effects when the permeability of the soil was greater than 10^{-11} cm^{-2} and the relative vapor density of the VOC to air was approximately 1.2 or greater.

Two-dimensional physical modeling of diesel fuel leaks in sand tanks was used by Johnson and Kreamer (1994) to determine liquid and vapor migration characteristics.

The dissolution of organic liquid entrapped in water-saturated glass beads was measured by Geller (1990) for pure toluene and a benzene-toluene mixture. The dissolution of the benzene-

toluene mixture demonstrated the change in aqueous concentration in response to the changing organic liquid composition. Up to the point where the available interfacial area limited the transfer, diffusion within the organic liquid did not affect mass transfer.

Annable (1991) conducted soil column experiments with soil containing three fluid phases, air, water, and gasoline, which were designed to simulate conditions in the unsaturated zone. Modeling the selective transport observed in experiments indicated that the majority of benzene, toluene, ethylbenzene, m&p-xylene, o-xylene, and naphthalene removal could be simulated acceptably using a chemical equilibrium based approach.

Alfossail (1986) investigated the effect of viscous forces and capillary forces on residual water saturation by conducting an experimental study of displacement of the wetting phase by a non-wetting phase. The experimental results showed that the residual water saturation was independent of flow rate when low viscosity oil displaced water in either high or low tension systems. A new dimensionless number was developed to indicate the effects of oil viscosity, flow rate and the interfacial tension.

Multicomponent transport of methane and trichloroethylene through air was examined by Abu-El-Sha'r (1993) under isobaric and non-isobaric conditions. He used experimental measurements to evaluate the applicability of three diffusional transport models: Fick's law, the Stefan-Maxwell equations, and the Dusty Gas Model (DGM). Comparisons indicated that for isobaric conditions, all models could accurately predict the measured fluxes. For non-isobaric

conditions, significant slip flux transport was observed and all models underestimated the measured fluxes.

Zhou (1994) conducted long-term and large-scale experiments to evaluate the migration of diesel and JP-5 fuels in sand and soil media in three dimensions. The transport of diesel in a sand medium was observed to be slower than that of JP-5 in both the horizontal and the vertical directions. Fuel transport in soil was more limited than in sand. The concentrations measured in the contaminated soil were much higher than that in sand.

A two-dimensional, multiphase flow experiment was conducted in the laboratory by Van Geel and Sykes (1994a). The saturation distribution of a lighter than water nonaqueous phase liquid as it migrated through a variably saturated sand medium was determined using image analysis techniques. The capillary pressures recorded by the pressure transducers were used to calculate the phase saturations based on a fully hysteretic capillary pressure-saturation algorithm. The static equilibrium capillary pressure-saturation relationships proved to be invalid immediately ahead of the LNAPL front. The capillary pressure-saturation relationships, appeared to be dynamic for short periods of time as the LNAPL front arrived at each transducer location. The presence of a trapped air phase as the LNAPL migrated through the unsaturated zone clearly affected the migration of the LNAPL and the maximum LNAPL saturation reached in the sand medium.

Table (2.1).is a summary of the experimental works that was identified during the present literature search. It may be concluded that:

- Dissolution of hydrocarbons from a residual oil zone to water could be determined by the partition coefficient of compounds and by the water/oil ratio.
- NAPL vapor transport may acceptably be modeled by Fickian diffusion law.
- NAPL removal may be acceptably simulated using a chemical equilibrium based approach.
- Residual water saturation was independent of flow rate when low viscosity oil displaced water.

Table (2.1) Summary of experimental models

Van der Waarden et al. (1971)	Dissolution of hydrocarbons from a residual oil zone to trickling water
Hunt et al. (1988)	Dissolution of NAPL in water and steam propagation
Swallow & Gschwend (1983)	Gaseous transport mechanisms
Johnson, R.L. (1988)	Transport mechanisms of VOCs
Johnson & Kreamer (1994)	2D physical model to determine liquid and vapor migration characteristics
Geller (1990)	Dissolution of pure toluene and a benzene-toluene mixture entrapped in water-saturated glass beads
Annable (1991)	Soil column experiments with soil containing three fluid phases: air, water, and gasoline, which were designed to simulate conditions in the unsaturated zone
Alfossail (1986)	The effect of viscous forces and capillary forces on residual water saturation
Abu-El-Sha'r (1993)	Evaluate the applicability of three diffusional transport models: Fick's law, the Stefan-Maxwell equations, and the Dusty Gas Model (DGM)
Zhou (1994)	To evaluate the migration of diesel and JP-5 fuels in sand and soil media in three dimensions
Van Geel and Sykes (1994)	2D, multiphase flow experiment with LNAPL

2.2 Analytical and numerical models

In the petroleum industry, «black oil simulators» were developed to simulate multi-dimensional, non-steady, three phase flow systems. In these models, water, oil, and gas were included. Flow equations for the three phases were written with respect to pressure in each phase and in the formulation, all the reactions and nonadvective flux terms were dropped. Solution techniques were first presented by Sheldon et al. (1959) and Stone and Gardner (1961) by a so called implicit pressure-explicit saturation (IMES) method. A second solution technique termed the Simultaneous Solution (SS) was introduced by Douglas et al. (1959) and extended by Coats et al. (1967) and Sheffield (1969). Stability restrictions on the time step were the major problem with these methods.

The final group of models that appeared in the oil industry were compositional models. These models simulate both the flow and transport of major species that exist in oil reservoirs and the interactions among them. These models are highly complicated and suffer from the same problems of «black oil simulators» (Al-Sheriadeh, 1993).

Recent interest by hydrologists and hydrogeologists in this field has been motivated by the possible disruption of water supply systems that may result as a consequence of an accidental oil spill. Their work is generally focused on modeling the flow, transport, remediation, and

recovery of the oil contaminants from the subsurface at levels above, below and within the water table.

Models in this area are grouped into three categories. The first group is analytical or semi-analytical and was developed in the early 1970's to describe the behavior of fuel oil spills in the subsurface. All models in this category treat the immiscible flow of chemical as a sharp interface problem with negligible smearing effects. The second group relaxes the sharp interface assumption and incorporates the capillary effect. The third group incorporates interphase transfer of mass, in addition to simple descriptions of the aqueous phase and vapor phase transport processes.

2.2.1 Sharp interface approach

The sharp interface approach or a piston flow model, which develops a time-distance profile for NAPL, is based on Darcy's law. Buckly and Leverett (1942), Mull (1971), Dracos (1978), Reible & Illangasekare (1989), and El-Kadi (1992 and 1994) developed analytical and semi-analytical approximations to describe the time evolution of a petroleum spill. The assumptions included in the sharp interface approach are as follows (El-Kadi, 1992):

1. The NAPL gas phase is assumed to be at constant pressure so only the liquid phase is modeled.

2. A sharp transition between NAPL-saturated and the dry condition is assumed; hence, the saturation-capillary relation is idealized as a rectangle.
3. Only air is displaced by infiltrating NAPL in the unsaturated zone.
4. The displacement of fluids is assumed as a piston flow, i.e., one fluid replaces the other, and hence only one mobile fluid may exist at a given location.
5. For one-dimensional infiltration, lateral spreading is ignored, i.e., the flow is assumed to be strictly vertical.
6. The water table is assumed to be too deep to have an influence on NAPL transport. This could be a serious limitation in some cases due to the large pressure gradient in water, which may affect NAPL movement.
7. Compressibility effects of the matrix and fluids are ignored.

The main advantages of this approach are, first the limited data requirement and second, the ease of model formulation and use.

Holzer (1976) used Hantush's theory for the formation of a fresh-water lens in an unconfined saline aquifer to analyze the decay of an oil lens overlying a water table. The theory is restricted to an isotropic media, a static and thick unconfined aquifer, no immobilization of other fluids, and is based on the Dupuit assumption. Although undoubtedly oversimplified, the theory when applied to a subsurface oil spill, nevertheless helps in the understanding of the temporal evolution of the oil lens. For this purpose, oil replaces fresh water and fresh water replaces the saline water in the theory. The equation describing the growth of the lens is:

$$H_m^2 = 4c.v.t.S^*(a/\sqrt{4vt}, a/\sqrt{4vt})$$

H_m = distance from base of lens to initial water table;

$$S^*(\alpha,\alpha) = \int_0^1 \mathrm{erf}(\alpha/\sqrt{\tau})\mathrm{erf}(\alpha/\sqrt{\tau})d\tau;$$

$c = w/2\delta(1+\delta)K$;

$v = K\delta H/\phi$;

$\delta = (\gamma_f - \gamma_o)/\gamma_o$;

$2a$ = dimension of square recharge area;

H = a weighted mean of areal distribution of the depth to the interface during a period of flow at the end of which the distribution of thickness of the spill is desired;

K = permeability (LT^{-1});

ϕ = porosity;

t = time;

w = recharge rate;

$\gamma_{f,o}$ = specific weight of fresh water and oil, respectively.

Hochmuth and Sunada (1985) also developed a numerical model based on the salt/fresh water analogy to simulate the behavior of two phase immiscible fluids in ground water systems for specific application to hydrocarbon spills and leaks. The model was a two-dimensional areal flow model using the finite element method. The vertically downward migration of the oil was

not simulated in the two dimensional areal model. Instead, the horizontal spread of the oil after reaching the water table was evaluated. The physical assumptions used to formulate the problem and their effect on the system were:

1.The Dupuit-Forchheimer approximation with a strictly horizontal flow

2. The flow of each phase obeys Darcy's law

3. The capillary pressure-saturation curve is idealized and is constant over the study area.

The validity of the model was demonstrated by comparing results with an analytical solution originally developed for fresh-water lenses in island aquifers and a laboratory investigation.

2.2.2 Immiscible phase approach

Because of the limitation of the first approach, other researchers applied numerical models like «black oil» reservoir simulators to simulate fluid flow with the provision of a transition zone within which a number of phases are mobile. This approach couples the equations for the water-NAPL-gas system and includes constitutive relations for saturation and relative permeability.

Two-dimensional equations for flow in a vertical plane have been developed by Faust (1985). The fully implicit equations are solved by a direct matrix technique and Newton-Raphson iteration for the nonlinear terms. His mathematical model is based on a simplification that

follows from the same assumption used in Richard's equation, namely that pressure gradients in the air are negligible and that the air pressure is at its atmospheric value. The conventional three-phase flow model has three governing partial differential equations for water, gas, and the nonaqueous liquid. The use of the simplifying assumption for hazardous waste applications eliminates the explicit treatment of the gas (air) equation. Since the governing equations are nonlinear and strongly coupled, the elimination of the air equation results in a numerical model that is less expensive to use. The most significant simplifying assumption is that pressure in the air phase is atmospheric. For the shallow system it is also appropriate to assume that densities and viscosities are pressure independent. Volatilization of the nonaqueous fluid is treated by considering it as a source/sink term. The two-dimensional model is based on a finite difference scheme utilizing a block-centered grid that allows variable spacing and approximation of irregular geometry. Depth is not necessarily aligned with the vertical direction. This permits simulation of a sloping aquifer. An implicit treatment leads to a system of 2N nonlinear equations for each time step. Each grid block is connected to, at most, four adjacent blocks so that each equation has a maximum of 5 unknown grid block values for both pressure and saturation, or 10 unknowns per equation. This set of nonlinear equations is linearized using a residual formulation with Newton-Raphson iteration. Application of the Newton-Raphson procedure to the nonlinear difference equations produces a system of linear equations that requires a solution for each iteration. The coefficient matrix of the linearized equation is banded but nonsymmetric. The matrix equation is solved using the Gauss-Doolittle decomposition for a banded matrix (Faust, 1985).

Osborne & Sykes (1986) developed a two phase, two dimensional model by using the finite element technique. Fluids and matrix compressibilities were negligible. Linear, isoparametric, quadrilateral elements were used and the set of partial differential equations was solved by the method of weighted residuals. The resulting set of nonlinear equations was resolved by a Newton-Raphson iterative technique. This model was applied to a field-contaminated site at the Hyde Park landfill in New Jersey. Simulation results significantly underpredicted the extent of the NAPL saturation observed in field testing.

Kuppusamy et al. (1987) developed a finite element model for multiphase flow through soil. The solution procedure used backward time integration with iteration by a modified Picard method to handle the nonlinear properties. The model was used to simulate laboratory experiments and a hypothetical field case involving NAPL near the soil surface due to leakage from an underground storage tank.

A finite element model was presented by Rajapaksa (1988) to simulate multiphase immiscible fluid flow in two and three dimensional heterogeneous oil reservoirs with irregular boundaries. The effect of gravity, rock compressibility and fluid compressibility was incorporated. The finite element method was used to discretize the spatial domain. The formulation of three-node triangular, four-node isoparametric quadrilateral and eight-node isoparametric brick elements was presented. The total simulation time is divided into equal small time increments. The unknown variables are approximated as a polynomial function of time over each time

increment. Thus a forward iterative scheme is used to advance the solution from one time increment to the next. A computer program was developed for the finite element model used to analyze the flow characteristics of complex oil reservoirs. The program has the capacity to selectively refine the finite element mesh in appropriate sub-regions of the domain (i.e., the surrounding area along the moving interface between the fluids, which is called the fluid interface) and to remove the mesh refinement in regions where it is not necessary (i.e., regions which are fully saturated). In this study the appropriate regions were selected based on the saturation of the injected fluid. The fluid interface is defined as the region in which the injecting fluid saturation is between 0.4 and 0.8, the fully saturated region is defined where this saturation is greater than 0.9. The ability to selectively refine or coarsen the finite element mesh is attempted only if three-node triangular elements and the four-node isoparametric quadrilateral elements are used to discretize the domain.

A two dimensional finite element model was also developed by Kaluarachchi & Parker (1989). A Galerkin weighted residual approach together with an upstream weighting technique was used to predict simultaneous flow of water and oil in a three fluid phase system with gas assumed at constant pressure. Picard and Newton-Raphson iteration were used and it was concluded that both schemes provided similar accuracy. They analyzed several example problems to show the accuracy of their model by checking that the mass balance criteria is satisfied within each phase of the system. Consumption of large amounts of CPU time was their main problem.

Chang (1991) developed a multiphase unsaturated zone contaminant transport (MUCT) model to simulate the simultaneous vertical flow of water and a second immiscible fluid in unsaturated porous media. The model couples multiphase flow equations with a multiphase solute transport equation. The multiphase flow equations were solved semi-analytically by applying finite difference computations. Multiphase solute transport was governed by a simplified three-phase flow advection-dispersion equation. The solute transport equation is solved analytically under the assumptions of a steady flow field and local partition equilibrium between phases. The solute transport is assumed to be strictly one dimensional; only longitudinal advection and dispersion are included. The model was evaluated by applying generic examples, mass balance, and sensitivity analyses to demonstrate the potential application of the model.

Wu et al. (1994) developed a numerical model in which the mathematical formulation was based on vertical integration of the three-dimensional two-phase flow equations. The concept of gravity-capillary vertical equilibrium (GCVE) in which a vertical balance of gravitational and capillary forces is assumed was incorporated within their formulation.. Simulation examples were provided to demonstrate model verification and utility.

2.2.3 Interphase mass transfer approach

Corapcioglu and Baehr (1985, 1987a, 1987b, 1987c) presented a series of models to simulate immiscible contaminant transport in soils. The first model was a single cell model as a

simplified version of a generalized system (Corapcioglu and Baehr, 1985). The entire system was represented by a single element. Such an approach yields conservative estimates of a single constituent contaminant as only advective solute transport is allowed. The model has been applied to study the fate and transport of individual hydrocarbon constituents in an unsaturated zone. The results predict the concentrations of each hydrocarbon in all phases in space and time allowing the user to estimate the amounts of hydrocarbons which enter the underlying aquifer or which leave the soil via volatilization into the atmosphere. In developing the model, they assumed that:

- The plume may be approximated by a series of rectangular blocks with one-dimensional transport for each block;
- After the discovery of a contamination incident, the source has been discontinued and the immiscible fluid is immobile, that is, the plume boundaries are not functions of time;
- fluid phases are isothermal and isobaric;
- soil water is at equilibrium with the immiscible phase;
- there is no partitioning of the contaminant into air or adsorbed phases;
- in the water phase, only advection transport is considered, diffusive and dispersive fluxes are neglected;
- the contaminating hydrocarbon is represented by a single constituent.

They found that model predictions were very sensitive to the soil complexity and furthermore, that sensitivity was a function of the thermodynamic properties of the contaminant. The single

cell model yields very conservative estimates, as much as two to four times that of the generalized model and sometimes higher. This is due to the fact that they neglected the vaporization in the air phase and considered only the advective transport in the water.

In their second model, Corapcioglu and Baehr (1987) developed a mathematical formulation to describe the transport and fate of a petroleum product. Transport of the contaminants can occur as solutes in soil water, vapors in the interstitial air, and as unaltered constituents in the oil phase. Governing equations were obtained by developing conservation of mass equations for the water, air, and oil phases, and for each contaminant constituent. An equilibrium model was assumed to partition constituent mass between the air, oil, water, and adsorbed phases. This simplified the mathematical complexity of the model, as phase specific conservation of mass equations (a kinetic description) were then not required to describe the contaminant transport. A method for estimating upper bound biodegradation rates was incorporated into the model by considering the subsurface transport of free oxygen. Changes in the composition of the phases due to mass transfer from natural chemical systems (e.g., water vapor, dissolved soil gases, carbonate systems) as well as other possible pollutants were assumed to be negligible. Solid exchange is mediated by only a wetting aqueous phase (water) in soils. The advective-dispersive model was applied to quantify the mass flux for the individual constituents of the fluid phases.

A numerical solution to the governing equations was also presented by Baehr and Corapcioglu (1987). This solution, obtained by using a finite difference scheme and a method of forward

projection to evaluate nonlinear coefficients, provided estimates of the flux of solubalized hydrocarbon constituents to groundwater from the portion of spill which remains trapped in the soil after routine remedial efforts to recover the product have ceased. The procedure was used to solve the one-dimensional (vertical) form of the system of nonlinear partial differential equations defining the transport for each constituent of the product. They assumed immobile oil and air phases. They also assumed that the immiscible phase is an insignificant mode of transport and neglected abiotic transformations. Other assumptions were a constant water flux, constant density of the water phase, and a homogeneous, isothermal soil with uniform moisture content.

An analytical solution to a one-dimensional diffusion equation was the third model developed by Baehr (1987) to examine the sensitivity of vapor and solute migration on partition coefficients and moisture content. There was no source or sink for immiscible constituents due to molecular transformation and the immiscible phase was at residual saturation. The air phase was assumed to be at atmospheric pressure and the porous medium was supposed homogeneous, isotropic, and under isothermal conditions. Equilibrium approximations were employed to partition contaminant mass between the air, water, and adsorbed phases outside the region contaminated by the organic liquid phase. Significant differences in the predicted transport between substances covering the range of possible partition coefficients justified the development of a higher-dimensional model for practical applications. Transport of gasoline constituents was simulated using the radially symmetric algorithm to identify those constituents with a high groundwater contamination potential. Aromatic constituents of gasoline dominate

the total hydrocarbon mass partitioned in the water in the unsaturated zone due to their high water/air partition coefficients relative to nonaromatic constituents. As the spill ages, aromatic dominance increases as nonaromatic constituents find their way more rapidly into the atmosphere. Because aromatic constituents are more soluble than nonaromatic constituents are, the significant hydrocarbon flux to the atmosphere does not result in a commensurate decline in groundwater contamination potential.

A comprehensive approach to the modeling of a chemical contamination was developed by Abriola and Pinder (1985b). With their approach, they could determine both fluid saturations and pollutant concentrations in each phase as functions of space and time in a heterogeneous porous medium. They also developed a one-dimensional numerical model which was designed to solve their system of governing equations. They assumed that the contaminant phase could consist of, at most, two organic species. One of them is assumed nonvolatile and insoluble in water. The other species may be a more volatile component, capable of crossing phase boundaries. Three other system components were soil, air, and water. Each of these components was assumed to exist in a single phase: the solid (s), gas (g), and water (w) phases, respectively. Thus, neither the formation and migration of water vapor nor the adsorption of water onto soil particles was included. There was also no consideration herein of possible adsorption or biological decay of species. Their analysis was restricted to contaminants that are only slightly water soluble. Under this restriction, any changes in water properties (such as density or viscosity) due to the presence of soluble organics or the exchange of these organics with other phases will be very small and can be neglected. Using volume averaging theory,

equations governing such migration were developed from basic conservation of mass principles for a two-component contaminating phase. The resulting equations form a system of three nonlinear partial differential equations in five unknowns: P_{ow} , P_{wg} , ω_2^o , ω_2^g , ω_2^w . On the basis of the concept of local equilibrium between the phases, two constraints relating mass fractions were formulated to close this mathematical system.

The numerical model of Abriola & Pinder (1985a) solves a system of equations using a technique that is known as the "simultaneous solution" (SS) method. This method is generally formulated using a finite difference discretization of the governing equations. Properties of the SS method have been examined in the oil industry literature for various linearized versions of the immiscible flow equations. An implicit finite difference simultaneous solution scheme is used to solve the system of governing equations. The standard or "variable tangent" Newton-Raphson method was the iterative scheme employed in their model. Dirichlet, or first-type boundary conditions, were incorporated into the system by replacing each mass balance equation at a boundary node i by an identity of the form

$$a_{kj}\, u_j \,|_i = c_k$$

where a_{kj} and c_k are specified. In addition to boundary conditions, a set of initial conditions must also be provided. For regions in which a fluid is absent, a finite, albeit very small, initial saturation of the purportedly absent phase exists everywhere in the domain. The full system of mass balance equations may then be solved at every node. A minimum saturation value of 10^{-4} was employed in their work.

Also, Pinder & Abriola, 1986 provided a broad overview of the problem of multiphase migration of organic chemicals in a porous medium. Equations governing the movement of NAPL and water in a saturated-unsaturated groundwater reservoir were presented along with a discussion of some of the theoretical underpinnings of these equations. They assumed in their development that there are no chemical reactions other than adsorption; the porous medium matrix is rigid; there are no external sources or sinks; and the air phase is immobile. A two-dimensional finite difference numerical model was used to simulate TCE migration.

Sheng (1986) developed a finite element model for multiphase flow through soil involving three immiscible fluids: namely air, water, and an organic fluid. A variational method was employed for the finite element formulation corresponding to the coupled differential equations governing the flow of the fluid phase porous medium system with constant air phase pressure. Constitutive relationships for fluid conductivities and saturations as functions of fluid pressures which may be calibrated from two-phase laboratory measurements, were employed in the finite element program. The solution procedure used iteration by a modified Picard method to handle the nonlinear properties and the backward method for a stable time integration. Laboratory experiments involving soil columns initially saturated with water and displaced by p-cymene (a benzene-derivative hydrocarbon) under constant pressure were simulated by the finite element model for validation purposes and for formulation of the constitutive properties. Transient water outflow predicted using independently measured capillary head-saturation data agreed well with observed outflow data. Two-dimensional simulations were presented for

eleven hypothetical field cases involving introduction of an organic fluid near the soil surface due to leakage from an underground storage tank. The subsequent transport of the organic fluid in the variably saturated vadose and groundwater zones was analyzed.

A model was developed to solve for the water phase flow together with the transport and density dependent gas phase flow and transport by Sleep and Sykes (1989). The expressions for dissolution, volatilization, and gas-liquid partitioning, employing the concept of an overall mass transfer coefficient, were incorporated into their model. The set of partial differential equations developed by them was solved for a two-dimensional, vertical, cross section using the Galerkin method of weighted residuals. The nonlinear water flow equations were solved iteratively, using a modified Newton-Raphson technique with an Aitken accelerator. The importance of gas phase processes in increasing subsurface contamination from volatile organics, and in dissipating residual amounts of these substances, was demonstrated.

A theoretical investigation of factors affecting the gas phase transport of evaporating organic liquids in the unsaturated zone was presented by Falta et al. (1989). Their numerical simulations showed that mass transfer due to density-driven flow may dominate the gas phase transport of some organic chemical vapors in the unsaturated zone.

Ryan & Cohen (1991) presented a one-dimensional multiphase mass transport model for the migration of NAPL containing sparingly water soluble organics in the unsaturated soil zone. Their model consisted of a two-phase immiscible flow model linked to a four-phase chemical

transport model. The coupled equations of the system were rearranged in dimensionless form to explore the driving forces in the flow and transport mechanisms in the porous media. Three resulting partial differential equations were solved by a trapezoidal finite difference scheme. For tracking and locating the front, they linked the dimensionless equations of flow to a mass balance equation, and solved them simultaneously for front location and saturation.

A 2D finite element model was developed to simulate 2-phase flow in heterogeneous media by Al-Sheriadeh (1993). In this model the pressure head to each fluid phase was selected as the primary variable for discretization. Formulation based on these variables will produce a proper basic irreducible form that ensures that continuity and compatibility conditions will be satisfied quite easily in any media. To avoid stability problems, a full implicit scheme in time was used with an adaptive time stepping procedure to enhance model practicality. Emphasis was placed on simulating heterogeneous cases by forcing continuity and compatibility conditions in the basis functions. To reduce mass balance error, he evaluated the capacity terms using the mean head analytic scheme proposed by Osborne and Sykes (1986). This scheme reduces the error reasonably well with rapid convergence in cases of heterogeneous media. This model was verified by comparing its results with an analytical solution developed by McWhorter and Sunada (1991) for a horizontal flow in homogeneous media and to those of a numerical model developed by Kaluarachchi and Parker (1989) for vertical flow in a homogeneous medium.

Binning (1994) presented a two-dimensional model of unsaturated zone multiphase air-water flow and contaminant transport. He used two approaches to write multiphase equations: with

the two individual phase pressures as dependent variables or using the global pressure-saturation approach of petroleum engineering. The two-pressure form of the equations was solved in two dimensions in both Cartesian and radial coordinates using a modified Picard linearization of the mixed form of the equations with a finite element method applied in space. In one dimension for incompressible fluids the pressure-saturation equations simplified because the pressure equation reduces to a trivial ordinary differential equation, leaving only the saturation equation to be solved numerically. The saturation equation was solved using a Modified Method of Characteristics (MMOC). A volatile contaminant was assumed to be transported in either phase or in both phases simultaneously. The contaminant partition between phases was described with an equilibrium distribution given by Henry's Law or via kinetic mass transfer. The resulting equations were solved using two methods: a lumped-in-time Galerkin finite element method using reduced integration, and the Eulerian Lagrangian Localized Adjoint Method (ELLAM). Both methods were applied in one and two dimensions and their relative merits were demonstrated and discussed. The ELLAM uses finite volume test functions and the method conserves mass both globally and locally. It is shown to have particularly good performance for advection dominated problems in regions of sharp changes in saturation. These could be overcome, but only at the expense of these difficulties and is clearly favored over the finite element solution.

Weaver et al. (1994) presented a model for simulation of subsurface releases of light nonaqueous phase liquids (LNAPLs). Transport of the NAPL through the unsaturated zone was assumed to be one-dimensional. Capillary pressure gradients were neglected except as

they influenced the infiltration of NAPL into the soil. The resulting equations for NAPL flow were hyperbolic and were solved by the generalized method of characteristics. The aquifer transport of the dissolved contaminant was simulated by using a two-dimensional, vertically averaged analytic solution of the advection-dispersion equation. The vertical extent of the contaminant was estimated from the recharge rate, ground water seepage velocity and vertical dispersivity, rather than assuming the contaminant is distributed over the entire aquifer thickness (Charbeneau et al., 1995).

Van Geel and Sykes (1994b) developed a two-dimensional finite difference model to simulate the movement of a LNAPL spill in a variably saturated zone. The numerical model allowed a non-hysteretic, a partially hysteretic and a fully hysteretic solution. Their model results compared well with the laboratory data presented by Van Geel and Sykes (1994a).

Guarnaccia and Pinder (1997) developed a two and three dimensional numerical model to simulate the transport and fate of NAPLs in near surface granular soils. Their model accommodates three mobile phases: water, NAPL and gas. The numerical solution algorithm is based on a Hermit collocation finite element discretization. Particular attention was paid to the development of a sub-model that describes three phase hysteretic permeability-saturation-pressure (k-S-P) relationships. The main disadvantage of this model is that the problem domain and individual elements must have a rectangular shape. Also, it needs many parameters which are usually hard to measure in the real cases.

A numerical model was developed by Munoz and Irarrazaval (1998) to describe the bioremediation of hydrocarbons in ground water aquifers considering aerobic degradation. The flow equation is solved by means of an alternating direction implicit finite difference method and the transport equations for the three solutes (hydrocarbons, oxygen, and microorganisms) are solved by applying the method of characteristics separately to each of the solutes. The model was verified against some available experimental data. Significant average relative errors were obtained from comparison between leached and degraded mass predictions and the experimental results. The Authors claimed that these differences may be due to the different conditions regarding the addition of nutrients in the columns, which were not accounted for in the model.

This literature review was intended to give a basic background of previous works of other researchers in analytical, experimental and numerical fields. As a result, analytical models are only suitable for simplified problems and are generally not applicable for the analysis of complicated real world problems. Physical and experimental models may be used for better understanding of phenomena but they cannot be used as prediction tools. The only remaining option is using numerical models. In the past three decades, a significant amount of work devoted to this area has been realized. However, most of the models in this group focus on a particular aspect of the problem, which is the transport part. The others are far more complicated and even suffer from stability and convergence restrictions, which make them difficult to use for practical applications. In the following chapters, a numerical model of multi

phase flow in the vadose zone is presented based on a conservative finite difference scheme known as the method of support-operators. The most advantages of this method are its relative simplicity and also it may be used to construct finite difference scheme on grids of arbitrary geometry.

Table (2.2) Analytical and numerical models

Analytical Models	Finite Difference models	Finite Element Models
Mull (1971)	Faust (1985)	Osborne & Sykes (1986)
Holzer (1976)	Abriola & Pinder (1985b)	Sheng (1986)
Dracos (1978)	Baehr & Corapcioglu (1987)	Kuppusamy et al. (1987)
Hochmuth & Sunada (1985)	Chang (1991)	Rajapaksa (1988)
Corapcioglu & Baehr (1985)	Van Geel & Sykes (1994b)	Kaluarachchi&Parker (1989)
Baehr (1987)	Munoz & Irarrazaval (1998)	Sleep & Sykes (1989)
Reible & Illangasekare (1989)		Katyal, et al. (1991)
Ryan & Cohen (1991)		Al-Sheriadeh (1993)
McWhorter & Sunda (1991)		Binning (1994)
El-Kadi (1994)		Guarnaccia & Pinder (1997)
Wu et al. (1994)		

CHAPTER III

MATHEMATICAL DESCRIPTION OF NON-AQUEOUS PHASE LIQUIDS (NAPLs) MOVEMENT IN POROUS MEDIA

In this chapter, mechanics and mathematics of the movement of non-aqueous phase liquids and their behavior in the subsurface are presented. In the vadose zone, consideration of NAPL migration must account for the interactions between the NAPL, the water, and the air. In the groundwater zone, interaction between the NAPL and water phases are important.

The entry of NAPL into porous media is controlled primarily by capillary phenomena arising from the facts that an interfacial tension is present between two mutually immiscible fluids (e.g. air/NAPL or water/NAPL), and that the pores are small. In addition, the wettability of the water/NAPL/solid system influences the conditions under which a NAPL enters a given permeable geologic medium. Wettability refers to the preferential spreading of one fluid over solid surfaces in a two-fluid system. Whereas the wetting fluid will tend to coat solid surfaces and occupy smaller openings in porous media, the nonwetting fluid will tend to be constructed to the larger openings (Cohen and Mercer, 1993). Most NAPLs of interest are non-wetting on geologic solids with respect to water, but wetting with respect to air. The forces driving subsurface NAPL movement depend on the density and viscosity of the NAPL, the pressures resulting from its release into the

subsurface, the intrinsic and relative permeability of the geological medium, capillary pressure, and the degree of NAPL saturation of the pore space in the medium. For NAPL movement to occur in wet media, these driving forces must overcome the capillary resistance. The NAPL in the larger pore openings must deform to pass through smaller pore throats to reach other pore openings. The pressure required for this deformational movement is the entry pressure. The value of the entry pressure is proportional to the interfacial tension between the NAPL and the water, and inversely is proportional to the size of the pore throats.

In the most general case, the equations governing the migration of NAPLs, in air and water, subject to mass transfer across phase boundaries, can be assembled from the following mass balance equation for the chemical component k in phase α (Kueper and Frind, 1996):

$$\frac{\partial}{\partial t}\left(\theta_\alpha \rho_\alpha \omega_k^\alpha\right) + \frac{\partial}{\partial x_i}\left(\theta_\alpha \rho_\alpha \omega_k^\alpha V_{\alpha,i}\right) - \frac{\partial}{\partial x_i} J_{k,i}^\alpha = I_k^\alpha + R_k^\alpha \qquad (3.1)$$

where θ_α is the fraction of bulk volume occupied by the α phase, ρ_α is the average mass density of α phase ω_k^α is the mass fraction of component k in the α phase, $V_{\alpha,i}$ is the velocity of the α phase in the i-th direction, $J^\alpha_{k,i}$ is the non-advective flux of k in the α phase in the i-th direction, I_k^α represents the transfer of k due to phase change and

diffusion across phase boundaries, and R_k^{α} is is the net mass transfer per unit porous media volume into(+) or out of (-) phase α. The following expressions obviously hold:

$$\begin{aligned} \sum_{k=1}^{n} \omega_k^{\alpha} &= 1 \\ \sum_{\alpha=1}^{N} \theta_k^{\alpha} &= 1 \\ \sum_{\alpha=1}^{N} I_k^{\alpha} &= 1 \end{aligned} \tag{3.2}$$

where n is the total number of components comprising phase α and N is the total number of phases.

The non-advective flux vector, $J^{\alpha}_{k,i}$, appearing in (3.1), accounts for the molecular diffusion and mechanical dispersion of component k within a given phase. It is often assumed that both of these are Fickian in nature and may be defined as(Kueper and Frind, 1996):

$$J_{k,i}^{\alpha} = -\theta_{\alpha}\tau_{\alpha,ij}D_0^{k,\alpha}\frac{\partial\left(\rho_{\alpha}\omega_k^{\alpha}\right)}{\partial x_j} - \theta_{\alpha}D_{m,ij}^{k,\alpha}\frac{\partial\left(\rho_{\alpha}\omega_k^{\alpha}\right)}{\partial x_j} \tag{3.3}$$

where $\tau_{\alpha,ij}$ is a tensor of phase tortusity coefficients, $D_0^{k,\alpha}$ is the free solution molecular diffusion coefficient of k in α, and $D_{m,ij}^{k,\alpha}$ is a mechanical dispersion tensor of k in α.

Velocity may be obtained from Darcy's law which has been used successfully in the petroleum literature to model multiphase flow in porous media. The generalized form of Darcy's law for multiphase flow may be written as (Pinder & Abriola, 1986):

$$V_{\alpha,i} = \frac{-k_{i,j}k_{r,\alpha}}{\mu_\alpha \theta_\alpha}(\nabla P_\alpha - \rho_\alpha g \frac{\partial z}{\partial x_j}) \qquad (3.4)$$

where

$k_{i,j}$ intrinsic permeability tensor, a function of the soil matrix [L^2];

$k_{r,\alpha}$ relative permeability of the matrix to the phase α ($0 \leq k_{r\alpha} \leq 1$);

μ_α dynamic viscosity of the α phase ;

P_α pressure of the α phase

g vector of gravitational acceleration directed downward [L/T^2].

z the vertical direction

ρ_α density [M/L^3]

In order to complete the set of equations required to represent NAPL migration in the subsurface, the various phase pressures must be coupled through capillary pressure relationships. For a general air-water-NAPL system, the following capillary pressures can be defined (Kueper and Frind, 1996):

$$P_{aw}(S_a, S_w) = P_a - P_w$$
$$P_{an}(S_a, S_n) = P_a - P_n \qquad (3.5)$$
$$P_{nw}(S_n, S_w) = P_n - P_w$$

where the subscripts a, n, and w are taken to represent air, NAPL, and water, respectively. The phase saturation, S_α, is expressed as a fraction of pore space and is related to the phase volume fraction by $S_\alpha = \theta_\alpha / \phi$ where ϕ is the porosity of the medium and it is clear that:

$$S_w + S_n + S_a = 1 \qquad (3.6)$$

LNAPLs transport may be roughly divided into four processes: infiltration, mound formation, spreading in the direction of flowing water, and migration of dissolved NAPL in the saturated zone (El-Kadi, 1994). Spreading of NAPL atop the water table is assumed to occur at the end of mound formation, and to develop due to water-table gradient and pressure gradient. The latter is caused by NAPL accumulation under the source on the top of the capillary fringe.

By substituting the equation (3.4) in (3.1) and neglecting the solute transport term in the equation (3.1), NAPL movement in the absence of mass transfer for water (w), NAPL (n), and air (a), is based on the following partial differential equations, which can be created by

summing equation (3.1) over all components comprising a given phase for a two dimensional Cartesian domain (Katyal et al. 1991):

$$\phi \frac{\partial S_w}{\partial t} = \frac{\partial}{\partial x}\left[Kw_{ij}\left(\frac{\partial h_w}{\partial x}\right)\right] + \frac{\partial}{\partial z}\left[Kw_{ij}\left(\frac{\partial h_w}{\partial z} + 1\right)\right] + \frac{R_w}{\rho_w} \tag{3.7}$$

$$\phi \frac{\partial S_n}{\partial t} = \frac{\partial}{\partial x}\left[Kn_{ij}\left(\frac{\partial h_n}{\partial x}\right)\right] + \frac{\partial}{\partial z}\left[Kn_{ij}\left(\frac{\partial h_n}{\partial z} + \frac{\rho_n}{\rho_w}\right)\right] + \frac{R_n}{\rho_n} \tag{3.8}$$

$$\phi \frac{\partial \rho_a S_a}{\partial t} = \frac{\partial}{\partial x}\left[\rho_a Ka_{ij}\left(\frac{\partial h_a}{\partial x}\right)\right] + \frac{\partial}{\partial z}\left[\rho_a Ka_{ij}\left(\frac{\partial h_a}{\partial z} + \frac{\rho_a}{\rho_w}\right)\right] + R_a \tag{3.9}$$

where $h_\alpha = P_\alpha / (\rho^*_w g)$ is the water height- equivalent pressure head of phase α; and ρ^*_w is the density of pure water.

Two constitutive relationships often used in the mathematical description of multi-phase liquid flow in porous media are the capillary pressure and relative permeability of the system as functions of saturation. Capillary pressure-saturation and relative permeability-saturation relationships have been studied extensively in soil science and Petroleum engineering.

3.1 Saturation-pressure relations

A variety of techniques are used in multiphase flow models for the estimation of these relationships. Almost the first equation to be used was Leverett's function (Leverett, 1941). It can be defined as:

$$J(S_w) = \frac{P_{nw1}}{\sigma_{n1w}}\left(\frac{k_1}{\phi_1}\right)^{1/2} = \frac{P_{nw2}}{\sigma_{n2w}}\left(\frac{k_2}{\phi_2}\right)^{1/2} \tag{3.10}$$

where

$J(S_w)$ Leverett's function;

σ_{nw} interfacial surface tension between the organic liquid phase and the aqueous phase;

When the systems have the same permeability and porosity ($k_1 = k_2$; $\varepsilon_1 = \varepsilon_2$), Leverett's function simplifies to

$$J(S_w) = \frac{P_{nw1}}{\sigma_{n1w}} = \frac{P_{nw2}}{\sigma_{n2w}} \tag{3.11}$$

or,

$$P_{nw2} = P_{nw1}\left(\frac{\sigma_{n2w}}{\sigma_{n1w}}\right) \tag{3.12}$$

Hence, the capillary pressure at a given saturation for an organic liquid-water system can be generated from, for example, the air-water capillary pressure-saturation relationship for that soil by knowing the ratio of the liquid-liquid interfacial tensions of the systems.

As the capillary pressure increases, the saturation of the wetting phase approaches some limiting value, S_{rw}. At this point, the wetting fluid loses its capability to move as a bulk phase in response to a hydraulic gradient and its movement is then dominated by advective-diffusive transport as a dispersed phase in the nonwetting fluid. When $\sigma_{nw} = 0$, only a single phase is present and, consequently, $S_{rw} = 0$. Therefore, one might expect that as $\sigma_{nw} \rightarrow 0$, $S_{rw} \rightarrow 0$. Yet, previous measurements do not always show this to be the case.

Measurement and experiments of Demond and Roberts (1991) showed that the form of Leverett's function is unable to estimate the residual saturation for organic liquid-water systems from air-water values, despite its ability to predict the displacement pressures for drainage and imbibition.

One of the most popular functions that empirically describe the soil water retention curve is that of Brooks and Corey (1964):

$$\theta = \begin{cases} \theta_r + (\theta_s - \theta_r)(ah)^{-\lambda} & (ah > 1) \\ \theta_s & (ah \le 1) \end{cases} \tag{3.13}$$

where θ_r and θ_s are the residual and saturated water contents, respectively, a is an empirical parameter (L^{-1}) whose inverse is often referred to as the air entry value or bubbling pressure, and λ is a pore-size distribution parameter affecting the slope of the retention function. Also, it may be written in dimensionless form as follows:

$$\bar{S}_w = \begin{cases} (ah)^{-\lambda} & (ah > 1) \\ 1 & (ah \le 1) \end{cases} \tag{3.14}$$

where $\bar{S}_w$ is the effective degree of saturation ($0 \le \bar{S}_w \le 1$) (Cory, 1994):

$$\bar{S}_w = \frac{\theta - \theta_r}{\theta_s - \theta_r} = \frac{S_w - S_{rw}}{1 - S_{rw}} \tag{3.15}$$

Several continuously differentiable equations have been proposed to improve the description of soil water retention near saturation. The most effective of them is the equation of Van Genuchten (1980):

$$\bar{S}_w = \left[1 + (\alpha h)^n\right]^{-m} \tag{3.16}$$

where α and n are empirical constants of the retention curve and m = 1-1/n. In a three phase system this equation can be written as (Falta, 1990):

$$\bar{S}_w = \left[1 + (\alpha\beta_{nw} h_{nw})^n\right]^{-m} \tag{3.17}$$

$$\bar{S}_n = \left[1 + (\alpha\beta_{an} h_{an})^n\right]^{-m} \tag{3.18}$$

where β_{an} is the scaling factor and may be approximated by the ratio of water surface tension to oil surface tension, β_{nw} is the scaling factor approximated by the ratio of water surface tension to oil-water interfacial tension, and $\bar{S}_n$ is effective NAPL saturation and is equal to:

$$\bar{S}_n = \frac{S_w + S_n - S_{rw}}{1 - S_{rw}} \tag{3.19}$$

Nimmo (1991) and Ross et al. (1991) found that the van Genuchten model is successful at high and medium water contents but often gives poor results at low water contents. This model does not account for the air entry value but does have an inflection point which allows better performance than the Brooks and Corey model for many soils, particularly for data near saturation (Assouline et al., 1998).

3.2 Permeability-saturation relations

The conductivity of the nonaqueous phase liquid is related to the water conductivity by

$$K_{napl} = K_{water} \frac{\nu_{water}}{\nu_{napl}} \tag{3.20}$$

where ν is the kinematic viscosity

When only part of the pore space is available for the flow of the chemical, the conductivity of the nonaqueous phase liquid must be modified by a relative permeability. Relative permeability is defined as the ratio of the phase permeability (or conductivity) at the actual volumetric content to the permeability (or conductivity) under saturated (i.e. pore filled) conditions. The concept of relative permeability accounts for the tendency for fluids to interfere with one another as they flow (Domenico and Schwartz, 1990).

$$K_w = K_{rw} K_{sw} \tag{3.21}$$

$$K_n = K_{rn} K_{sw} \left(\nu_w / \nu_n \right) \tag{3.22}$$

$$K_a = K_{ra} K_{sw} \left(\nu_w / \nu_a \right) \tag{3.23}$$

where K_p is the phase conductivity [L/T]; K_{rp} is the relative permeability of phase p; and K_{sw} is the saturated conductivity tensor for water [L/t].

Accurate in situ measurements of the unsaturated hydraulic conductivity is usually expensive and time-consuming. Using theoretical methods, which predict the conductivity from more easily measured soil fluid retention data, is an alternative to direct measurements. Most of these models are based on statistical pore-size distribution models. Childs and Collis-George(1950), Burdine (1953), Milington and Quirk (1961), and Mualem (1976) are some examples of this kind of models. Implementation of these predictive conductivity models still requires independently measured soil fluid retention data.

The use of analytical functions in soil fluid flow studies allows for a more efficient representation and comparison of hydraulic properties of different soils and soil horizons. Because of their simplicity and ease of use, they are very popular in numerical studies of unsaturated flow.

Leverett and Lewis (1941) reported the first experimental investigation of relative permeability in three-phase systems. They concluded that relative permeability to water in water-oil-gas systems was a function only of water saturation, while gas permeability was primarily dependent on gas saturation and only mildly dependent on water saturation. Oil permeability varied in a more complex manner with strong dependence on the saturation of all phases. Reible & Illangasekare (1989) have observed that the correlation for relative permeability presented by Brooks and Corey adequately predict the relative permeability of a nonaqueous phase in an initially air and residual water filled vadose zone. In terms of

fluid volumetric content (θ), this relationship can be written for the infiltration phase (which is assumed wetting with respect to air)

$$\frac{k(\theta)}{k} = k_r = \left[\frac{\theta - \theta_r}{\phi - \theta_r}\right]^{(2+3b)/b} \tag{3.24}$$

Here, b is a grain size parameter that varies from about 2.8 in sands to about 10 in clay soils (Baehr, 1984). Baehr (1984) based on the work of Brooks and Corey obtained the following expressions for relative permeabilities:

$$K_{rw} = \frac{\bar{S}_w^2\left(S_w^{\frac{2+\lambda}{\lambda}} - S_{rw}^{\frac{2+\lambda}{\lambda}}\right)}{1 - S_{rw}^{\frac{2+\lambda}{\lambda}}} \tag{3.25}$$

$$K_{rn} = \left(1 - S_{rw}\right)\left(3\bar{S}_w^{\,2} + 3\bar{S}_w S_n + S_n^2\right)\left[\frac{\left(S_w + S_n\right)^{\frac{2+\lambda}{\lambda}} - S_w^{\frac{2+\lambda}{\lambda}}}{1 - S_{rw}^{\frac{2+\lambda}{\lambda}}}\right] \tag{3.26}$$

$$K_{ra} = \left(1 - S_{rw}\right)\left[\frac{1 - \left(\bar{S}_w + S_n\right)^3}{1 - \bar{S}_w - S_n}\right]\left[\frac{1 - \left(S_w + S_n\right)^{\frac{2+\lambda}{\lambda}}}{1 - S_{rw}^{\frac{2+\lambda}{\lambda}}}\right] \tag{3.26}$$

Because of the difficulty in measuring three phase relative permeability, however, two phase data is often used to predict three phase relationships. Faust (1985) has presented a relationship for this purpose based on the work of Stone (1973)

$$K_{rn} = K^{*}_{rnw}\left[\left(\frac{K_{rnw}}{K^{*}_{rnw}} + K_{rw}\right)\left(\frac{K_{rna}}{K^{*}_{rnw}} + K_{ra}\right) - \left(K_{rw} - K_{ra}\right)\right] \quad (3.27)$$

Kool and Parker (1987) and Parker et al. (1987) have extended this approach to hysteretic relative permeability and capillary pressure relationships. Parker et al. (1987) derived the following relations from Mualem's (1976) model:

$$K_{rw} = \bar{S}_w^{1/2}\left[1 - \left(1 - \bar{S}_w^{1/m}\right)^m\right]^2 \quad (3.28)$$

$$K_{rn} = \left(\bar{S}_t - \bar{S}_w\right)^{1/2}\left[\left(1 - \bar{S}_w^{1/m}\right)^m - \left(1 - \bar{S}_t^{1/m}\right)^m\right]^2 \quad (3.29)$$

$$K_{ra} = \left(1 - \bar{S}_t\right)^{1/2}\left(1 - \bar{S}_t^{1/m}\right)^{2m} \quad (3.30)$$

where S_t and $\bar{S}_t$ are defined as follows:

$$S_t = S_w + S_n = 1 - S_a \quad (3.31)$$

$$\bar{S}_t = \frac{S_w + S_n - S_{rw}}{1 - S_{rw}} \quad (3.32)$$

For the Van Genuchten model, Al-Sheriadeh (1993) presented the following relationships:

$$K_{rw} = \bar{S}_w^{2}\left[1-\left(1-\bar{S}_w^{1/m}\right)^{m}\right]^{2} \tag{3.33}$$

$$K_{rn} = \left(1-\bar{S}_w^{2}\right)\left[1-\bar{S}_w^{1/m}\right]^{2m} \tag{3.34}$$

Also, for the Brooks-Corey model he suggested:

$$K_{rw} = \bar{S}_w^{\frac{2+3\lambda}{\lambda}} \tag{3.35}$$

$$K_{rn} = \left(1-\bar{S}_w^{2}\right)\left(1-\bar{S}_w^{\frac{2+\lambda}{\lambda}}\right) \tag{3.36}$$

Typical curves showing both Van Genuchten and Brooks-Corey constitutive relationships for a soil with $\lambda = 2$ and the same soil with Van Genuchten parameter $\alpha = 0.04$ cm^{-1} and $n = 3.41$ are shown in figure 3.1. The nonwetting fluid relative permeabilities obtained by the B&C model are lower than the ones obtained by the VG model. Therefore, the advance of the nonwetting fluid front in a domain, which is initially filled with the wetting fluid, is expected to be slower using the B&G functions than the one obtained with the VG functions. Also, there is no significant difference between the VG models developed by Parker and Al-Sheriadeh and between B&G functions used by Baehr and Al-Sheriadeh.

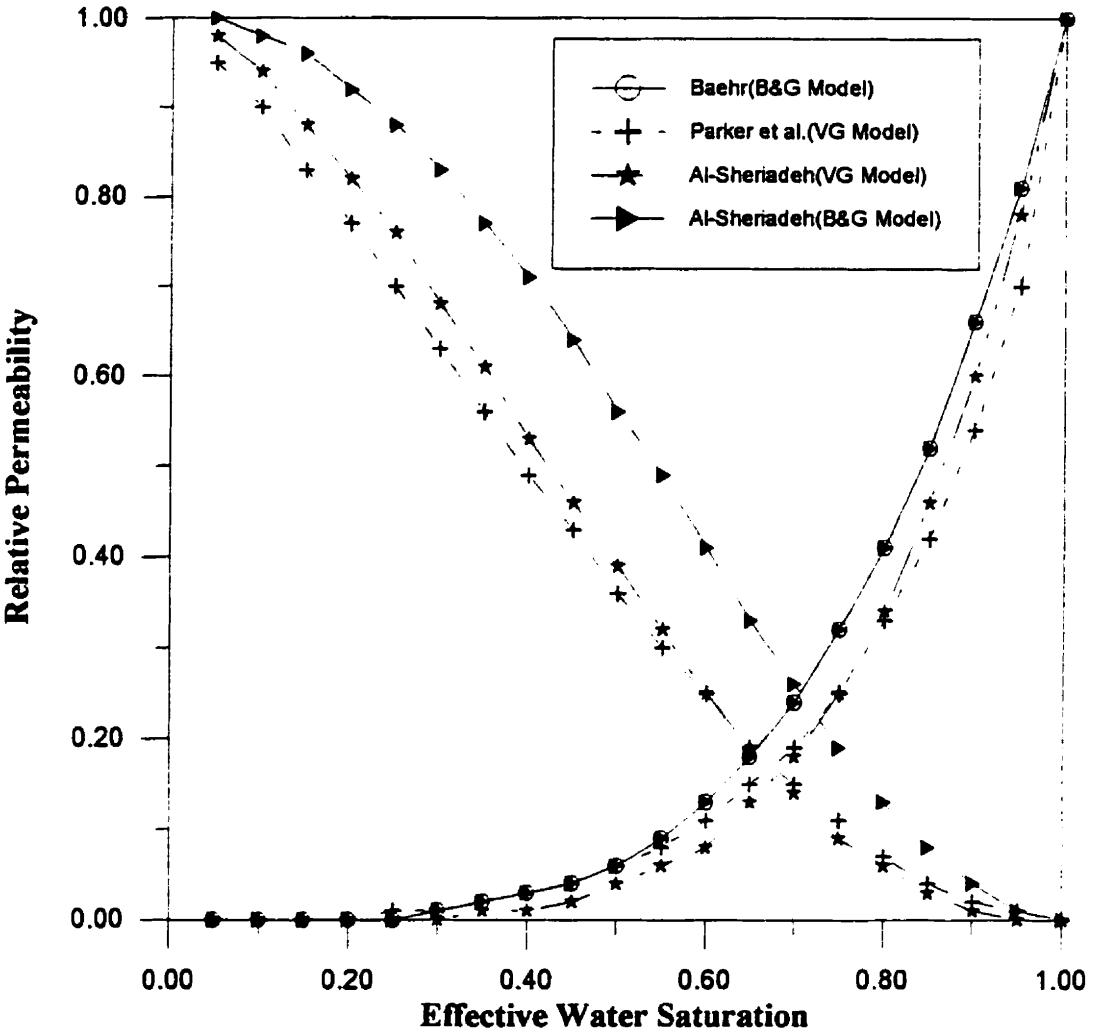

Figure (3.1) Typical curve showing the relative permeability function

3.3 Mass transfer processes

A variety of classical theories have been developed to predict mass transfer rates across interphase boundaries. The application of these theories has been limited to very simple systems where the area of contact of the phases, the geometry of the phase interfaces and the distribution of the phases within the pores are known. In chemical engineering, mass

transfer processes in separation equipment are represented by first-order expressions in which the mass transfer driving forces are proportional to the difference between equilibrium and actual concentrations.

If $\bar{c}$ represents the bulk concentration (mass/volume of porous medium) of an immobilized organic compound in the porous medium, then the rate of dissolution of the organic compound can be described by (Sleep & Sykes, 1989):

$$\left[\frac{d\bar{c}}{dt}\right]_D = \phi S_w \lambda_D (C_w - C_{wm}) \tag{3.37}$$

where λ_D is the dissolution rate constant [1/T]; C_w is the concentration [M/L^3] of organic compound in the water phase; and $C_{w\,m}$ is the equilibrium concentration of the organic compound in the water phase[M/L^3].

An expression similar to that used for dissolution rates was used for volatilization of pure organic liquid into the air phase by Sleep & Sykes (1989). The rate of decay of the residual due to volatilization is then

$$\left[\frac{d\bar{c}}{dt}\right]_V = \phi S_a \lambda_v (C_a - C_{am}) \tag{3.38}$$

where λ_V is the mass transfer coefficient for volatilization of organic compounds in the vapor phase; C_a is the concentration in the gas phase; and $C_{a\ m}$ is the equilibrium concentration in the vapor phase, determined by the vapor pressure of the pure compound.

Some dissolved contaminants may interact with the aquifer solids encountered along the flow path through adsorption, partitioning, ion exchange, and other processes. In the case of some groundwater contaminants, such as certain halogenated organic solvents, the interaction, called sorption, is often affected in a significant way by only two factors: the contaminant's hydrophobicity (its antipathy to dissolving in water) and the fraction of solid organic matter in the aquifer solids (organic carbon content). In a homogeneous aquifer therefore, sorption of a hydrophobic organic solute should theoretically be constant in space and time. If the sorptive interaction is at equilibrium and completely reversible, the solute should move at a constant average velocity equal to the groundwater average velocity, divided by the "retardation factor". Such a contaminant is said to be linearly retarded.

The simple hydrophobic sorption and retardation model may not be applicable in all cases. For example, sorption by mineral surfaces may approach or exceed that by the solid organic matter if the ratio of mineral surface areas is large. In addition, there is evidence that in some cases, sorption equilibrium may require weeks or months and thus may not always be reached in the field.

Certain organic groundwater contaminants can be biologically transformed by micro-organisms attached to solid surfaces within the aquifer. The attached bacteria obtain energy and nutrients from the groundwater flowing by and may form a biofilm as their numbers increase. Energy for growth is obtained from oxidation of organic substrates or inorganic compounds, such as hydrogen or reduced forms of iron, nitrogen, or sulfur (Mackay et al., 1985).

3.4 Gas compressibility

When gas phase is considered in simulation, the gas compressibility may be taken into account. The gas compressibility is described by the following linear relation (Katyal, 1991):

$$\rho_a = \lambda h_a + \rho_a^0 + \rho_a^c \tag{3.38}$$

where λ is the gas compressibility taken to be 1.17×10^{-6} gcm^{-4}, ρ_a^0 is the density of native soil air taken to be 1.12×10^{-3} gcm^{-3}, and ρ_a^c is the density of contaminants in the gas phase.

3.5 Summary

The presented governing equations and relationships will be used to construct a numerical solution to simulate the flow of water, NAPL, and gas in subsurface. The desired physical characteristics and limitations of this model are as follows:

- Simulating the flow of water, NAPL and air simultaneously. Also, gaseous phase and/or nonaqueous phase can be absent in simulation.
- Extended Van Genuchten relationships are chosen to define the constitutive relationships of soil.
- Heterogeneity of porous media is considered in the model.
- Water and NAPL densities are constant.
- Gas phase can be considered as compressible or incompressible fluid.
- Solute transport due to convection, dispersion and diffusion is not considered either in water or gas phase.
- Hysteresis in constitutive relationships is not taken into account.
- NAPL is a single component fluid.
- Dissolution and volatilization are only considered from NAPL to water and gas phase, respectively and it is calculated in sink term.
- The model do not consider biodegradation, decay and adsorption/desorption

CHAPTER IV

NUMERICAL ANALYSIS

The partial differential equations that were developed in chapter 2 are highly nonlinear, as both the hydraulic conductivity and fluid pressure heads depend on the saturations. Exact analytical solutions are only possible for simplified cases under a number of restrictive assumptions. On the other hand, numerical methods are powerful tools in approximating the solution to these differential equations.

Modeling becomes increasingly difficult as: 1) the number of physical processes increase; 2) the shape of the physical domain becomes more complex, and 3) boundary conditions are made more realistic. The development of the discrete algorithms that capture all the important characteristics of such physical problems becomes more difficult with this increasing complexity. Thus, it is important to have a discretization method that is sufficiently general so that it may be applied to a wide range of physical systems.

The partial differential equations may be numerically formulated using finite differences, finite elements, boundary elements, or finite volume techniques. The appropriate discretization scheme is applied to a system of nodal points that is superimposed on the soil depth-time region under consideration. With specification of the initial and boundary

conditions, the differential problem is transformed into a system of linear or nonlinear algebraic equations that may be solved by various methods.

The finite element method is a numerical method through which any continuous function may be approximated by a discrete model which consists of a set of values of the given function (eventually with its derivatives) at a finite number of preselected points in its domain, together with piecewise approximations of the function over a finite number of connected disjunct subdomains (Kazda, 1990). An important aspect of the finite element method is that we can consider an individual element to be completely disjoint from the element mesh, and approximate the unknown function locally over it, independent of the element location and of the behavior of the unknown function in neighboring elements.

The boundary element method consists of integrals in which products are present between an auxiliary function and unknown potentials and normal boundary fluxes defined on a domain boundary (Fidelibus and Lenti, 1996). The boundary is divided into small segments that are characterized by nodes. The distribution of potentials and normal boundary fluxes depend on nodal values of these quantities, collected by means of interpolation functions. Consequently, the more accurate the description of the above quantities on the boundary is, the more effective will be the solution provided by the method. The main difficulties lie in correctly defining the normal boundary flux

discontinuities; these may be encountered at the boundary corners, either when covering the external boundary of the domain, or when covering a subregion boundary.

The finite volume method is based on an integral form of the equation to be solved. This method was introduced into the field of numerical fluid dynamics by McDonald (1971) and MacCormack and Paullay (1972). Due to its integral formulation, an arbitrary mesh may be used. In addition, by the direct discretization of the integral form of the conservation laws, it may be ensured that the basic quantities such as mass, momentum and energy will also remain conserved at the discrete level.

Finite difference methods are one of the most widely used techniques for the approximate solution of the partial differential equations. The finite difference solution for partial differential equations is implemented in two stages:

- Writing a difference approximation to the differential equation.
- Using some computational technique for resolving the resulting set of algebraic equations.

The following steps are used in a finite difference method (Shashkov, 1996):

1. The continuous domain is replaced by a discrete set of nodes, called the grid.

2. Instead of a function of continuous arguments, a function of discrete arguments is considered. The value of this function is defined at the nodes of the grid or at other elements of the grid and is called the grid function.
3. The derivatives entering into the differential equations and the boundary conditions are approximated by the difference expression, thus the differential problem is transformed into a system of linear or nonlinear algebraic equations.

In this thesis, the *support-operators* method is considered to be a discrete model of the continuum physical system. Many of the standard finite difference methods and also the finite volume method are special cases of the support-operators method (Shashkov, 1996). Unlike elementary finite difference methods, the support-operators method may be used to construct finite difference schemes on grids of arbitrary geometry.

The support-operators method was chosen over the finite element method due to its relative simplicity and the fact that there was no priori reason to expect that the finite element method would provide superior results. A standard argument in support of the finite element method is noting its greater versatility in handling irregular boundaries. Such an argument is no longer valid in the present context, since an irregular mesh may also be handled by the support-operators method

4.1 Method of support-operators

There are two basic types of restrictions imposed on finite difference schemes, FDS, (Shashkov, 1996):

- The first being approximation and stability restrictions stipulating the convergence of the approximate solution as the mesh size is made small enough.
- The second type of requirement refers to the retention by the FDS of the important properties of the differential equations. The most important of these properties is conservation of FDS.

In this thesis, we demonstrate the possibility of constructing FDS by using the support-operators method. The method was developed by A. Favorskii, A. Samarskii, M. Shashkov, and V. Tishkin (Samarskii et al., 1981 and 1982) over a number of years. There are five main steps in the support-operators method of constructing conservative finite difference schemes for equations of mathematical physics (Shashkov, 1996):

1. First, the original equations are written in terms of invariant first-order differential operators such as divergence, gradient, and curl. At this point, it is important to understand which properties of the invariant differential operators imply the

conservation laws and other main features of the original system of differential equations

2. Choosing where the scalar, vector, and tensor functions are to be located in the grid. There are two possibilities. The first possibility is to use nodal discretization for the scalar function and a cell-centered discretization of the Cartesian component vector function. A second possibility is to use nodal discretization for the Cartesian component of the vector function and cell-centered discretization for the scalar functions.
3. The choice of the prime operator must be made. This operator must be one of a first order differential operator that is used in the formulation of the original equations. A difference analog for this operator is given by definition. Then all other difference operators are derived from the definition of the discretization of the prime operator and difference analogs of integral identities. In the case of nodal discretization of the vector function, it is natural to use the divergence as the prime operator. In the case of nodal discretization of the scalar function, it is natural to use the operator gradient as the prime.
4. The formulas for other difference operators, called derived operators, are derived using the expression for the prime operator and the form of difference analogs of the integral identities.
5. Finally, if we have discrete analogs of the differential operators, which form the original differential equations, then we may derive the FDS by substituting the discrete operators for differential operators.

4.2 Grid in two dimensions

For practical applications the use of a non-uniform grid is very useful and important. The simplest example of a grid in 2-D is a rectangle (Figure 4.1). Clearly, the grid consists of points formed by the intersection of lines. For identification of nodes one can use two indices i,j. The rectangle with vertices (i,j), (i+1,j), (i+1,j+1), (i,j+1) , called a cell or mesh, is used for identification of this cell. The index of the lower left vertex (i,j) is used to denote the cell by $\Omega_{i,j}$ (Figure 4.2).

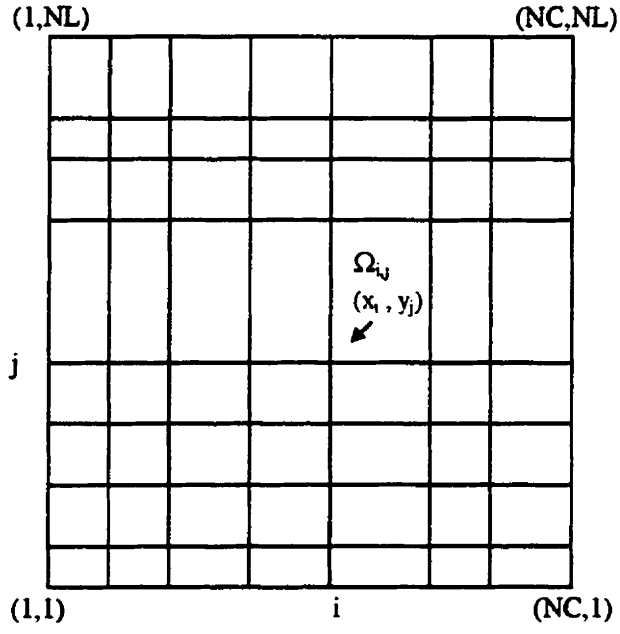

Figure (4-1) Non-uniform rectangular grid

A more complicated example of a grid in 2-D is called a logically rectangular grid (Figure 4.3). This grid has the same structure as the rectangular grid that makes it possible to use two indices for identification of the nodes.

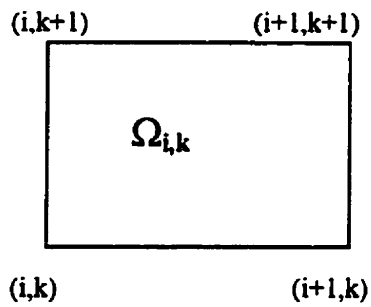

Figure (4-2) Typical mesh of rectangular grid

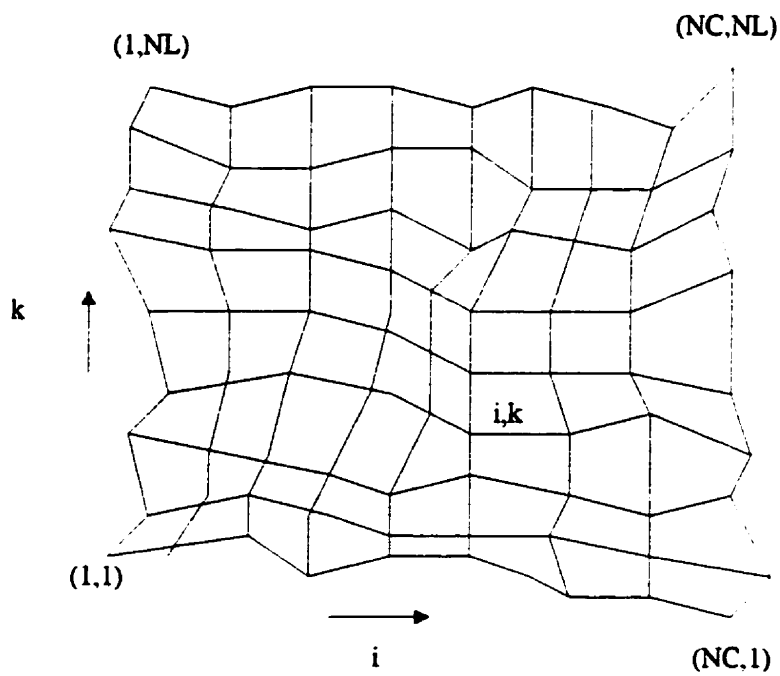

Figure (4-3) Logically rectangular grid

4.3 Difference operators

To construct the difference operator we will use Green's formula for the first partial derivative of u with respect to x and y. This theorem can be considered as defining the avarage of the gradient of a scalar u as a function of its values at the boundaries of the volume under consideration. Since for an arbitrary volume Ω

$$\int_{\Omega} \bar{\nabla} u d\Omega = \oint_{S} u d\vec{S}$$

where S is the closed boundary surface, we can define the averaged gradients as:

$$\left(\frac{\partial u}{\partial x}\right)_{\Omega} = \frac{1}{\Omega}\int_{\Omega}\frac{\partial u}{\partial x}d\Omega = \frac{1}{\Omega}\oint_{S} u\, I_x . d\vec{S}$$

and

$$\left(\frac{\partial u}{\partial y}\right)_{\Omega} = \frac{1}{\Omega}\int_{\Omega}\frac{\partial u}{\partial y}d\Omega = \frac{1}{\Omega}\oint_{S} u\, I_y . d\vec{S}$$

where I_x and I_y are unit vectors in x and y directions, respectively.

For two-dimensional control cells Ω, after partial integration, we obtain:

$$\left(\frac{\partial u}{\partial x}\right)_{\Omega} = \frac{1}{\Omega}\oint_{S} u\, dy = -\frac{1}{\Omega}\oint_{S} y\, du \qquad (4.1.1)$$

Similarly, the averaged y-derivatives are obtained from:

$$\left(\frac{\partial u}{\partial y}\right)_{\Omega} = \frac{1}{\Omega}\oint_{S} u\, dx = -\frac{1}{\Omega}\oint_{S} x\, du \qquad (4.1.2)$$

For the discrete case, the role of Ω is played by the grid cell $\Omega_{i,k}$. Therefore S is the union of sides. For approximation of the contour integral on the right-hand side of 4.1, we divide the contour integral into four integrals over each of the corresponding sides of the quadrangle $\Omega_{i,k}$ and for the approximate evaluation of each integral, we use the trapezoidal rule. As a result, one can obtain the following expression (Shashkov, 1996):

$$\left(\frac{\partial u}{\partial x}\right)_{i,k} = \frac{1}{\Omega_{i,k}}\left[\frac{u_{i+1,k}+u_{i,k}}{2}\left(z_{i+1,k}-z_{i,k}\right)+\frac{u_{i+1,k+1}+u_{i+1,k}}{2}\left(z_{i+1,k+1}-z_{i,k+1}\right)\right.$$
$$\left.+\frac{u_{i,k+1}+u_{i+1,k+1}}{2}\left(z_{i,k+1}-z_{i+1,k+1}\right)+\frac{u_{i,k}+u_{i,k+1}}{2}\left(z_{i,k}-z_{i,k+1}\right)\right] \tag{4.2}$$

Collecting the coefficients, we may transform the formula to a more simple form:

$$\left(\frac{\partial u}{\partial x}\right)_{i,k} = \frac{1}{2\Omega_{i,k}}\left[\left(u_{i+1,k+1}-u_{i,k}\right)\left(z_{i,k+1}-z_{i+1,k}\right)\right.$$
$$\left.-\left(u_{i,k+1}-u_{i+1,k}\right)\left(z_{i+1,k+1}-z_{i,k}\right)\right] \tag{4.3}$$

In a similar way we can derive the formula for operator $\partial u/\partial z$:

$$\left(\frac{\partial u}{\partial z}\right)_{i,k} = -\frac{1}{2\Omega_{i,k}}\left[\left(u_{i+1,k+1}-u_{i,k}\right)\left(x_{i,k+1}-x_{i+1,k}\right)\right.$$
$$\left.-\left(u_{i,k+1}-u_{i+1,k}\right)\left(x_{i+1,k+1}-x_{i,k}\right)\right] \tag{4.4}$$

For the second order derivative $\partial(Ax)/\partial x$ in which Ax is the operator $\partial/\partial x$ we can write:

$$\left(\frac{\partial Ax}{\partial x}\right)_{i,k} = -\left(\frac{z_{i-1,k} - z_{i,k-1}}{2} Ax_{i-1,k-1} - \frac{z_{i,k+1} - z_{i+1,k}}{2} Ax_{i,k} + \frac{z_{i+1,k} - z_{i,k-1}}{2} Ax_{i,k-1} - \frac{z_{i,k+1} - z_{i-1,k}}{2} Ax_{i-1,k}\right) / VN_{i,k} \tag{4.5}$$

Similarly in the z direction we get:

$$\left(\frac{\partial Az}{\partial z}\right)_{i,k} = -\left(\frac{x_{i-1,k} - x_{i,k-1}}{2} Az_{i-1,k-1} - \frac{x_{i,k+1} - x_{i+1,k}}{2} Az_{i,k} + \frac{x_{i+1,k} - x_{i,k-1}}{2} Az_{i,k-1} - \frac{x_{i,k+1} - x_{i-1,k}}{2} Az_{i-1,k}\right) / VN_{i,k} \tag{4.6}$$

where

$$VN_{i,k} = \frac{1}{4}\left(\Omega_{i,k} + \Omega_{i-1,k} + \Omega_{i-1,k-1} + \Omega_{i,k-1}\right) \tag{4.7}$$

The stencils for these operators are shown in figure 4.4. Applying these operators to the right hand side of equation 3.7 which is as follows:

$$\phi \frac{\partial S_w}{\partial t} = \frac{\partial}{\partial x}\left[Kw_{ij}\left(\frac{\partial h_w}{\partial x}\right)\right] + \frac{\partial}{\partial z}\left[Kw_{ij}\left(\frac{\partial h_w}{\partial z} + 1\right)\right] + \frac{R_w}{\rho_w}$$

we obtain:

$$
\left\{\left[\frac{z_{i-1,k}-z_{i,k-1}}{2}*\left(Kxx_{i-1,k-1}\left(\left(hw_{i,k}-hw_{i-1,k-1}\right)\left(z_{i-1,k}-z_{i,k-1}\right)-\right.\right.\right.\right.
$$

$$
\left.\left(hw_{i-1,k}-hw_{i,k-1}\right)\left(z_{i,k}-z_{i-1,k-1}\right)\right)/\left(2\Omega_{i-1,k-1}\right)-
$$

$$
Kxz_{i-1,k-1}\left(\left(hw_{i,k}-hw_{i-1,k-1}\right)\left(x_{i-1,k}-x_{i,k-1}\right)-\right.
$$

$$
\left.\left.\left(hw_{i-1,k}-hw_{i,k-1}\right)\left(x_{i,k}-x_{i-1,k-1}\right)\right)/\left(2\Omega_{i-1,k-1}\right)\right)+
$$

$$
\frac{z_{i,k+1}-z_{i+1,k}}{2}*\left(Kxx_{i,k}\left(\left(hw_{i+1,k+1}-hw_{i,k}\right)\left(z_{i,k+1}-z_{i+1,k}\right)-\right.\right.
$$

$$
\left.\left(hw_{i,k+1}-hw_{i+1,k}\right)\left(z_{i+1,k+1}-z_{i,k}\right)\right)/\left(2\Omega_{i,k}\right)-
$$

$$
Kxz_{i,k}\left(\left(hw_{i+1,k+1}-hw_{i,k}\right)\left(x_{i,k+1}-x_{i+1,k}\right)-\right.
$$

$$
\left.\left.\left(hw_{i,k+1}-hw_{i+1,k}\right)\left(x_{i+1,k+1}-x_{i,k}\right)\right)/\left(2\Omega_{i,k}\right)\right)+
$$

$$
\frac{z_{i+1,k}-z_{i,k-1}}{2}*\left(Kxx_{i,k-1}\left(\left(hw_{i+1,k}-hw_{i,k-1}\right)\left(z_{i,k}-z_{i+1,k-1}\right)-\right.\right.
$$

$$
\left.\left(hw_{i,k}-hw_{i+1,k-1}\right)\left(z_{i+1,k}-z_{i,k-1}\right)\right)/\left(2\Omega_{i,k-1}\right)-
$$

$$
Kxz_{i,k-1}\left(\left(hw_{i+1,k}-hw_{i,k-1}\right)\left(x_{i,k}-x_{i+1,k-1}\right)-\right.
$$

$$
\left.\left.\left(hw_{i,k}-hw_{i+1,k-1}\right)\left(x_{i+1,k}-x_{i,k-1}\right)\right)/\left(2\Omega_{i,k-1}\right)\right)+
$$

$$
\frac{z_{i,k+1}-z_{i-1,k}}{2}*\left(Kxx_{i-1,k}\left(\left(hw_{i,k+1}-hw_{i-1,k}\right)\left(z_{i-1,k+1}-z_{i,k}\right)-\right.\right.
$$

$$
\left.\left(hw_{i-1,k+1}-hw_{i,k}\right)\left(z_{i,k+1}-z_{i-1,k}\right)\right)/\left(2\Omega_{i-1,k}\right)-
$$

$$
Kxz_{i-1,k}\left(\left(hw_{i,k+1}-hw_{i-1,k}\right)\left(x_{i-1,k+1}-x_{i,k}\right)-\right.
$$

$$
\left.\left.\left.\left(hw_{i-1,k+1}-hw_{i,k}\right)\left(x_{i,k+1}-x_{i-1,k}\right)\right)/\left(2\Omega_{i-1,k}\right)\right)\right]-
$$

$$
\begin{aligned}
&\Bigg[\frac{x_{i-1,k}-x_{i,k-1}}{2}*\Big(Kxz_{i-1,k-1}\Big(\big(hw_{i,k}-hw_{i-1,k-1}\big)\big(z_{i-1,k}-z_{i,k-1}\big)-\\
&\quad\big(hw_{i-1,k}-hw_{i,k-1}\big)\big(z_{i,k}-z_{i-1,k-1}\big)\Big)/\big(2\Omega_{i-1,k-1}\big)-\\
&\quad Kzz_{i-1,k-1}\Big(\big(hw_{i,k}-hw_{i-1,k-1}\big)\big(x_{i-1,k}-x_{i,k-1}\big)-\\
&\quad\big(hw_{i-1,k}-hw_{i,k-1}\big)\big(x_{i,k}-x_{i-1,k-1}\big)\Big)/\big(2\Omega_{i-1,k-1}\big)\Big)+\\
&\frac{x_{i,k+1}-x_{i+1,k}}{2}*\Big(Kxz_{i,k}\Big(\big(hw_{i+1,k+1}-hw_{i,k}\big)\big(z_{i,k+1}-z_{i+1,k}\big)-\\
&\quad\big(hw_{i,k+1}-hw_{i+1,k}\big)\big(z_{i+1,k+1}-z_{i,k}\big)\Big)/\big(2\Omega_{i,k}\big)-\\
&\quad Kzz_{i,k}\Big(\big(hw_{i+1,k+1}-hw_{i,k}\big)\big(z_{i,k+1}-z_{i+1,k}\big)-\\
&\quad\big(hw_{i,k+1}-hw_{i+1,k}\big)\big(z_{i+1,k+1}-z_{i,k}\big)\Big)/\big(2\Omega_{i,k}\big)\Big)+\\
&\frac{x_{i+1,k}-x_{i,k-1}}{2}*\Big(Kxz_{i,k-1}\Big(\big(hw_{i+1,k}-hw_{i,k-1}\big)\big(z_{i,k}-z_{i+1,k-1}\big)-\\
&\quad\big(hw_{i,k}-hw_{i+1,k-1}\big)\big(z_{i+1,k}-z_{i,k-1}\big)\Big)/\big(2\Omega_{i,k-1}\big)-\\
&\quad Kzz_{i,k-1}\Big(\big(hw_{i+1,k}-hw_{i,k-1}\big)\big(x_{i,k}-x_{i+1,k-1}\big)-\\
&\quad\big(hw_{i,k}-hw_{i+1,k-1}\big)\big(x_{i+1,k}-x_{i,k-1}\big)\Big)/\big(2\Omega_{i,k-1}\big)\Big)+\\
&\frac{x_{i,k+1}-x_{i-1,k}}{2}*\Big(Kxz_{i-1,k}\Big(\big(hw_{i,k+1}-hw_{i-1,k}\big)\big(z_{i-1,k+1}-z_{i,k}\big)-\\
&\quad\big(hw_{i-1,k+1}-hw_{i,k}\big)\big(z_{i,k+1}-z_{i-1,k}\big)\Big)/\big(2\Omega_{i-1,k}\big)-\\
&\quad Kzz_{i-1,k}\Big(\big(hw_{i,k+1}-hw_{i-1,k}\big)\big(x_{i-1,k+1}-x_{i,k}\big)-\\
&\quad\big(hw_{i-1,k+1}-hw_{i,k}\big)\big(x_{i,k+1}-x_{i-1,k}\big)\Big)\Big)\Big\}/VN_{i,k}+\\
&\quad\Big[\big(Kzz_{i+1,k+1}-Kzz_{i,k}\big)\big(x_{i,k+1}-x_{i+1,k}\big)-\\
&\quad\big(Kzz_{i,k+1}-Kzz_{i+1,k}\big)\big(x_{i+1,k+1}-x_{i,k}\big)\Big]/\big(2\Omega_{i,k}\big)
\end{aligned}
\tag{4.8}
$$

Similar discretization relationships may be written for equations 3.8 and 3.9.

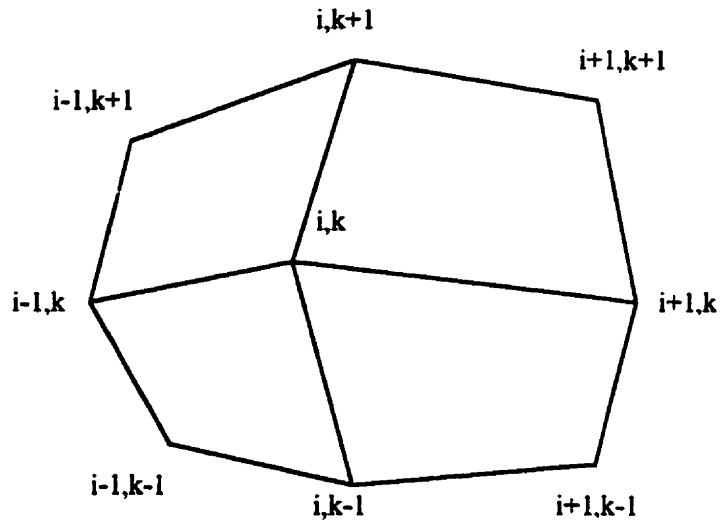

Figure (4.4) Stencil for operators ∂Ax/∂x and ∂Az/∂z

In order to discretize the left hand side of the equation (3.7), we introduce a grid in time as follows:

$$t_0 = 0 \, , \, t_{n+1} = t_n + \Delta t \, , \, n=0,1,\ldots$$

where Δt is called the time step. Methods with a variable time step are usually used when the coefficients of the differential equations have some singularity as the functions of time. To approximate a time derivative, we can use the formula

$$\left(\frac{\partial S}{\partial t}\right)\Big|_{(x_i,t_n)} \approx \frac{S_i^{n+1} - S_i^n}{\Delta t}$$

This approximation has a first-order truncation error for $t=t_n$, because

$$\frac{S_i^{n+1} - S_i^n}{\Delta t_n} = \frac{\partial S}{\partial t}\Big|_{(i,n)} + \frac{\Delta t_n}{2}\frac{\partial^2 S}{\partial t^2}\Big|_{(i,n)} + O\left((\Delta t_n)^2\right)$$

It is also easy to see that for $t = t_{n+1/2} = 0.5(t_n+t_{n+1})$, we have a second-order truncation error

$$\frac{S_i^{n+1} - S_i^n}{\Delta t_n} = \left.\frac{\partial S}{\partial t}\right|_{(i,n+1/2)} + O\left((\Delta t_n)^2\right)$$

The simplest finite difference scheme for the unsteady problem is an explicit scheme. It is called explicit because one can compute values at the new n+1 time level using an explicit formula. The right hand side of equation (3.7) only contains values at the old time step so the left hand side may be calculated by marching forward in time. The disadvantage of the explicit method is its limitation on time step size for numerical stability. This restriction results in a prohibitive cost to improve spatial accuracy because the maximum possible time step needs to be reduced to a very small value. Consequently, this method is not recommended for general transient problems.

When the values of unknowns at the right hand side of equation (3.7) are considered at the new time level, t_{n+1} , we obtain the implicit scheme. A system of algebraic equations must be solved at each time level. The time marching procedure starts with given initial values for heads of water, NAPL, and air. These initial conditions can have an important effect on the solution especially at the start of the computation. The implicit scheme is unconditionally stable for any size of time step. Since the accuracy of the scheme is only first-order in time, small time steps are still needed to ensure accuracy. The implicit method is recommended for general purpose transient calculations because of its robustness and unconditional stability.

A variable time step is used to increase the efficiency of the solution based on the following relationships:

$$\Delta t_n = \beta \Delta t_{n+1}$$

where β is a coefficient greater than 1 and will cause the increasing of Δt in each new time level. The maximum possible time step will ensure that it will not reach an undesirable value.

4.4 Boundary conditions

Mathematical models consist of the governing equations, boundary conditions, and initial conditions. Boundary conditions are mathematical statements specifying the dependent variable (head) or the derivative of the dependent variable (flux) at the boundaries of the problem domain.

Correct selection of boundary conditions is a critical step in model design. In steady-state simulations, the boundaries largely determine the flow pattern. Boundary conditions influence transient solutions when the effects of the transient stresses reach the boundary. In this case, the boundaries must be selected so that the simulated effect is realistic. According to Franke et al. (1987), setting boundary conditions is the step in model design that is most subject to serious error.

Let G be the bounded region on the plane $x=(x_1,x_2)$ and Γ the boundary of G. To find the continuity solution in the closed domain $G+\Gamma$, which satisfies one of the following boundary conditions:

Type 1. Specified head boundaries (Dirichlet conditions) for which head is given.

$$u=\mu_1(x), \qquad x\in\Gamma,$$

Type 2. Specified flow boundaries (Neumann conditions) for which the derivative of head (flux) across the boundary is given. A no-flow boundary condition is set by specifying flux to be zero.

$$\frac{\partial u}{\partial \vec{n}}=\mu_2(x) \quad x\in\Gamma,$$

Where $\frac{\partial u}{\partial \vec{n}}$ is the directional derivative in direction $\vec{n}$, and $\vec{n}$ is the outward unit normal to Γ, means that flux is given on the boundary.

Type 3. Head-dependent flow boundaries (Robin or mixed boundary conditions) for which flux across the boundary is calculated given a boundary head value. This type of

boundary condition is sometimes called a mixed boundary condition because it relates boundary heads to boundary flows.

$$K\frac{\partial u}{\partial \vec{n}} + \alpha(u) = \gamma \qquad x \in \Gamma,$$

From the physical viewpoint, this condition means that there is an inflow/outflow discharge because of head difference.

In order to apply Robin boundary condition to the model, we have to modify the equation (3.8) for nodes on boundaries. For example on the bottom boundary and in the left corner we have:

For i=2,...,M-1 :

$$
\begin{aligned}
&-\left\{\left[\frac{z_{i,2}-z_{i+1,1}}{2}*\right.\right.\\
&\left(Kxx_{i,1}\left(\left(hw_{i+1,2}-hw_{i,1}\right)\left(z_{i,2}-z_{i+1,2}\right)-\left(hw_{i,2}-hw_{i+1,1}\right)\left(z_{i+1,2}-z_{i,1}\right)\right)/\left(2\Omega_{i,1}\right)-\right.\\
&Kxz_{i,1}\left(\left(hw_{i+1,2}-hw_{i,1}\right)\left(x_{i,2}-x_{i+1,1}\right)-\left(hw_{i,2}-hw_{i+1,1}\right)\left(x_{i+1,2}-x_{i,1}\right)\right)/\left(2\Omega_{i,1}\right)\Big)-\\
&\frac{z_{i,2}-z_{i=1,1}}{2}*\\
&\left(Kxx_{i-1,1}\left(\left(hw_{i,2}-hw_{i-1,1}\right)\left(z_{i-1,2}-z_{i,1}\right)-\left(hw_{i-1,2}-hw_{i,1}\right)\left(z_{i,2}-z_{i-1,1}\right)\right)/\left(2\Omega_{i-1,1}\right)-\right.\\
&Kxz_{i-1,1}\left(\left(hw_{i,2}-hw_{i-1,1}\right)\left(x_{i-1,2}-x_{i,1}\right)-\left(hw_{i-1,2}-hw_{i,1}\right)\left(x_{i,2}-x_{i-1,1}\right)\right)/\left(2\Omega_{i-1,1}\right)\Big)\Big]-\\
&\left[\frac{x_{i,2}-x_{i+1,1}}{2}*\right.\\
&\left(Kxz_{i,1}\left(\left(hw_{i+1,2}-hw_{i,1}\right)\left(z_{i,2}-z_{i+1,2}\right)-\left(hw_{i,2}-hw_{i+1,1}\right)\left(z_{i+1,2}-z_{i,1}\right)\right)/\left(2\Omega_{i,1}\right)-\right.\\
&Kzz_{i,1}\left(\left(hw_{i+1,2}-hw_{i,1}\right)\left(x_{i,2}-x_{i+1,1}\right)-\left(hw_{i,2}-hw_{i+1,1}\right)\left(x_{i+1,2}-x_{i,1}\right)\right)/\left(2\Omega_{i,1}\right)\Big)-\\
&\frac{x_{i,2}-x_{i=1,1}}{2}*\\
&\left(Kxz_{i-1,1}\left(\left(hw_{i,2}-hw_{i-1,1}\right)\left(z_{i-1,2}-z_{i,1}\right)-\left(hw_{i-1,2}-hw_{i,1}\right)\left(z_{i,2}-z_{i-1,1}\right)\right)/\left(2\Omega_{i-1,1}\right)-\right.\\
&Kxz_{i-1,1}\left(\left(hw_{i,2}-hw_{i-1,1}\right)\left(x_{i-1,2}-x_{i,1}\right)-\left(hw_{i-1,2}-hw_{i,1}\right)\left(x_{i,2}-x_{i-1,1}\right)\right)/\left(2\Omega_{i-1,1}\right)\Big)\Big\}/l_{i,1}+\\
&\alpha_{i,1}hw_{i,1}=\gamma_{i,1}
\end{aligned}
\tag{4.9}
$$

For the corner node (1,1) we get

$$
\begin{aligned}
&\left\{\left[\frac{z_{1,2}-z_{2,1}}{2}*\right.\right.\\
&Kxx_{1,1}\left(\left(hw_{2,2}--hw_{1,1}\right)\left(z_{1,2}-z_{2,1}\right)-\left(hw_{1,2}-hw_{2,1}\right)\left(z_{2,2}-z_{1,1}\right)\right)/\left(2\Omega_{1,1}\right)-\\
&Kxz_{1,1}\left(\left(hw_{2,2}--hw_{1,1}\right)\left(x_{1,2}-x_{2,1}\right)-\left(hw_{1,2}-hw_{2,1}\right)\left(x_{2,2}-x_{1,1}\right)\right)/\left(2\Omega_{1,1}\right)\Big)\Big]-\\
&\left[\frac{x_{1,2}-x_{2,1}}{2}*\right.\\
&Kxz_{1,1}\left(\left(hw_{2,2}--hw_{1,1}\right)\left(z_{1,2}-z_{2,1}\right)-\left(hw_{1,2}-hw_{2,1}\right)\left(z_{2,2}-z_{1,1}\right)\right)/\left(2\Omega_{1,1}\right)-\\
&Kzz_{1,1}\left(\left(hw_{2,2}--hw_{1,1}\right)\left(x_{1,2}-x_{2,1}\right)-\left(hw_{1,2}-hw_{2,1}\right)\left(x_{2,2}-x_{1,1}\right)\right)/\left(2\Omega_{1,1}\right)\Big)\Big\}/l_{1,1}+\\
&\alpha_{1,1}hw_{1,1}=\gamma_{1,1}
\end{aligned}
\tag{4.10}
$$

4.5 Method of solution

The Newton-Raphson method for solving scalar algebraic and transcendental equations is well known for its simplicity and effectiveness. This method provides a powerful tool for the theoretical as well as the numerical investigation of nonlinear operator equations. The Newton-Raphson method is often recommended for highly nonlinear problems for which the Picard scheme may fail or provides slow convergence (Huyakorn and Pinder, 1983).

A system of non-linear equations may be written as follows:

$$\begin{aligned} &f_1(x_1, x_2, \ldots, x_m) = 0, \\ &f_2(x_1, x_2, \ldots, x_m) = 0, \\ &\ldots\ldots\ldots\ldots\ldots\ldots\ldots \\ &\ldots\ldots\ldots\ldots\ldots\ldots\ldots \\ &f_m(x_1, x_2, \ldots, x_m) = 0, \end{aligned} \tag{4.9}$$

where f_i , i=1,2,...,m is a function of variables x_1 , x_2 , ..., x_m . Suppose that the values $x_i^{(k)}$ are known at some iteration number k. Then by using the Taylor series for functions f_i (x_1 , x_2 , ..., x_m) at point $x^{(k)} = (x_1^{(k)}, x_2^{(k)}, \ldots, x_m^{(k)})^T$ it can be written:

$$\sum_{j=1}^{m}\left(x_j^{(k+1)} - x_j^{(k)}\right)\frac{\partial f_i\left(x^{(k)}\right)}{\partial x_j} + f_i\left(x^{(k)}\right) = 0, \quad i = 1,2,\ldots,m. \tag{4.10}$$

If we use notations

$$F(x) = \left(f_1(x), f_2(x), \ldots, f_m(x)\right)^T$$

and

$$F'(x) = \begin{bmatrix} \frac{\partial f_1(x)}{\partial x_1} & \frac{\partial f_1(x)}{\partial x_2} & \cdots & \frac{\partial f_1(x)}{\partial x_m} \\ \frac{\partial f_2(x)}{\partial x_1} & \frac{\partial f_2(x)}{\partial x_2} & \cdots & \frac{\partial f_2(x)}{\partial x_m} \\ \cdots & \cdots & \cdots & \cdots \\ \frac{\partial f_1(x)}{\partial x_1} & \frac{\partial f_1(x)}{\partial x_2} & \cdots & \frac{\partial f_1(x)}{\partial x_m} \end{bmatrix}$$

then the matrix form of 4.10 will be as follows:

$$F'\left(x^{(k)}\right)\left(x^{(k+1)} - x^{(k)}\right) + F\left(x^{(k)}\right) = 0 \qquad (4.11)$$

To determine $x^{(k+1)}$ we must solve the system of linear equations expressed by (4.11) or, in other words, we must invert the matrix $F'(x^{(k)})$ at each iteration. The components of the Jacobian matrix, F'(x), have been determined analytically and expressed in Appendix I at the end of this dissertation.

For each grid there are (NPHASE) unknowns, where NPHASE is the number of phases considered in the simulation. The unknowns are the hydraulic head for the water, h_w , for

the NAPL, h_n , and for the air, h_a . The non-linearities inherent in the above equations are the relative permeability and saturation. The equations are coupled because in all of them more than one primary variable appears concurrently. Required input data for flow analysis consists of initial conditions, soil hydraulic properties, fluid properties, time integration parameters, boundary condition data and mesh geometry. The solution algorithm is outlined in Table 4.1.

Table (4.1) Solution algorithm

1)	Provide initial guesses h_w , h_n , and h_a for each node
2)	Substitute the guesses into the discretized equations and find $F(x^{(k)})$
3)	Evaluate the terms in the Jacobian matrix
4)	Solve for Δh_w , Δh_n , Δh_a
5)	Update guesses for primary variables:
	$h_w^{\,1} = h_w^{\,0} + \Delta h_w$, $h_n^{\,1} = h_n^{\,0} + \Delta h_n$, $h_a^{\,1} = h_a^{\,0} + \Delta h_a$
6)	if $\Delta h_w > \varepsilon_w$ or $\Delta h_n > \varepsilon_n$ or $\Delta h_a > \varepsilon_a$ then go to step 2

The convergence criterion for phase p is as follows (Katyal, 1991):

$$\left|h_p^{n+1} - h_p^n\right| \le e_r \left|h_p^n\right| + e_a$$

where e_r is the relative convergence error and e_a is the absolute convergence error for phase p.

To avoid numerical difficulties in cases where extreme changes in the pressure heads occur as in sharp fronts or at the line of contact between different soils in a heterogeneous medium, all the derivatives in the Jacobian matrix were evaluated analytically rather than numerically. As is evident, the solution vector is posed in terms of pressure head changes over the current time step rather than the unknown heads themselves so as to reduce round off errors when the variation in the magnitude of the pressure heads is very large (Huyakorn and Pinder, 1993). This can be understood easily by noting that pressure head at low wetting saturations can be very large, while the change in the pressure head is not. Another problem can occur regarding phase saturation relationships and their derivatives with respect to pressure as it appears in the Jacobian matrix. These relationships produce values which are either very large or too small in the solution matrices in the limit when the saturation approaches either zero or one. At zero saturation, the terms K_{rw}, $\partial K_{rw}/\partial h$, $\partial K_m/\partial h$ and $\partial S_w/\partial h$ become too small which produce insignificant values at the diagonal of the linear system for the nodes that correspond to the full saturation of the non-wetting phase. Similarly, when the saturation is unity, the terms K_m, $\partial K_{rw}/\partial h$, $\partial K_m/\partial h$ and $\partial S_n/\partial h$ become too small. In order to circumvent these problems the effective saturations were allowed to vary only between the limits 1×10^{-6} and $1.0-1\times10^{-6}$ in the solution algorithm (Al-Sheriadeh, 1993).

A comparison of the model capabilities with similar models are shown in Table (4.2)

Table (4.2) Comparison of capabilities of different numerical models for multi-phase flow.

	Numerical Scheme	No. of Phases	No. of Dimen-sions	Transport Model in Gas	Transport Model in water	Hysteresis	Gas Compressibility	Irregular Boundaries
Faust (1985)	FD*	2	2	No	No	No	No	No
Osborne&Sykes (1986)	FE**	2	2	No	No	No	No	No
Katyal (1991)	FE	3	2	No	Yes	No	Yes	No
Al-Sheriadeh (1993)	FE	2	2	No	No.	No	No	No
Van Geel & Sykes (1994)	FD	2	2	No	No	Yes	No	No
Guaranccia & Pinder (1997)	FE	3	2&3	Yes	Yes	Yes	Yes	No
Mohammadi & Kahawita	MS***	3	2	No	No	No	Yes	Yes

* Finite Difference
** Finite Element
*** Method of Support-Operators

CHAPTER V

MODEL VALIDATION AND VERIFICATION

In general, models must be validated in order to establish not only their credibility but also their limitations (Waddill and Parker, 1997). In order to validate a model, Van der Heijde et al. (1984) recommend a three level testing procedure. Level 1 involves verification of the model's computer code. During level 2, the model is tested under a variety of hypothetical conditions, and model performance may be evaluated through code inter-comparison. Level 3 involves validating the model against independent field or laboratory data. In the absence of adequate field or laboratory data sets, validation of models may be limited to level 1 and 2 testing (Beljin and van der Heijde, 1989). Since it is impossible to test all conditions for which a model may be applied, model validity cannot be established absolutely. Instead, each validation scenario confirms a degree of accuracy that applies to the specific conditions of the scenario.

To demonstrate that the numerical model developed here converges to a correct solution, verification should be carried out against exact analytical solutions. However, in general, analytical solutions exist only for a range of restricted problems with many terms in the original equations being either simplified or totally neglected.. Furthermore, the solutions are obtained for very simple boundary conditions. It is not possible to have an analytical solution that can handle the non-linearities in multiphase flow problems. It is only possible

to compare the results given by the model against solutions for various linearized forms of the problem. Therefore, the numerical model cannot be verified in the classical sense. There are few analytical solutions available for water and NAPL flow in variably saturated soils. Two analytical solutions for water flow and one for NAPL flow are used here.

5.1 Analytical solutions

The first example involves a one-dimensional steady vertical water flow in a 6 meter soil profile, consisting of 2 m of fine sand, overlying 2 m of silty clay loam, overlying another 2 m of fine sand. Table (5.1) shows the hydraulic parameters for these two soils. A flux of 1.6×10^{-4} cm/s and a pressure head of 0 cm were specified for the upper and lower boundaries of the model domain, respectively. The analytical solution developed by Rockhold and Fayer (1997) is based on the exact solution for the Gardner (1958) exponential hydraulic conductivity function. They extended the exact solution for use with arbitrary hydraulic property functions, or measured K(h) data, by approximating lnK(h) with piecewise-linear curve segments and integrating analytically, segment by segment. The domain was discretized into 60 cells with 10 cm height. Figure (5.1) shows the water pressure head distribution for example 1. In general, there is a good agreement between analytical and numerical solutions. The whole simulation was done in 6 minutes with a PC-Pentium 200 processor.

Table (5.1) Soil hydraulic parameters for Examples 1 and 2 (After Rockhold et al., 1997)

Material	K_s cm/s	$\propto$ cm^{-1}	n	θ_s	θ_r
Berino loamy fine sand	6.26×10^{-3}	0.0208	2.2390	0.3658	0.0286
Glendale silty caly loam	1.52×10^{-4}	0.0104	1.3954	0.4686	0.1060

In the second example, a 5.85-m-deep lysimeter, packed with alternating, 20-cm-thick layers of silty clay loam and loamy fine sand , was irrigated with water at a rate of 2.38×10^{-5} cm/s (Wierenga et al., 1988). Water content and pressure head were monitored in the lysimeter during the experiment using a neutron probe and tensiometers. The steady state pressure head distribution in the lysimeter was simulated using the analytical solution technique by Rockhold et al. (1997). Soil parameters are the same as those in test problem 1 (Table 5.1) except α which is α= 0.028 for this test. A flux of 2.38×10^{-5} cm/s and a pressure head of -200 cm were the upper and lower boundaries of the flow domain, respectively. The domain was divided into 58 one-dimensional cells. The height of the first cell at the bottom was 25 cm and then for the remaining cells it was 10 cm. Observed data, the analytical solution and the numerical results for pressure head and water content are compared in Figure (5.2) and (5.3). Given the uncertainties in the model parameters and potential measurement errors, the overall agreement between the observed data, the analytical results, and the simulated pressure head and water content distributions for this example is considered to be good.

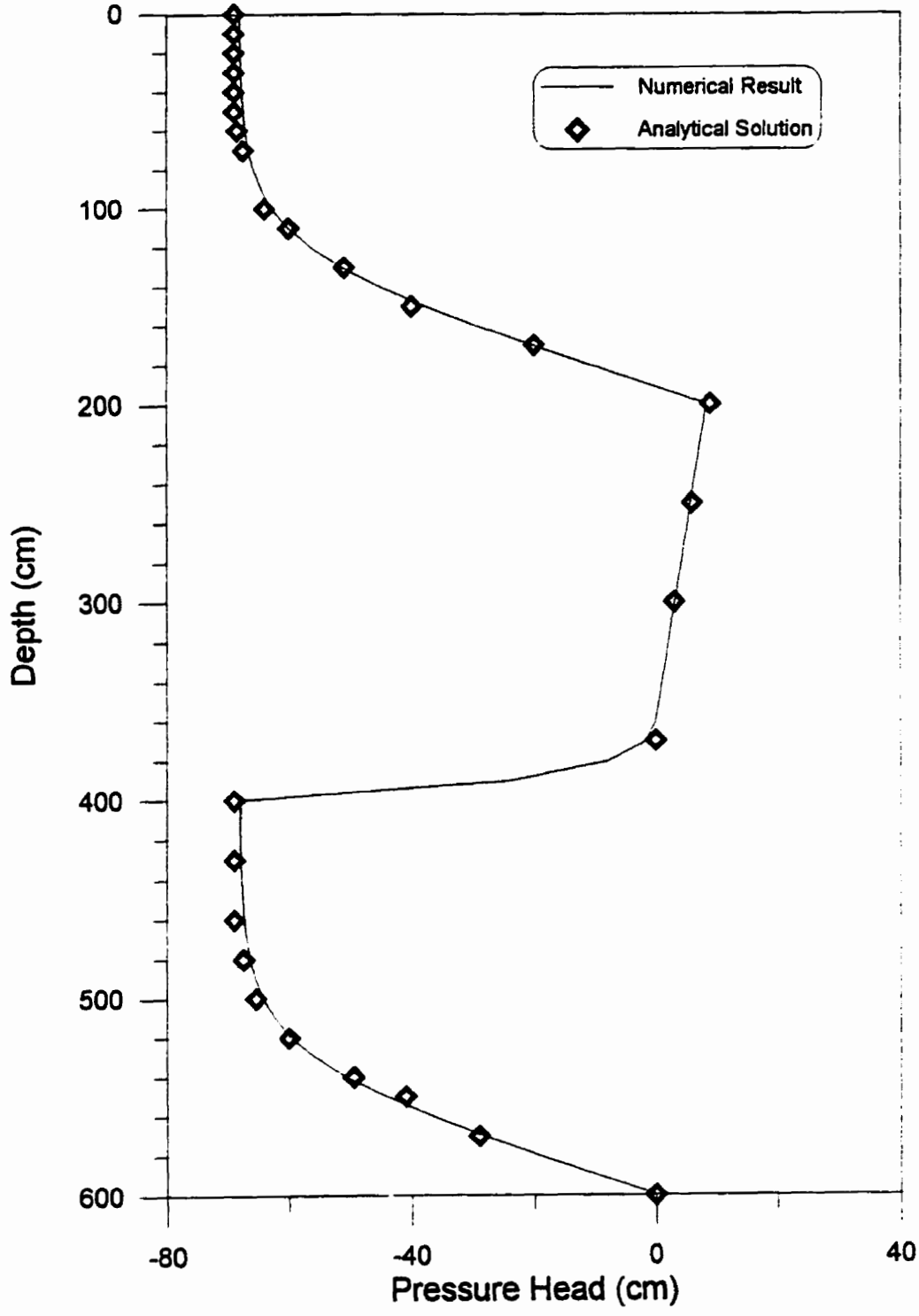

Figure (5.1) Water Pressure Head Distribution

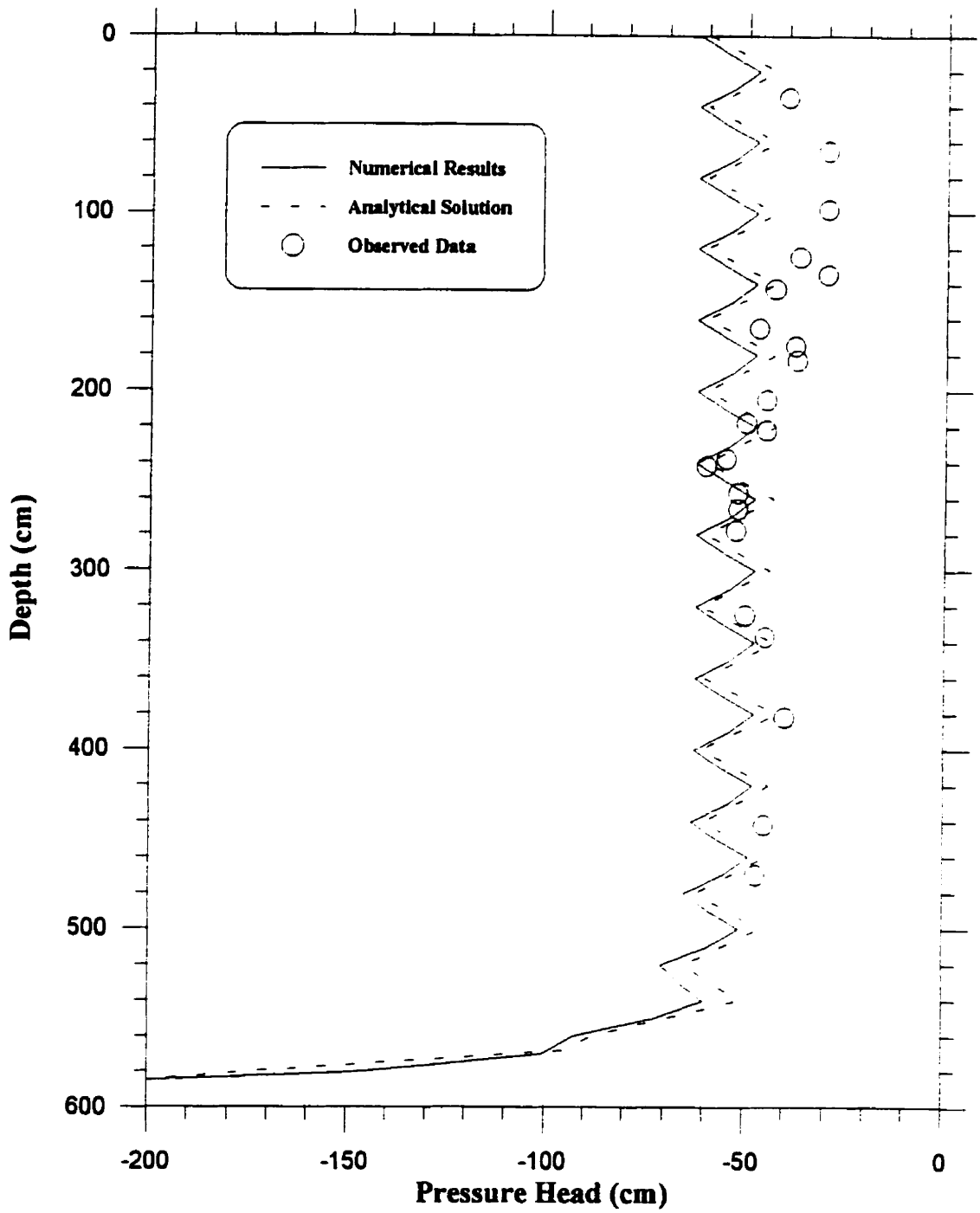

Figure (5.2) Soil-Water Head Distribution

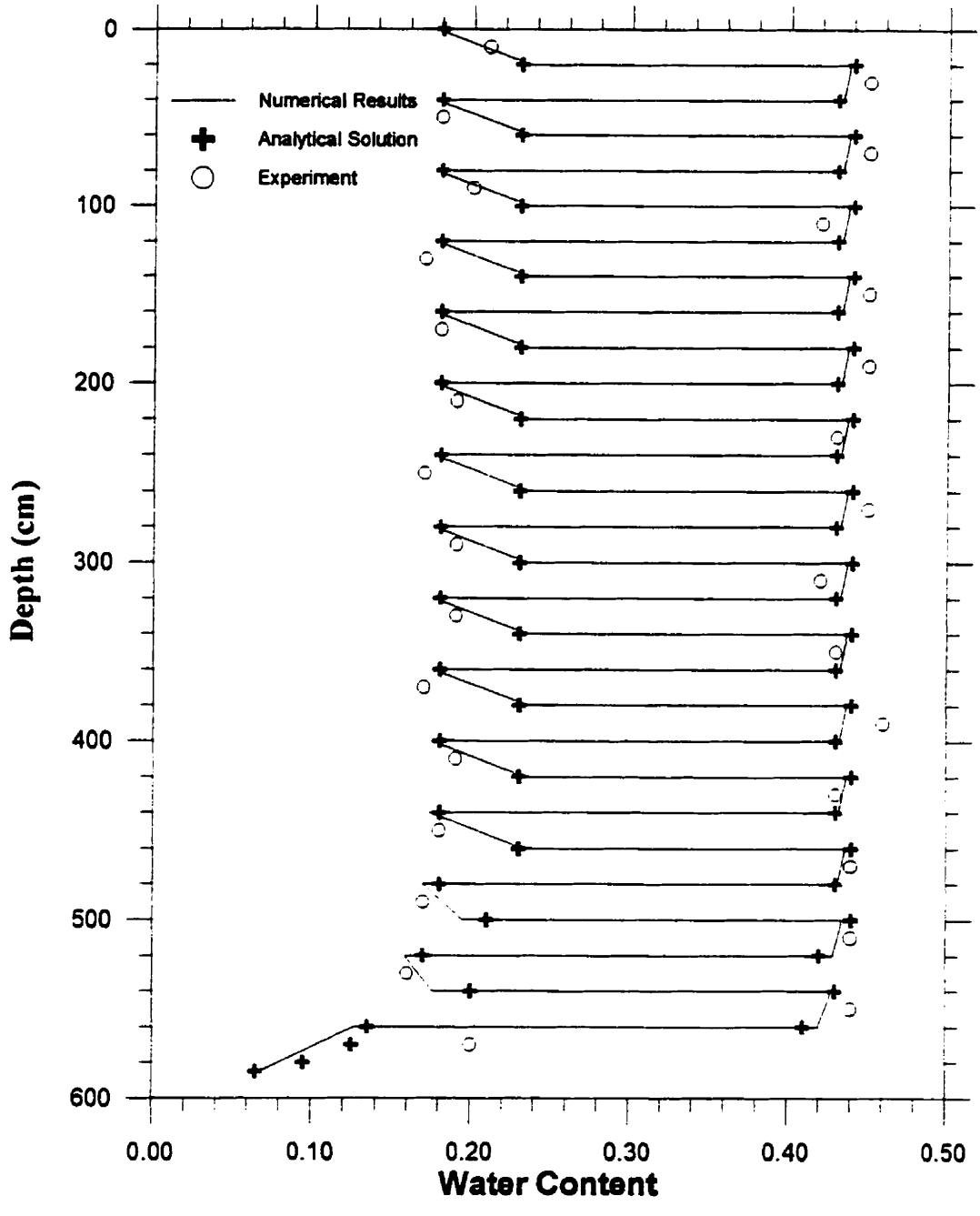

Figure (5.3) Water Content Distribution

The third example represents a linear waterflood of a petroleum reservoir. An analytical solution for this one-dimensional problem is given by Buckley and Leverett (1942) for the case of zero capillary pressure. Buckley and Leverett (1942) introduced the following equation for this idealized case:

$$\left(\frac{dx}{dt}\right)_S = \frac{q_t}{\phi}\left(\frac{dF_w}{dS}\right)_S \tag{5.1}$$

where q_t s the total flux rate q_w+q_{nw}, F_w has the physical meaning of the ratio of the net wetting phase flux at (x,t) to the net influx of wetting phase. If the permeability ratio of K_{nw}/K_w as a function of S is known, dF_w/dS can be evaluated as a function of S. When S is known Equation (5.1) can be integrated to give the saturation distribution for any t>0. The integration of Equation (5.1) with respect to time gives

$$(x)_S = \frac{Q_i(t)}{\phi A}\left(\frac{dF_w}{dS}\right)_S \tag{5.2}$$

in which $Q_i(t)$ is the cumulative total volume of fluid flowing through an area A in an interval of time t, $(x)_S$ is the distance traveled along x by the plane of saturation S in the same interval of time. An illustrative example to this analytical solution is given by Faust (1985). Data for this problem are given in Table (5.2). In this example water is injected in one end and it is displacing the nonwetting fluid in a fully NAPL saturated one dimensional domain along the x-direction. 40 cells each 7.62 m in length were used to discretize the domain. Figure (5.4) shows the comparison between the analytical solution and the numerical results for this problem.

Table (5.2) Data used in the one-dimensional water flood problem

Parameter	Value
Permeability	2.96×10^{-13} m^2
Porosity	0.2
Reservoir length	304.8 m
Cross-sectional area	929 m^2
Oil viscosity	0.001 kg m^{-1} s^{-1}
Water viscosity	0.001 kg m^{-1} s^{-1}
Oil density	1000 kg m^{-3}
Water density	1000 kg m^{-3}
Initial water saturation	0.16
Initial pressure head	70.29 m
Injection rate	1.399×10^{-4} m^3/s
Residual saturation for water	0.16
Residual saturation for oil	0.2

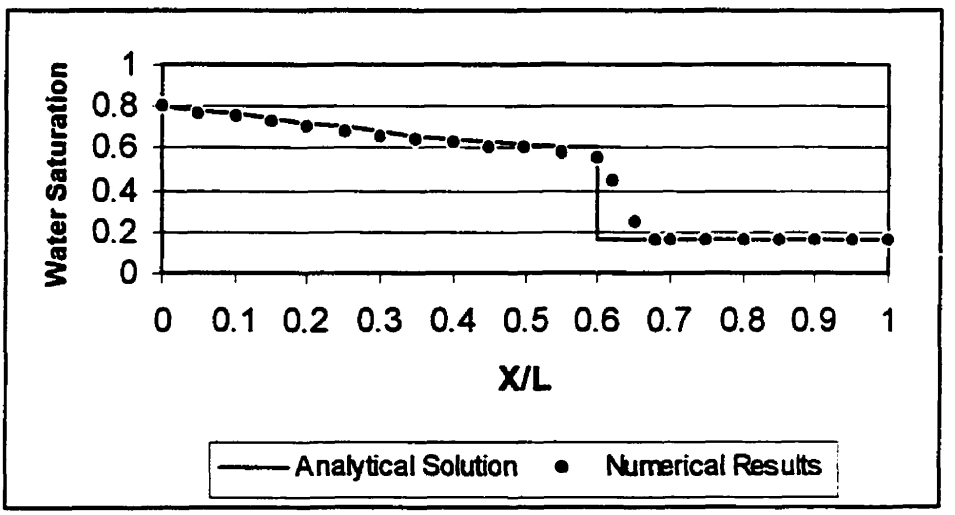

Figure (5.4) Saturation profile of waterflood problem

5.2 One dimensional unsaturated flow experiment

Experimental work may be used as a useful tool in order to verify a numerical model. In this regard, the following works from other researchers have been chosen.

The first experiment involves one dimensional infiltration and redistribution of oil in a sand column (Al-Sheriadeh, 1993). A transparent Plexiglas column was dry packed in a homogeneous manner with #125 sand to a height of 120 cm. The sample was slowly saturated with water supplied at the bottom. After 24 hours, the column was de-saturated slowly by pulling water out using a pump connected to a supply tube at the bottom of the column until the water saturation throughout the sand column reached an irreducible water saturation of 0.22. A lighter than water nonaqueous fluid, Soltrol 220, was spilled instantaneously on the top of the sand to form a falling ponding depth source, which was initially at 19.0 cm. Oil saturations every two cm along the column were recorded by a gamma attenuation device. Soil properties and fluid physical properties are presented in table (5.3). A one-dimensional mesh with 60 cells was used for this example. Each cell had 2 cm height. By using a PC-computer with a Pentium 200 processor, the simulation last 7 minutes.

Table (5.3) Soil and fluid physical properties for the first experiment (Al-Sheriadeh, 1993)

$K_s = 0.42$ cm/min	$\rho_n = 0.789$ g/cm^3
$\alpha = 0.019$ cm^{-1}	$\mu_n = 6.12$ cp
$n = 3.55$	$\beta_{an} = 2.63$
$\phi = 0.4$	$\beta_{nw} = 1.69$
$S_r = 0.22$	$\rho_w = 1.0$ g/cm^3
	$\mu_w = 1.0$ cp

Since measured parameters and the inferred relative permeability function are subject to possible measurement error, the model simulated saturation was not able to fit the observed profile without any parameter adjustments. The first 28 minutes was used to calibrate the hydraulic conductivity and then the calibrated value was used to validate the model results beyond 28 minutes and these values were compared with observation. It was found that a value of 0.54 cm/min gave the best fit to the observed data. Figures (5.5) to (5.8) show the NAPL saturation at 28, 51, 144, and 363 minutes after the beginning of the experiment. Good agreement between the observed and simulated results is evident.

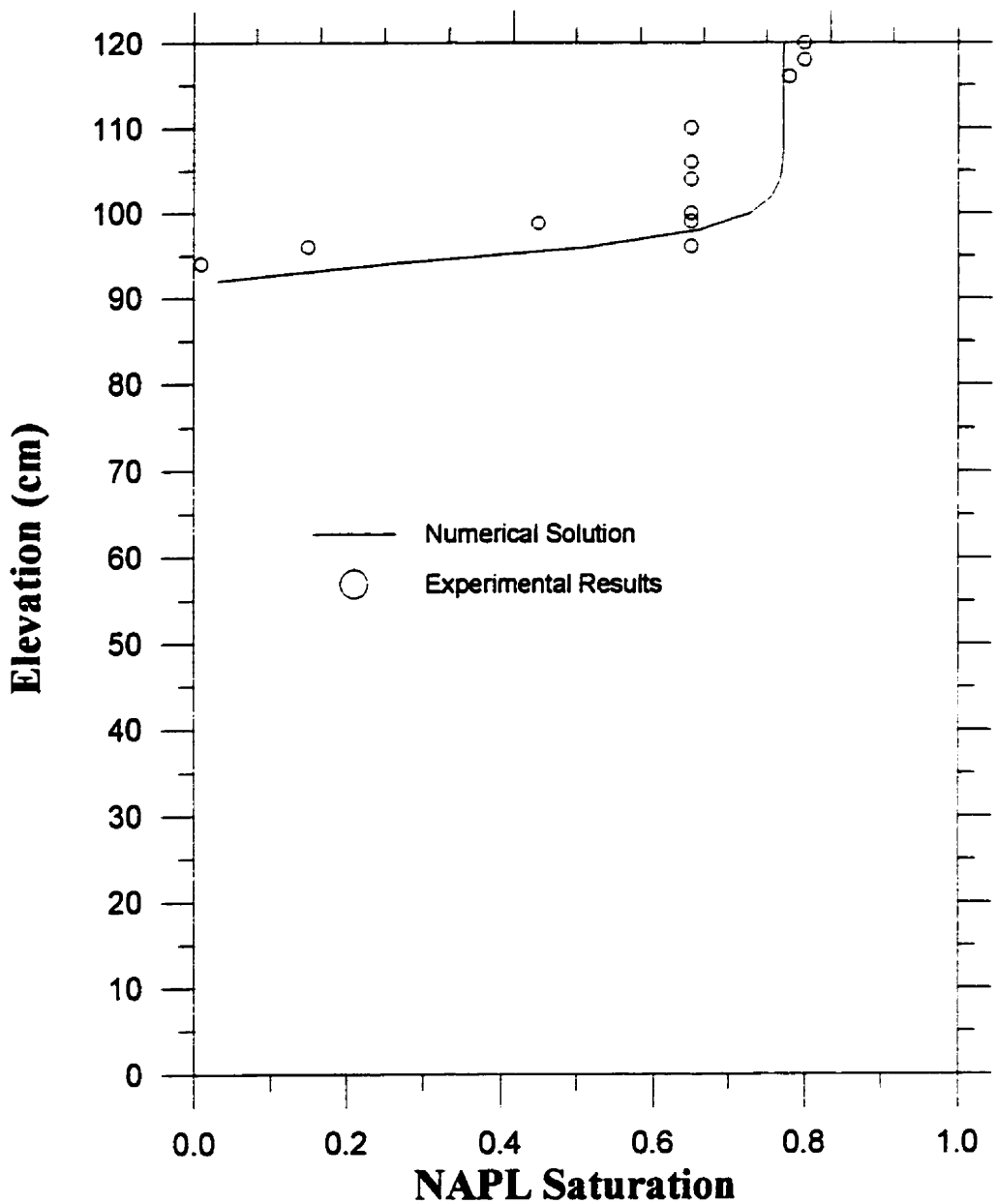

Figure (5.5) Numerical and experimental results at T=28.0 min

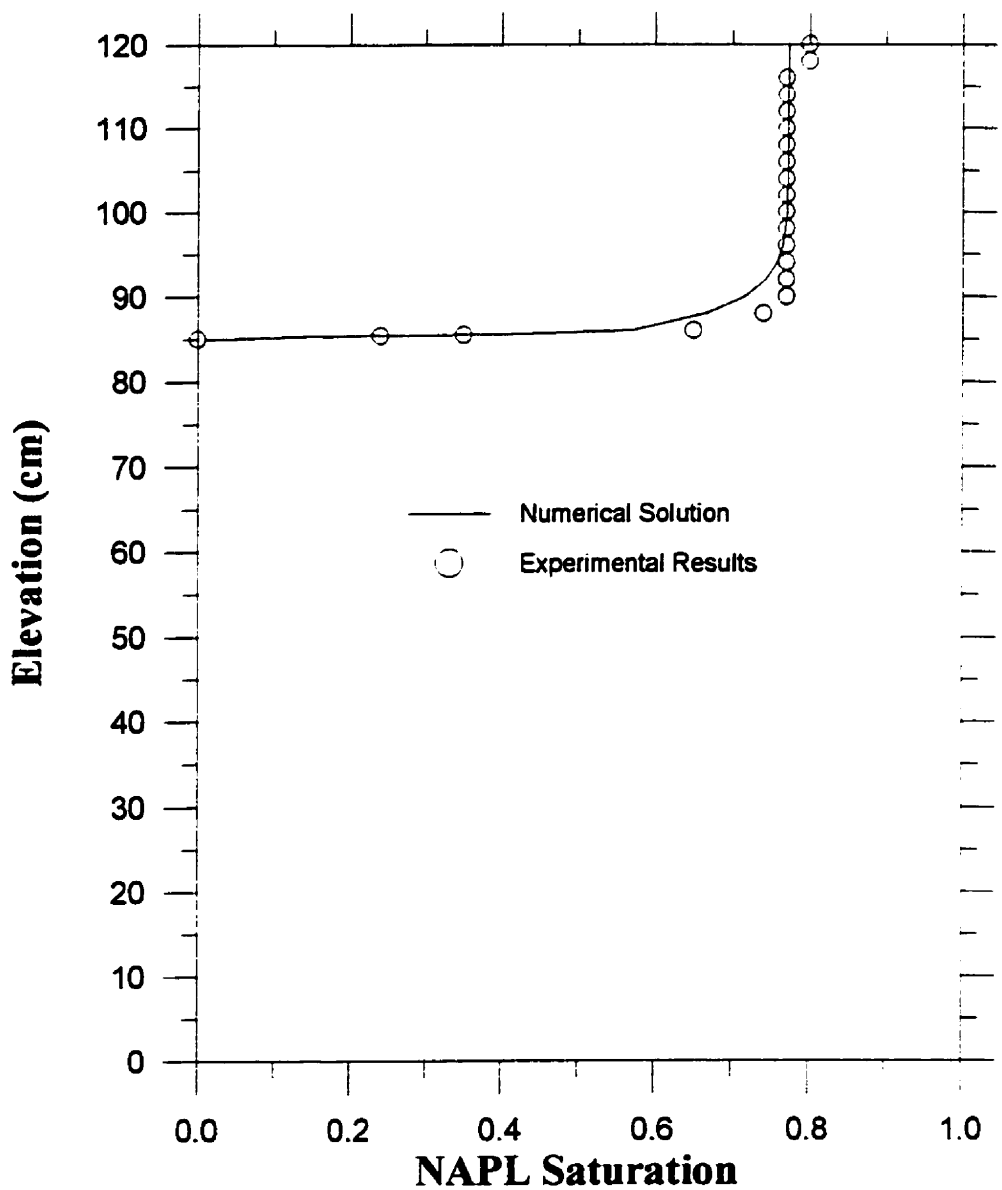

Figure (5.6) Numerical and experimental results at T=51.0 min

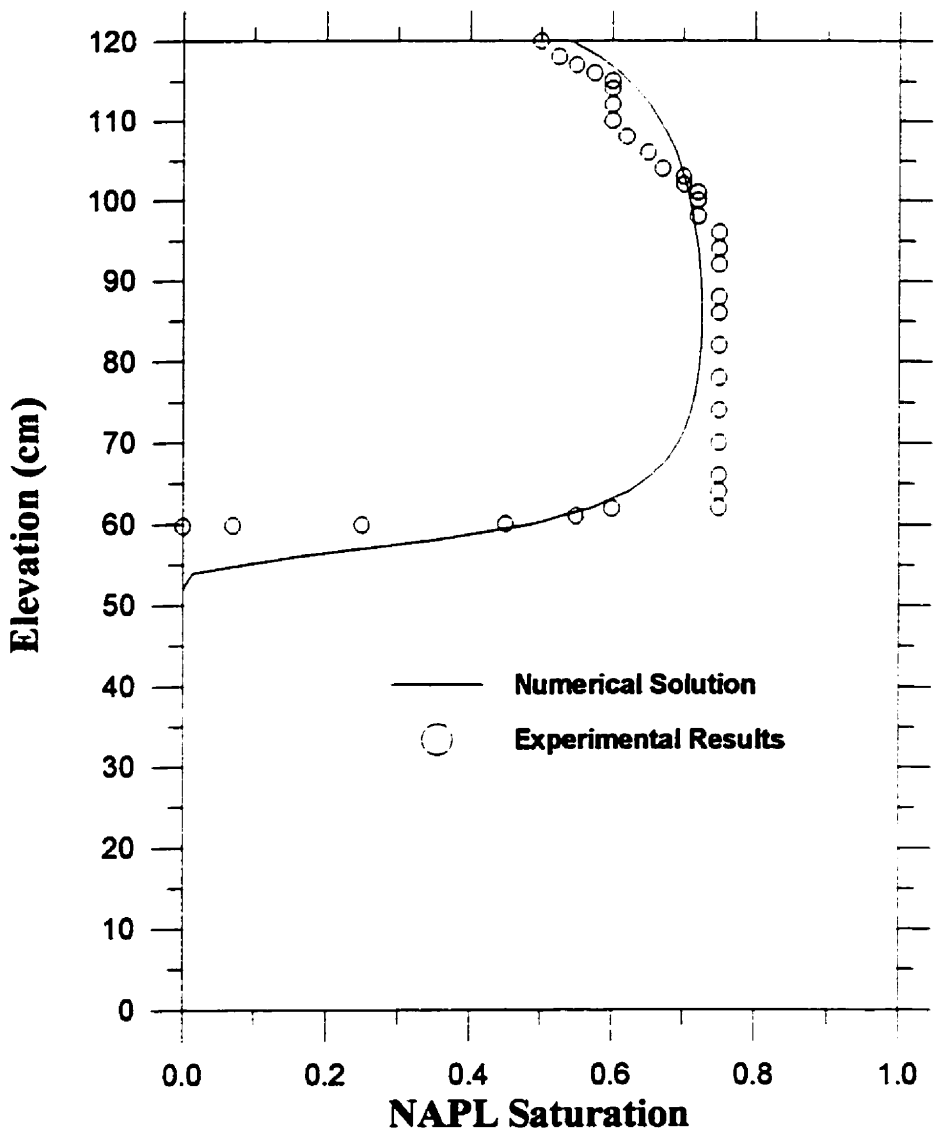

Figure (5.7) Numerical and experimental results at T=144 min

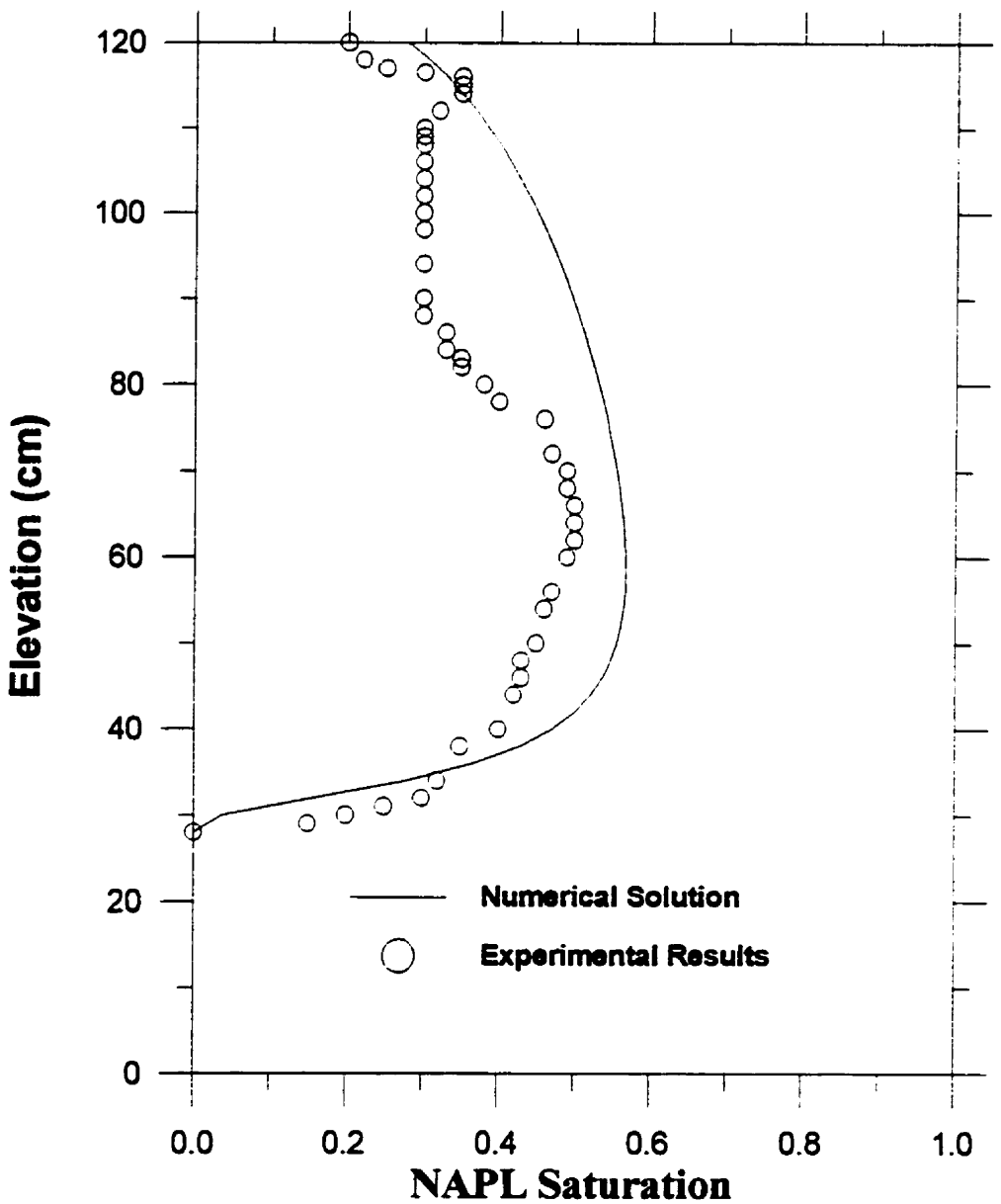

Figure (5.8) Numerical and experimental results at T=363 min

5.3 Two-dimensional LNAPL spill

In this test a comparison between the results from the current model and the experimental work of Van Geel and Sykes (1995 a and b) is made. An experimental box 1.5 m in length, 1.2 m in height and 6 cm in depth was filled with a well-sorted silica sand. Two liters of n-heptane were allowed to infiltrate the sand under a 3-cm prescribed head boundary condition. The spill was dispersed over a 10 cm by 6 cm area located at the center of the top boundary and lasted 18.67 min. The model parameters are presented in Table (5.4). A symmetric no-flow boundary was assumed along the center of the experimental box and therefore only half the domain was modeled. 27 nodes in the z-direction and 18 nodes in the x-direction were used in the discretization. In z direction, the first 15 cells had 4 cm height, then from node 16 to node 25, 9 cells, 5 cm and the last 2 cells were 3.5 and 6 cm, respectively. In x direction, the first three cells were 2 cm long, then 2 cells were 2.5 cm, 11 cells were 5 cm, and the last cell was 9 cm long. Since the LNAPL spill was conducted in a small, stainless steel rectangular cross section, which penetrated the sand to a depth of 3 cm, a permeability several orders of magnitude less than the sand, was assigned to 9 cm immediately outside the spill area to simulate the impermeable spill box. Figure (5.9) shows the comparison between the numerical and the experimental results. The velocity vectors of NAPL contaminant are illustrated in Figures (5.10) and (5.11) for time 1120 sec and 3000 sec.

Table (5.4) Soil and fluid physical properties for the second experiment (Van Geel and Sykes, 1994)

$K_x = 2.0\times10^{-4}$ cm/s	$\rho_n = 0.685$ g/cm^3
$K_z = 1.0\times10^{-4}$ cm/s	$\mu_n = 0.409$ cp
$\alpha = 0.0271$ cm^{-1}	$\beta_{an} = 3.65$
$n = 5.72$	$\beta_{nw} = 1.95$
$\phi = 0.374$	$\rho_w = 1.0$ g/cm^3
$S_{rw} = 0.17$	$\mu_w = 1.0$ cp

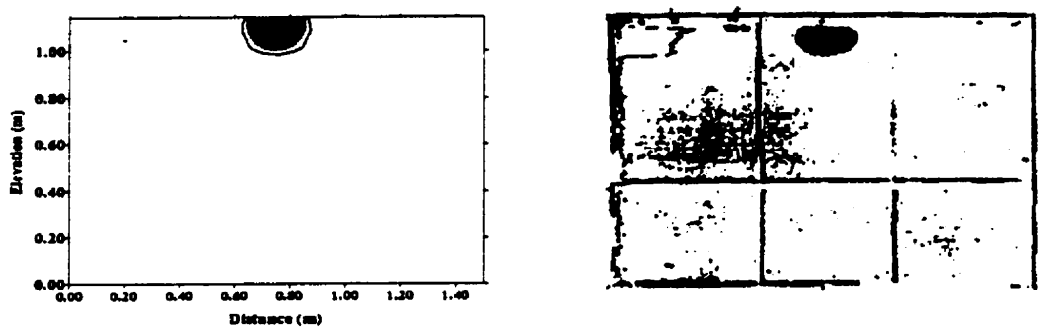

Time = 120 sec

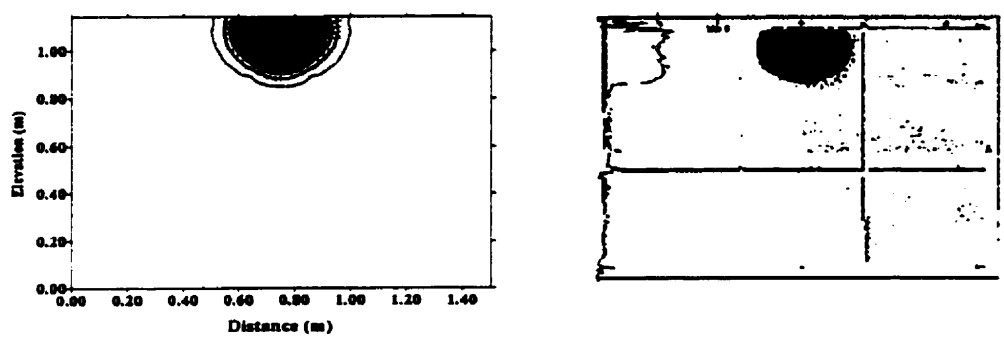

Time = 600 sec

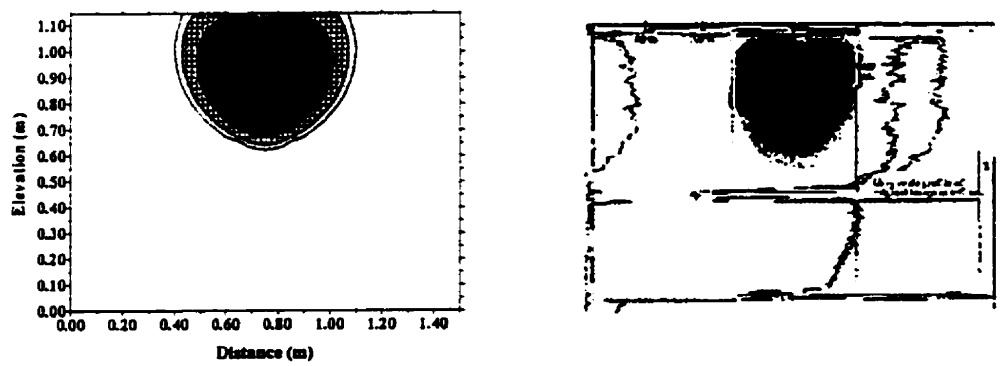

Time = 3000 sec

Figure (5.9) Comparison of numerical (left) and experimental (right) results for the second experiment (Van Geel and Sykes, 1994)

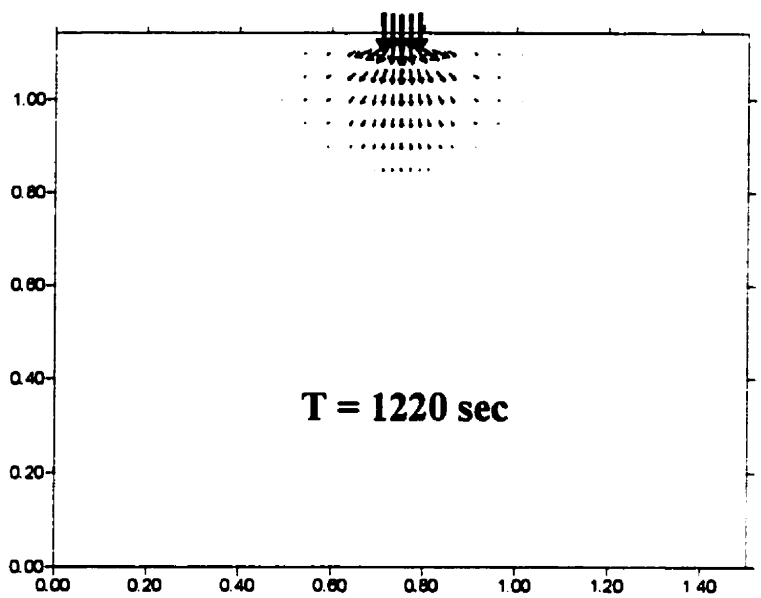

Figure (5.10) Computed velocity vectors for Van Geel and Sykes (1994) Experiment at T=1120 sec.

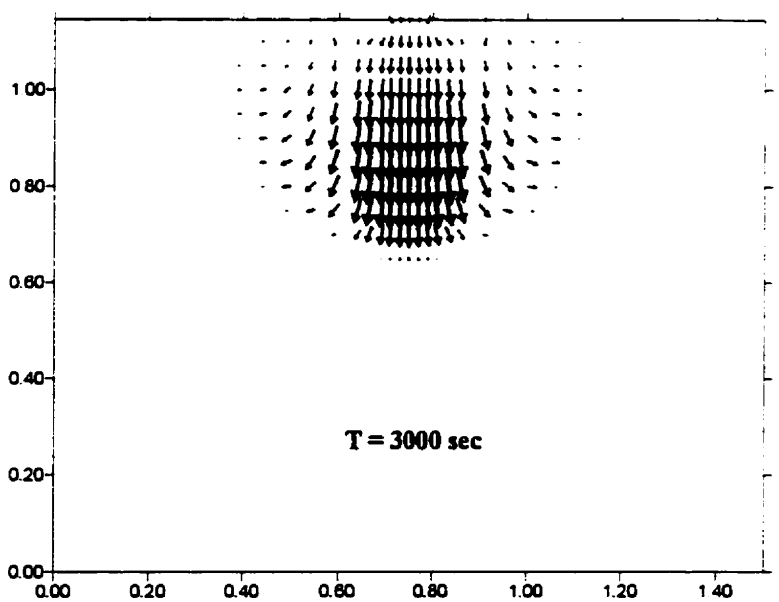

Figure (5.11) Computed velocity vectors for Van Geel and Sykes (1994) Experiment at T=3000 sec.

5.4 Model applications

In order to demonstrate the capabilities of the present model, two hypothetical tests are presented here.

5.4.1 Test No. 1

The first example involves a spill of Tetrachloroethylene in an irregular domain. This simulation is performed in two stages. In stage one, 3.013 liters of Tetrachloroethylene infiltrate into the soil under a head of -0.25 m along a width of 2 m (Figure 5.12). The soil is homogeneous and its properties are given in Table (5.5). The water table is situated at a depth of 2.2 m and the impermeable layer is at a depth of 5 m below the surface. The length of the domain in the x-direction is assumed to be 8 m. Boundary conditions for the water phase to the left and right of the domain below the water table are of Dirichlet type and all other boundaries are impermeable for the water phase. For the oil phase, the boundary conditions are "no flow" except at the infiltration zone, which is a Dirichlet condition. Stage one is terminated after 10 days.

Stage 2 of the problem involves a continuation of stage 1. Tetrachloroethylene is permitted to distribute for 25 days under no flow boundary conditions for NAPL. Boundary conditions for water are the same as they were in stage 1.

Table (5.5) Soil and fluid physical properties for test problem 1.

$K_x = 5$ m/d	$\rho_n = 1620$ kg/m^3
$K_z = 2$ m/d	$\mu_n = 0.9$ cp
$\alpha = 3.0$ m^{-1}	$\beta_{an} = 2.3$
$n = 2.8$	$\beta_{nw} = 1.77$
$\phi = 0.4$	$\rho_w = 1000.0$ kg/m^3
$S_{rw} = 0.1$	$\mu_w = 1.0$ cp

Dissolution in water and volatilization to air from NAPL are considered in this stage. The equilibrium partition coefficient between NAPL and water is 493 gr/gr and between air and water is 0.24 gr/gr. By the end of stage 2, the NAPL plume has reached the lower aquifer boundary. However, a substantial volume of the spill is still retained in the zone above the water table as residual saturation. The oil saturation distribution at the end of stage 1 and 2 are shown in figures (5.13) and (5.14). Table (5.6) shows the results of mass distribution between three phases: free product, in water phase and in gas phase. A mass balance test was used to measure of the numerical accuracy of the solution. Here, the model uses, as a criterion, the mass residual, M_r, compared with the difference between the initial mass, M_i, and the net mass flux, N_f.

$$\text{Error} = \frac{100 M_r}{M_i - N_f} \tag{11}$$

where $M_r = \Delta M_s - N_f$ and ΔM_s is the change in mass stored in the aquifer [M]. This simulation took 97 minutes to be completed with a PC-computer with a Pentium 200 processor.

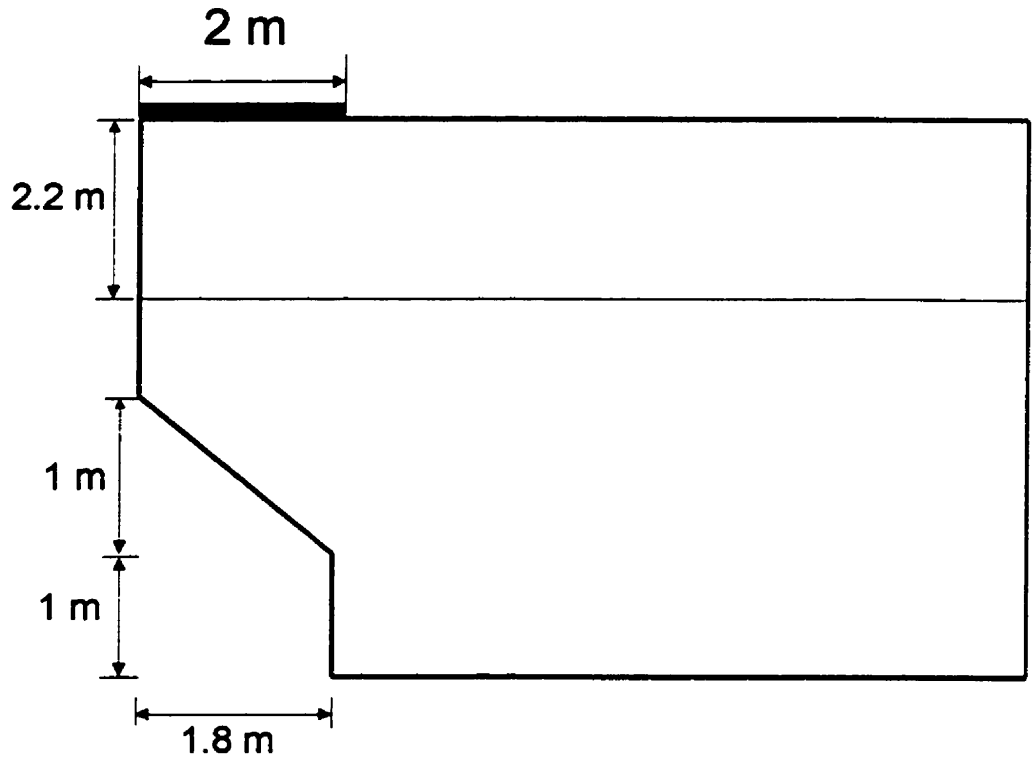

Figure (5.12) Domain used in test problem 1

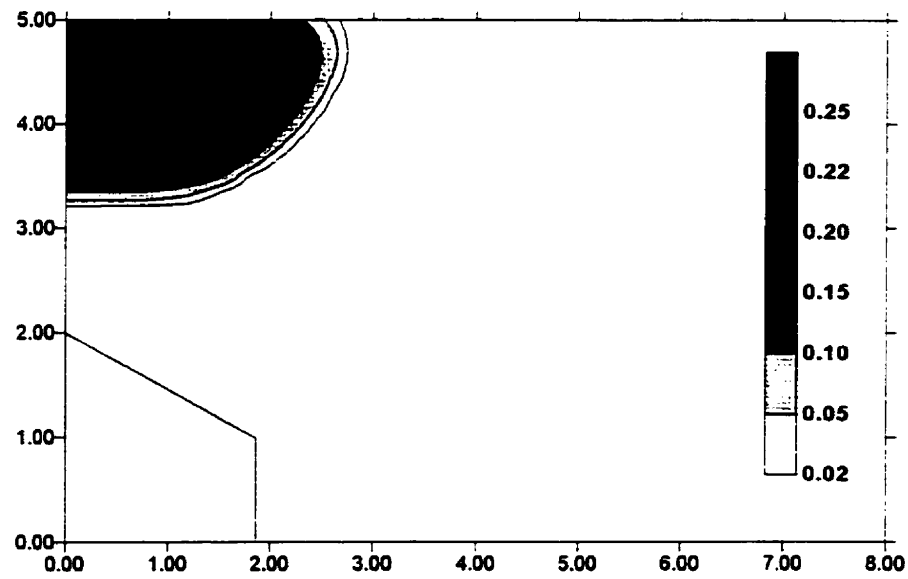

Figure (5.13) NAPL saturation at the end of stage 1 for test problem 1.

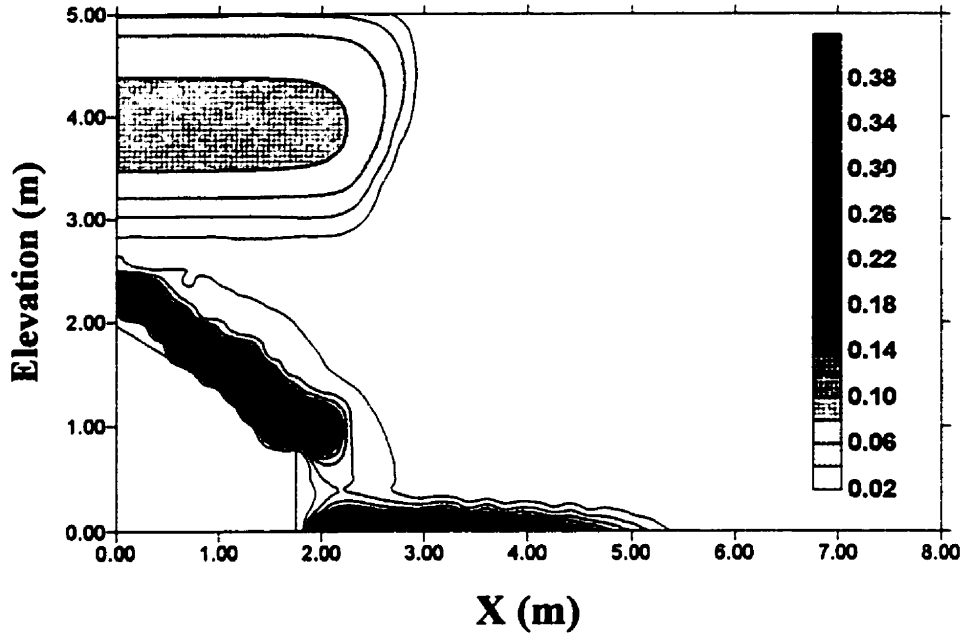

Figure (5.14) NAPL saturation at the end of stage 2 for test problem 1.

Table (5.6) NAPL distribution between phases and mass balance error in Test No.1

Time (day)	Free NAPL (ℓ)	Dissolved NAPL (ℓ)	Vaporized NAPL (ℓ)	Net Change (ℓ)	Net Outflow(ℓ)	Error (%)
1	3.0003	0.00934	0.00332	0.0127	0.0127	0.0014
3	2.9890	0.01627	0.00632	0.0240	0.0226	0.0475
5	2.9715	0.02818	0.01160	0.0415	0.0398	0.0578
10	2.9209	0.07480	0.03244	0.0921	0.1072	-0.5184
15	2.8797	0.11492	0.04943	0.1333	0.1644	-1.0782
20	2.8265	0.14134	0.06080	0.1865	0.2021	-0.5533
25	2.7761	0.17428	0.07612	0.2369	0.2504	-0.5649

5.4.2 Test No. 2

The second test involves simulation of a three-phase flow in an unsaturated zone. A three meter deep by five meter long box is filled with coarse homogeneous sand. A water table is maintained near the bottom of the sand column with a small head differential imposed such that water flows from left to right. The water table on the left has is an elevation of 2.69 meters while on the right it is 2.7 meters. A zone near the top center is filled with sand and residual TCE as the contaminant vapor source. The simulation is performed in three stages. At the first stage, which lasts 2.78 hours, the initially saturated sand is allowed to drain, thereby creating a steady-state moisture profile.

The physical and hydraulic characteristics of the soil and the NAPL are shown in Table (5.7). At the second stage from 2.78 to 48 hours the TCE vapor is applied to the domain. In stage 3, remediation is simulated with vacuum pumping in the unsaturated zone. A vacuum well is assumed to be placed in the center of the contaminated zone and screened over 30 cm from a depth of 22.5 cm to 52.5 cm. The discharge rate is considered to be 0.02 liters per second for 12 hours. Figure (5.15) and figure (5.16) show the TCE gas saturations at the end of stages 2 and 3. During stage three, 1.07 m^3 of NAPL gas is removed from the unsaturated zone.

Table (5.7) Soil and fluid physical properties for test problem 2.

$K_x = 2.1\times10^{-6}$ cm/s	$\rho_n = 0.00553$ g/cm^3
$K_z = 2.1\times10^{-6}$ cm/d	$\mu_n = 0.0002$ p
$\alpha = 0.156$ cm^{-1}	$\beta_{an} = 2.46$
$n = 4.26$	$\beta_{nw} = 2.16$
$\phi = 0.47$	$\rho_w = 0.9982$ g/cm^3
$S_{rw} = 0.2$	$\mu_w = 0.01$ p

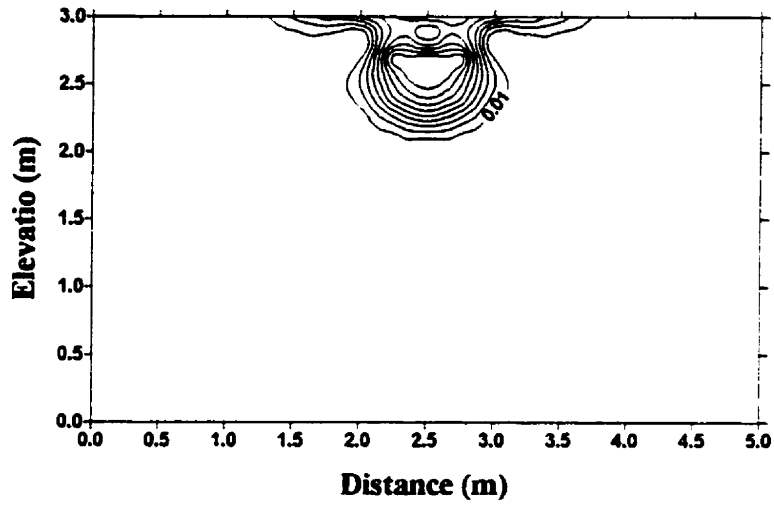

Figure (5.15) NAPL gas saturation at the end of stage 2

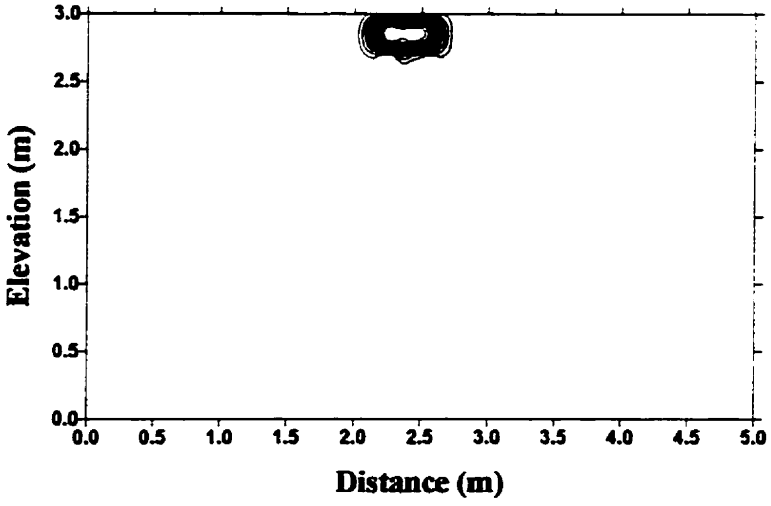

Figure (5.16) NAPL gas saturation at the end of stage 3

CHAPTER VI

LABORATORY EXPERIMENTS

The physical processes governing the flow of an immiscible organic liquid in a variably-saturated porous medium has been investigated with a laboratory experiment at the Hydrodynamic Laboratory of Ecole Polytechnique of Montreal. The working medium used in the flow container was composed of two different clean Silica sands which were supplied by Unimin Canada Ltd. The effective diameter of sands, D_{50}, were 0.25 and 0.10 mm, respectively. For the first sand, 10 percent of grains retained on 20 mesh or coarser and for the finer grained sand, 10 percent retained on 40 mesh or coarser. Also, a series of preliminary tests were conducted to determine the sand characteristics including capillary pressure-water content relationships and saturated hydraulic conductivities.

6.1 Capillary pressure-water content relationships

Water retention curves for the sands were determined using the ASTM (1981) standard test method for capillary-moisture relationships. This test method covers the determination of capillary-moisture relationships for coarse-and medium-textured soils as indicated by the soil-moisture tension relations for tensions between 10 and 101 kPa (0.1 and 1 atm). Under equilibrium conditions, moisture tension is defined as the equivalent negative gage pressure, or suction, corresponding to a specified soil moisture content (ASTM, 1981).

An assembly of the apparatus is shown in Figure (6.1). In order to saturate the porous plates, it was installed in the pressure container. The container was then filled with water, and the lid on the container was locked. The pressure was set to 101 kPa or 776 mmHg (1 atm or 15 psi), and was maintained for several hours under pressure until there was no further bubbling of air from the outlet.

Saturated soil samples were then placed in contact with the saturated porous plate installed within the pressure chamber. The bottom of each plate is covered by a rubber membrane to be airtight and is maintained at atmospheric pressure by means of a small drain tube and opening through the side of the pressure chamber. A desired air pressure admitted to the pressure chamber, and consequently to the top of the porous plate, creates a pressure drop across the porous plate. The saturated soil samples on the plates establish equilibrium with the water in the plate. The water, held at a tension less than the pressure drop across the porous plate, will then move out of the soil, through the plate, and out through the drain tube. When water has ceased to flow from the sample and porous plate (indicating equilibrium for that particular tension), the moisture content of each sample is determined. A series of these tests at various tensions were done to prepare the capillary pressure-water content curve (Figures 6.2 ad 6.3).

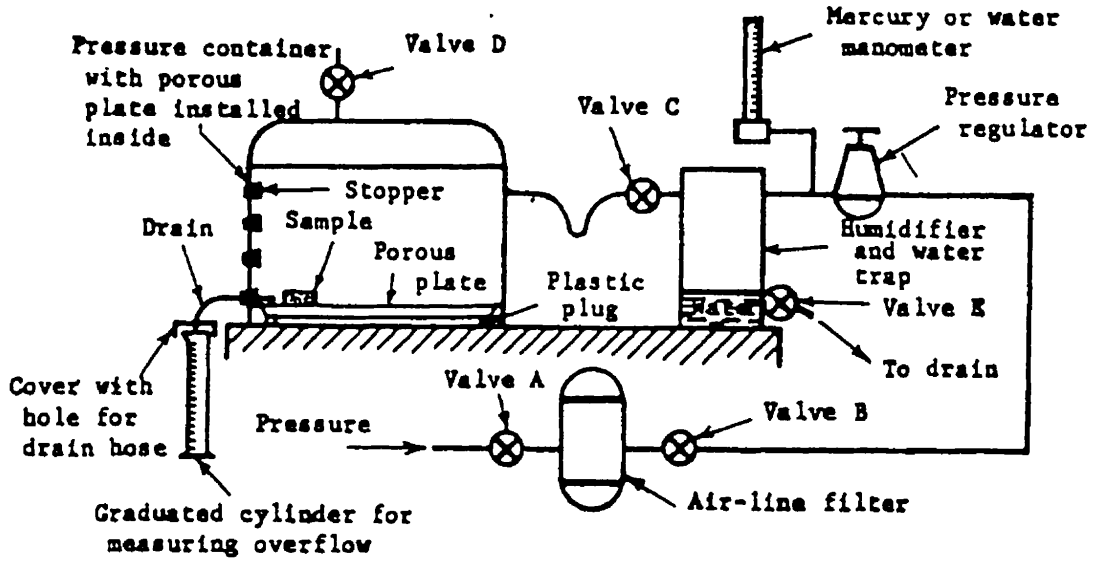

Figure (6.1) Schematic assembly of porous plate tension apparatus

An EPA program, RETC, was used to analyze the soil water retention function and estimate the constitutive parameters of the sands (van Genuchten et al., 1991). The program uses the parametric models of Brooks-Corey (1964) and van Genuchten (1980) to represent the soil water retention curve, and the theoretical pore-size distribution models of Mualem (1976) and Burdine (1953) to predict the unsaturated hydraulic conductivity function from observed soil water retention data. Figure (6.2) and (6.3) show the predicted retention curve for two types of sands. Also, logarithm of pressure heads verses the volumetric water contents are illustrated in Figures (6.4) and (6.5). The estimated constitutive parameters for sand with effective size d=0.25 mm are α=0.0893 cm^{-1} and n=2.8090. For sand with d=0.15 mm those parameters are α=0.022 cm^{-1} and n=2.997.

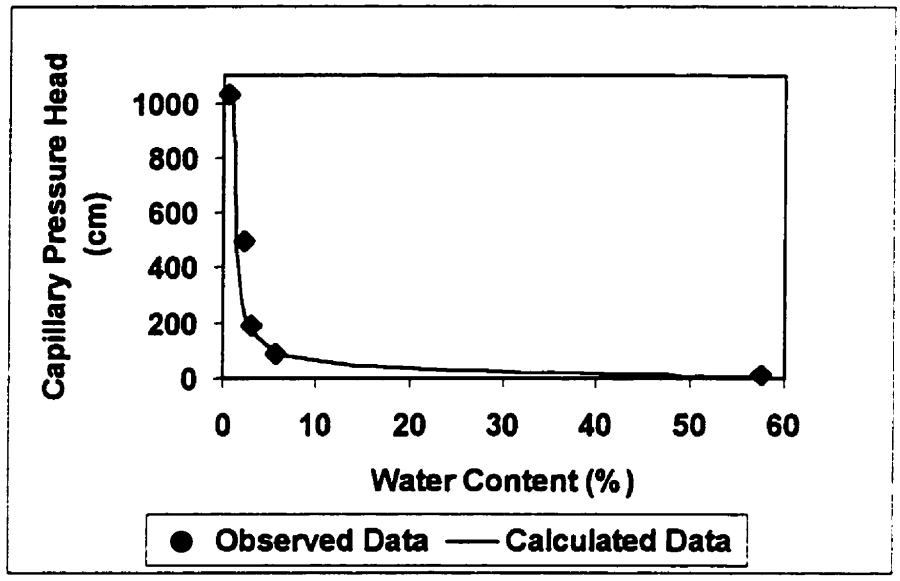

Figure (6.2) Retention curve for sand with effective size d=0.25 mm

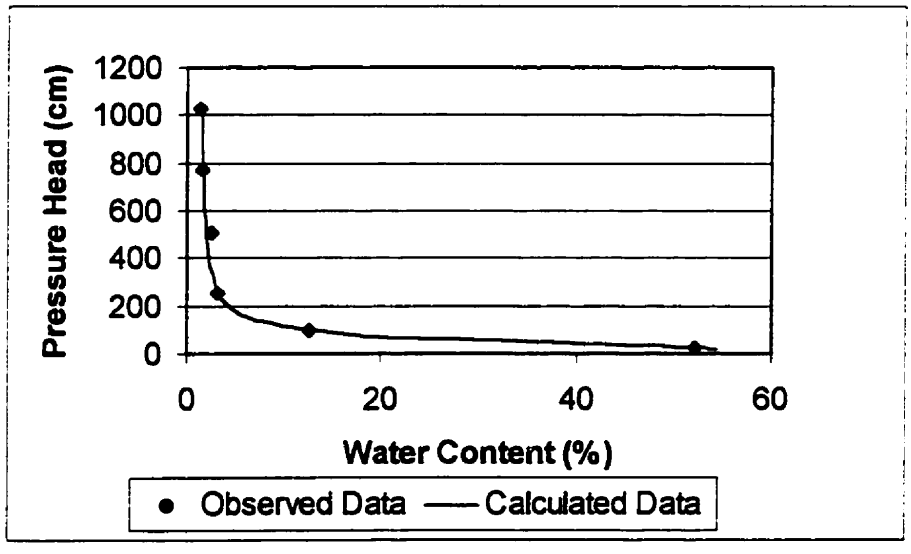

Figure (6.3) Retention curve for sand with effective size d=0.15 mm

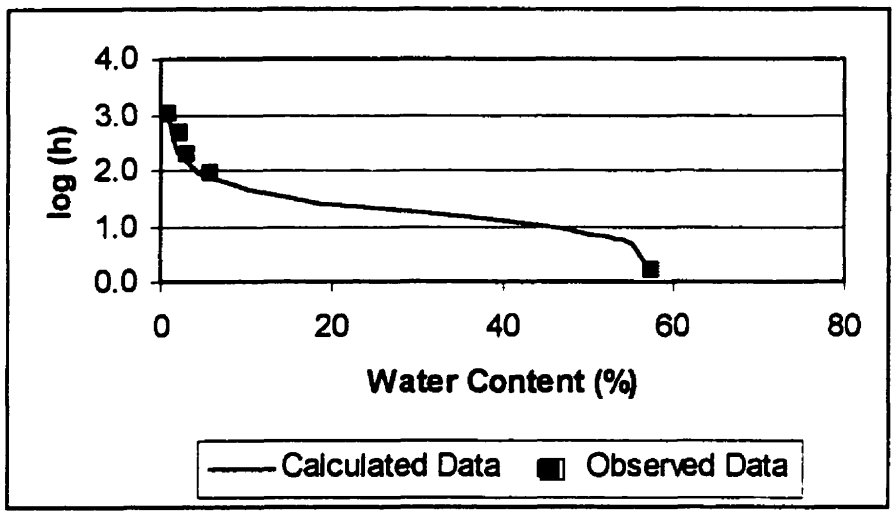

Figure (6.4) Logarithm of pressure heads verses the water contents for sand d=0.25

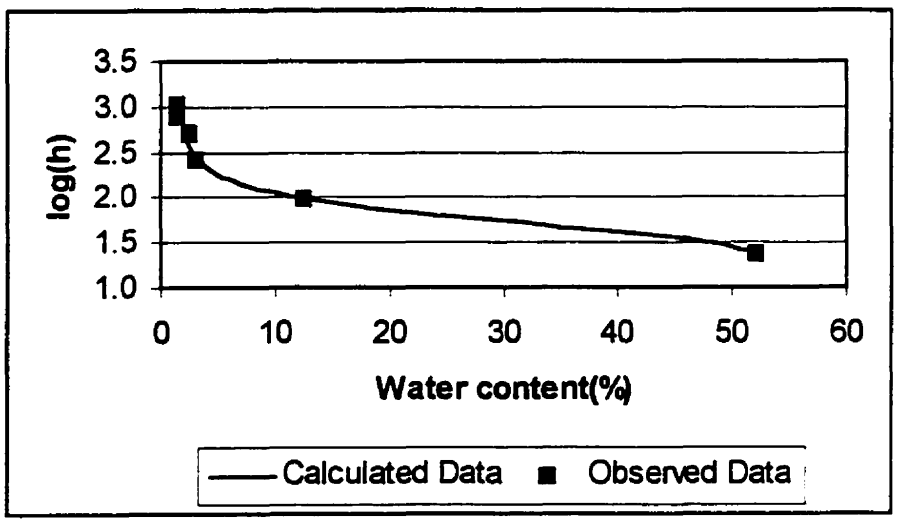

Figure (6.5) Logarithm of pressure heads verses the water contents for sand d=0.15

6.2 Saturated hydraulic conductivity test

These tests were performed to determine the saturated hydraulic conductivities by a constant-head method. Hydraulic conductivity in unsaturated porous media is related to the saturated hydraulic conductivity by the following relationship

$$K = k_r \cdot K_s$$

where K is the unsaturated hydraulic conductivity, k_r is relative permeability, and K_s is the saturated hydraulic conductivity.

A permeameter as shown in Figure (6.6) was used for the tests. It has a specimen cylinder of 15.3 cm in diameter. The permeameter is fitted with : (1) a reinforced screen at the bottom with permeability greater than that of sands but with a sufficiently small opening to prevent movement of particles; (2) manometer outlets for measuring the loss of head, *h*, over a length, *l* , of 15 cm.; (3) a reinforced screen with a spring attached to the top for applying light spring pressure; (4) constant-head filter tank to supply water and to remove most of the air from tap water. At the beginning of the tests, a vacuum pump was used to evacuate the air adhering to soil particles and from the voids. This was followed by a slow saturation of the specimen from the bottom upward under full vacuum in order to free any remaining air in the specimen.

For each sand, three different hydraulic gradients were applied and the test was repeated for each hydraulic gradient to eliminate, as much as possible, any errors. A summary of

the results is shown in Table (6.1) while Figures (6.7) and (6.8) illustrate the relationships between hydraulic gradients and flux.

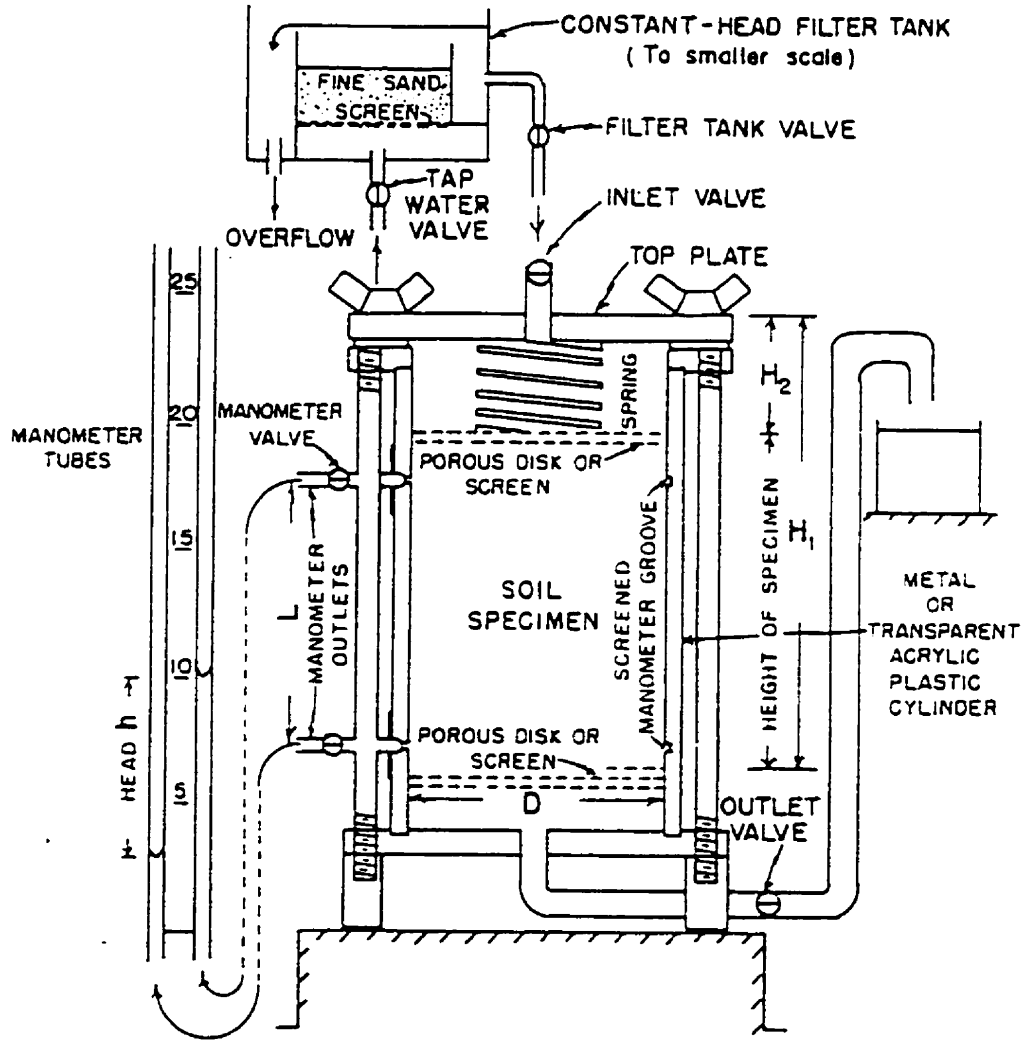

Figure (6.6) Constant head permeameter

Table (6.1) Summary of permeability test results

		Sand No. 1 (d=0.15)			Sand No.2 (d=0.25)	
Test No.	**Δh (m)**	**Q (m^3/s) $\times 10^3$**	**K (m/s) $\times 10^2$**	**Δh (m)**	**Q (m^3/s) $\times 10^3$**	**K (m/s) $\times 10^2$**
1-1	0.197	5.876	0.024	0.510	9.889	0.158
1-2	0.176	5.966	0.028	0.520	9.640	0.151
2-1	0.233	7.703	0.027	0.830	13.696	0.135
2-2	0.231	7.770	0.027	0.800	13.445	0.137
3-1	0.298	10.090	0.028	0.129	20.089	0.127
3-2	0.290	9.922	0.028	0.126	19.209	0.124
Average			0.0272			0.1314

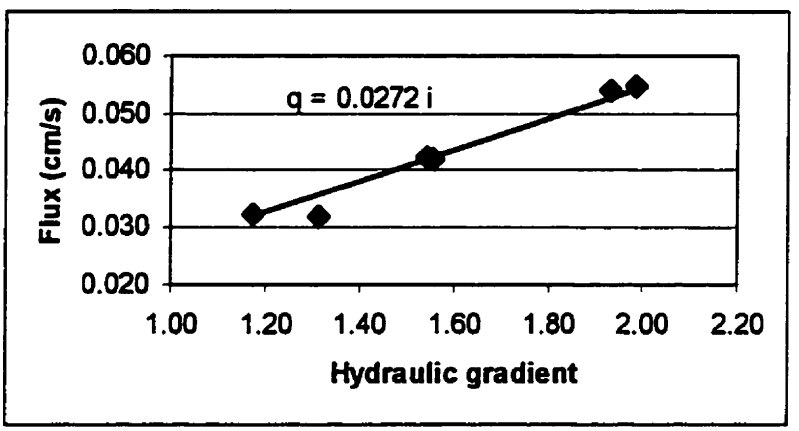

Figure (6.7) Permeability test for sand No. 1 (d=0.15 mm)

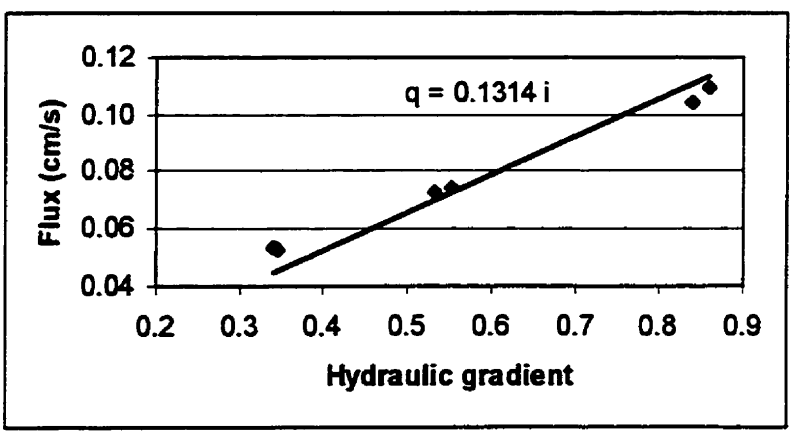

Figure (6.8) Permeability test for sand No. 2 (d=0.25 mm)

6.3 Experimental setup and procedure

The experiment was conducted in a relatively narrow (8 cm width) flow container. A sketch of the container, including important variables and parameters, is shown in Figure (6.9). The flow container has four chambers: an inlet head chamber, a working chamber, an outlet head chamber and a NAPL source chamber. The working chamber was layered with two different sands. The bottom layer of 27.5 cm height was filled with fine grain sand, d=0.10 mm. It was then covered with 10 cm of coarse grain sand, d=0.25 mm. The top layer was 16.5 cm of the fine grain sand. The inside dimensions of the sand filled chamber were 137 × 54 × 8 cm. The lower left corner of the porous medium was chosen as the origin of a (x,y)-coordinate system.

The front side of the flow container was made of glass in order to be able to visualize the plume movement. The side panels were made of Plexiglas and after cutting the two panels to the right dimensions, a large number of 1/32" holes were drilled through the plates. They were then shielded with geotextile membranes to prevent the movement of sand through the holes.

During the experiment, the head, h_1 (L), in the inlet head chamber and the head, h_2 (L) in the outlet chamber were kept constant. The heads were controlled by adjusting the placement of the water drainage hole on the side panels of the chamber.

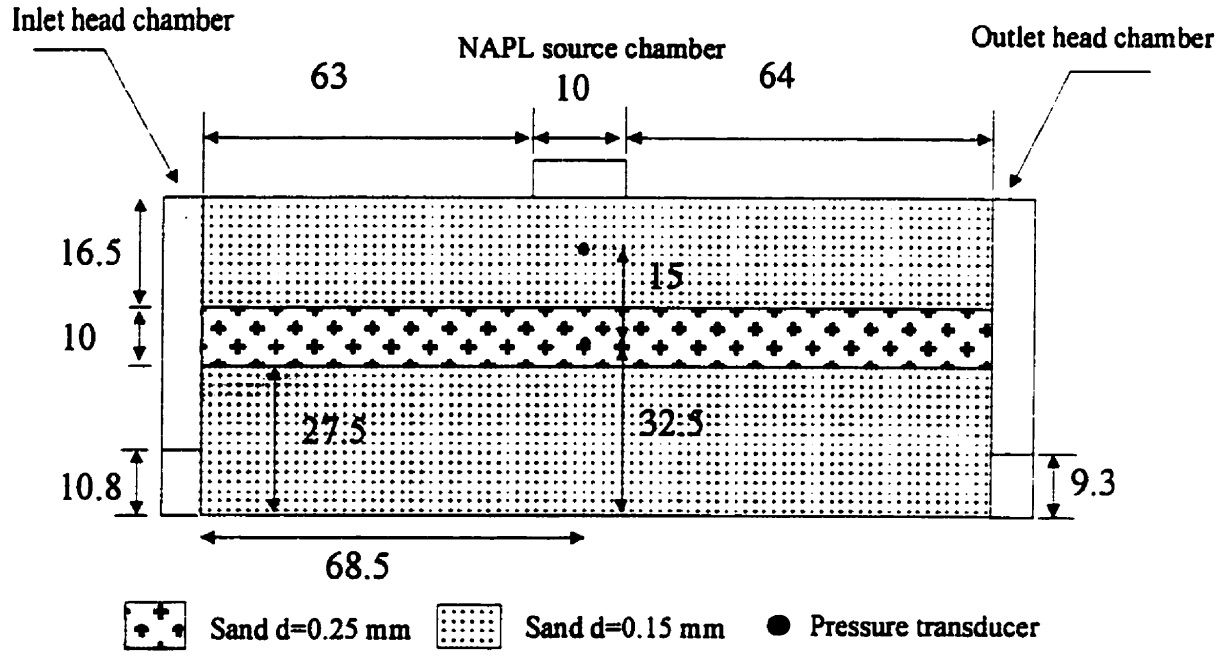

Figure (6.9) Sketch of the flow container

Two Validyne Model DP15 pressure transducers were used to measure the fluid pressure or suction in the soil (Figure 6.10). These pressure transducers are designed for low and medium pressure measurements and provide laboratory accuracy. The pressure sensing element is a flat diaphragm of magnetic stainless steel, clamped between case halves of the same material, in a symmetrical assembly. Pick-off coils, embedded in the case halves, sense the diaphragm deflection through the variable reluctance principle. The embedded coils are covered with a non-magnetic stainless layer, so that the pressure cavity presents a completely stainless exposure to the working fluid. Vent valves facilitate complete liquid filling for dynamic measurement.

The carrier demodulator supplied with the pressure transducers provides a DC output signal that may be adjusted in the range of 0 to 10 Volts. The instrument furnishes a regulated carrier excitation of 5 Vrms, 5 KHz sine wave to the two inductance ratio arms of the transducer. The resulting output is demodulated and amplified using the integrated circuit, and gives a uniform frequency response from steady state to 1000 Hz.

The pressure transducers were tested prior to use in the laboratory. They were calibrated using a manometer and the relationships between pressure head and output voltage were determined (Figures 6.11 and 6.12). As can be seen, the behavior of these instruments is very linear.

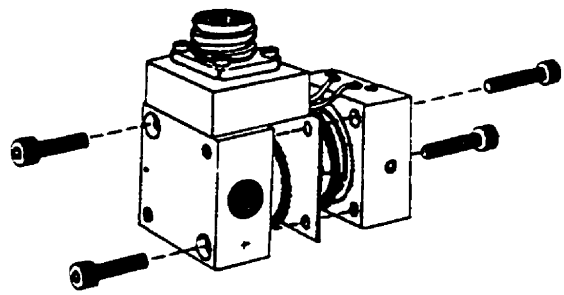

Figure (6.10) Pressure transducer

The pressure transducers were connected to a porous cup to measure negative fluid pressures. In order to obtain accurate pressure readings, extreme care was taken in filling the transducer and porous cup cavity with fluid to ensure that there was no trapped air.

The porous cups used to measure the pressures in the LNAPL phase were treated with chlorotrimethysilane to render them hydrophobic and wetting to the LNAPL phase (Lenhard et al., 1988).

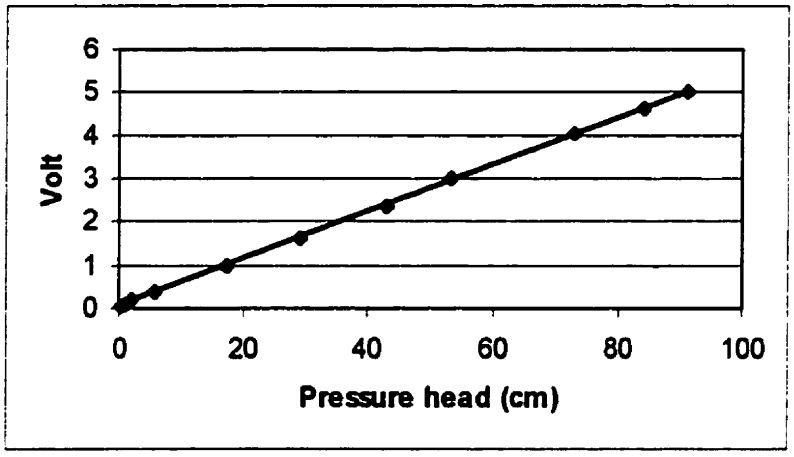

Figure (6.11) Calibration line for diaphragm 5 PSI

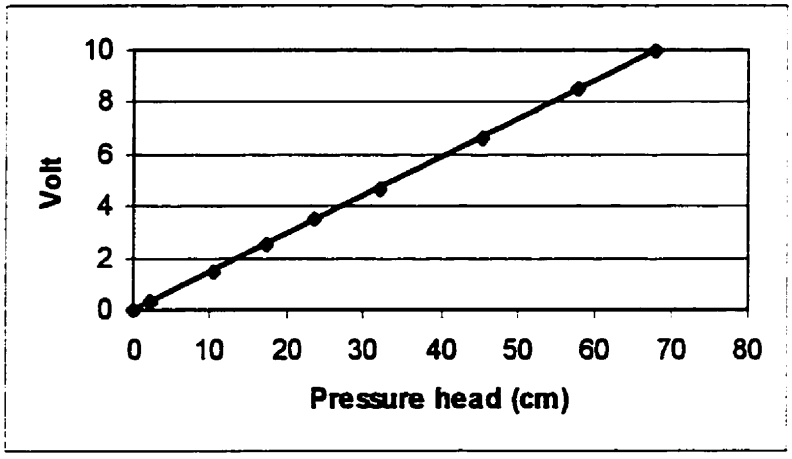

Figure (6.12) Calibration line for diaphragm 1 PSI

The transducers were mounted on the reverse side of the experimental box one at the center line situated 32.5 cm from the bottom of the box and the other was installed directly above the first at a point 47.5 cm from the bottom of the box.

6.4 Experimental results

The LNAPL, n-heptane, was selected for this test due to its low density, water solubility and vapor pressure. The characteristics of n-heptane are given in Table (6.2). The LANPL spill was initiated at the soil surface in the infiltration chamber which was 10 cm long and with a 3 cm head. In order to visualize the infiltrated LNAPL, SUDAN III color was used. The development of the recharge mound was followed by recording the transducer voltage readings. The constant head of LNAPL was kept for 375 seconds and then discontinued. The LNAPL continued to move down and readings were continued for another 825 seconds. The voltage readings were recorded from the two transducers and then converted to relative pressure head using the calibration curves. Figure (6.13) shows the results for transducer number one which was installed in the fine sand. The second transducer did not provide a satisfactory result. The cause may be attributed to several factors such as: not using enough chlorotrimetysilane, a higher pressure range, 5 psi, for that transducer, thus reducing its sensitivity, and/or existence of air inside the transducer. The shape of the NAPL infiltration front versus time was documented photographically (Figures 6.14 to 6.17).

As may be noted, the NAPL movement through the coarse-grained sand encountered a higher entry pressure when the finer-grained layer at the bottom was contacted. Initially, the contaminant descends and spreads out fairly symmetrically. On encountering the layer of fine grained sand however, a higher entry pressure is required and this causes lateral spreading and accumulation of heptane on the finer-grained layer.

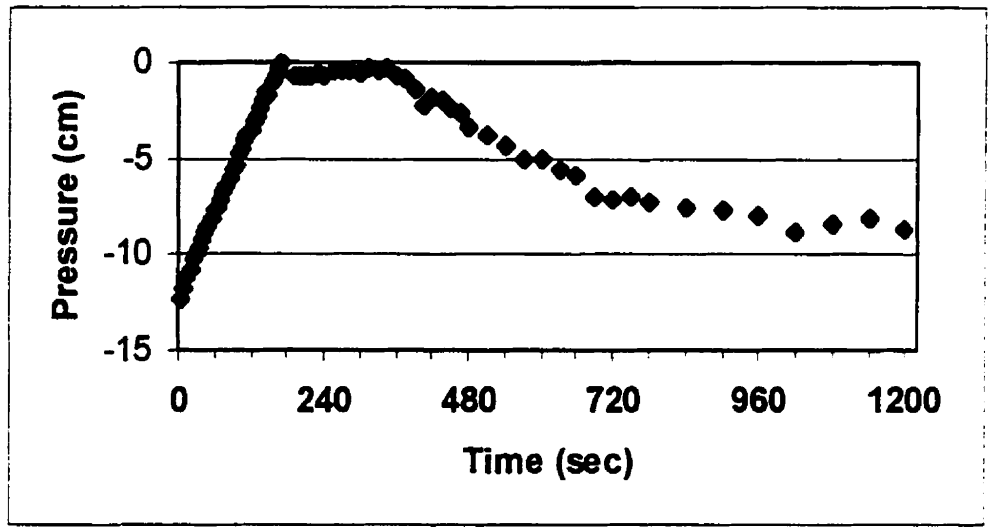

Figure (6.13) Pressure head measured by transducer No. 1

Figure (6.14) LNAPL distribution at t=120 sec

Figure (6.15) LNAPL distribution at t=375 sec.

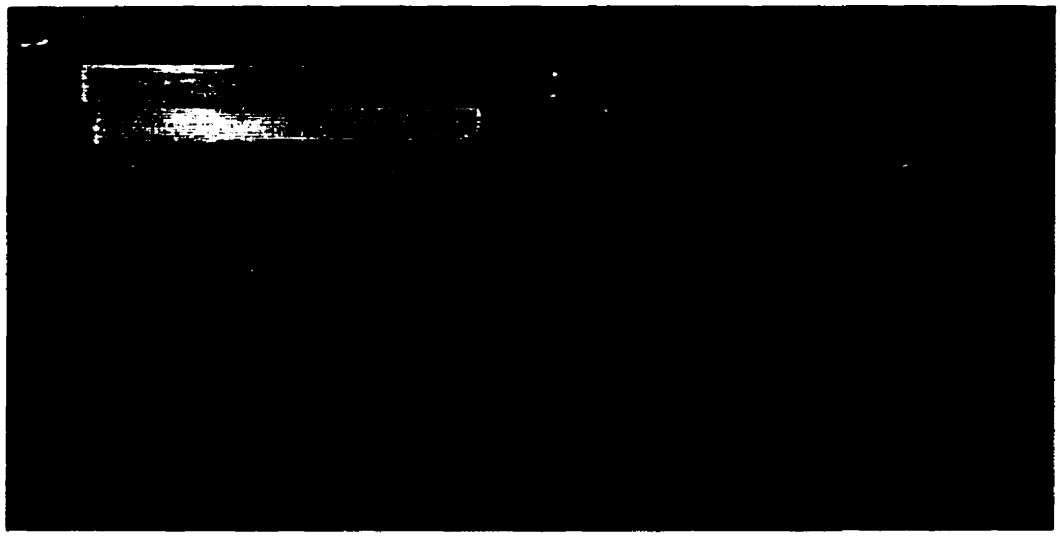

Figure (6.16) LNAPL distribution at t=620 sec

Figure (6.17) LNAPL distribution at t=1220 sec.

6.5 Numerical simulation of laboratory experiment

The laboratory LNAPL spill just presented was simulated using the numerical model. A summary of the input parameters used for the model simulations is presented in Tables (6.2) and (6.3). The scaling parameters, β_{an} and β_{nw}, are based on the work of Van Geel and Sykes (1994) for heptane. The input and output files for this simulation are presented in Appendix II. It is considered that Sudan III has no modifying effects on the viscosity and the density of heptane.

Table (6.2) Fluid properties used in simulating the laboratory experiment

Parameter	Value
Density of water	998.2 kg/m^3
Density of heptane	685.8 kg/m^3
Viscosity of water	0.0010 Pa.s
Viscosity of heptane	0.000409 Pa.s
Scaling parameters:	
β_{nw}	1.95
β_{an}	3.65

The discretization consisted of 25 nodes in the horizontal x-direction and 29 nodes in the y-direction. The LNAPL spill was conducted in the infiltration chamber. In order to prevent the lateral movement of LNAPL at the surface of the sand, two stainless-steel

plates which penetrated the sand to a depth of 2 cm were installed on the two sides of infiltration chamber.

Table (6.3) Soil properties used in simulating the laboratory experiment

Parameter	Fine sand (d=0.15 mm)	Coarse sand(d=0.25mm)
Porosity	0.525	0.565
Permeability	2.757×10^{-11} m^2	1.328×10^{-10} m^2
Water residual saturation	0.015	0.007
NAPL residual saturation	0.010	0.005
van Genuchten parameters		
α	0.0228 cm^{-1}	0.0893 cm^{-1}
n	3.00	2.81

The LNAPL spill was modeled for a period of 375 sec. During this period slight changes to the physical properties of the sands and fluids were made to find the best agreement between the numerical results and experimental data. These changes were as follows:

- The vertical hydraulic conductivity of coarse sand was increased to 1.532×10^{-8} cm while the horizontal hydraulic conductivity was kept the same.
- The parameter α for fine sand was increased to 0.0328 cm^{-1} .

After this period, the model was run for 825 sec without the LNAPL spill. The resulting pressure head for LNAPL has been compared with the measured data and illustrated in Figure (6.18). Also, the distributin of heptane is compared with the experimental results in

Figure (6.19). The computed NAPL velocity vectors for the end of spill period and end of migration period are presented in Figures (6.20) and (6.21).

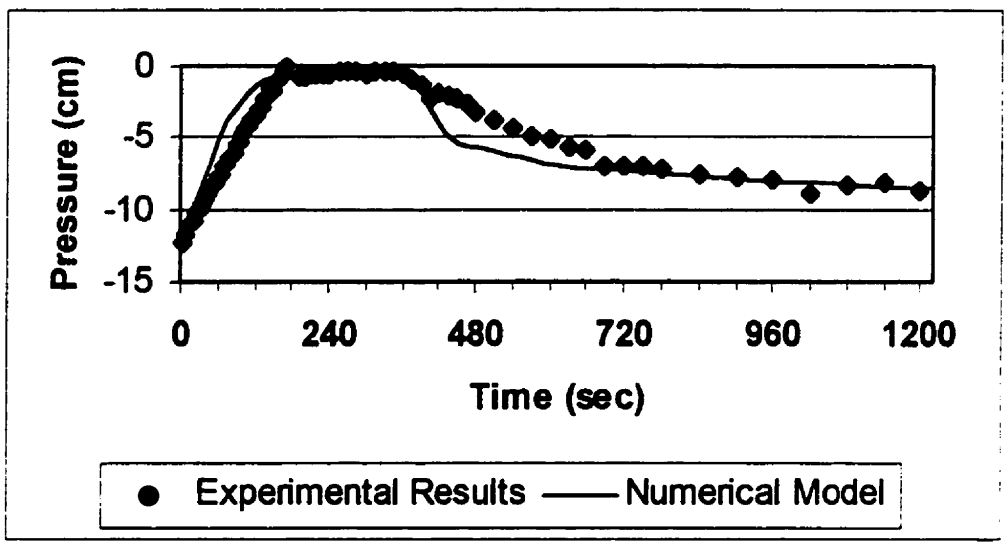

Figure (6.18) Comparison between pressure head measured at transducer No. 1 with numerical model

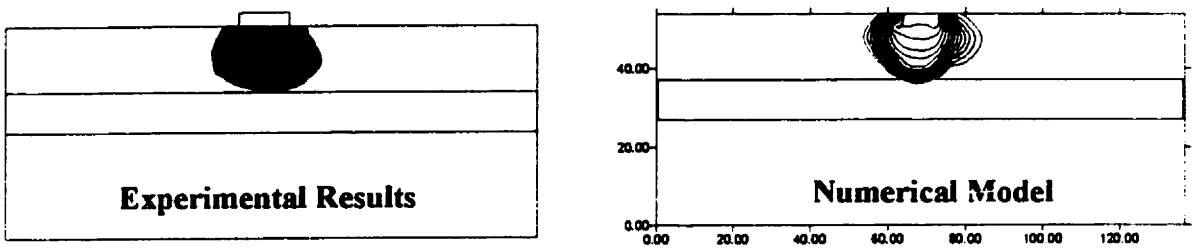

T = 120 sec , Spill Period

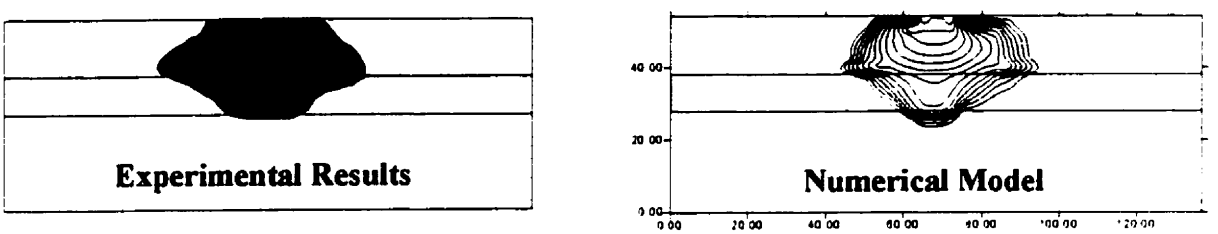

T = 375 sec , End of Spill Period

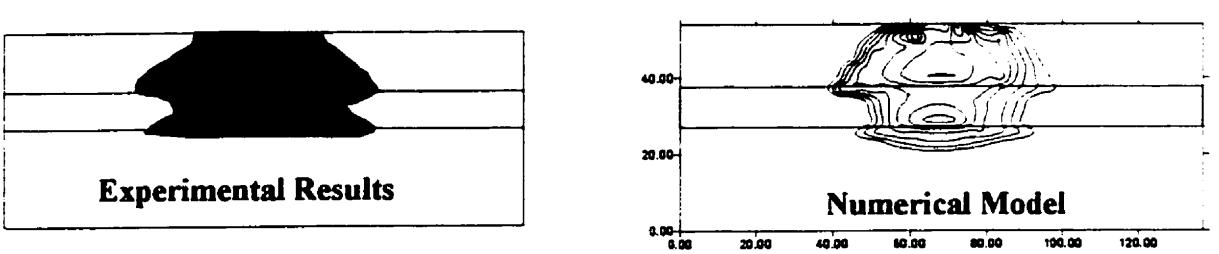

T = 620 sec , Migration Period

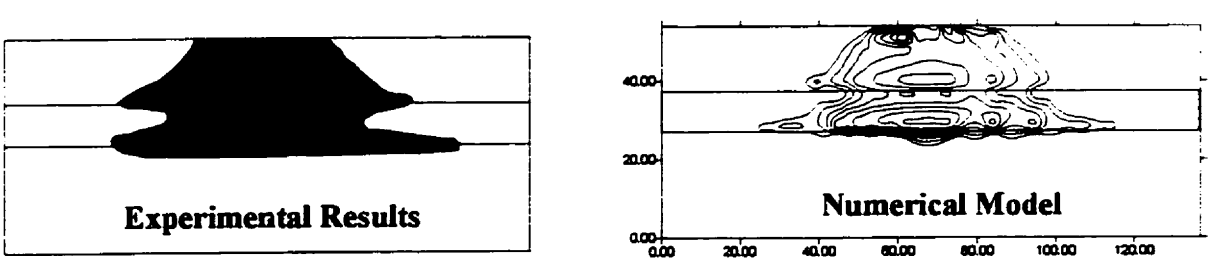

T = 1220 sec , End of Experiment

Figure (6.19) Comparison between numerical and laboratory experimental results

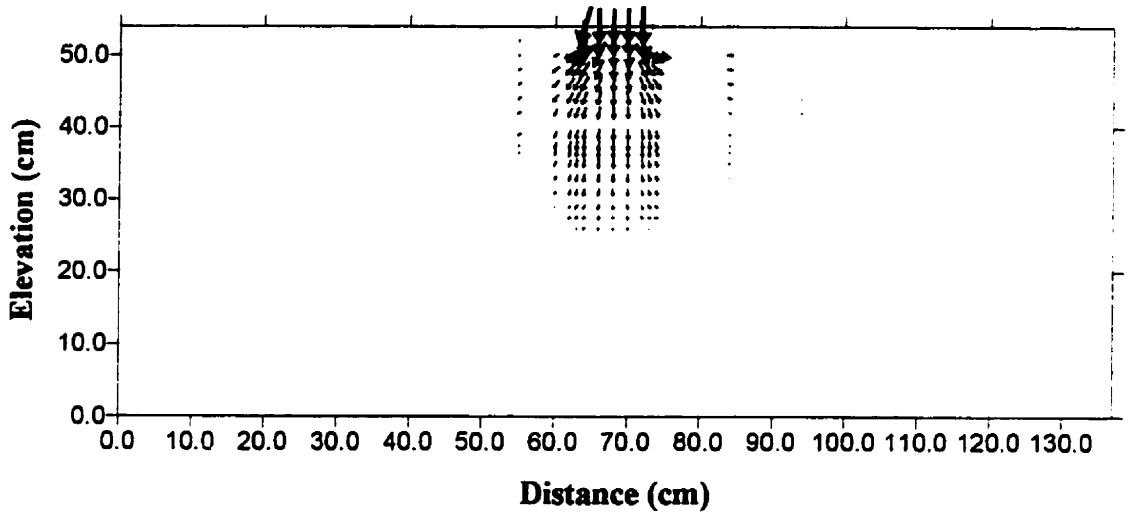

Figure (6.20) Computed NAPL velocity vectors for experimental results at T=375

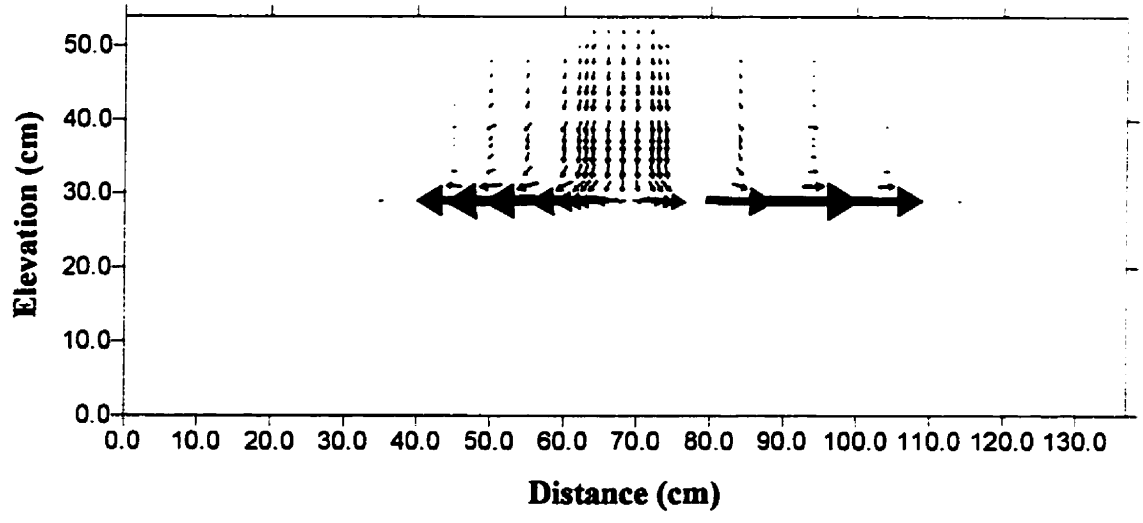

Figure (6.21) Computed NAPL velocity vectors for experimental results at T=1220

CHAPTER VII

SENSIVITY ANALYSIS

Several simulations were carried out in order to determine the sensitivity of the model with respect to the various parameters involved. The parameters of interest were: hydraulic conductivity, porosity, the van Genuchten parameters, and the NAPL hydraulic head. The results of these simulations are illustrated and discussed below.

7.1 Hydraulic conductivity

To illustrate the importance of hydraulic conductivity when modeling NAPL movement, test simulations were performed for the physical situation shown in Figure (7.1). The domain is 10 m long and 5 m tall. A constant water table is maintained at the bottom of the domain. A NAPL due to a spill is supposed to infiltrate into the subsurface from a pool 5 cm depth in the middle of the top boundary. The porosity is equal to 0.43, water residual saturation is 0.09 and NAPL residual saturation is 0.1. The NAPL is considered to be Benzene with specific gravity and viscosity being respectively 0.878 and 0.65 cp. Capillary pressure curve scaling parameters are equal to $\beta_{an} = 2.6075$ $\beta_{nw} = 2.5190$. The soil is assumed to be a homogeneous loamy sand with Van Genuchten parameters α = 12.4 and n = 2.3.

The model was run for 7200 sec for four different hydraulic conductivities as follows:

$$Ks_1 = 2.0\times10^{-5}\ m/s$$

$$Ks_2 = 4.0\times10^{-5}\ m/s$$

$$Ks_3 = 8.0\times10^{-5}\ m/s$$

$$Ks_4 = 8.0\times10^{-4}\ m/s$$

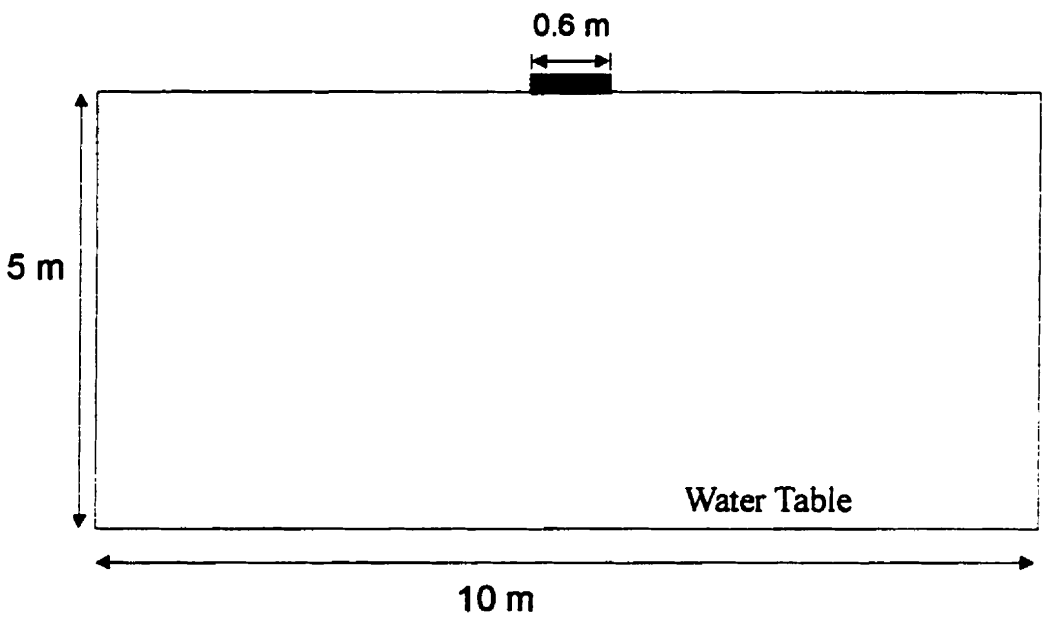

Figure 7.1)Simulation domain for hydraulic conductivity test

The results for these four runs are illustrated in Figure (7.2). Also, Figures (7.3) to (7.6) demonstrate the results in three-dimensional view . Figure (7.7) shows the relationship between hydraulic conductivity and the intruded volume of NAPL

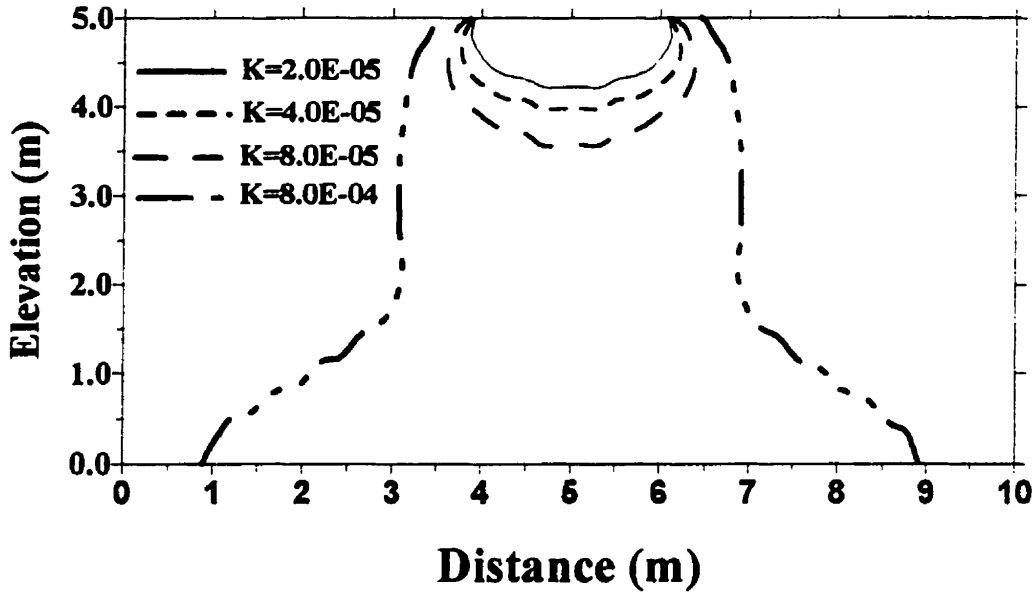

Figure 7.2) NAPL saturation for different hydraulic conductivity

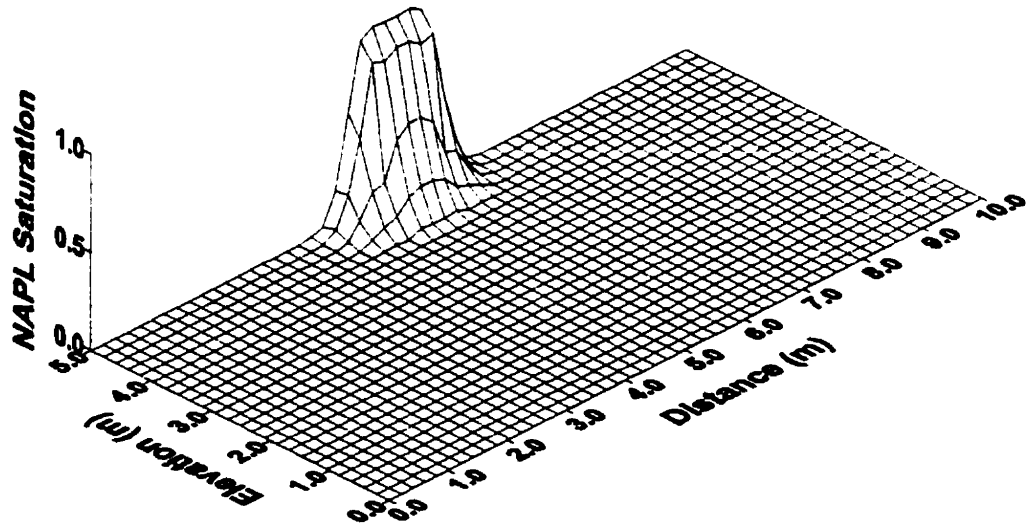

Figure 7.3) NAPL movement with K_s=2.0E-05 m/s

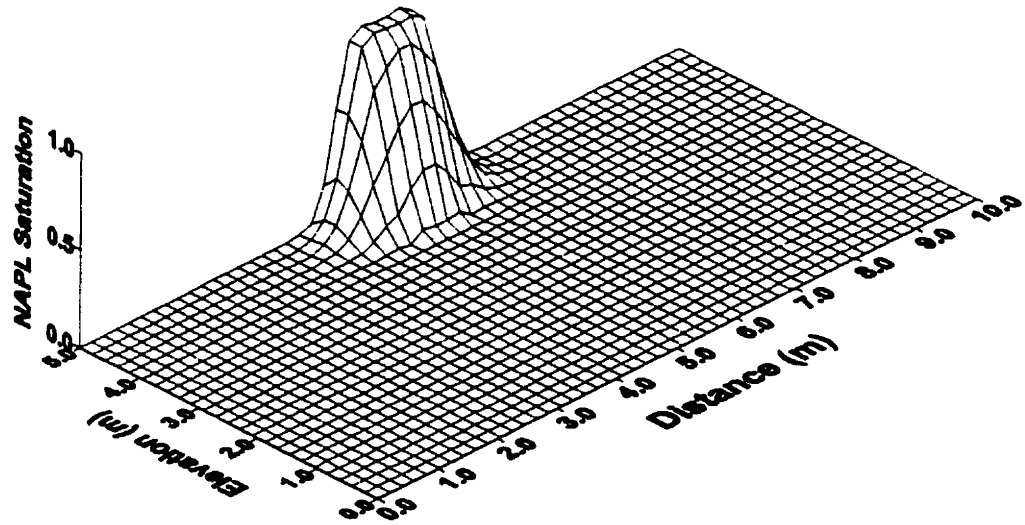

Figure 7.4) NAPL movement with K_s=4.0E-05 m/s

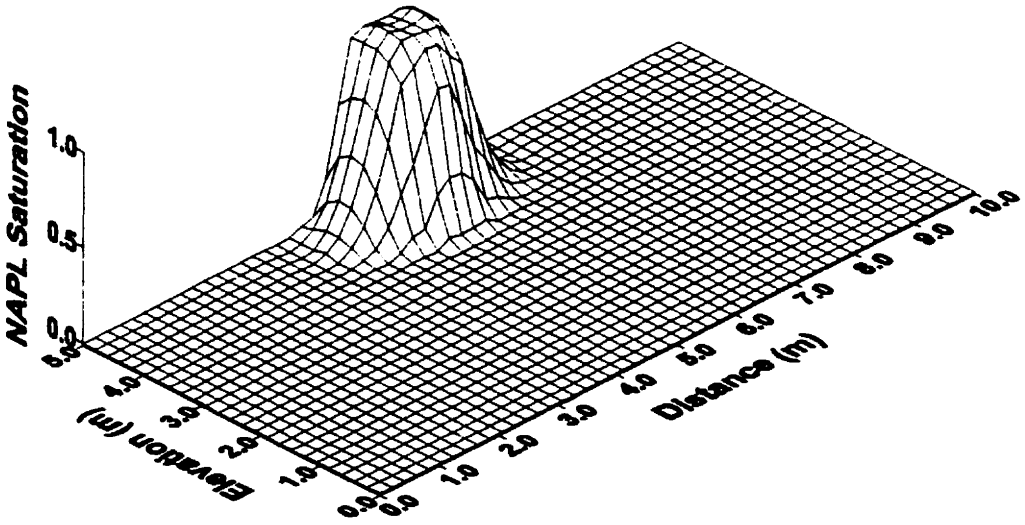

Figure 7.5) NAPL movement with K_s=8.0E-05 m/s

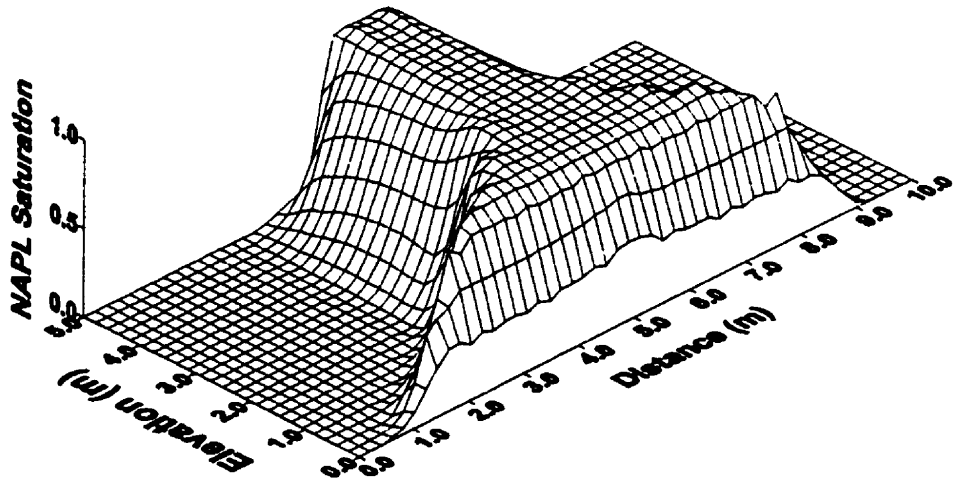

Figure 7.6) NAPL movement with K_s=8.0E-04 m/s

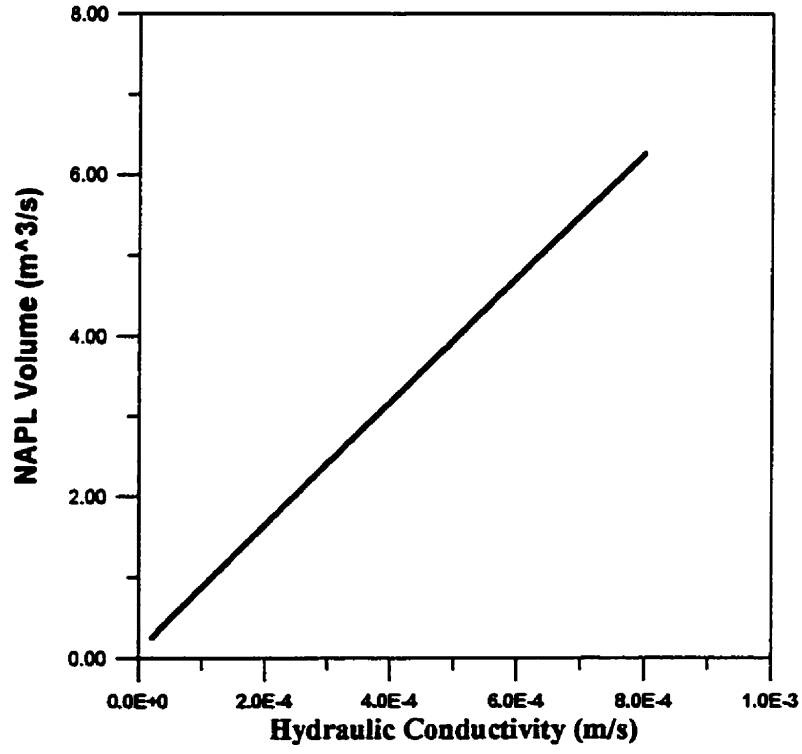

Figure 7.7) Entered NAPL volume and hydraulic conductivity relationship

7.2 Porosity

For this test problem, the same domain and physical properties were used. This time the hydraulic conductivity was kept constant at $K_s = 4.0 \times 10^{-5}$ m/s and the model was run for three different soil porosities, which were 0.30, 0.43, 0.60. Resulting NAPL saturations due to these three simulations have been compared in Figure (7.8). The intruded NAPL volumes are 0.381, 0.413, and 0.451 m^3, respectively.

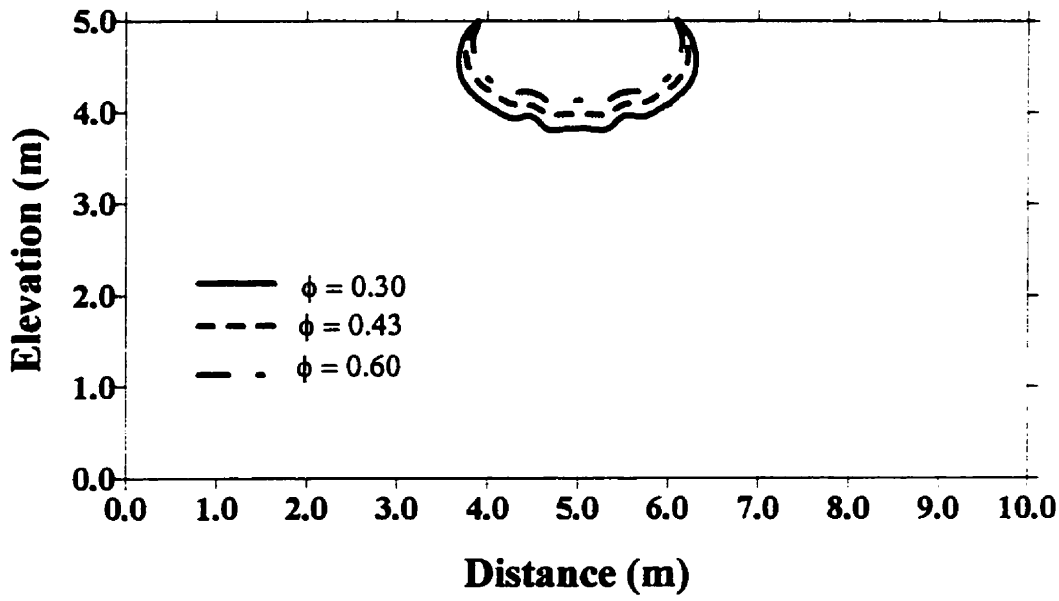

Figure 7.8) NAPL saturation for different Porosity

7.3 Van Genuchten parameters

To investigate whether the constitutive parameters in the van Genuchten relationships have an important effect on the distribution of NAPL in the unsaturated zone, two-dimensional simulations were carried out in the domain displayed in Figure (7.1). The soil hydraulic conductivity was 4.0×10^{-5} m/s and three different sets of VG parameters were chosen:

1) α=0.5 m^{-1}; n=1.1

2) α=3.6 m^{-1}; n=1.6

3) α=12.4 m^{-1}; n=2.3

NAPL saturation distributions in the unsaturated zone are shown in Figure (7.9) and the volume of NAPL at the end of the simulations are 0.081, 0.413, 0.442 m^3 .

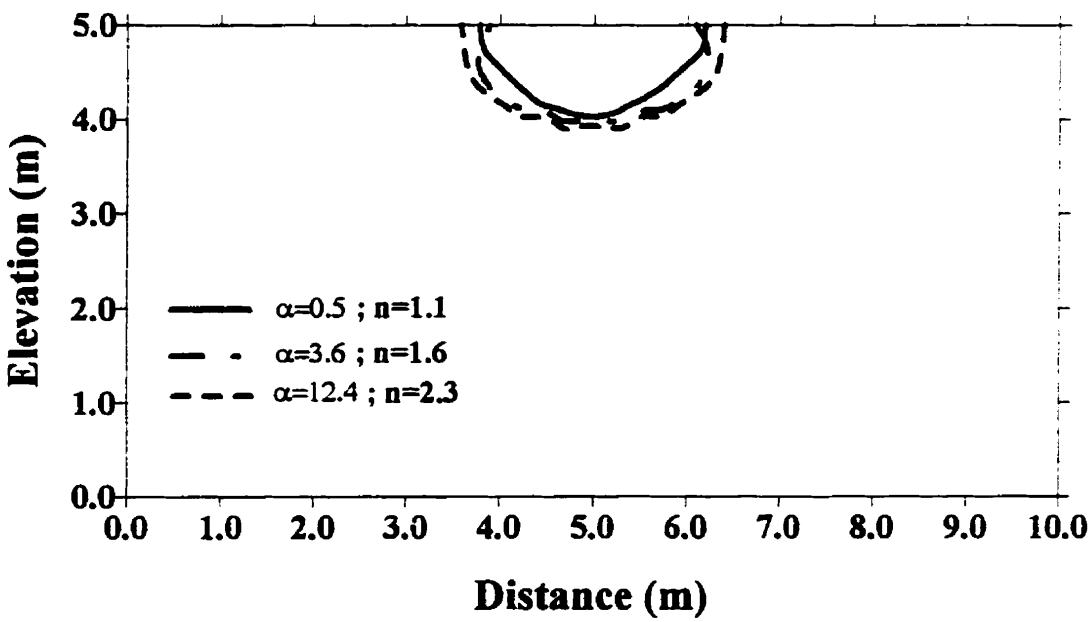

Figure 7.9) NAPL saturation distribution for different VG parameters

7.4 NAPL hydraulic head in infiltration area

In order to illustrate the influence of the NAPL hydraulic head in the infiltration area, the same domain as in previous test was used with different hydraulic heads. Other parameters remained constant and only the hydraulic head was changed to 1, 5, 10, and 20 cm, respectively. The NAPL saturation distributions are shown in Figure (7.10) and NAPL volume for these values were 0.371, 0.413, 0.462, and 0.541, respectively.

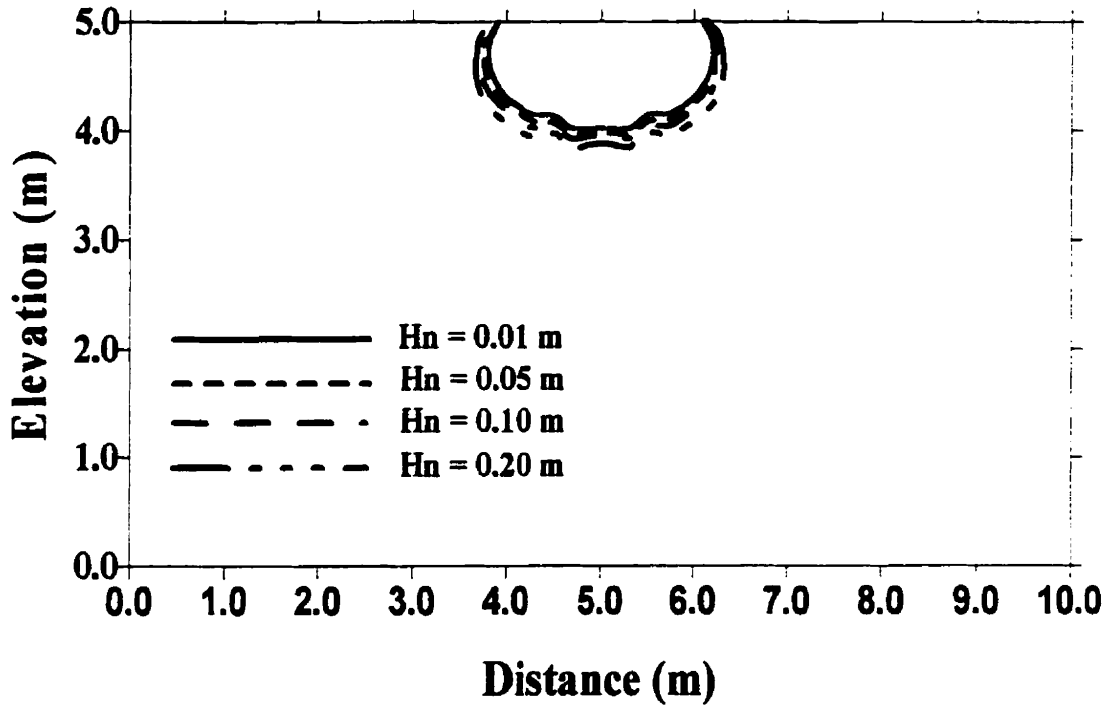

Figure 7.10) NAPL saturation Distribution for different infiltration head

7.5 Discussion

An examination of the results from the numerical simulation clearly indicates the significant influence of the hydraulic conductivity on intrusion depth. An increase in the hydraulic conductivity results in a corresponding increase in NAPL saturation and intruded volume. The results are all the more significant when it is realized that the simulation was run for a period of only two hours. Turning now to the tests using different porosities, it may be seen that the influence of the porosity is much less marked. However, once more it must not be forgotten that the differences are noticeable after only two hours. Typical predictive computations would be executed for a much longer time period, perhaps spanning several years and therefore, it must be concluded that the influence of varying porosity is likely to be significant. The same order of variability in the results are observed with the van Genuchten parameters and with the NAPL hydraulic head.

A general conclusion that may be drawn detailed knowledge of the soil characteristics is desirable in order for any model to provide reliable estimates of NAPL intrusion. In the absence of this detailed data, a sound approach would be to determine the variability of the soil characteristics and provide confidence intervals on the position (and dilution) of the contaminant plume.

CHAPTER VIII

CONCLUSION

In this dissertation, an attempt has been made to numerically simulate the propagation of a multi-phase flow of NAPL in the unsaturated zone of heterogeneous porous media. The model is formulated in a two-dimensional vertical cross section. The mass transfer process, including dissolution of NAPL in the water phase and volatilization of NAPL to the gas phase, is represented by a simple, physically-based first-order mass transfer mechanism in the sink term.

A finite difference scheme using the method of support-operators was applied to discretize the governing partial differential equations. This method which was used for the first time to the field of hydrogeology may be used to construct a finite difference scheme on grids of arbitrary structure. The support-operators method was chosen over the finite element method due to its relative simplicity and the fact that there was no priori reason to expect that finite element methods would afford superior results. A standard argument in support of the finite element method is noting its greater versatility in handling irregular boundaries. Such an argument is no longer valid in the present context, since an irregular mesh may also be handled by the support-operators method. Furthermore, since the method is based on an integral formulation, conservation of variable quantities is assured.

The governing equations were posed in terms of hydraulic pressure heads, since pressure is continuous at fluid and material interfaces.

The support-operators method gives rise to a series of simultaneous algebraic nonlinear equations that must be resolved. A fully coupled Newton-Raphson technique was chosen to handle the nonlinearity and solve the equations sequentially in an iterative fashion. The nonlinearities inherent in the governing equations are the relative permeability $K_{r\alpha}=K_{r\alpha}(h_\alpha)$, saturation $S_\alpha = S_\alpha (h_\alpha)$, and gas phase density $\rho_a = \rho_a (h_a)$. The equations are coupled because in all equations more than one primary variable appears concurrently. The Jacobian matrices were evaluated analytically not only to obtain more stable solutions in heterogeneous soil media but also to speed up the computations.

Three phase permeability-saturation-capillary pressure relations are defined by an extension of the Van Genuchten model. In some situations where one of the fluids in the flow domain approaches irreducible or full saturation, the behavior of the constitutive relationships requires careful handling. These problems were circumvented in the model by imposing upper and lower bounds to the values of these relationships.

Since very few experiments containing a LNAPL flow were available and none of them was done in a heterogeneous porous medium, a laboratory experiment was conducted to provide a better understanding of the physical behavior of multi-phase flow in the

unsaturated zone and verify the model against a heterogeneous case. The experimental investigation contained two main sets of laboratory tests:

1) Some independent tests in order to find the physical characteristics of the soil such as saturated hydraulic conductivity, soil-moisture retention curves, and the dry density;

2) LNAPL flow using n-heptane.

The results of the experiment proved that the NAPL moving downward from a coarse-grained material will encounter a higher entry pressure when a finer-grained layer is contacted. This behavior caused the spreading of heptane above the fine sand at the interface between the coarse and fine sand in the laboratory experiment. The NAPL migrated preferentially along the coarse-grained layer, and did not substantially penetrate the fine-grained layer. The numerical model was able to successfully simulate the experimentally observed behavior of the LNAPL.

Using experimental results and also analytical and experimental works of other researchers, the numerical model was then further calibrated and verified. The model may be used to simulate the complete movement of NAPLs from underground storage tanks or oil spills in variably saturated porous media. It may also be used to analyze two-phase flow of water and NAPL in a system in which gas is either absent or present but at constant pressure. Required input data for flow analysis consists of initial conditions, soil hydraulic properties, fluid properties, time integration parameters, boundary condition

data and mesh geometry. The program will predict the pressure head and saturation of the three phases at every node at specified output intervals. Its numerical scheme, the method of support-operators, allows the model to be applied on an irregular boundary without adding to the complexity of the solution.

The sensitivity analysis of model parameters showed that hydraulic conductivity has the most significant influence on the flow of NAPL compared to the other soil characteristics. High porosity of the media may limit the area of contaminated soil due to its high capacity of containing the pollutant.

It is recommended that further work in this area include the following:

- Addition of a solute transport option to the present model to improve its applicability to real cases so that complete simulation may be realized with a single model.
- Although the model developed in this study takes a variety of complex processes into account there are nevertheless some other processes which should be considered in the modeling of the phenomenon, such as hysteresis, radioactive decay and biodegradation.
- Fractured media is an important source for water supply in many areas and movement of NAPLs in this media needs special consideration. The pattern of NAPL movement and ultimate distribution in fractured geologic media is controlled primarily by the orientation and interconnection of the fractures.

- This investigation could be extended to three-dimensions to study the phenomena more accurately.
- Many NAPLs are mixtures of several chemical compounds. Each compound may have a different solubility or volatility. The chemical composition of NAPL and plume would therefore, change as it migrates within the soil. The laboratory experiment and numerical method may be extended for multi-component fluids which would offer simulations one step closer to reality.

REFERENCES

ABRIOLA, L.M. and PINDER, G.F. (1985a). A multiphase approach to the modelling of porous media contaminated by organic compounds, 1, Equation development. Water Resour. Res. 21(1), 11-18.

ABRIOLA, L.M. and PINDER, G.F. (1985b). A multiphase approach to the modeling of porous media contaminated by organic compounds, 2, Numerical simulation. Water Resour. Res. 21(1), 19-26.

ABU-EL-SHA'R, W.Y. (1993). Experimental assessment of multicomponent gas transport flux mechanisms in subsurface systems. Ph.D. Dissertation, The University of Michigan, USA.

ALFOSSAIL, KHALID ABDULLA (1986). Factors affecting residual wetting phase saturation. Ph.D. Dissertation, University of Southern California, USA.

AL-SHERIADEH, M.S. (1993). Modeling of transport of nonaqueous phase contaminants in heterogeneous aquifers. Ph.D. Dissertation, University of Colorado(Boulder), USA.

ANNABLE, MICHAEL DAVID (1991). Aqueous phase transport in soils contaminated with a multi-component liquid hydrocarbon and subjected to vapor flow. Ph.D. Dissertation, Michigan State university, USA.

ASSOULINE, A., TESSIER, D., and BRUAND, A. (1998). A conceptual model of the soil water retention curve, Water Resour. Res., 34(2), 223-231.

BAEHR, A.L. (1987). Selective transport of hydrocarbons in the unsaturated zone due to aqueous and vapor phase partitioning. Water Resour. Res., 23(10), 1926-1938.

BAEHR, A.L. and CORAPCIOGLU, M.Y. (1987). A compositional multiphase model for groundwater contamination by petroleum products, 2, Numerical solution. Water Resour. Res., 23(1), 201-213.

BEAR, J. (1972). Dynamics of fluids in porous media. American Elsevier, New York, 764p.

BELJIN, M.A. and VAN DER HEIJDE, P.K.M. (1989). Testing, verification, and validation of two-dimensional solute transport models. Groundwater Contamination: Use of Models in Decision Making, Ed. By G. Jousma et. al. Kluwer Academic, 121-137.

BINNING, P.J. (1994). Modeling unsaturated zone flow and contaminant transport in the air and water phases. Ph.D. Dissertation, Princeton University, USA.

BROOKS, R.J. and COREY, A.T. (1964). Hydraulic properties of porous media, Hydro. Pap. 3, Colorado State University, Fort Collins.

BURDINE, N.T. (1953). Relative permeability calculations from pore size distribution data. Trans. AIME 198, 71-78.

BUCKLEY, S.E. and LEVERETT, M.C. (1942). Mechanism of fluid displacement in sands, Am. Inst. Min. Eng., 146, 107-116.

CHANG, C.C. (1991). Multiphase unsaturated zone contaminant transport model for source term definition in ground water. Ph.D. Dissertation, Rice University, USA.

CHARBENEAU, R.J., WEAVER, J.W., and LIEN, B.K. (1995). The hydrocarbon spill screening model (HSSM)-Volume 2: Theoretical background and source codes., U.S. EPA Report EPA/600/R-94/039b, Ada, Oklahama, 259p.

CHILDS E.C. and COLLIS-GEORGE, N. (1950). The permeability of porous materials, Proc. Roy. Soc., Ser. A, 201, 392-405.

CORAPCIOGLU, M.Y. and BAEHR, A.L. (1985). Immiscible contaminant transport in soils and groundwater with an emphasis on gasoline hydrocarbons system of differential equation Vs. single cell model. Water Sci. Technol., 17, 23-37.

CORAPCIOGLU, M.Y. and BAEHR, A.L. (1987). A compositional multiphase model for groundwater contamination by petroleum products: 1, Theoretical considerations. Water Resour. Res., 23(1), 191-200.

COREY, A.T. (1994). Mechanics of immiscible fluids in porous media. Water Resources Publication, Fort Collins, 252 p.

DEMOND, A.H. and ROBERTS, P.V. (1991). Effect of interfacial forces on two-phase capillary pressure-saturation relationships. Water Resour. Res., 27(3), 423-435.

DOMENICO, P.A. and SCHWARTZ, F.W. (1990). Physical and chemical hydrogeology. John Wiley & Sons, New York, 824p.

DRACOS, T. (1978). Theoretical considerations and practical implications on the infiltration of hydrocarbons in aquifers. Proc. IAH Int. Symp. on Ground water pollution by oil hydrocarbons, June 5-9, Prague, pp. 127-137.

EL-KADI, A.I. (1992). Applicability of sharp-interface models for NAPL transport: 1, Infiltration. Ground Water, 30(6), 849-856.

EL-KADI, A.I. (1994). Applicability of sharp-interface models for NAPL transport: 2, Spreading of a LNAPL. Ground Water, 32(5), 784-793.

FALTA, W.R., JAVANDEL, I., PRUESS, K. (1989). Density-driven flow of gas in the unsaturated zone due to the evaporation of volatile organic compounds. Water Resour. Res., 25 (10), 2159-2169.

FALTA, W.R., PRUESS, K., JAVANDEL, I., and WITHERSPOON, P.A. (1989). Numerical modeling of steam injection for the removal of non aqueous phase liquids from the subsurface: 1. Numerical formulation. Water Resour. Res., 28 (2), 433-449.

FAUST, C. (1985). Transport of immiscible fluids within and below the unsaturated zone: A numerical model. Water Resour. Res., 21, 587-596.

FEENSTRA, S., CHERRY, J.A. and PARKER, B. (1996). Conceptual models for behavior of dense non-aqueous phase liquids (DNAPLs) in the subsurface. In: Dense chlorinated solvents and other DNAPLs in groundwater, Eds: Pankow,J.F.; Cherry,J.A., Waterloo Press, Portland, 53-88.

FETTER, C.W. (1993). Contaminant Hydrogeology. Macmillan Pub., New York, 458p.

FIDELIBUS, C. and LENTI, V. (1996). A BEM code for ground-water problems in multizoned domains with normal boundary flux discontinuities, Ground Water, 34(5), 943-948.

FRANKE, O.L., REILLY, T.E., and BENNETT, G.D. (1987). Definition of boundary conditions in the analysis of saturated ground-water flow systems: An introduction, USGS Techniques of Water-Resources Investigations, 03-B5, 15p.

GARDNER, W.R. (1958). Some steady-state solutions of the unsaturated moisture flow equation with application to evaporation from water table, Soil Science, 85, 228-232

GELLER, JIL TALKOVSKY (1990). Dissolution of non-aqueous phase organic liquids in porous media. Ph.D. Dissertation, University of California, Berkeley, USA.

GUARNACCIA, J. and PINDER, G. (1997). NAPL_Simulator Documentation: User's Guide, U.S. EPA , Ada, Oklahoma, 228 p.

HOCHMUTH, D.P. and SUNADA, D.K. (1985). Groundwater model of two phase immiscible flow in coarse material. Ground Water, 23(5), 617-626.

HOLZER, T.L. (1976). Application of groundwater flow theory to a subsurface oil spill. Ground Water, 14(3), 138-145.

HUNT, J.R., SITTAR, N. and UDELL, K.S. (1988). Non-aqueous phase liquid transport and cleanup, 2, Experimental studies. Water Resour. Res., 24(8), 1259-1269.

HUYAKORN, P.S., and PINDER, G.F. (1983). Computational Methods in Subsurface Flow, Academic Press.

JOHNSON, R.L. (1988). Direct comparison of vapor-, free-product and aqueous-phase monitoring for gasoline leaks from underground storage tanks. Proposal submitted to Philip Durgin, Project Officer, U.S. Environmental Protection Agency, Environmental Monitoring Systems Laboratory, Las Vegas.

JOHNSON, T.E. and KREAMER, D.K. (1994). Physical and mathematical modeling of diesel fuel liquid and vapor movement in porous media. Ground Water, 32(4), 551-569.

KALUARACHCHI, J.J. and PARKER, J.C. (1989). An efficient finite element method for modeling multiphase flow. Water Resour. Res., 25(1), 43-54.

KATYAL, A.K., KALUARACHCHI, J.J. and PARKER, J.C. (1991). MOFAT: A two-dimensional finite element program for multiphase flow and multicomponent transport. User's Guide, U.S. EPA , Ada, Oklahoma, 228 p.

KAZDA, I. (1990). Finite element technique in groundwater flow studies. Elsevier Science Publishers, Amsterdam, 313 p.,

KOOL, J.B. and PARKER, J.C. (1987). Development and evaluation of closed-form expressions for hysteretic soil hydraulic properties. Water Resour. Res., 23(1), 105.

KUEPER, B.H. and FRIND, E.O. (1996). Numerical simulation of the migration of Dense Non-Aqueous Phase Liquids (DNAPLs) in porous media. In: Dense chlorinated solvents and other DNAPLs in groundwater, Eds: Pankow,J.F.; Cherry,J.A., Waterloo Press, Portland, 129-144.

KUPPUSAMY, T., SHENG, J.J., PARKER, J.C. and LENHARD, R.J. (1987). Finite element analysis of multiphase immiscible flow through soils. Water Resour. Res., 23, 625-631.

LEVERETT, M.C. (1941). Capillary behavior in porous solids. Trans. AIME, 142, 152-169.

LEVERETT, M.C. and LEWIS, W.B. (1941). Steady flow of gas-oil-water mixtures through unconsolidated sands. Trans. Am. Inst. Min. Metall. Pet. Eng., 142, 107-116.

MACCORMACK, R.W. and PAULLAY, A.J. (1972). Computational efficiency achived by time splitting of finite difference operators, AIAA Paper, 72-154, San Diego.

MCDONALD, P.W. (1971). The computation of transonic flow through two-dimensional gas turbine cascades. ASME Paper, 71-GT-89.

MACKAY, D.M., ROBERTS, P.V. and CHERRY, J.A. (1985). Transport of organic contaminants in groundwater. Environ. Sci. Technol., 19(5), 384-392.

MILINGTON, R.J. and QUIRK, J.P. (1961). Permeability of porous solids. Trans Faraday Soc., 57, 1200-1206.

MUALEM,Y. (1976). A new model for predicting the hydraulic conductivity of unsaturated porous media. Water Resour. Res., 12(3), 513-522.

MULL, R. (1971). Migration of oil products in the subsoil with regard to ground water pollution by oil. In: Advances in water pollution research, Ed: Jenkins,S.H., Pergamon Press, 1-8.

MUNOZ, J.F. and IRARRAZAVAL, M.J. (1998). A numerical model for simulation of bioremediation of hydrocarbons in aquifers. Ground Water, 36(2), 215-224.

NIMMO, J. R., (1991). Comment on the treatment of residual water content in "A consistent set of parametric models for the two-phase flow of immiscible fluids in the subsurface" by L. Luckner et al., Water Resour. Res. , 27 , 661–662.

OSBORNE, M. and SYKES, J. (1986). Numerical Modeling of Immiscible organic transport at the Hyde Park Landfill. Water Resour. Res., 22(1), 25-33.

PARKER, J.C., LENHARD, R.J. and KUPPUSAMY, T. (1987). A parametric model for constitutive properties governing multiphase flow in porous media. Water Resour. Res., 23(4), 618-624.

PINDER, G.F. and ABRIOLA, L.M. (1986). On the simulation of nonaqueous phase organic compounds in the subsurface. Water Resour. Res., 22(9), 109S-119S.

RAJAPAKSA, YATENDRA (1988). Finite element modeling of flow of immiscible fluids in heteregeneous, irregular shaped reservoirs using a self-adapting mesh. Ph.D. Dissertation, The University of Oklahama, USA.

REIBLE, D. and ILLANGASEKARE, T. (1989). Subsurface processes of non-aqueous phase contaminants. In: Intermedia pollutant transport: Modeling and field measurements, Eds: D.T. Allen, Y. Cohen and I.R. Kaplan, Plenum, New York.

ROCKHOLD, M.L., SIMMONS, C.S. and FAYER, M.J., (1997). An analytical solution technique for one-dimensional, steady vertical water flow in layered soils. Water Resour. Res., 33(4), 897-902.

ROSS, P. J., J. WILLIAMS, and K. L. BRISTOW, (1991). Equations for extending water-retention curves to dryness, Soil Sci. Soc. Am. J. , 55, 923–927.

RYAN, P.A. and COHEN, Y. (1991). One-dimensional subsurface transport of a non-aqueous phase liquid containing sparingly water soluble organics: A front-Tracking model. Water Resour. Res., 27(7), 1487-1500.

SAMARSKII, A.A., TISHKIN, V.F., FAVORSKII, A.P., and SHASHKOV, M. (1981). Operational finite difference schemes, Diff. Eqns., 17(7), 854-862.

SAMARSKII, A.A., TISHKIN, V.F., FAVORSKII, A.P., and SHASHKOV, M. (1982). Employment of the Reference-operator method in the construction of finite difference analogs of tensor operations, Diff. Eqns., 18(7), 881-885.

SHASHKOV, M. (1996). Conservative finite-difference methods on general grids, CRC Press, New York, 359 p.

SHENG, J. (1986). Multiphase immiscible flow through porous media. Ph.D. Dissertation, Virginia Polytechnic Institute and State University. 146 p.

SLEEP, B.E. and SYKES, J.F. (1989). Modeling the transport of volatile organics in variably saturated media. Water Resour. Res., 25(1), 81-92.

STONE, H.L. (1973). Estimation of three-phase relative permeability and residual oil data. J. Can. Petrol. Technol., 12, 53-61.

SWALLOW, J.A. and GSCHWEND, P.M. (1983). Volatilization of organic compounds from unconfined aquifers. Proceedings from the third National Symposium on Aquifer Restoration and Groundwater Monitoring, National Water Well Assoc., 327-333.

VAN DAM, J. (1967). The migration of hydrocarbons in a water bearing stratum, The Joint Problems of the Oil and Water Industries, P. Hepple, Elsevier Science Publishers, 55-96.

VAN DER HEIJDE, P.K.M., HUYAKORN, P.S. and MERCER, J.W. (1984). Testing and validation of groundwater models. Proc. Practical Applications of Ground-Water Modeling, NWWA/IGWMC Conference, Columbus, OH, Aug. 19-20.

VAN DER WAARDEN, M., BRIDIE, A.L.A.M. and GROENWOUD, W.M. (1971). Transport of mineral oil components to groundwater, I, Model experiments on the transfer of hydrocarbons from a residual oil zone to trickling water. Water Res., 5(5), 213-226.

VAN GEEL, P.J and SYKES, J.F. (1995a). Laboratory and model simulations of a LNAPL spill in a variably-saturated sand: 1. Laboratory experiment and image analysis techniques. Journal of Contaminant Hydrology, 17(1), 1-25.

VAN GEEL, P.J and SYKES, J.F. (1995b). Laboratory and model simulations of a LNAPL spill in a variably-saturated sand: 2. Comparison of laboratory and model results, Journal of Contaminant Hydrology, 17(1), 27-53.

VAN GENUCHTEN, M.Th, (1980). A closed-form equation for predicting the hydraulic conductivity of unsaturated soils. Soil Sci. Soc. Am. J., 44, 892-899.

VAN GENUCHTEN, M.Th, LEIJ, F.J., YATES, S.R., (1980). The RETC code for quantifying the hydraulic functions of unsaturated soils, US-EPA, EPA/600/2-91/065, 92 pp.

WADDILL, D.W. and PARKER, J.C., (1997). A semianalytical model to predict recovery of light, nonaqueous phase liquids from unconfined aquifers, Ground Water, 35(2), 280-290.

WEAVER, J.W., CHARBENEAU, R.J., LIEN, B.K., and PROVOST, J.B. (1994). The hydrocarbon spill screening model (HSSM)-Volume 1: User's guide. U.S. EPA Report EPA/600/R-94/039a, 212p.

WIERENGA, P.J., BACHELET, D., BILSJIE, J.R., ELABD, D.B., HUDSON, D.B., NASH, M., PORRO, I., STRONG, W.R., TOORMAN, A. and VINSON, J. (1988). Validation of stochastic flow and transport models for unsaturated soils, Res. Rep. 88-SS-03, 224 pp., New Mexico St. Univ., Las Cruces, USA.

WU, Y.S., HUYAKORN, P.S. and PARK, N.S. (1994). A vertical equilibrium model for assessing nonaqueous phase liquid contamination and remediation of groundwater systems. Water Resour. Res., 30(4), 903-912.

ZHOU, JUN (1994). Numerical and experimental analysis of diesel and JP-5 transport in unsaturated soils. Ph.D. Dissertation, University of California, Los Angeles, USA.

APPENDIX I: JACOBIAN MATRIX COMPONENTS

For (i=2,…,M-1; k=2,…N-1) the derivatives of equation (4.8) for Jacobean matrix are as follows:

$$\frac{\partial F}{\partial h_{i+1,k-1}} = -\frac{1}{4}\frac{1}{VN_{i,k}}\left[\left(x_{i-1,k}-x_{i,k-1}\right)^2\frac{Kz_{i-1,k-1}}{\Omega_{i-1,k-1}}\right.$$
$$\left.-2\left(x_{i-1,k}-x_{i,k-1}\right)\left(z_{i-1,k}-z_{i,k-1}\right)\frac{Kxz_{i-1,k-1}}{\Omega_{i-1,k-1}}+\left(z_{i+1,k}-z_{i,k-1}\right)^2\frac{Kx_{i,k-1}}{\Omega_{i,k-1}}\right]$$

$$\frac{\partial F}{\partial h_{i,k-1}} = \frac{1}{4}\frac{1}{VN_{i,k}}\left[\left(x_{i-1,k}-x_{i,k-1}\right)\left(x_{i,k}-x_{i-1,k-1}\right)\frac{Kz_{i-1,k-1}}{\Omega_{i-1,k-1}}\right.$$
$$+\left(x_{i-1,k}-x_{i,k-1}\right)\left(z_{i,k}-z_{i-1,k-1}\right)\frac{Kxz_{i-1,k-1}}{\Omega_{i-1,k-1}}-\left(x_{i+1,k}-x_{i,k-1}\right)\left(x_{i,k}-x_{i+1,k-1}\right)\frac{Kz_{i,k-1}}{\Omega_{i,k-1}}$$
$$-\left(x_{i+1,k}-x_{i,k-1}\right)\left(z_{i,k}-z_{i+1,k-1}\right)\frac{Kxz_{i,k-1}}{\Omega_{i,k-1}}+\left(z_{i-1,k}-z_{i,k-1}\right)\left(z_{i,k}-z_{i-1,k-1}\right)\frac{Kx_{i-1,k-1}}{\Omega_{i-1,k-1}}$$
$$+\left(z_{i-1,k}-z_{i,k-1}\right)\left(x_{i,k}-x_{i-1,k-1}\right)\frac{Kxz_{i-1,k-1}}{\Omega_{i-1,k-1}}-\left(z_{i+1,k}-z_{i,k-1}\right)\left(z_{i,k}-z_{i+1,k-1}\right)\frac{Kx_{i,k-1}}{\Omega_{i,k-1}}$$
$$\left.-\left(z_{i+1,k}-z_{i,k-1}\right)\left(x_{i,k}-x_{i+1,k-1}\right)\frac{Kxz_{i,k-1}}{\Omega_{i,k-1}}\right]$$

$$\frac{\partial F}{\partial h_{i+1,k-1}} = \frac{1}{4}\frac{1}{VN_{i,k}}\left[\left(x_{i+1,k}-x_{i,k-1}\right)^2\frac{Kz_{i,k-1}}{\Omega_{i,k-1}}\right.$$
$$\left.+2\left(x_{i+1,k}-x_{i,k-1}\right)\left(z_{i+1,k}-z_{i,k-1}\right)\frac{Kxz_{i,k-1}}{\Omega_{i,k-1}}+\left(z_{i+1,k}-z_{i,k-1}\right)^2\frac{Kx_{i,k-1}}{\Omega_{i,k-1}}\right]$$

$$\frac{\partial F}{\partial h_{i-1,k}} = -\frac{1}{4}\frac{1}{VN_{i,k}}\left[\left(x_{i-1,k}-x_{i,k-1}\right)\left(x_{i,k}-x_{i-1,k-1}\right)\frac{Kz_{i-1,k-1}}{\Omega_{i-1,k-1}}\right.$$
$$+\left(x_{i-1,k}-x_{i,k-1}\right)\left(z_{i,k}-z_{i-1,k-1}\right)\frac{Kxz_{i-1,k-1}}{\Omega_{i-1,k-1}}+\left(x_{i,k+1}-x_{i-1,k}\right)\left(x_{i-1,k+1}-x_{i,k}\right)\frac{Kz_{i-1,k}}{\Omega_{i-1,k}}$$
$$+\left(x_{i,k+1}-x_{i-1,k}\right)\left(z_{i-1,k+1}-z_{i,k}\right)\frac{Kxz_{i-1,k}}{\Omega_{i-1,k}}+\left(z_{i-1,k}-z_{i,k-1}\right)\left(z_{i,k}-z_{i-1,k-1}\right)\frac{Kx_{i-1,k-1}}{\Omega_{i-1,k-1}}$$
$$+\left(z_{i-1,k}-z_{i,k-1}\right)\left(x_{i,k}-x_{i-1,k-1}\right)\frac{Kxz_{i-1,k-1}}{\Omega_{i-1,k-1}}+\left(z_{i,k+1}-z_{i-1,k}\right)\left(z_{i-1,k+1}-z_{i,k}\right)\frac{Kx_{i-1,k}}{\Omega_{i-1,k}}$$
$$\left.+\left(z_{i,k+1}-z_{i-1,k}\right)\left(x_{i-1,k+1}-x_{i,k}\right)\frac{Kxz_{i-1,k}}{\Omega_{i-1,k}}\right]$$

$$\frac{\partial F}{\partial h_{i,k}} = \frac{1}{4}\frac{1}{VN_{i,k}}\left[\left(x_{i-1,k}-x_{i,k-1}\right)^2\frac{Kz_{i-1,k-1}}{\Omega_{i-1,k-1}}-\left(x_{i,k+1}-x_{i+1,k}\right)^2\frac{Kz_{i,k}}{\Omega_{i,k}}\right.$$
$$-\left(x_{i+1,k}-x_{i,k-1}\right)^2\frac{Kz_{i,k-1}}{\Omega_{i,k-1}}+\left(x_{i,k+1}-x_{i-1,k}\right)^2\frac{Kz_{i-1,k}}{\Omega_{i-1,k}}+\left(z_{i-1,k}-z_{i,k-1}\right)^2\frac{Kx_{i-1,k-1}}{\Omega_{i-1,k-1}}$$
$$\left.-\left(z_{i,k+1}-z_{i+1,k}\right)^2\frac{Kx_{i,k}}{\Omega_{i,k}}+\left(x_{i+1,k}-x_{i,k-1}\right)^2\frac{Kx_{i,k-1}}{\Omega_{i,k-1}}+\left(z_{i,k+1}-z_{i-1,k}\right)^2\frac{Kx_{i-1,k}}{\Omega_{i-1,k}}\right]$$

$$\frac{\partial F}{\partial h_{i+1,k}} = \frac{1}{4}\frac{1}{VN_{i,k}}\left[\left(x_{i,k+1}-x_{i+1,k}\right)\left(x_{i+1,k+1}-x_{i,k}\right)\frac{Kz_{i,k}}{\Omega_{i,k}}+\left(x_{i,k+1}-x_{i+1,k}\right)\left(z_{i+1,k+1}-z_{i,k}\right)\frac{Kxz_{i,k}}{\Omega_{i,k}}\right.$$
$$+\left(x_{i+1,k}-x_{i,k-1}\right)\left(x_{i,k}-x_{i+1,k-1}\right)\frac{Kz_{i,k-1}}{\Omega_{i,k-1}}+\left(x_{i+1,k}-x_{i,k-1}\right)\left(z_{i,k}-z_{i+1,k-1}\right)\frac{Kxz_{i,k-1}}{\Omega_{i,k-1}}$$
$$+\left(z_{i,k+1}-z_{i+1,k}\right)\left(z_{i+1,k+1}-z_{i,k}\right)\frac{Kx_{i,k}}{\Omega_{i,k}}+\left(z_{i,k+1}-z_{i+1,k}\right)\left(x_{i+1,k+1}-x_{i,k}\right)\frac{Kxz_{i,k}}{\Omega_{i,k}}$$
$$\left.+\left(z_{i+1,k}-z_{i,k-1}\right)\left(z_{i,k}-z_{i+1,k-1}\right)\frac{Kx_{i,k-1}}{\Omega_{i,k-1}}+\left(z_{i+1,k}-z_{i,k-1}\right)\left(x_{i,k}-x_{i+1,k-1}\right)\frac{Kxz_{i,k-1}}{\Omega_{i,k-1}}\right]$$

$$\frac{\partial F}{\partial h_{i-1,k+1}} = -\frac{1}{4}\frac{1}{VN_{i,k}}\left[\left(x_{i,k+1}-x_{i-1,k}\right)^2\frac{Kz_{i-1,k}}{\Omega_{i-1,k}} - 2\left(x_{i,k+1}-x_{i-1,k}\right)\left(z_{i,k+1}-z_{i-1,k}\right)\frac{Kxz_{i-1,k}}{\Omega_{i-1,k}} + \left(z_{i,k+1}-z_{i-1,k}\right)^2\frac{Kx_{i-1,k}}{\Omega_{i-1,k}}\right]$$

$$\begin{aligned}\frac{\partial F}{\partial h_{i,k+1}} = \frac{1}{4}\frac{1}{VN_{i,k}}\Big[&\left(x_{i,k+1}-x_{i-1,k}\right)\left(x_{i-1,k+1}-x_{i,k}\right)\frac{Kz_{i-1,k}}{\Omega_{i-1,k}} + \left(x_{i,k+1}-x_{i-1,k}\right)\left(z_{i-1,k+1}-z_{i,k}\right)\frac{Kxz_{i-1,k}}{\Omega_{i-1,k}}\\ &-\left(x_{i,k+1}-x_{i+1,k}\right)\left(x_{i+1,k+1}-x_{i,k}\right)\frac{Kz_{i,k}}{\Omega_{i,k}} - \left(x_{i,k+1}-x_{i+1,k}\right)\left(z_{i+1,k+1}-z_{i,k}\right)\frac{Kxz_{i,k}}{\Omega_{i,k}}\\ &+\left(z_{i,k+1}-z_{i-1,k}\right)\left(z_{i-1,k+1}-z_{i,k}\right)\frac{Kx_{i-1,k}}{\Omega_{i-1,k}} + \left(z_{i,k+1}-z_{i-1,k}\right)\left(x_{i-1,k+1}-x_{i,k}\right)\frac{Kxz_{i-1,k}}{\Omega_{i-1,k}}\\ &+\left(z_{i,k+1}-z_{i+1,k}\right)\left(z_{i+1,k+1}-z_{i,k}\right)\frac{Kx_{i,k}}{\Omega_{i,k}} + \left(z_{i,k+1}-z_{i+1,k}\right)\left(x_{i+1,k+1}-x_{i,k}\right)\frac{Kxz_{i,k}}{\Omega_{i,k}}\Big]\end{aligned}$$

$$\frac{\partial F}{\partial h_{i+1,k+1}} = \frac{1}{4}\frac{1}{VN_{i,k}}\left[\left(x_{i,k+1}-x_{i+1,k}\right)^2\frac{Kz_{i,k}}{\Omega_{i,k}} + 2\left(x_{i,k+1}-x_{i+1,k}\right)\left(z_{i,k+1}-z_{i+1,k}\right)\frac{Kxz_{i,k}}{\Omega_{i,k}} + \left(z_{i,k+1}-z_{i+1,k}\right)^2\frac{Kx_{i,k}}{\Omega_{i,k}}\right]$$

For boundary nodes, (i=1; k=2,N-1) we get the following non-zero components:

$$\frac{\partial F}{\partial h_{i,k-1}} = \frac{1}{4}\frac{1}{VN_{i,k}}\left[-\left(x_{i+1,k}-x_{i,k-1}\right)\left(x_{i,k}-x_{i+1,k-1}\right)\frac{Kz_{i,k-1}}{\Omega_{i,k-1}} - \left(x_{i+1,k}-x_{i,k-1}\right)\left(z_{i,k}-z_{i+1,k-1}\right)\frac{Kxz_{i,k-1}}{\Omega_{i,k-1}} - \left(z_{i+1,k}-z_{i,k-1}\right)\left(z_{i,k}-z_{i+1,k-1}\right)\frac{Kx_{i,k-1}}{\Omega_{i,k-1}} - \left(z_{i+1,k}-z_{i,k-1}\right)\left(x_{i,k}-x_{i+1,k-1}\right)\frac{Kxz_{i,k-1}}{\Omega_{i,k-1}}\right]$$

$$\frac{\partial F}{\partial h_{i,k}} = \frac{1}{4}\frac{1}{VN_{i,k}}\left[-\left(x_{i,k+1}-x_{i+1,k}\right)^2\frac{Kz_{i,k}}{\Omega_{i,k}}-\left(x_{i+1,k}-x_{i,k-1}\right)^2\frac{Kz_{i,k-1}}{\Omega_{i,k-1}}\right.$$
$$\left.-\left(z_{i,k+1}-z_{i+1,k}\right)^2\frac{Kx_{i,k}}{\Omega_{i,k}}+\left(x_{i+1,k}-x_{i,k-1}\right)^2\frac{Kx_{i,k-1}}{\Omega_{i,k-1}}\right]$$

$$\frac{\partial F}{\partial h_{i+1,k-1}} = \frac{1}{4}\frac{1}{VN_{i,k}}\left[\left(x_{i+1,k}-x_{i,k-1}\right)^2\frac{Kz_{i,k-1}}{\Omega_{i,k-1}}\right.$$
$$\left.+2\left(x_{i+1,k}-x_{i,k-1}\right)\left(z_{i+1,k}-z_{i,k-1}\right)\frac{Kxz_{i,k-1}}{\Omega_{i,k-1}}+\left(z_{i+1,k}-z_{i,k-1}\right)^2\frac{Kx_{i,k-1}}{\Omega_{i,k-1}}\right]$$

$$\frac{\partial F}{\partial h_{i,k+1}} = \frac{1}{4}\frac{1}{VN_{i,k}}\left[-\left(x_{i,k+1}-x_{i+1,k}\right)\left(x_{i+1,k+1}-x_{i,k}\right)\frac{Kz_{i,k}}{\Omega_{i,k}}\right.$$
$$-\left(x_{i,k+1}-x_{i+1,k}\right)\left(z_{i+1,k+1}-z_{i,k}\right)\frac{Kxz_{i,k}}{\Omega_{i,k}}+\left(z_{i,k+1}-z_{i+1,k}\right)\left(z_{i+1,k+1}-z_{i,k}\right)\frac{Kx_{i,k}}{\Omega_{i,k}}$$
$$\left.+\left(z_{i,k+1}-z_{i+1,k}\right)\left(x_{i+1,k+1}-x_{i,k}\right)\frac{Kxz_{i,k}}{\Omega_{i,k}}\right]$$

$$\frac{\partial F}{\partial h_{i+1,k}} = \frac{1}{4}\frac{1}{VN_{i,k}}\left[\left(x_{i,k+1}-x_{i+1,k}\right)\left(x_{i+1,k+1}-x_{i,k}\right)\frac{Kz_{i,k}}{\Omega_{i,k}}+\left(x_{i,k+1}-x_{i+1,k}\right)\left(z_{i+1,k+1}-z_{i,k}\right)\frac{Kxz_{i,k}}{\Omega_{i,k}}\right.$$
$$+\left(x_{i+1,k}-x_{i,k-1}\right)\left(x_{i,k}-x_{i+1,k-1}\right)\frac{Kz_{i,k-1}}{\Omega_{i,k-1}}+\left(x_{i+1,k}-x_{i,k-1}\right)\left(z_{i,k}-z_{i+1,k-1}\right)\frac{Kxz_{i,k-1}}{\Omega_{i,k-1}}$$
$$+\left(z_{i,k+1}-z_{i+1,k}\right)\left(z_{i+1,k+1}-z_{i,k}\right)\frac{Kx_{i,k}}{\Omega_{i,k}}+\left(z_{i,k+1}-z_{i+1,k}\right)\left(x_{i+1,k+1}-x_{i,k}\right)\frac{Kxz_{i,k}}{\Omega_{i,k}}$$
$$\left.+\left(z_{i+1,k}-z_{i,k-1}\right)\left(z_{i,k}-z_{i+1,k-1}\right)\frac{Kx_{i,k-1}}{\Omega_{i,k-1}}+\left(z_{i+1,k}-z_{i,k-1}\right)\left(x_{i,k}-x_{i+1,k-1}\right)\frac{Kxz_{i,k-1}}{\Omega_{i,k-1}}\right]$$

$$\frac{\partial F}{\partial h_{i+1,k+1}} = \frac{1}{4}\frac{1}{VN_{i,k}}\left[\left(x_{i,k+1}-x_{i+1,k}\right)^2\frac{Kz_{i,k}}{\Omega_{i,k}} + 2\left(x_{i,k+1}-x_{i+1,k}\right)\left(z_{i,k+1}-z_{i+1,k}\right)\frac{Kxz_{i,k}}{\Omega_{i,k}} + \left(z_{i,k+1}-z_{i+1,k}\right)^2\frac{Kx_{i,k}}{\Omega_{i,k}}\right]$$

$$\frac{\partial F}{\partial h_{i-1,k-1}} = 0 \;\; ; \;\; \frac{\partial F}{\partial h_{i-1,k}} = 0 \;\; ; \;\; \frac{\partial F}{\partial h_{i-1,k+1}} = 0$$

For (i=2,...M ; k=1), we get:

$$\frac{\partial F}{\partial h_{i-1,k}} = -\frac{1}{4}\frac{1}{VN_{i,k}}\left[+\left(x_{i,k+1}-x_{i-1,k}\right)\left(x_{i-1,k+1}-x_{i,k}\right)\frac{Kz_{i-1,k}}{\Omega_{i-1,k}} + \left(x_{i,k+1}-x_{i-1,k}\right)\left(z_{i-1,k+1}-z_{i,k}\right)\frac{Kxz_{i-1,k}}{\Omega_{i-1,k}} + \left(z_{i,k+1}-z_{i-1,k}\right)\left(z_{i-1,k+1}-z_{i,k}\right)\frac{Kx_{i-1,k}}{\Omega_{i-1,k}} + \left(z_{i,k+1}-z_{i-1,k}\right)\left(x_{i,k}-x_{i+1,k-1}\right)\frac{Kxz_{i,k-1}}{\Omega_{i,k-1}}\right]$$

$$\frac{\partial F}{\partial h_{i,k}} = \frac{1}{4}\frac{1}{VN_{i,k}}\left[-\left(x_{i,k+1}-x_{i+1,k}\right)^2\frac{Kz_{i,k}}{\Omega_{i,k}} + \left(x_{i,k+1}-x_{i-1,k}\right)^2\frac{Kz_{i-1,k}}{\Omega_{i-1,k}} - \left(z_{i,k+1}-z_{i+1,k}\right)^2\frac{Kx_{i,k}}{\Omega_{i,k}} + \left(z_{i,k+1}-z_{i-1,k}\right)^2\frac{Kx_{i-1,k}}{\Omega_{i-1,k}}\right]$$

$$\frac{\partial F}{\partial h_{i+1,k}} = \frac{1}{4}\frac{1}{VN_{i,k}}\left[\left(x_{i,k+1}-x_{i+1,k}\right)\left(x_{i+1,k+1}-x_{i,k}\right)\frac{Kz_{i,k}}{\Omega_{i,k}} + \left(x_{i,k+1}-x_{i+1,k}\right)\left(z_{i+1,k+1}-z_{i,k}\right)\frac{Kxz_{i,k}}{\Omega_{i,k}} + \left(z_{i,k+1}-z_{i+1,k}\right)\left(z_{i+1,k+1}-z_{i,k}\right)\frac{Kx_{i,k}}{\Omega_{i,k}} + \left(z_{i,k+1}-z_{i+1,k}\right)\left(x_{i+1,k+1}-x_{i,k}\right)\frac{Kxz_{i,k}}{\Omega_{i,k}}\right]$$

$$\frac{\partial F}{\partial h_{i-1,k+1}} = -\frac{1}{4}\frac{1}{VN_{i,k}}\left[\left(x_{i,k+1}-x_{i-1,k}\right)^2\frac{Kz_{i-1,k}}{\Omega_{i-1,k}} - 2\left(x_{i,k+1}-x_{i-1,k}\right)\left(z_{i,k+1}-z_{i-1,k}\right)\frac{Kxz_{i-1,k}}{\Omega_{i-1,k}} + \left(z_{i,k+1}-z_{i-1,k}\right)^2\frac{Kx_{i-1,k}}{\Omega_{i-1,k}}\right]$$

$$\begin{aligned}\frac{\partial F}{\partial h_{i,k+1}} = \frac{1}{4}\frac{1}{VN_{i,k}}\Big[&\left(x_{i,k+1}-x_{i-1,k}\right)\left(x_{i-1,k+1}-x_{i,k}\right)\frac{Kz_{i-1,k}}{\Omega_{i-1,k}} + \left(x_{i,k+1}-x_{i-1,k}\right)\left(z_{i-1,k+1}-z_{i,k}\right)\frac{Kxz_{i-1,k}}{\Omega_{i-1,k}}\\ &-\left(x_{i,k+1}-x_{i+1,k}\right)\left(x_{i+1,k+1}-x_{i,k}\right)\frac{Kz_{i,k}}{\Omega_{i,k}} - \left(x_{i,k+1}-x_{i+1,k}\right)\left(z_{i+1,k+1}-z_{i,k}\right)\frac{Kxz_{i,k}}{\Omega_{i,k}}\\ &+\left(z_{i,k+1}-z_{i-1,k}\right)\left(z_{i-1,k+1}-z_{i,k}\right)\frac{Kx_{i-1,k}}{\Omega_{i-1,k}} + \left(z_{i,k+1}-z_{i-1,k}\right)\left(x_{i-1,k+1}-x_{i,k}\right)\frac{Kxz_{i-1,k}}{\Omega_{i-1,k}}\\ &+\left(z_{i,k+1}-z_{i+1,k}\right)\left(z_{i+1,k+1}-z_{i,k}\right)\frac{Kx_{i,k}}{\Omega_{i,k}} + \left(z_{i,k+1}-z_{i+1,k}\right)\left(x_{i+1,k+1}-x_{i,k}\right)\frac{Kxz_{i,k}}{\Omega_{i,k}}\Big]\end{aligned}$$

$$\frac{\partial F}{\partial h_{i+1,k+1}} = \frac{1}{4}\frac{1}{VN_{i,k}}\left[\left(x_{i,k+1}-x_{i+1,k}\right)^2\frac{Kz_{i,k}}{\Omega_{i,k}} + 2\left(x_{i,k+1}-x_{i+1,k}\right)\left(z_{i,k+1}-z_{i+1,k}\right)\frac{Kxz_{i,k}}{\Omega_{i,k}} + \left(z_{i,k+1}-z_{i+1,k}\right)^2\frac{Kx_{i,k}}{\Omega_{i,k}}\right]$$

For (i=M ; k=2,…,N), the non-zero elements are:

$$\frac{\partial F}{\partial h_{i+1,k-1}} = -\frac{1}{4}\frac{1}{VN_{i,k}}\left[\left(x_{i-1,k}-x_{i,k-1}\right)^2\frac{Kz_{i-1,k-1}}{\Omega_{i-1,k-1}} - 2\left(x_{i-1,k}-x_{i,k-1}\right)\left(z_{i-1,k}-z_{i,k-1}\right)\frac{Kxz_{i-1,k-1}}{\Omega_{i-1,k-1}} + \left(z_{i+1,k}-z_{i,k-1}\right)^2\frac{Kx_{i,k-1}}{\Omega_{i,k-1}}\right]$$

$$\frac{\partial F}{\partial h_{i,k-1}} = \frac{1}{4}\frac{1}{VN_{i,k}}\left[\left(x_{i-1,k}-x_{i,k-1}\right)\left(x_{i,k}-x_{i-1,k-1}\right)\frac{Kz_{i-1,k-1}}{\Omega_{i-1,k-1}}\right.$$
$$+\left(x_{i-1,k}-x_{i,k-1}\right)\left(z_{i,k}-z_{i-1,k-1}\right)\frac{Kxz_{i-1,k-1}}{\Omega_{i-1,k-1}}+\left(z_{i-1,k}-z_{i,k-1}\right)\left(z_{i,k}-z_{i-1,k-1}\right)\frac{Kx_{i-1,k-1}}{\Omega_{i-1,k-1}}$$
$$\left.+\left(z_{i-1,k}-z_{i,k-1}\right)\left(x_{i,k}-x_{i-1,k-1}\right)\frac{Kxz_{i-1,k-1}}{\Omega_{i-1,k-1}}\right]$$

$$\frac{\partial F}{\partial h_{i-1,k}} = -\frac{1}{4}\frac{1}{VN_{i,k}}\left[\left(x_{i-1,k}-x_{i,k-1}\right)\left(x_{i,k}-x_{i-1,k-1}\right)\frac{Kz_{i-1,k-1}}{\Omega_{i-1,k-1}}\right.$$
$$+\left(x_{i-1,k}-x_{i,k-1}\right)\left(z_{i,k}-z_{i-1,k-1}\right)\frac{Kxz_{i-1,k-1}}{\Omega_{i-1,k-1}}+\left(x_{i,k+1}-x_{i-1,k}\right)\left(x_{i-1,k+1}-x_{i,k}\right)\frac{Kz_{i-1,k}}{\Omega_{i-1,k}}$$
$$+\left(x_{i,k+1}-x_{i-1,k}\right)\left(z_{i-1,k+1}-z_{i,k}\right)\frac{Kxz_{i-1,k}}{\Omega_{i-1,k}}+\left(z_{i-1,k}-z_{i,k-1}\right)\left(z_{i,k}-z_{i-1,k-1}\right)\frac{Kx_{i-1,k-1}}{\Omega_{i-1,k-1}}$$
$$+\left(z_{i-1,k}-z_{i,k-1}\right)\left(x_{i,k}-x_{i-1,k-1}\right)\frac{Kxz_{i-1,k-1}}{\Omega_{i-1,k-1}}+\left(z_{i,k+1}-z_{i-1,k}\right)\left(z_{i-1,k+1}-z_{i,k}\right)\frac{Kx_{i-1,k}}{\Omega_{i-1,k}}$$
$$\left.+\left(z_{i,k+1}-z_{i-1,k}\right)\left(x_{i,k}-x_{i+1,k-1}\right)\frac{Kxz_{i,k-1}}{\Omega_{i,k-1}}\right]$$

$$\frac{\partial F}{\partial h_{i,k}} = \frac{1}{4}\frac{1}{VN_{i,k}}\left[\left(x_{i-1,k}-x_{i,k-1}\right)^2\frac{Kz_{i-1,k-1}}{\Omega_{i-1,k-1}}+\left(x_{i,k+1}-x_{i-1,k}\right)^2\frac{Kz_{i-1,k}}{\Omega_{i-1,k}}\right.$$
$$\left.+\left(z_{i-1,k}-z_{i,k-1}\right)^2\frac{Kx_{i-1,k-1}}{\Omega_{i-1,k-1}}+\left(z_{i,k+1}-z_{i-1,k}\right)^2\frac{Kx_{i-1,k}}{\Omega_{i-1,k}}\right]$$

$$\frac{\partial F}{\partial h_{i,k+1}} = \frac{1}{4}\frac{1}{VN_{i,k}}\left[\left(x_{i,k+1}-x_{i-1,k}\right)\left(x_{i-1,k+1}-x_{i,k}\right)\frac{Kz_{i-1,k}}{\Omega_{i-1,k}}\right.$$
$$+\left(x_{i,k+1}-x_{i-1,k}\right)\left(z_{i-1,k+1}-z_{i,k}\right)\frac{Kxz_{i-1,k}}{\Omega_{i-1,k}}+\left(z_{i,k+1}-z_{i-1,k}\right)\left(z_{i-1,k+1}-z_{i,k}\right)\frac{Kx_{i-1,k}}{\Omega_{i-1,k}}$$
$$\left.+\left(z_{i,k+1}-z_{i-1,k}\right)\left(x_{i-1,k+1}-x_{i,k}\right)\frac{Kxz_{i-1,k}}{\Omega_{i-1,k}}\right]$$

For (i=2,…,M ; k=N), the non-zero elements are:

$$\frac{\partial F}{\partial h_{i+1,k-1}} = -\frac{1}{4}\frac{1}{VN_{i,k}}\left[\left(x_{i-1,k} - x_{i,k-1}\right)^2 \frac{Kz_{i-1,k-1}}{\Omega_{i-1,k-1}}\right.$$
$$\left. - 2\left(x_{i-1,k} - x_{i,k-1}\right)\left(z_{i-1,k} - z_{i,k-1}\right)\frac{Kxz_{i-1,k-1}}{\Omega_{i-1,k-1}} + \left(z_{i+1,k} - z_{i,k-1}\right)^2 \frac{Kx_{i,k-1}}{\Omega_{i,k-1}}\right]$$

$$\frac{\partial F}{\partial h_{i,k-1}} = \frac{1}{4}\frac{1}{VN_{i,k}}\left[\left(x_{i-1,k} - x_{i,k-1}\right)\left(x_{i,k} - x_{i-1,k-1}\right)\frac{Kz_{i-1,k-1}}{\Omega_{i-1,k-1}}\right.$$
$$+ \left(x_{i-1,k} - x_{i,k-1}\right)\left(z_{i,k} - z_{i-1,k-1}\right)\frac{Kxz_{i-1,k-1}}{\Omega_{i-1,k-1}} - \left(x_{i+1,k} - x_{i,k-1}\right)\left(x_{i,k} - x_{i+1,k-1}\right)\frac{Kz_{i,k-1}}{\Omega_{i,k-1}}$$
$$- \left(x_{i+1,k} - x_{i,k-1}\right)\left(z_{i,k} - z_{i+1,k-1}\right)\frac{Kxz_{i,k-1}}{\Omega_{i,k-1}} + \left(z_{i-1,k} - z_{i,k-1}\right)\left(z_{i,k} - z_{i-1,k-1}\right)\frac{Kx_{i-1,k-1}}{\Omega_{i-1,k-1}}$$
$$+ \left(z_{i-1,k} - z_{i,k-1}\right)\left(x_{i,k} - x_{i-1,k-1}\right)\frac{Kxz_{i-1,k-1}}{\Omega_{i-1,k-1}} - \left(z_{i+1,k} - z_{i,k-1}\right)\left(z_{i,k} - z_{i+1,k-1}\right)\frac{Kx_{i,k-1}}{\Omega_{i,k-1}}$$
$$\left. - \left(z_{i+1,k} - z_{i,k-1}\right)\left(x_{i,k} - x_{i+1,k-1}\right)\frac{Kxz_{i,k-1}}{\Omega_{i,k-1}}\right]$$

$$\frac{\partial F}{\partial h_{i+1,k-1}} = \frac{1}{4}\frac{1}{VN_{i,k}}\left[\left(x_{i+1,k} - x_{i,k-1}\right)^2 \frac{Kz_{i,k-1}}{\Omega_{i,k-1}}\right.$$
$$\left. + 2\left(x_{i+1,k} - x_{i,k-1}\right)\left(z_{i+1,k} - z_{i,k-1}\right)\frac{Kxz_{i,k-1}}{\Omega_{i,k-1}} + \left(z_{i+1,k} - z_{i,k-1}\right)^2 \frac{Kx_{i,k-1}}{\Omega_{i,k-1}}\right]$$

$$\frac{\partial F}{\partial h_{i-1,k}} = -\frac{1}{4}\frac{1}{VN_{i,k}}\left[\left(x_{i-1,k} - x_{i,k-1}\right)\left(x_{i,k} - x_{i-1,k-1}\right)\frac{Kz_{i-1,k-1}}{\Omega_{i-1,k-1}}\right.$$
$$+\left(x_{i-1,k} - x_{i,k-1}\right)\left(z_{i,k} - z_{i-1,k-1}\right)\frac{Kxz_{i-1,k-1}}{\Omega_{i-1,k-1}} + \left(z_{i-1,k} - z_{i,k-1}\right)\left(z_{i,k} - z_{i-1,k-1}\right)\frac{Kx_{i-1,k-1}}{\Omega_{i-1,k-1}}$$
$$\left.+\left(z_{i-1,k} - z_{i,k-1}\right)\left(x_{i,k} - x_{i-1,k-1}\right)\frac{Kxz_{i-1,k-1}}{\Omega_{i-1,k-1}}\right]$$

$$\frac{\partial F}{\partial h_{i,k}} = \frac{1}{4}\frac{1}{VN_{i,k}}\left[\left(x_{i-1,k} - x_{i,k-1}\right)^2\frac{Kz_{i-1,k-1}}{\Omega_{i-1,k-1}}\right.$$
$$\left.-\left(x_{i+1,k} - x_{i,k-1}\right)^2\frac{Kz_{i,k-1}}{\Omega_{i,k-1}} + \left(z_{i-1,k} - z_{i,k-1}\right)^2\frac{Kx_{i-1,k-1}}{\Omega_{i-1,k-1}} + \left(x_{i+1,k} - x_{i,k-1}\right)^2\frac{Kx_{i,k-1}}{\Omega_{i,k-1}}\right]$$

$$\frac{\partial F}{\partial h_{i+1,k}} = \frac{1}{4}\frac{1}{VN_{i,k}}\left[\left(x_{i+1,k} - x_{i,k-1}\right)\left(x_{i,k} - x_{i+1,k-1}\right)\frac{Kz_{i,k-1}}{\Omega_{i,k-1}}\right.$$
$$+\left(x_{i+1,k} - x_{i,k-1}\right)\left(z_{i,k} - z_{i+1,k-1}\right)\frac{Kxz_{i,k-1}}{\Omega_{i,k-1}} + \left(z_{i+1,k} - z_{i,k-1}\right)\left(z_{i,k} - z_{i+1,k-1}\right)\frac{Kx_{i,k-1}}{\Omega_{i,k-1}}$$
$$\left.+\left(z_{i+1,k} - z_{i,k-1}\right)\left(x_{i,k} - x_{i+1,k-1}\right)\frac{Kxz_{i,k-1}}{\Omega_{i,k-1}}\right]$$

For corner node (1,1), we get:

$$\frac{\partial F}{\partial h_{i,k}} = \frac{1}{4}\frac{1}{VN_{i,k}}\left[-\left(x_{i,k+1} - x_{i+1,k}\right)^2\frac{Kz_{i,k}}{\Omega_{i,k}} - \left(z_{i,k+1} - z_{i+1,k}\right)^2\frac{Kx_{i,k}}{\Omega_{i,k}}\right]$$

$$\frac{\partial F}{\partial h_{i+1,k}} = \frac{1}{4}\frac{1}{VN_{i,k}}\left[\left(x_{i,k+1} - x_{i+1,k}\right)\left(x_{i+1,k+1} - x_{i,k}\right)\frac{Kz_{i,k}}{\Omega_{i,k}} + \left(x_{i,k+1} - x_{i+1,k}\right)\left(z_{i+1,k+1} - z_{i,k}\right)\frac{Kxz_{i,k}}{\Omega_{i,k}}\right.$$
$$\left.+\left(z_{i,k+1} - z_{i+1,k}\right)\left(z_{i+1,k+1} - z_{i,k}\right)\frac{Kx_{i,k}}{\Omega_{i,k}} + \left(z_{i,k+1} - z_{i+1,k}\right)\left(x_{i+1,k+1} - x_{i,k}\right)\frac{Kxz_{i,k}}{\Omega_{i,k}}\right]$$

$$\frac{\partial F}{\partial h_{i,k+1}} = \frac{1}{4}\frac{1}{VN_{i,k}}\left[-\left(x_{i,k+1}-x_{i+1,k}\right)\left(x_{i+1,k+1}-x_{i,k}\right)\frac{Kz_{i,k}}{\Omega_{i,k}}\right.$$
$$-\left(x_{i,k+1}-x_{i+1,k}\right)\left(z_{i+1,k+1}-z_{i,k}\right)\frac{Kxz_{i,k}}{\Omega_{i,k}}+\left(z_{i,k+1}-z_{i+1,k}\right)\left(z_{i+1,k+1}-z_{i,k}\right)\frac{Kx_{i,k}}{\Omega_{i,k}}$$
$$\left.+\left(z_{i,k+1}-z_{i+1,k}\right)\left(x_{i+1,k+1}-x_{i,k}\right)\frac{Kxz_{i,k}}{\Omega_{i,k}}\right]$$

$$\frac{\partial F}{\partial h_{i+1,k+1}} = \frac{1}{4}\frac{1}{VN_{i,k}}\left[\left(x_{i,k+1}-x_{i+1,k}\right)^2\frac{Kz_{i,k}}{\Omega_{i,k}}+2\left(x_{i,k+1}-x_{i+1,k}\right)\left(z_{i,k+1}-z_{i+1,k}\right)\frac{Kxz_{i,k}}{\Omega_{i,k}}\right.$$
$$\left.+\left(z_{i,k+1}-z_{i+1,k}\right)^2\frac{Kx_{i,k}}{\Omega_{i,k}}\right]$$

For corner node (M,1), we get:

$$\frac{\partial F}{\partial h_{i-1,k}} = -\frac{1}{4}\frac{1}{VN_{i,k}}\left[\left(x_{i,k+1}-x_{i-1,k}\right)\left(x_{i-1,k+1}-x_{i,k}\right)\frac{Kz_{i-1,k}}{\Omega_{i-1,k}}\right.$$
$$+\left(x_{i,k+1}-x_{i-1,k}\right)\left(z_{i-1,k+1}-z_{i,k}\right)\frac{Kxz_{i-1,k}}{\Omega_{i-1,k}}+\left(z_{i,k+1}-z_{i-1,k}\right)\left(z_{i-1,k+1}-z_{i,k}\right)\frac{Kx_{i-1,k}}{\Omega_{i-1,k}}$$
$$\left.+\left(z_{i,k+1}-z_{i-1,k}\right)\left(x_{i-1,k+1}-x_{i,k}\right)\frac{Kxz_{i-1,k}}{\Omega_{i-1,k}}\right]$$

$$\frac{\partial F}{\partial h_{i,k}} = \frac{1}{4}\frac{1}{VN_{i,k}}\left[-\left(x_{i+1,k}-x_{i,k-1}\right)^2\frac{Kz_{i,k-1}}{\Omega_{i,k-1}}-\left(z_{i,k+1}-z_{i+1,k}\right)^2\frac{Kx_{i,k}}{\Omega_{i,k}}\right]$$

$$\frac{\partial F}{\partial h_{i-1,k+1}} = -\frac{1}{4}\frac{1}{VN_{i,k}}\left[\left(x_{i,k+1}-x_{i-1,k}\right)^2\frac{Kz_{i-1,k}}{\Omega_{i-1,k}}-2\left(x_{i,k+1}-x_{i-1,k}\right)\left(z_{i,k+1}-z_{i-1,k}\right)\frac{Kxz_{i-1,k}}{\Omega_{i-1,k}}\right.$$
$$\left.+\left(z_{i,k+1}-z_{i-1,k}\right)^2\frac{Kx_{i-1,k}}{\Omega_{i-1,k}}\right]$$

$$\frac{\partial F}{\partial h_{i,k+1}} = \frac{1}{4}\frac{1}{VN_{i,k}}\left[\left(x_{i,k+1}-x_{i-1,k}\right)\left(x_{i-1,k+1}-x_{i,k}\right)\frac{Kz_{i-1,k}}{\Omega_{i-1,k}}\right.$$
$$+\left(x_{i,k+1}-x_{i-1,k}\right)\left(z_{i-1,k+1}-z_{i,k}\right)\frac{Kxz_{i-1,k}}{\Omega_{i-1,k}}+\left(z_{i,k+1}-z_{i-1,k}\right)\left(z_{i-1,k+1}-z_{i,k}\right)\frac{Kx_{i-1,k}}{\Omega_{i-1,k}}$$
$$\left.+\left(z_{i,k+1}-z_{i-1,k}\right)\left(x_{i-1,k+1}-x_{i,k}\right)\frac{Kxz_{i-1,k}}{\Omega_{i-1,k}}\right]$$

For corner node (1,N), we get:

$$\frac{\partial F}{\partial h_{i+1,k-1}} = \frac{1}{4}\frac{1}{VN_{i,k}}\left[\left(x_{i+1,k}-x_{i,k-1}\right)^2\frac{Kz_{i,k-1}}{\Omega_{i,k-1}}\right.$$
$$\left.+2\left(x_{i+1,k}-x_{i,k-1}\right)\left(z_{i+1,k}-z_{i,k-1}\right)\frac{Kxz_{i,k-1}}{\Omega_{i,k-1}}+\left(z_{i+1,k}-z_{i,k-1}\right)^2\frac{Kx_{i,k-1}}{\Omega_{i,k-1}}\right]$$

$$\frac{\partial F}{\partial h_{i,k}} = \frac{1}{4}\frac{1}{VN_{i,k}}\left[-\left(x_{i+1,k}-x_{i,k-1}\right)^2\frac{Kz_{i,k-1}}{\Omega_{i,k-1}}+\left(x_{i,k+1}-x_{i-1,k}\right)^2\frac{Kz_{i-1,k}}{\Omega_{i-1,k}}\right.$$
$$\left.+\left(x_{i+1,k}-x_{i,k-1}\right)^2\frac{Kx_{i,k-1}}{\Omega_{i,k-1}}\right]$$

$$\frac{\partial F}{\partial h_{i+1,k}} = \frac{1}{4}\frac{1}{VN_{i,k}}\left[\left(x_{i+1,k}-x_{i,k-1}\right)\left(x_{i,k}-x_{i+1,k-1}\right)\frac{Kz_{i,k-1}}{\Omega_{i,k-1}}\right.$$
$$+\left(x_{i+1,k}-x_{i,k-1}\right)\left(z_{i,k}-z_{i+1,k-1}\right)\frac{Kxz_{i,k-1}}{\Omega_{i,k-1}}+\left(z_{i+1,k}-z_{i,k-1}\right)\left(z_{i,k}-z_{i+1,k-1}\right)\frac{Kx_{i,k-1}}{\Omega_{i,k-1}}$$
$$\left.+\left(z_{i+1,k}-z_{i,k-1}\right)\left(x_{i,k}-x_{i+1,k-1}\right)\frac{Kxz_{i,k-1}}{\Omega_{i,k-1}}\right]$$

For corner node (M,N), we get:

$$\frac{\partial F}{\partial h_{i+1,k-1}} = -\frac{1}{4}\frac{1}{VN_{i,k}}\left[\left(x_{i-1,k} - x_{i,k-1}\right)^2 \frac{Kz_{i-1,k-1}}{\Omega_{i-1,k-1}}\right.$$
$$\left. - 2\left(x_{i-1,k} - x_{i,k-1}\right)\left(z_{i-1,k} - z_{i,k-1}\right)\frac{Kxz_{i-1,k-1}}{\Omega_{i-1,k-1}} + \left(z_{i+1,k} - z_{i,k-1}\right)^2 \frac{Kx_{i,k-1}}{\Omega_{i,k-1}}\right]$$

$$\frac{\partial F}{\partial h_{i,k-1}} = \frac{1}{4}\frac{1}{VN_{i,k}}\left[\left(x_{i-1,k} - x_{i,k-1}\right)\left(x_{i,k} - x_{i-1,k-1}\right)\frac{Kz_{i-1,k-1}}{\Omega_{i-1,k-1}}\right.$$
$$+ \left(x_{i-1,k} - x_{i,k-1}\right)\left(z_{i,k} - z_{i-1,k-1}\right)\frac{Kxz_{i-1,k-1}}{\Omega_{i-1,k-1}} + \left(z_{i-1,k} - z_{i,k-1}\right)\left(z_{i,k} - z_{i-1,k-1}\right)\frac{Kx_{i-1,k-1}}{\Omega_{i-1,k-1}}$$
$$\left. + \left(z_{i-1,k} - z_{i,k-1}\right)\left(x_{i,k} - x_{i-1,k-1}\right)\frac{Kxz_{i-1,k-1}}{\Omega_{i-1,k-1}}\right]$$

$$\frac{\partial F}{\partial h_{i,k}} = \frac{1}{4}\frac{1}{VN_{i,k}}\left[\left(x_{i-1,k} - x_{i,k-1}\right)^2 \frac{Kz_{i-1,k-1}}{\Omega_{i-1,k-1}} + \left(z_{i-1,k} - z_{i,k-1}\right)^2 \frac{Kx_{i-1,k-1}}{\Omega_{i-1,k-1}}\right]$$

APPENDIX II: INPUT AND OUTPUT DATA FILE FOR LABORATORY EXPERIMENT SIMULATION

List of input data parameters are as follows:

NROW	Number of rows
NCOL	Number of columns
MXIT	Maximum number of iteration
NSTAT	=0 no change in source/sink value Vs time
	=1 Read new source/sink values from data file in every time step
NPHASE	Number of phases in the system
IRES	=0 start from initial condition at t=0
	=1 restart problem and read initial condition from previous solution
ITRN	=0 no mass transfer between phases
	=1 considering mass transfer due to dissolution and volatilization
TSTR	Starting time of simulation
DT	Time step
TMAX	Maximum simulation time
TPRN	Time interval for printout of the results
TOLF	Relative allowable error
TOLX	Absolute allowable error
NCBEG(k)	Beginning column number in each row
NCEND(k)	Final column number in each row
FAC1	Conversion factor number 1
FAC2	Conversion factor number 2
DEFA	Default value for reading each set of data

IPRN	=0 not to print the read data in output
	=1 print the read data in output
ITYPEW	For defining the boundary conditions for water:
	=0 internal nodes
	= negative number, prescribed head for water phase
	= positive number, prescribed flow for water phase
ITYPEN	For defining the boundary condition for NAPL (same as ITYPEW)
TSHW	Time for defining the schedule of each boundary condition for water head
VSHW	Value for defining the schedule of each boundary condition for water head
TSHN	Time for defining the schedule of each boundary condition for NAPL head
VSHN	Value for defining the schedule of each boundary condition for NAPL head
TSFN	Time for defining the schedule of each boundary condition for NAPL flow
VSFN	Value for defining the schedule of each boundary condition for NAPL flow
X	x-coordinates of nodes in x direction
Z	z-coordinates of nodes in z direction
RHOW	Density of water
VMUW	Viscosity of water
RHON	Density of NAPL
VMUN	Viscosity of NAPL
VMUA	Viscosity of air
betanw	NAPL-water scaling parameter, β_{nw}
betaan	Air-NAPL scaling parameter, β_{an}
NMAT	Number of soil materials
AF2	parameter α in VG relationships
VVN2	parameter n in VG relationships
TSRW2	Residual water saturation
TSNP2	Residual NAPL saturation
PORS2	Porosity

pmr2	Saturated hydraulic conductivity
zk	Ration of conductivity in z direction to that in x direction, Kz/Kx
KMAT	Material type of each node
IFW	=0 initial condition for water is calculated from bilinear interpolation
	=1 read initial condition for each node from data file
IFN	=0 no initial condition for NAPL
	=1 initial condition for NAPL is calculated from bilinear interpolation
	=2 read initial condition for each node from data file
WP1	Value of water head in left boundary
WP2	Value of water head in right boundary

INPUT FILE

Laboratory Experiment-Mohammadi&Kahawita
NROW,NCOL,MXIT,NSTAT,NPHASE,IRES,ITRN
29,25,30,2,0,0
TSTR,DT,TMAX,TPRN,TOLF,TOLX
0,0.01,375,60,.1,0.001
NCBEG(k),NCEND(k)
1,25
1,25
1,25
1,25
1,25
1,25
1,25
1,25
1,25
1,25
1,25
1,25
1,25
1,25
1,25
1,25
1,25
1,25
1,25
1,25
1,25

1,25
1,25
1,25
1,25
1,25
1,25
1,25
ITYPEW
1.0,1.0,0.0,0 : FAC1,FAC2,DEFA,IPRN
1,1,1.,2,1,1.0,3,1,1.0,4,1,1.0,5,1,1.0,6,1,1.0
7,1,1.0,8,1,1.0,9,1,1.0,10,1,1.0,11,1,1.0,12,1,1.0
13,1,1.0,14,1,1.0,15,1,1.0,16,1,1.0,17,1,1.0,18,1,1.0
19,1,1.0,20,1,1.0,21,1,1.0,22,1,1.0,23,1,1.0,24,1,1.0
25,1,1.,1,2,-1.,25,2,-2.,1,3,-3.,25,3,-4.,1,4,-5.
25,4,-6.,1,5,-7.,25,5,-8.,1,6,-9.,25,6,-10.,1,7,-11.
25,7,1.,1,8,1.,25,8,1.,1,9,1.,25,9,1.,1,10,1.
25,10,1.,1,11,1.,25,11,1.,1,12,1.,25,12,1.,1,13,1.
25,14,1.,1,15,1.,25,15,1.,1,16,1.,25,16,1.,1,17,1.
25,17,1.,1,18,1.,25,18,1.,1,19,1.,25,19,1.,1,20,1.
25,20,1.,1,21,1.,25,21,1.,1,22,1.,25,22,1.,1,23,1.
25,23,1.,1,24,1.,25,24,1.,1,25,1.,25,25,1.,1,26,1.
25,26,1.,1,27,1.,25,27,1.,1,28,1.,25,28,1.,1,29,1.
2,29,1.,3,29,1.,4,29,1.,5,29,1.,6,29,1.,7,29,1.
8,29,1.,9,29,1.,10,29,1.,11,29,1.,12,29,1.,13,29,1.
14,29,1.,15,29,1.,16,29,1.,17,29,1.,18,29,1.,19,29,1.
20,29,1.,21,29,1.,22,29,1.,23,29,1.,24,29,1.,25,29,1.
0,0,0.,0,0,0.,0,0,0.,0,0,0.,0,0,0.,0,0,0.
ITYPEN
1.0,1.0,1.0,0
1,1,1.,2,1,1.0,3,1,1.0,4,1,1.0,5,1,1.0,6,1,1.0
7,1,1.0,8,1,1.0,9,1,1.0,10,1,1.0,11,1,1.0,12,1,1.0
13,1,1.0,14,1,1.0,15,1,1.0,16,1,1.0,17,1,1.0,18,1,1.0
19,1,1.0,20,1,1.0,21,1,1.0,22,1,1.0,23,1,1.0,24,1,1.0
25,1,1.,1,2,1.,25,2,1.,1,3,1.,25,3,1.,1,4,1.
25,4,1.,1,5,1.,25,5,1.,1,6,1.,25,6,1.,1,7,1.
25,7,1.,1,8,1.,25,8,1.,1,9,1.,25,9,1.,1,10,1.
25,10,1.,1,11,1.,25,11,1.,1,12,1.,25,12,1.,1,13,1.
25,14,1.,1,15,1.,25,15,1.,1,16,1.,25,16,1.,1,17,1.
25,17,1.,1,18,1.,25,18,1.,1,19,1.,25,19,1.,1,20,1.
25,20,1.,1,21,1.,25,21,1.,1,22,1.,25,22,1.,1,23,1.
25,23,1.,1,24,1.,25,24,1.,1,25,1.,25,25,1.,1,26,1.
25,26,1.,1,27,1.,25,27,1.,1,28,1.,25,28,1.,1,29,1.
2,29,1.,3,29,1.,4,29,1.,5,29,1.,6,29,1.,7,29,1.

8,29,1.,9,29,1.,10,29,1.,11,29,1.,12,29,-12.,13,29,-12.
14,29,-12.,15,29,-12.,16,29,-12.,17,29,1.,18,29,1.,19,29,1.
20,29,1.,21,29,1.,22,29,1.,23,29,1.,24,29,1.,25,29,1.
0,0,0.,0,0,0.,0,0,0.,0,0,0.,0,0,0.,0,0,0.,0,0,0.
TSHW,VSHW Schedules for water head at boundaries
0.,10.8
10.,10.8
100.,10.8
9999.0,10.8
0.,9.3
10.,9.3
100.,9.3
9999.0,9.3
0.,8.8
10.,8.8
100.,8.8
9999.,8.8
0.,7.3
10.,7.3
100.,7.3
9999.,7.3
0.,6.8
10.,6.8
100.,6.8
9999.,6.8
0.,5.3
10.,5.3
100.,5.3
9999.,5.3
0.,4.8
10.,4.8
100.,4.8
9999.,4.8
0.,3.3
10.,3.3
100.,3.3
9999.,3.3
0.,2.8
10.,2.8
100.,2.8
9999.,2.8
0.,1.3
10.,1.3

100.,1.3
9999.,1.3
0.,0.8
10.,0.8
100.,0.8
9999.,0.8
TSHN, VSHN Schedules for NAPL head at boundaries
0.,3.0
10.,3.0
100.,3.0
9999.,3.0
TSFN,VSFN Schedules for Water and NAPL flow at boundaries
0.,0.0
10.,0.0
100.,0.0
9999.,0.0
X
0.0,5.0,15.0,25.0,35.0,45.0
50.0,55.0,60.0,62.0,63.0,64.0
66.0,68.5,70.0,72.0,73.0,74.0
84.0,94.0,104.0,114.0,124.0,134.0
137.0
Z
0.0,2.0,4.0,6.0,8.0,10.0
12.0,14.0,16.0,18.0,20.0,22.0
24.0,26.0,27.5,29.0,31.0,32.5
35.0,36.5,37.5,39.0,42.0,44.0
46.0,47.5,50.0,52.0,54.0
RHOW,VMUW,RHON,VMUN,VMUA,betanw,betaan
998.2,0.001,685.8,.000409,0.00001,1.95,3.65
NMAT
3
AF2,VVN2,TSRW2,TSNP2,PORS2,pmr2,zk=Kz/Kx
0.0328,3.00,0.0157,0.01,0.525,.027,1.0
0.0893,2.81,.00100,0.01,0.575,0.13,1.1538
0.0271,5.72,0.17,0.01,0.374,1.0e-24,1.0
KMAT : Material type of each node
1.0,1.0,1.0,0
1,16,2.0,2,16,2.0,3,16,2.0,4,16,2.0,5,16,2.0,6,16,2.0
7,16,2.0,8,16,2.0,9,16,2.0,10,16,2.0,11,16,2.0,12,16,2.0
13,16,2.0,14,16,2.0,15,16,2.0,16,16,2.0,17,16,2.0,18,16,2.0
19,16,2.0,20,16,2.0,21,16,2.0,22,16,2.0,23,16,2.0,24,16,2.0
25,16,2.0,1,17,2.0,2,17,2.0,3,17,2.0,4,17,2.0,5,17,2.0

6,17,2.0,7,17,2.0,8,17,2.0,9,17,2.0,10,17,2.0,11,17,2.0
12,17,2.0,13,17,2.0,14,17,2.0,15,17,2.0,16,17,2.0,17,17,2.0
18,17,2.0,19,17,2.0,20,17,2.0,21,17,2.0,22,17,2.0,23,17,2.0
24,17,2.0,25,17,2.0,1,18,2.0,2,18,2.0,3,18,2.0,4,18,2.0
5,18,2.0,6,18,2.0,7,18,2.0,8,18,2.0,9,18,2.0,10,18,2.0
11,18,2.0,12,18,2.0,13,18,2.0,14,18,2.0,15,18,2.0,16,18,2.0
17,18,2.0,18,18,2.0,19,18,2.0,20,18,2.0,21,18,2.0,22,18,2.0
23,18,2.0,24,18,2.0,25,18,2.0,1,19,2.0,2,19,2.0,3,19,2.0
4,19,2.0,5,19,2.0,6,19,2.0,7,19,2.0,8,19,2.0,9,19,2.0
10,19,2.0,11,19,2.0,12,19,2.0,13,19,2.0,14,19,2.0,15,19,2.0
16,19,2.0,17,19,2.0,18,19,2.0,19,19,2.0,20,19,2.0,21,19,2.0
22,19,2.0,23,19,2.0,24,19,2.0,25,19,2.0,1,20,2.0,2,20,2.0
3,20,2.0,4,20,2.0,5,20,2.0,6,20,2.0,7,20,2.0,8,20,2.0
9,20,2.0,10,20,2.0,11,20,2.0,12,20,2.0,13,20,2.0,14,20,2.0
15,20,2.0,16,20,2.0,17,20,2.0,18,20,2.0,19,20,2.0,20,20,2.0
21,20,2.0,22,20,2.0,23,20,2.0,24,20,2.0,25,20,2.0,1,21,2.0
2,21,2.0,3,21,2.0,4,21,2.0,5,21,2.0,6,21,2.0,7,21,2.0
8,21,2.0,9,21,2.0,10,21,2.0,11,21,2.0,12,21,2.0,13,21,2.0
14,21,2.0,15,21,2.0,16,21,2.0,17,21,2.0,18,21,2.0,19,21,2.0
20,21,2.0,22,21,2.0,23,21,2.0,24,21,2.0,25,21,2.0,8,27,3.0
9,27,3.0,10,27,3.0,11,27,3.0,17,27,3.0,18,27,3.0,19,27,3.0
20,27,3.0,8,28,3.0,9,28,3.0,10,28,3.0,11,28,3.0,17,28,3.0
18,28,3.0,19,28,3.0,20,28,3.0,0,0,0.0,0,0,0.0,0,0,0.0
IFW,IFN
0,0
WP1,WP2
10.8,9.3

OUTPUT FILE

Laboratory Experiment-Mohammadi&Kahawita

Initial Conditions

X	Z	Hw	Hn	Ha	Sw	Sn	Sa
.000	.000	10.800	10.800	.000	1.00000	.00000	.00000
5.000	.000	10.745	10.745	.000	1.00000	.00000	.00000
15.000	.000	10.636	10.636	.000	1.00000	.00000	.00000
25.000	.000	10.526	10.526	.000	1.00000	.00000	.00000
35.000	.000	10.417	10.417	.000	1.00000	.00000	.00000
45.000	.000	10.307	10.307	.000	1.00000	.00000	.00000
50.000	.000	10.253	10.253	.000	1.00000	.00000	.00000
55.000	.000	10.198	10.198	.000	1.00000	.00000	.00000

60.000	.000	10.143	10.143	.000	1.00000	.00000	.00000
62.000	.000	10.121	10.121	.000	1.00000	.00000	.00000
63.000	.000	10.110	10.110	.000	1.00000	.00000	.00000
64.000	.000	10.099	10.099	.000	1.00000	.00000	.00000
66.000	.000	10.077	10.077	.000	1.00000	.00000	.00000
68.500	.000	10.050	10.050	.000	1.00000	.00000	.00000
70.000	.000	10.034	10.034	.000	1.00000	.00000	.00000
72.000	.000	10.012	10.012	.000	1.00000	.00000	.00000
73.000	.000	10.001	10.001	.000	1.00000	.00000	.00000
74.000	.000	9.990	9.990	.000	1.00000	.00000	.00000
84.000	.000	9.880	9.880	.000	1.00000	.00000	.00000
94.000	.000	9.771	9.771	.000	1.00000	.00000	.00000
104.000	.000	9.661	9.661	.000	1.00000	.00000	.00000
114.000	.000	9.552	9.552	.000	1.00000	.00000	.00000
124.000	.000	9.442	9.442	.000	1.00000	.00000	.00000
134.000	.000	9.333	9.333	.000	1.00000	.00000	.00000
137.000	.000	9.300	9.300	.000	1.00000	.00000	.00000
.000	2.000	8.800	8.800	.000	1.00000	.00000	.00000
5.000	2.000	8.745	8.745	.000	1.00000	.00000	.00000
15.000	2.000	8.636	8.636	.000	1.00000	.00000	.00000
25.000	2.000	8.526	8.526	.000	1.00000	.00000	.00000
35.000	2.000	8.417	8.417	.000	1.00000	.00000	.00000
45.000	2.000	8.307	8.307	.000	1.00000	.00000	.00000
50.000	2.000	8.253	8.253	.000	1.00000	.00000	.00000
55.000	2.000	8.198	8.198	.000	1.00000	.00000	.00000
60.000	2.000	8.143	8.143	.000	1.00000	.00000	.00000
62.000	2.000	8.121	8.121	.000	1.00000	.00000	.00000
63.000	2.000	8.110	8.110	.000	1.00000	.00000	.00000
64.000	2.000	8.099	8.099	.000	1.00000	.00000	.00000
66.000	2.000	8.077	8.077	.000	1.00000	.00000	.00000
68.500	2.000	8.050	8.050	.000	1.00000	.00000	.00000
70.000	2.000	8.034	8.034	.000	1.00000	.00000	.00000
72.000	2.000	8.012	8.012	.000	1.00000	.00000	.00000
73.000	2.000	8.001	8.001	.000	1.00000	.00000	.00000
74.000	2.000	7.990	7.990	.000	1.00000	.00000	.00000
84.000	2.000	7.880	7.880	.000	1.00000	.00000	.00000
94.000	2.000	7.771	7.771	.000	1.00000	.00000	.00000
104.000	2.000	7.661	7.661	.000	1.00000	.00000	.00000
114.000	2.000	7.552	7.552	.000	1.00000	.00000	.00000
124.000	2.000	7.442	7.442	.000	1.00000	.00000	.00000
134.000	2.000	7.333	7.333	.000	1.00000	.00000	.00000
137.000	2.000	7.300	7.300	.000	1.00000	.00000	.00000
.000	4.000	6.800	6.800	.000	1.00000	.00000	.00000
5.000	4.000	6.745	6.745	.000	1.00000	.00000	.00000
15.000	4.000	6.636	6.636	.000	1.00000	.00000	.00000
25.000	4.000	6.526	6.526	.000	1.00000	.00000	.00000
35.000	4.000	6.417	6.417	.000	1.00000	.00000	.00000
45.000	4.000	6.307	6.307	.000	1.00000	.00000	.00000
50.000	4.000	6.253	6.253	.000	1.00000	.00000	.00000
55.000	4.000	6.198	6.198	.000	1.00000	.00000	.00000
60.000	4.000	6.143	6.143	.000	1.00000	.00000	.00000

62.000	4.000	6.121	6.121	.000	1.00000	.00000	.00000
63.000	4.000	6.110	6.110	.000	1.00000	.00000	.00000
64.000	4.000	6.099	6.099	.000	1.00000	.00000	.00000
66.000	4.000	6.077	6.077	.000	1.00000	.00000	.00000
68.500	4.000	6.050	6.050	.000	1.00000	.00000	.00000
70.000	4.000	6.034	6.034	.000	1.00000	.00000	.00000
72.000	4.000	6.012	6.012	.000	1.00000	.00000	.00000
73.000	4.000	6.001	6.001	.000	1.00000	.00000	.00000
74.000	4.000	5.990	5.990	.000	1.00000	.00000	.00000
84.000	4.000	5.880	5.880	.000	1.00000	.00000	.00000
94.000	4.000	5.771	5.771	.000	1.00000	.00000	.00000
104.000	4.000	5.661	5.661	.000	1.00000	.00000	.00000
114.000	4.000	5.552	5.552	.000	1.00000	.00000	.00000
124.000	4.000	5.442	5.442	.000	1.00000	.00000	.00000
134.000	4.000	5.333	5.333	.000	1.00000	.00000	.00000
137.000	4.000	5.300	5.300	.000	1.00000	.00000	.00000
.000	6.000	4.800	4.800	.000	1.00000	.00000	.00000
5.000	6.000	4.745	4.745	.000	1.00000	.00000	.00000
15.000	6.000	4.636	4.636	.000	1.00000	.00000	.00000
25.000	6.000	4.526	4.526	.000	1.00000	.00000	.00000
35.000	6.000	4.417	4.417	.000	1.00000	.00000	.00000
45.000	6.000	4.307	4.307	.000	1.00000	.00000	.00000
50.000	6.000	4.253	4.253	.000	1.00000	.00000	.00000
55.000	6.000	4.198	4.198	.000	1.00000	.00000	.00000
60.000	6.000	4.143	4.143	.000	1.00000	.00000	.00000
62.000	6.000	4.121	4.121	.000	1.00000	.00000	.00000
63.000	6.000	4.110	4.110	.000	1.00000	.00000	.00000
64.000	6.000	4.099	4.099	.000	1.00000	.00000	.00000
66.000	6.000	4.077	4.077	.000	1.00000	.00000	.00000
68.500	6.000	4.050	4.050	.000	1.00000	.00000	.00000
70.000	6.000	4.034	4.034	.000	1.00000	.00000	.00000
72.000	6.000	4.012	4.012	.000	1.00000	.00000	.00000
73.000	6.000	4.001	4.001	.000	1.00000	.00000	.00000
74.000	6.000	3.990	3.990	.000	1.00000	.00000	.00000
84.000	6.000	3.880	3.880	.000	1.00000	.00000	.00000
94.000	6.000	3.771	3.771	.000	1.00000	.00000	.00000
104.000	6.000	3.661	3.661	.000	1.00000	.00000	.00000
114.000	6.000	3.552	3.552	.000	1.00000	.00000	.00000
124.000	6.000	3.442	3.442	.000	1.00000	.00000	.00000
134.000	6.000	3.333	3.333	.000	1.00000	.00000	.00000
137.000	6.000	3.300	3.300	.000	1.00000	.00000	.00000
.000	8.000	2.800	2.800	.000	1.00000	.00000	.00000
5.000	8.000	2.745	2.745	.000	1.00000	.00000	.00000
15.000	8.000	2.636	2.636	.000	1.00000	.00000	.00000
25.000	8.000	2.526	2.526	.000	1.00000	.00000	.00000
35.000	8.000	2.417	2.417	.000	1.00000	.00000	.00000
45.000	8.000	2.307	2.307	.000	1.00000	.00000	.00000
50.000	8.000	2.253	2.253	.000	1.00000	.00000	.00000
55.000	8.000	2.198	2.198	.000	1.00000	.00000	.00000
60.000	8.000	2.143	2.143	.000	1.00000	.00000	.00000
62.000	8.000	2.121	2.121	.000	1.00000	.00000	.00000

63.000	8.000	2.110	2.110	.000	1.00000	.00000	.00000
64.000	8.000	2.099	2.099	.000	1.00000	.00000	.00000
66.000	8.000	2.077	2.077	.000	1.00000	.00000	.00000
68.500	8.000	2.050	2.050	.000	1.00000	.00000	.00000
70.000	8.000	2.034	2.034	.000	1.00000	.00000	.00000
72.000	8.000	2.012	2.012	.000	1.00000	.00000	.00000
73.000	8.000	2.001	2.001	.000	1.00000	.00000	.00000
74.000	8.000	1.990	1.990	.000	1.00000	.00000	.00000
84.000	8.000	1.880	1.880	.000	1.00000	.00000	.00000
94.000	8.000	1.771	1.771	.000	1.00000	.00000	.00000
104.000	8.000	1.661	1.661	.000	1.00000	.00000	.00000
114.000	8.000	1.552	1.552	.000	1.00000	.00000	.00000
124.000	8.000	1.442	1.442	.000	1.00000	.00000	.00000
134.000	8.000	1.333	1.333	.000	1.00000	.00000	.00000
137.000	8.000	1.300	1.300	.000	1.00000	.00000	.00000
.000	10.000	.800	.800	.000	1.00000	.00000	.00000
5.000	10.000	.745	.745	.000	1.00000	.00000	.00000
15.000	10.000	.636	.636	.000	1.00000	.00000	.00000
25.000	10.000	.526	.526	.000	1.00000	.00000	.00000
35.000	10.000	.417	.417	.000	1.00000	.00000	.00000
45.000	10.000	.307	.307	.000	1.00000	.00000	.00000
50.000	10.000	.253	.253	.000	1.00000	.00000	.00000
55.000	10.000	.198	.198	.000	1.00000	.00000	.00000
60.000	10.000	.143	.143	.000	1.00000	.00000	.00000
62.000	10.000	.121	.121	.000	1.00000	.00000	.00000
63.000	10.000	.110	.110	.000	1.00000	.00000	.00000
64.000	10.000	.099	.099	.000	1.00000	.00000	.00000
66.000	10.000	.077	.077	.000	1.00000	.00000	.00000
68.500	10.000	.050	.050	.000	1.00000	.00000	.00000
70.000	10.000	.034	.034	.000	1.00000	.00000	.00000
72.000	10.000	.012	.012	.000	1.00000	.00000	.00000
73.000	10.000	.001	.001	.000	1.00000	.00000	.00000
74.000	10.000	-.010	-.004	.000	1.00000	.00000	.00000
84.000	10.000	-.120	-.042	.000	1.00000	.00000	.00000
94.000	10.000	-.229	-.080	.000	1.00000	.00000	.00000
104.000	10.000	-.339	-.118	.000	1.00000	.00000	.00000
114.000	10.000	-.448	-.156	.000	1.00000	.00000	.00000
124.000	10.000	-.558	-.194	.000	1.00000	.00000	.00000
134.000	10.000	-.667	-.232	.000	1.00000	.00000	.00000
137.000	10.000	-.700	-.244	.000	1.00000	.00000	.00000
.000	12.000	-1.200	-.418	.000	.99990	.00000	.00010
5.000	12.000	-1.255	-.437	.000	.99990	.00000	.00010
15.000	12.000	-1.364	-.475	.000	.99990	.00000	.00010
25.000	12.000	-1.474	-.513	.000	.99980	.00000	.00020
35.000	12.000	-1.583	-.551	.000	.99980	.00000	.00020
45.000	12.000	-1.693	-.589	.000	.99980	.00000	.00020
50.000	12.000	-1.747	-.609	.000	.99970	.00000	.00030
55.000	12.000	-1.802	-.627	.000	.99970	.00000	.00030
60.000	12.000	-1.857	-.647	.000	.99970	.00000	.00030
62.000	12.000	-1.879	-.654	.000	.99970	.00000	.00030
63.000	12.000	-1.890	-.658	.000	.99970	.00000	.00030

64.000	12.000	-1.901	-.662	.000	.99970	.00000	.00030
66.000	12.000	-1.923	-.669	.000	.99970	.00000	.00030
68.500	12.000	-1.950	-.679	.000	.99960	.00000	.00040
70.000	12.000	-1.966	-.685	.000	.99960	.00000	.00040
72.000	12.000	-1.988	-.692	.000	.99960	.00000	.00040
73.000	12.000	-1.999	-.696	.000	.99960	.00000	.00040
74.000	12.000	-2.010	-.700	.000	.99960	.00000	.00040
84.000	12.000	-2.120	-.738	.000	.99950	.00000	.00050
94.000	12.000	-2.229	-.776	.000	.99950	.00000	.00050
104.000	12.000	-2.339	-.814	.000	.99940	.00000	.00060
114.000	12.000	-2.448	-.853	.000	.99930	.00000	.00070
124.000	12.000	-2.558	-.891	.000	.99920	.00000	.00080
134.000	12.000	-2.667	-.929	.000	.99910	.00000	.00090
137.000	12.000	-2.700	-.940	.000	.99910	.00000	.00090
.000	14.000	-3.200	-1.114	.000	.99840	.00000	.00160
5.000	14.000	-3.255	-1.133	.000	.99840	.00000	.00160
15.000	14.000	-3.364	-1.171	.000	.99820	.00000	.00180
25.000	14.000	-3.474	-1.210	.000	.99800	.00000	.00200
35.000	14.000	-3.583	-1.248	.000	.99780	.00000	.00220
45.000	14.000	-3.693	-1.286	.000	.99760	.00000	.00240
50.000	14.000	-3.747	-1.305	.000	.99750	.00000	.00250
55.000	14.000	-3.802	-1.324	.000	.99740	.00000	.00260
60.000	14.000	-3.857	-1.343	.000	.99730	.00000	.00270
62.000	14.000	-3.879	-1.351	.000	.99720	.00000	.00280
63.000	14.000	-3.890	-1.355	.000	.99720	.00000	.00280
64.000	14.000	-3.901	-1.358	.000	.99720	.00000	.00280
66.000	14.000	-3.923	-1.366	.000	.99710	.00000	.00290
68.500	14.000	-3.950	-1.375	.000	.99710	.00000	.00290
70.000	14.000	-3.966	-1.381	.000	.99700	.00000	.00300
72.000	14.000	-3.988	-1.389	.000	.99700	.00000	.00300
73.000	14.000	-3.999	-1.393	.000	.99700	.00000	.00300
74.000	14.000	-4.010	-1.396	.000	.99690	.00000	.00310
84.000	14.000	-4.120	-1.434	.000	.99670	.00000	.00330
94.000	14.000	-4.229	-1.473	.000	.99640	.00000	.00360
104.000	14.000	-4.339	-1.511	.000	.99610	.00000	.00390
114.000	14.000	-4.448	-1.549	.000	.99580	.00000	.00420
124.000	14.000	-4.558	-1.587	.000	.99550	.00000	.00450
134.000	14.000	-4.667	-1.625	.000	.99520	.00000	.00480
137.000	14.000	-4.700	-1.637	.000	.99510	.00000	.00490
.000	16.000	-5.200	-1.811	.000	.99340	.00000	.00660
5.000	16.000	-5.255	-1.830	.000	.99320	.00000	.00680
15.000	16.000	-5.364	-1.868	.000	.99270	.00000	.00730
25.000	16.000	-5.474	-1.906	.000	.99230	.00000	.00770
35.000	16.000	-5.583	-1.944	.000	.99180	.00000	.00820
45.000	16.000	-5.693	-1.982	.000	.99130	.00000	.00870
50.000	16.000	-5.747	-2.001	.000	.99110	.00000	.00890
55.000	16.000	-5.802	-2.020	.000	.99080	.00000	.00920
60.000	16.000	-5.857	-2.039	.000	.99060	.00000	.00940
62.000	16.000	-5.879	-2.047	.000	.99050	.00000	.00950
63.000	16.000	-5.890	-2.051	.000	.99040	.00000	.00960
64.000	16.000	-5.901	-2.055	.000	.99040	.00000	.00960

66.000	16.000	-5.923	-2.062	.000	.99020	.00000	.00980
68.500	16.000	-5.950	-2.072	.000	.99010	.00000	.00990
70.000	16.000	-5.966	-2.078	.000	.99000	.00000	.01000
72.000	16.000	-5.988	-2.085	.000	.98990	.00000	.01010
73.000	16.000	-5.999	-2.089	.000	.98990	.00000	.01010
74.000	16.000	-6.010	-2.093	.000	.98980	.00000	.01020
84.000	16.000	-6.120	-2.131	.000	.98930	.00000	.01070
94.000	16.000	-6.229	-2.169	.000	.98870	.00000	.01130
104.000	16.000	-6.339	-2.207	.000	.98810	.00000	.01190
114.000	16.000	-6.448	-2.245	.000	.98750	.00000	.01250
124.000	16.000	-6.558	-2.283	.000	.98680	.00000	.01320
134.000	16.000	-6.667	-2.322	.000	.98620	.00000	.01380
137.000	16.000	-6.700	-2.333	.000	.98600	.00000	.01400
.000	18.000	-7.200	-2.507	.000	.98260	.00000	.01740
5.000	18.000	-7.255	-2.526	.000	.98230	.00000	.01770
15.000	18.000	-7.364	-2.564	.000	.98150	.00000	.01850
25.000	18.000	-7.474	-2.602	.000	.98060	.00000	.01940
35.000	18.000	-7.583	-2.641	.000	.97980	.00000	.02020
45.000	18.000	-7.693	-2.679	.000	.97890	.00000	.02110
50.000	18.000	-7.747	-2.698	.000	.97850	.00000	.02150
55.000	18.000	-7.802	-2.717	.000	.97800	.00000	.02200
60.000	18.000	-7.857	-2.736	.000	.97760	.00000	.02240
62.000	18.000	-7.879	-2.743	.000	.97740	.00000	.02260
63.000	18.000	-7.890	-2.747	.000	.97730	.00000	.02270
64.000	18.000	-7.901	-2.751	.000	.97720	.00000	.02280
66.000	18.000	-7.923	-2.759	.000	.97700	.00000	.02300
68.500	18.000	-7.950	-2.768	.000	.97680	.00000	.02320
70.000	18.000	-7.966	-2.774	.000	.97670	.00000	.02330
72.000	18.000	-7.988	-2.782	.000	.97650	.00000	.02350
73.000	18.000	-7.999	-2.786	.000	.97640	.00000	.02360
74.000	18.000	-8.010	-2.789	.000	.97630	.00000	.02370
84.000	18.000	-8.120	-2.827	.000	.97530	.00000	.02470
94.000	18.000	-8.229	-2.865	.000	.97440	.00000	.02560
104.000	18.000	-8.339	-2.904	.000	.97340	.00000	.02660
114.000	18.000	-8.448	-2.942	.000	.97230	.00000	.02770
124.000	18.000	-8.558	-2.980	.000	.97130	.00000	.02870
134.000	18.000	-8.667	-3.018	.000	.97020	.00000	.02980
137.000	18.000	-8.700	-3.030	.000	.96990	.00000	.03010
.000	20.000	-9.200	-3.204	.000	.96460	.00000	.03540
5.000	20.000	-9.255	-3.223	.000	.96400	.00000	.03600
15.000	20.000	-9.364	-3.261	.000	.96280	.00000	.03720
25.000	20.000	-9.474	-3.299	.000	.96150	.00000	.03850
35.000	20.000	-9.583	-3.337	.000	.96030	.00000	.03970
45.000	20.000	-9.693	-3.375	.000	.95900	.00000	.04100
50.000	20.000	-9.747	-3.394	.000	.95830	.00000	.04170
55.000	20.000	-9.802	-3.413	.000	.95760	.00000	.04240
60.000	20.000	-9.857	-3.432	.000	.95690	.00000	.04310
62.000	20.000	-9.879	-3.440	.000	.95670	.00000	.04330
63.000	20.000	-9.890	-3.444	.000	.95650	.00000	.04350
64.000	20.000	-9.901	-3.448	.000	.95640	.00000	.04360
66.000	20.000	-9.923	-3.455	.000	.95610	.00000	.04390

68.500	20.000	-9.950	-3.465	.000	.95580	.00000	.04420
70.000	20.000	-9.966	-3.470	.000	.95560	.00000	.04440
72.000	20.000	-9.988	-3.478	.000	.95530	.00000	.04470
73.000	20.000	-9.999	-3.482	.000	.95520	.00000	.04480
74.000	20.000	-10.010	-3.486	.000	.95500	.00000	.04500
84.000	20.000	-10.120	-3.524	.000	.95360	.00000	.04640
94.000	20.000	-10.229	-3.562	.000	.95220	.00000	.04780
104.000	20.000	-10.339	-3.600	.000	.95070	.00000	.04930
114.000	20.000	-10.448	-3.638	.000	.94930	.00000	.05070
124.000	20.000	-10.558	-3.676	.000	.94770	.00000	.05230
134.000	20.000	-10.667	-3.714	.000	.94620	.00000	.05380
137.000	20.000	-10.700	-3.726	.000	.94580	.00000	.05420
.000	22.000	-11.200	-3.900	.000	.93840	.00000	.06160
5.000	22.000	-11.255	-3.919	.000	.93760	.00000	.06240
15.000	22.000	-11.364	-3.957	.000	.93590	.00000	.06410
25.000	22.000	-11.474	-3.995	.000	.93420	.00000	.06580
35.000	22.000	-11.583	-4.033	.000	.93240	.00000	.06760
45.000	22.000	-11.693	-4.072	.000	.93070	.00000	.06930
50.000	22.000	-11.747	-4.091	.000	.92980	.00000	.07020
55.000	22.000	-11.802	-4.110	.000	.92890	.00000	.07110
60.000	22.000	-11.857	-4.129	.000	.92800	.00000	.07200
62.000	22.000	-11.879	-4.136	.000	.92760	.00000	.07240
63.000	22.000	-11.890	-4.140	.000	.92740	.00000	.07260
64.000	22.000	-11.901	-4.144	.000	.92720	.00000	.07280
66.000	22.000	-11.923	-4.152	.000	.92690	.00000	.07310
68.500	22.000	-11.950	-4.161	.000	.92640	.00000	.07360
70.000	22.000	-11.966	-4.167	.000	.92610	.00000	.07390
72.000	22.000	-11.988	-4.174	.000	.92580	.00000	.07420
73.000	22.000	-11.999	-4.178	.000	.92560	.00000	.07440
74.000	22.000	-12.010	-4.182	.000	.92540	.00000	.07460
84.000	22.000	-12.120	-4.220	.000	.92350	.00000	.07650
94.000	22.000	-12.229	-4.258	.000	.92160	.00000	.07840
104.000	22.000	-12.339	-4.297	.000	.91970	.00000	.08030
114.000	22.000	-12.448	-4.335	.000	.91780	.00000	.08220
124.000	22.000	-12.558	-4.373	.000	.91580	.00000	.08420
134.000	22.000	-12.667	-4.411	.000	.91390	.00000	.08610
137.000	22.000	-12.700	-4.422	.000	.91330	.00000	.08670
.000	24.000	-13.200	-4.596	.000	.90390	.00000	.09610
5.000	24.000	-13.255	-4.615	.000	.90280	.00000	.09720
15.000	24.000	-13.364	-4.654	.000	.90070	.00000	.09930
25.000	24.000	-13.474	-4.692	.000	.89860	.00000	.10140
35.000	24.000	-13.583	-4.730	.000	.89640	.00000	.10360
45.000	24.000	-13.693	-4.768	.000	.89420	.00000	.10580
50.000	24.000	-13.747	-4.787	.000	.89310	.00000	.10690
55.000	24.000	-13.802	-4.806	.000	.89200	.00000	.10800
60.000	24.000	-13.857	-4.825	.000	.89090	.00000	.10910
62.000	24.000	-13.879	-4.833	.000	.89040	.00000	.10960
63.000	24.000	-13.890	-4.837	.000	.89020	.00000	.10980
64.000	24.000	-13.901	-4.840	.000	.89000	.00000	.11000
66.000	24.000	-13.923	-4.848	.000	.88950	.00000	.11050
68.500	24.000	-13.950	-4.858	.000	.88900	.00000	.11100

70.000	24.000	-13.966	-4.863	.000	.88860	.00000	.11140
72.000	24.000	-13.988	-4.871	.000	.88820	.00000	.11180
73.000	24.000	-13.999	-4.875	.000	.88790	.00000	.11210
74.000	24.000	-14.010	-4.879	.000	.88770	.00000	.11230
84.000	24.000	-14.120	-4.917	.000	.88540	.00000	.11460
94.000	24.000	-14.229	-4.955	.000	.88310	.00000	.11690
104.000	24.000	-14.339	-4.993	.000	.88080	.00000	.11920
114.000	24.000	-14.448	-5.031	.000	.87850	.00000	.12150
124.000	24.000	-14.558	-5.069	.000	.87610	.00000	.12390
134.000	24.000	-14.667	-5.107	.000	.87380	.00000	.12620
137.000	24.000	-14.700	-5.119	.000	.87300	.00000	.12700
.000	26.000	-15.200	-5.293	.000	.86190	.00000	.13810
5.000	26.000	-15.255	-5.312	.000	.86070	.00000	.13930
15.000	26.000	-15.364	-5.350	.000	.85820	.00000	.14180
25.000	26.000	-15.474	-5.388	.000	.85570	.00000	.14430
35.000	26.000	-15.583	-5.426	.000	.85320	.00000	.14680
45.000	26.000	-15.693	-5.464	.000	.85060	.00000	.14940
50.000	26.000	-15.747	-5.484	.000	.84940	.00000	.15060
55.000	26.000	-15.802	-5.503	.000	.84810	.00000	.15190
60.000	26.000	-15.857	-5.522	.000	.84680	.00000	.15320
62.000	26.000	-15.879	-5.529	.000	.84630	.00000	.15370
63.000	26.000	-15.890	-5.533	.000	.84600	.00000	.15400
64.000	26.000	-15.901	-5.537	.000	.84580	.00000	.15420
66.000	26.000	-15.923	-5.544	.000	.84530	.00000	.15470
68.500	26.000	-15.950	-5.554	.000	.84460	.00000	.15540
70.000	26.000	-15.966	-5.560	.000	.84420	.00000	.15580
72.000	26.000	-15.988	-5.567	.000	.84370	.00000	.15630
73.000	26.000	-15.999	-5.571	.000	.84340	.00000	.15660
74.000	26.000	-16.010	-5.575	.000	.84320	.00000	.15680
84.000	26.000	-16.120	-5.613	.000	.84060	.00000	.15940
94.000	26.000	-16.229	-5.651	.000	.83800	.00000	.16200
104.000	26.000	-16.339	-5.689	.000	.83530	.00000	.16470
114.000	26.000	-16.448	-5.727	.000	.83270	.00000	.16730
124.000	26.000	-16.558	-5.766	.000	.83000	.00000	.17000
134.000	26.000	-16.667	-5.804	.000	.82740	.00000	.17260
137.000	26.000	-16.700	-5.815	.000	.82660	.00000	.17340
.000	27.500	-16.700	-5.815	.000	.82660	.00000	.17340
5.000	27.500	-16.755	-5.834	.000	.82520	.00000	.17480
15.000	27.500	-16.864	-5.872	.000	.82250	.00000	.17750
25.000	27.500	-16.974	-5.911	.000	.81980	.00000	.18020
35.000	27.500	-17.083	-5.949	.000	.81710	.00000	.18290
45.000	27.500	-17.193	-5.987	.000	.81440	.00000	.18560
50.000	27.500	-17.247	-6.006	.000	.81300	.00000	.18700
55.000	27.500	-17.302	-6.025	.000	.81160	.00000	.18840
60.000	27.500	-17.357	-6.044	.000	.81020	.00000	.18980
62.000	27.500	-17.379	-6.052	.000	.80970	.00000	.19030
63.000	27.500	-17.390	-6.055	.000	.80940	.00000	.19060
64.000	27.500	-17.401	-6.059	.000	.80910	.00000	.19090
66.000	27.500	-17.423	-6.067	.000	.80860	.00000	.19140
68.500	27.500	-17.450	-6.076	.000	.80790	.00000	.19210
70.000	27.500	-17.466	-6.082	.000	.80750	.00000	.19250

72.000	27.500	-17.488	-6.090	.000	.80690	.00000	.19310
73.000	27.500	-17.499	-6.094	.000	.80670	.00000	.19330
74.000	27.500	-17.510	-6.097	.000	.80640	.00000	.19360
84.000	27.500	-17.620	-6.135	.000	.80360	.00000	.19640
94.000	27.500	-17.729	-6.174	.000	.80080	.00000	.19920
104.000	27.500	-17.839	-6.212	.000	.79800	.00000	.20200
114.000	27.500	-17.948	-6.250	.000	.79520	.00000	.20480
124.000	27.500	-18.058	-6.288	.000	.79240	.00000	.20760
134.000	27.500	-18.167	-6.326	.000	.78960	.00000	.21040
137.000	27.500	-18.200	-6.338	.000	.78870	.00000	.21130
.000	29.000	-18.200	-6.338	.000	.50000	.00000	.50000
5.000	29.000	-18.255	-6.357	.000	.49900	.00000	.50100
15.000	29.000	-18.364	-6.395	.000	.49710	.00000	.50290
25.000	29.000	-18.474	-6.433	.000	.49520	.00000	.50480
35.000	29.000	-18.583	-6.471	.000	.49330	.00000	.50670
45.000	29.000	-18.693	-6.509	.000	.49150	.00000	.50850
50.000	29.000	-18.747	-6.528	.000	.49060	.00000	.50940
55.000	29.000	-18.802	-6.547	.000	.48960	.00000	.51040
60.000	29.000	-18.857	-6.566	.000	.48870	.00000	.51130
62.000	29.000	-18.879	-6.574	.000	.48840	.00000	.51160
63.000	29.000	-18.890	-6.578	.000	.48820	.00000	.51180
64.000	29.000	-18.901	-6.582	.000	.48800	.00000	.51200
66.000	29.000	-18.923	-6.589	.000	.48760	.00000	.51240
68.500	29.000	-18.950	-6.599	.000	.48720	.00000	.51280
70.000	29.000	-18.966	-6.604	.000	.48690	.00000	.51310
72.000	29.000	-18.988	-6.612	.000	.48650	.00000	.51350
73.000	29.000	-18.999	-6.616	.000	.48630	.00000	.51370
74.000	29.000	-19.010	-6.620	.000	.48620	.00000	.51380
84.000	29.000	-19.120	-6.658	.000	.48440	.00000	.51560
94.000	29.000	-19.229	-6.696	.000	.48260	.00000	.51740
104.000	29.000	-19.339	-6.734	.000	.48080	.00000	.51920
114.000	29.000	-19.448	-6.772	.000	.47900	.00000	.52100
124.000	29.000	-19.558	-6.810	.000	.47730	.00000	.52270
134.000	29.000	-19.667	-6.848	.000	.47550	.00000	.52450
137.000	29.000	-19.700	-6.860	.000	.47500	.00000	.52500
.000	31.000	-20.200	-7.034	.000	.46720	.00000	.53280
5.000	31.000	-20.255	-7.053	.000	.46640	.00000	.53360
15.000	31.000	-20.364	-7.091	.000	.46470	.00000	.53530
25.000	31.000	-20.474	-7.129	.000	.46310	.00000	.53690
35.000	31.000	-20.583	-7.167	.000	.46150	.00000	.53850
45.000	31.000	-20.693	-7.206	.000	.45980	.00000	.54020
50.000	31.000	-20.747	-7.225	.000	.45900	.00000	.54100
55.000	31.000	-20.802	-7.244	.000	.45820	.00000	.54180
60.000	31.000	-20.857	-7.263	.000	.45740	.00000	.54260
62.000	31.000	-20.879	-7.270	.000	.45710	.00000	.54290
63.000	31.000	-20.890	-7.274	.000	.45690	.00000	.54310
64.000	31.000	-20.901	-7.278	.000	.45680	.00000	.54320
66.000	31.000	-20.923	-7.286	.000	.45640	.00000	.54360
68.500	31.000	-20.950	-7.295	.000	.45600	.00000	.54400
70.000	31.000	-20.966	-7.301	.000	.45580	.00000	.54420
72.000	31.000	-20.988	-7.308	.000	.45550	.00000	.54450

73.000	31.000	-20.999	-7.312	.000	.45530	.00000	.54470
74.000	31.000	-21.010	-7.316	.000	.45520	.00000	.54480
84.000	31.000	-21.120	-7.354	.000	.45360	.00000	.54640
94.000	31.000	-21.229	-7.392	.000	.45200	.00000	.54800
104.000	31.000	-21.339	-7.430	.000	.45050	.00000	.54950
114.000	31.000	-21.448	-7.469	.000	.44890	.00000	.55110
124.000	31.000	-21.558	-7.507	.000	.44740	.00000	.55260
134.000	31.000	-21.667	-7.545	.000	.44580	.00000	.55420
137.000	31.000	-21.700	-7.556	.000	.44540	.00000	.55460
.000	32.500	-21.700	-7.556	.000	.44540	.00000	.55460
5.000	32.500	-21.755	-7.575	.000	.44460	.00000	.55540
15.000	32.500	-21.864	-7.613	.000	.44310	.00000	.55690
25.000	32.500	-21.974	-7.652	.000	.44160	.00000	.55840
35.000	32.500	-22.083	-7.690	.000	.44010	.00000	.55990
45.000	32.500	-22.193	-7.728	.000	.43870	.00000	.56130
50.000	32.500	-22.247	-7.747	.000	.43790	.00000	.56210
55.000	32.500	-22.302	-7.766	.000	.43720	.00000	.56280
60.000	32.500	-22.357	-7.785	.000	.43650	.00000	.56350
62.000	32.500	-22.379	-7.793	.000	.43620	.00000	.56380
63.000	32.500	-22.390	-7.796	.000	.43600	.00000	.56400
64.000	32.500	-22.401	-7.800	.000	.43590	.00000	.56410
66.000	32.500	-22.423	-7.808	.000	.43560	.00000	.56440
68.500	32.500	-22.450	-7.817	.000	.43520	.00000	.56480
70.000	32.500	-22.466	-7.823	.000	.43500	.00000	.56500
72.000	32.500	-22.488	-7.831	.000	.43470	.00000	.56530
73.000	32.500	-22.499	-7.835	.000	.43460	.00000	.56540
74.000	32.500	-22.510	-7.838	.000	.43440	.00000	.56560
84.000	32.500	-22.620	-7.877	.000	.43300	.00000	.56700
94.000	32.500	-22.729	-7.915	.000	.43160	.00000	.56840
104.000	32.500	-22.839	-7.953	.000	.43010	.00000	.56990
114.000	32.500	-22.948	-7.991	.000	.42870	.00000	.57130
124.000	32.500	-23.058	-8.029	.000	.42730	.00000	.57270
134.000	32.500	-23.167	-8.067	.000	.42590	.00000	.57410
137.000	32.500	-23.200	-8.079	.000	.42550	.00000	.57450
.000	35.000	-24.200	-8.427	.000	.41330	.00000	.58670
5.000	35.000	-24.255	-8.446	.000	.41260	.00000	.58740
15.000	35.000	-24.364	-8.484	.000	.41130	.00000	.58870
25.000	35.000	-24.474	-8.522	.000	.41000	.00000	.59000
35.000	35.000	-24.583	-8.560	.000	.40880	.00000	.59120
45.000	35.000	-24.693	-8.598	.000	.40750	.00000	.59250
50.000	35.000	-24.747	-8.617	.000	.40690	.00000	.59310
55.000	35.000	-24.802	-8.637	.000	.40620	.00000	.59380
60.000	35.000	-24.857	-8.656	.000	.40560	.00000	.59440
62.000	35.000	-24.879	-8.663	.000	.40540	.00000	.59460
63.000	35.000	-24.890	-8.667	.000	.40520	.00000	.59480
64.000	35.000	-24.901	-8.671	.000	.40510	.00000	.59490
66.000	35.000	-24.923	-8.678	.000	.40490	.00000	.59510
68.500	35.000	-24.950	-8.688	.000	.40460	.00000	.59540
70.000	35.000	-24.966	-8.694	.000	.40440	.00000	.59560
72.000	35.000	-24.988	-8.701	.000	.40410	.00000	.59590
73.000	35.000	-24.999	-8.705	.000	.40400	.00000	.59600

74.000	35.000	-25.010	-8.709	.000	.40390	.00000	.59610
84.000	35.000	-25.120	-8.747	.000	.40260	.00000	.59740
94.000	35.000	-25.229	-8.785	.000	.40140	.00000	.59860
104.000	35.000	-25.339	-8.823	.000	.40020	.00000	.59980
114.000	35.000	-25.448	-8.861	.000	.39900	.00000	.60100
124.000	35.000	-25.558	-8.899	.000	.39780	.00000	.60220
134.000	35.000	-25.667	-8.938	.000	.39660	.00000	.60340
137.000	35.000	-25.700	-8.949	.000	.39620	.00000	.60380
.000	36.500	-25.700	-8.949	.000	.39620	.00000	.60380
5.000	36.500	-25.755	-8.968	.000	.39560	.00000	.60440
15.000	36.500	-25.864	-9.006	.000	.39440	.00000	.60560
25.000	36.500	-25.974	-9.044	.000	.39320	.00000	.60680
35.000	36.500	-26.083	-9.083	.000	.39210	.00000	.60790
45.000	36.500	-26.193	-9.121	.000	.39090	.00000	.60910
50.000	36.500	-26.247	-9.140	.000	.39030	.00000	.60970
55.000	36.500	-26.302	-9.159	.000	.38980	.00000	.61020
60.000	36.500	-26.357	-9.178	.000	.38920	.00000	.61080
62.000	36.500	-26.379	-9.186	.000	.38900	.00000	.61100
63.000	36.500	-26.390	-9.189	.000	.38880	.00000	.61120
64.000	36.500	-26.401	-9.193	.000	.38870	.00000	.61130
66.000	36.500	-26.423	-9.201	.000	.38850	.00000	.61150
68.500	36.500	-26.450	-9.210	.000	.38820	.00000	.61180
70.000	36.500	-26.466	-9.216	.000	.38800	.00000	.61200
72.000	36.500	-26.488	-9.224	.000	.38780	.00000	.61220
73.000	36.500	-26.499	-9.227	.000	.38770	.00000	.61230
74.000	36.500	-26.510	-9.231	.000	.38760	.00000	.61240
84.000	36.500	-26.620	-9.269	.000	.38650	.00000	.61350
94.000	36.500	-26.729	-9.307	.000	.38530	.00000	.61470
104.000	36.500	-26.839	-9.346	.000	.38420	.00000	.61580
114.000	36.500	-26.948	-9.384	.000	.38310	.00000	.61690
124.000	36.500	-27.058	-9.422	.000	.38200	.00000	.61800
134.000	36.500	-27.167	-9.460	.000	.38090	.00000	.61910
137.000	36.500	-27.200	-9.471	.000	.38060	.00000	.61940
.000	37.500	-26.700	-9.297	.000	.38560	.00000	.61440
5.000	37.500	-26.755	-9.316	.000	.38510	.00000	.61490
15.000	37.500	-26.864	-9.354	.000	.38390	.00000	.61610
25.000	37.500	-26.974	-9.393	.000	.38280	.00000	.61720
35.000	37.500	-27.083	-9.431	.000	.38170	.00000	.61830
45.000	37.500	-27.193	-9.469	.000	.38060	.00000	.61940
50.000	37.500	-27.247	-9.488	.000	.38010	.00000	.61990
55.000	37.500	-27.302	-9.507	.000	.37950	.00000	.62050
60.000	37.500	-27.357	-9.526	.000	.37900	.00000	.62100
62.000	37.500	-27.379	-9.534	.000	.37880	.00000	.62120
63.000	37.500	-27.390	-9.538	.000	.37870	.00000	.62130
64.000	37.500	-27.401	-9.541	.000	.37860	.00000	.62140
66.000	37.500	-27.423	-9.549	.000	.37830	.00000	.62170
68.500	37.500	-27.450	-9.559	.000	.37810	.00000	.62190
70.000	37.500	-27.466	-9.564	.000	.37790	.00000	.62210
72.000	37.500	-27.488	-9.572	.000	.37770	.00000	.62230
73.000	37.500	-27.499	-9.576	.000	.37760	.00000	.62240
74.000	37.500	-27.510	-9.580	.000	.37750	.00000	.62250

84.000	37.500	-27.620	-9.618	.000	.37640	.00000	.62360
94.000	37.500	-27.729	-9.656	.000	.37530	.00000	.62470
104.000	37.500	-27.839	-9.694	.000	.37430	.00000	.62570
114.000	37.500	-27.948	-9.732	.000	.37320	.00000	.62680
124.000	37.500	-28.058	-9.770	.000	.37220	.00000	.62780
134.000	37.500	-28.167	-9.808	.000	.37110	.00000	.62890
137.000	37.500	-28.200	-9.820	.000	.37080	.00000	.62920
.000	39.000	-28.200	-9.820	.000	.53300	.00000	.46700
5.000	39.000	-28.255	-9.839	.000	.53170	.00000	.46830
15.000	39.000	-28.364	-9.877	.000	.52930	.00000	.47070
25.000	39.000	-28.474	-9.915	.000	.52680	.00000	.47320
35.000	39.000	-28.583	-9.953	.000	.52440	.00000	.47560
45.000	39.000	-28.693	-9.991	.000	.52190	.00000	.47810
50.000	39.000	-28.747	-10.010	.000	.52070	.00000	.47930
55.000	39.000	-28.802	-10.029	.000	.51950	.00000	.48050
60.000	39.000	-28.857	-10.048	.000	.51830	.00000	.48170
62.000	39.000	-28.879	-10.056	.000	.51780	.00000	.48220
63.000	39.000	-28.890	-10.060	.000	.51750	.00000	.48250
64.000	39.000	-28.901	-10.064	.000	.51730	.00000	.48270
66.000	39.000	-28.923	-10.071	.000	.51680	.00000	.48320
68.500	39.000	-28.950	-10.081	.000	.51620	.00000	.48380
70.000	39.000	-28.966	-10.087	.000	.51580	.00000	.48420
72.000	39.000	-28.988	-10.094	.000	.51540	.00000	.48460
73.000	39.000	-28.999	-10.098	.000	.51510	.00000	.48490
74.000	39.000	-29.010	-10.102	.000	.51490	.00000	.48510
84.000	39.000	-29.120	-10.140	.000	.51250	.00000	.48750
94.000	39.000	-29.229	-10.178	.000	.51010	.00000	.48990
104.000	39.000	-29.339	-10.216	.000	.50770	.00000	.49230
114.000	39.000	-29.448	-10.254	.000	.50530	.00000	.49470
124.000	39.000	-29.558	-10.292	.000	.50300	.00000	.49700
134.000	39.000	-29.667	-10.330	.000	.50060	.00000	.49940
137.000	39.000	-29.700	-10.342	.000	.49990	.00000	.50010
.000	42.000	-31.200	-10.864	.000	.46890	.00000	.53110
5.000	42.000	-31.255	-10.883	.000	.46780	.00000	.53220
15.000	42.000	-31.364	-10.922	.000	.46570	.00000	.53430
25.000	42.000	-31.474	-10.960	.000	.46350	.00000	.53650
35.000	42.000	-31.583	-10.998	.000	.46130	.00000	.53870
45.000	42.000	-31.693	-11.036	.000	.45920	.00000	.54080
50.000	42.000	-31.747	-11.055	.000	.45810	.00000	.54190
55.000	42.000	-31.802	-11.074	.000	.45710	.00000	.54290
60.000	42.000	-31.857	-11.093	.000	.45600	.00000	.54400
62.000	42.000	-31.879	-11.101	.000	.45560	.00000	.54440
63.000	42.000	-31.890	-11.104	.000	.45540	.00000	.54460
64.000	42.000	-31.901	-11.108	.000	.45520	.00000	.54480
66.000	42.000	-31.923	-11.116	.000	.45470	.00000	.54530
68.500	42.000	-31.950	-11.125	.000	.45420	.00000	.54580
70.000	42.000	-31.966	-11.131	.000	.45390	.00000	.54610
72.000	42.000	-31.988	-11.139	.000	.45350	.00000	.54650
73.000	42.000	-31.999	-11.143	.000	.45330	.00000	.54670
74.000	42.000	-32.010	-11.146	.000	.45310	.00000	.54690
84.000	42.000	-32.120	-11.184	.000	.45100	.00000	.54900

94.000	42.000	-32.229	-11.223	.000	.44890	.00000	.55110
104.000	42.000	-32.339	-11.261	.000	.44680	.00000	.55320
114.000	42.000	-32.448	-11.299	.000	.44470	.00000	.55530
124.000	42.000	-32.558	-11.337	.000	.44270	.00000	.55730
134.000	42.000	-32.667	-11.375	.000	.44060	.00000	.55940
137.000	42.000	-32.700	-11.387	.000	.44000	.00000	.56000
.000	44.000	-33.200	-11.561	.000	.43080	.00000	.56920
5.000	44.000	-33.255	-11.580	.000	.42980	.00000	.57020
15.000	44.000	-33.364	-11.618	.000	.42780	.00000	.57220
25.000	44.000	-33.474	-11.656	.000	.42590	.00000	.57410
35.000	44.000	-33.583	-11.694	.000	.42390	.00000	.57610
45.000	44.000	-33.693	-11.732	.000	.42200	.00000	.57800
50.000	44.000	-33.747	-11.751	.000	.42100	.00000	.57900
55.000	44.000	-33.802	-11.770	.000	.42000	.00000	.58000
60.000	44.000	-33.857	-11.790	.000	.41910	.00000	.58090
62.000	44.000	-33.879	-11.797	.000	.41870	.00000	.58130
63.000	44.000	-33.890	-11.801	.000	.41850	.00000	.58150
64.000	44.000	-33.901	-11.805	.000	.41830	.00000	.58170
66.000	44.000	-33.923	-11.812	.000	.41790	.00000	.58210
68.500	44.000	-33.950	-11.822	.000	.41740	.00000	.58260
70.000	44.000	-33.966	-11.828	.000	.41720	.00000	.58280
72.000	44.000	-33.988	-11.835	.000	.41680	.00000	.58320
73.000	44.000	-33.999	-11.839	.000	.41660	.00000	.58340
74.000	44.000	-34.010	-11.843	.000	.41640	.00000	.58360
84.000	44.000	-34.120	-11.881	.000	.41450	.00000	.58550
94.000	44.000	-34.229	-11.919	.000	.41260	.00000	.58740
104.000	44.000	-34.339	-11.957	.000	.41070	.00000	.58930
114.000	44.000	-34.448	-11.995	.000	.40880	.00000	.59120
124.000	44.000	-34.558	-12.033	.000	.40700	.00000	.59300
134.000	44.000	-34.667	-12.072	.000	.40510	.00000	.59490
137.000	44.000	-34.700	-12.083	.000	.40460	.00000	.59540
.000	46.000	-35.200	-12.257	.000	.39620	.00000	.60380
5.000	46.000	-35.255	-12.276	.000	.39530	.00000	.60470
15.000	46.000	-35.364	-12.314	.000	.39360	.00000	.60640
25.000	46.000	-35.474	-12.352	.000	.39180	.00000	.60820
35.000	46.000	-35.583	-12.391	.000	.39000	.00000	.61000
45.000	46.000	-35.693	-12.429	.000	.38830	.00000	.61170
50.000	46.000	-35.747	-12.448	.000	.38740	.00000	.61260
55.000	46.000	-35.802	-12.467	.000	.38650	.00000	.61350
60.000	46.000	-35.857	-12.486	.000	.38560	.00000	.61440
62.000	46.000	-35.879	-12.493	.000	.38530	.00000	.61470
63.000	46.000	-35.890	-12.497	.000	.38510	.00000	.61490
64.000	46.000	-35.901	-12.501	.000	.38490	.00000	.61510
66.000	46.000	-35.923	-12.509	.000	.38460	.00000	.61540
68.500	46.000	-35.950	-12.518	.000	.38420	.00000	.61580
70.000	46.000	-35.966	-12.524	.000	.38390	.00000	.61610
72.000	46.000	-35.988	-12.532	.000	.38360	.00000	.61640
73.000	46.000	-35.999	-12.535	.000	.38340	.00000	.61660
74.000	46.000	-36.010	-12.539	.000	.38320	.00000	.61680
84.000	46.000	-36.120	-12.577	.000	.38150	.00000	.61850
94.000	46.000	-36.229	-12.616	.000	.37980	.00000	.62020

104.000	46.000	-36.339	-12.654	.000	.37810	.00000	.62190
114.000	46.000	-36.448	-12.692	.000	.37640	.00000	.62360
124.000	46.000	-36.558	-12.730	.000	.37470	.00000	.62530
134.000	46.000	-36.667	-12.768	.000	.37300	.00000	.62700
137.000	46.000	-36.700	-12.780	.000	.37250	.00000	.62750
.000	47.500	-36.700	-12.780	.000	.37250	.00000	.62750
5.000	47.500	-36.755	-12.799	.000	.37170	.00000	.62830
15.000	47.500	-36.864	-12.837	.000	.37010	.00000	.62990
25.000	47.500	-36.974	-12.875	.000	.36840	.00000	.63160
35.000	47.500	-37.083	-12.913	.000	.36680	.00000	.63320
45.000	47.500	-37.193	-12.951	.000	.36510	.00000	.63490
50.000	47.500	-37.247	-12.970	.000	.36430	.00000	.63570
55.000	47.500	-37.302	-12.989	.000	.36350	.00000	.63650
60.000	47.500	-37.357	-13.008	.000	.36270	.00000	.63730
62.000	47.500	-37.379	-13.016	.000	.36240	.00000	.63760
63.000	47.500	-37.390	-13.020	.000	.36220	.00000	.63780
64.000	47.500	-37.401	-13.024	.000	.36210	.00000	.63790
66.000	47.500	-37.423	-13.031	.000	.36180	.00000	.63820
68.500	47.500	-37.450	-13.041	.000	.36140	.00000	.63860
70.000	47.500	-37.466	-13.046	.000	.36110	.00000	.63890
72.000	47.500	-37.488	-13.054	.000	.36080	.00000	.63920
73.000	47.500	-37.499	-13.058	.000	.36060	.00000	.63940
74.000	47.500	-37.510	-13.062	.000	.36050	.00000	.63950
84.000	47.500	-37.620	-13.100	.000	.35890	.00000	.64110
94.000	47.500	-37.729	-13.138	.000	.35730	.00000	.64270
104.000	47.500	-37.839	-13.176	.000	.35570	.00000	.64430
114.000	47.500	-37.948	-13.214	.000	.35420	.00000	.64580
124.000	47.500	-38.058	-13.252	.000	.35260	.00000	.64740
134.000	47.500	-38.167	-13.290	.000	.35110	.00000	.64890
137.000	47.500	-38.200	-13.302	.000	.35060	.00000	.64940
.000	50.000	-39.200	-13.650	.000	.33690	.00000	.66310
5.000	50.000	-39.255	-13.669	.000	.33620	.00000	.66380
15.000	50.000	-39.364	-13.707	.000	.33470	.00000	.66530
25.000	50.000	-39.474	-13.745	.000	.33330	.00000	.66670
35.000	50.000	-39.583	-13.783	.000	.33190	.00000	.66810
45.000	50.000	-39.693	-13.822	.000	.33040	.00000	.66960
50.000	50.000	-39.747	-13.841	.000	.32970	.00000	.67030
55.000	50.000	-39.802	-13.860	.000	.32900	.00000	.67100
60.000	50.000	-39.857	-13.879	.000	.32830	.00000	.67170
62.000	50.000	-39.879	-13.886	.000	.32800	.00000	.67200
63.000	50.000	-39.890	-13.890	.000	.32790	.00000	.67210
64.000	50.000	-39.901	-13.894	.000	.32770	.00000	.67230
66.000	50.000	-39.923	-13.902	.000	.32750	.00000	.67250
68.500	50.000	-39.950	-13.911	.000	.32710	.00000	.67290
70.000	50.000	-39.966	-13.917	.000	.32690	.00000	.67310
72.000	50.000	-39.988	-13.925	.000	.32660	.00000	.67340
73.000	50.000	-39.999	-13.928	.000	.32650	.00000	.67350
74.000	50.000	-40.010	-13.932	.000	.32630	.00000	.67370
84.000	50.000	-40.120	-13.970	.000	.32490	.00000	.67510
94.000	50.000	-40.229	-14.008	.000	.32360	.00000	.67640
104.000	50.000	-40.339	-14.047	.000	.32220	.00000	.67780

114.000	50.000	-40.448	-14.085	.000	.32080	.00000	.67920
124.000	50.000	-40.558	-14.123	.000	.31940	.00000	.68060
134.000	50.000	-40.667	-14.161	.000	.31810	.00000	.68190
137.000	50.000	-40.700	-14.172	.000	.31770	.00000	.68230
.000	52.000	-41.200	-14.346	.000	.31160	.00000	.68840
5.000	52.000	-41.255	-14.366	.000	.31100	.00000	.68900
15.000	52.000	-41.364	-14.404	.000	.30960	.00000	.69040
25.000	52.000	-41.474	-14.442	.000	.30830	.00000	.69170
35.000	52.000	-41.583	-14.480	.000	.30710	.00000	.69290
45.000	52.000	-41.693	-14.518	.000	.30580	.00000	.69420
50.000	52.000	-41.747	-14.537	.000	.30510	.00000	.69490
55.000	52.000	-41.802	-14.556	.000	.30490	.00000	.69510
60.000	52.000	-41.857	-14.575	.000	.30410	.00000	.69590
62.000	52.000	-41.879	-14.583	.000	.30380	.00000	.69620
63.000	52.000	-41.890	-14.587	.000	.30370	.00000	.69630
64.000	52.000	-41.901	-14.590	.000	.30340	.00000	.69660
66.000	52.000	-41.923	-14.598	.000	.30310	.00000	.69690
68.500	52.000	-41.950	-14.608	.000	.30280	.00000	.69720
70.000	52.000	-41.966	-14.613	.000	.30260	.00000	.69740
72.000	52.000	-41.988	-14.621	.000	.30230	.00000	.69770
73.000	52.000	-41.999	-14.625	.000	.30220	.00000	.69780
74.000	52.000	-42.010	-14.629	.000	.30210	.00000	.69790
84.000	52.000	-42.120	-14.667	.000	.30060	.00000	.69940
94.000	52.000	-42.229	-14.705	.000	.29920	.00000	.70080
104.000	52.000	-42.339	-14.743	.000	.29830	.00000	.70170
114.000	52.000	-42.448	-14.781	.000	.29710	.00000	.70290
124.000	52.000	-42.558	-14.819	.000	.29590	.00000	.70410
134.000	52.000	-42.667	-14.857	.000	.29470	.00000	.70530
137.000	52.000	-42.700	-14.869	.000	.29430	.00000	.70570
.000	54.000	-43.200	-15.043	.000	.28880	.00000	.71120
5.000	54.000	-43.255	-15.062	.000	.28820	.00000	.71180
15.000	54.000	-43.364	-15.100	.000	.28710	.00000	.71290
25.000	54.000	-43.474	-15.138	.000	.28590	.00000	.71410
35.000	54.000	-43.583	-15.176	.000	.28470	.00000	.71530
45.000	54.000	-43.693	-15.214	.000	.28360	.00000	.71640
50.000	54.000	-43.747	-15.233	.000	.28300	.00000	.71700
55.000	54.000	-43.802	-15.252	.000	.28050	.00000	.71950
60.000	54.000	-43.857	-15.272	.000	.27990	.00000	.72010
62.000	54.000	-43.879	-15.279	.000	.27970	.00000	.72030
63.000	54.000	-43.890	-15.283	.000	.27960	.00000	.72040
64.000	54.000	-43.901	-15.287	.000	.28140	.00000	.71860
66.000	54.000	-43.923	-15.295	.000	.28120	.00000	.71880
68.500	54.000	-43.950	-15.304	.000	.28090	.00000	.71910
70.000	54.000	-43.966	-15.310	.000	.28070	.00000	.71930
72.000	54.000	-43.988	-15.317	.000	.28050	.00000	.71950
73.000	54.000	-43.999	-15.321	.000	.27840	.00000	.72160
74.000	54.000	-44.010	-15.325	.000	.27830	.00000	.72170
84.000	54.000	-44.120	-15.363	.000	.27710	.00000	.72290
94.000	54.000	-44.229	-15.401	.000	.27600	.00000	.72400
104.000	54.000	-44.339	-15.439	.000	.27690	.00000	.72310
114.000	54.000	-44.448	-15.477	.000	.27580	.00000	.72420

124.000	54.000	-44.558	-15.516	.000	.27470	.00000	.72530
134.000	54.000	-44.667	-15.554	.000	.27360	.00000	.72640
137.000	54.000	-44.700	-15.565	.000	.27330	.00000	.72670

INITIAL VOLUME OF WATER = 2704.0810
INITIAL VOLUME OF OIL = .0000

Time = 375

.000	.000	10.800	8.777	.000	1.00000	.00000	.00000
5.000	.000	10.753	8.769	.000	1.00000	.00000	.00000
15.000	.000	10.679	8.700	.000	1.00000	.00000	.00000
25.000	.000	10.639	8.641	.000	1.00000	.00000	.00000
35.000	.000	10.637	8.590	.000	1.00000	.00000	.00000
45.000	.000	10.674	8.552	.000	1.00000	.00000	.00000
50.000	.000	10.702	8.539	.000	1.00000	.00000	.00000
55.000	.000	10.727	8.525	.000	1.00000	.00000	.00000
60.000	.000	10.738	8.503	.000	1.00000	.00000	.00000
62.000	.000	10.736	8.492	.000	1.00000	.00000	.00000
63.000	.000	10.733	8.485	.000	1.00000	.00000	.00000
64.000	.000	10.728	8.478	.000	1.00000	.00000	.00000
66.000	.000	10.715	8.461	.000	1.00000	.00000	.00000
68.500	.000	10.691	8.436	.000	1.00000	.00000	.00000
70.000	.000	10.673	8.419	.000	1.00000	.00000	.00000
72.000	.000	10.643	8.394	.000	1.00000	.00000	.00000
73.000	.000	10.626	8.380	.000	1.00000	.00000	.00000
74.000	.000	10.608	8.366	.000	1.00000	.00000	.00000
84.000	.000	10.378	8.203	.000	1.00000	.00000	.00000
94.000	.000	10.120	8.035	.000	1.00000	.00000	.00000
104.000	.000	9.890	7.876	.000	1.00000	.00000	.00000
114.000	.000	9.699	7.731	.000	1.00000	.00000	.00000
124.000	.000	9.530	7.602	.000	1.00000	.00000	.00000
134.000	.000	9.356	7.488	.000	1.00000	.00000	.00000
137.000	.000	9.300	7.478	.000	1.00000	.00000	.00000
.000	2.000	8.800	7.359	.000	1.00000	.00000	.00000
5.000	2.000	8.752	7.350	.000	1.00000	.00000	.00000
15.000	2.000	8.678	7.280	.000	1.00000	.00000	.00000
25.000	2.000	8.639	7.222	.000	1.00000	.00000	.00000
35.000	2.000	8.636	7.173	.000	1.00000	.00000	.00000
45.000	2.000	8.673	7.135	.000	1.00000	.00000	.00000
50.000	2.000	8.702	7.124	.000	1.00000	.00000	.00000
55.000	2.000	8.728	7.110	.000	1.00000	.00000	.00000
60.000	2.000	8.740	7.089	.000	1.00000	.00000	.00000
62.000	2.000	8.738	7.078	.000	1.00000	.00000	.00000
63.000	2.000	8.735	7.072	.000	1.00000	.00000	.00000
64.000	2.000	8.731	7.064	.000	1.00000	.00000	.00000
66.000	2.000	8.718	7.048	.000	1.00000	.00000	.00000
68.500	2.000	8.694	7.023	.000	1.00000	.00000	.00000
70.000	2.000	8.675	7.006	.000	1.00000	.00000	.00000
72.000	2.000	8.645	6.981	.000	1.00000	.00000	.00000

73.000	2.000	8.628	6.967	.000	1.00000	.00000	.00000
74.000	2.000	8.610	6.952	.000	1.00000	.00000	.00000
84.000	2.000	8.379	6.788	.000	1.00000	.00000	.00000
94.000	2.000	8.120	6.622	.000	1.00000	.00000	.00000
104.000	2.000	7.889	6.464	.000	1.00000	.00000	.00000
114.000	2.000	7.698	6.318	.000	1.00000	.00000	.00000
124.000	2.000	7.530	6.189	.000	1.00000	.00000	.00000
134.000	2.000	7.356	6.074	.000	1.00000	.00000	.00000
137.000	2.000	7.300	6.063	.000	1.00000	.00000	.00000
.000	4.000	6.800	5.858	.000	1.00000	.00000	.00000
5.000	4.000	6.750	5.846	.000	1.00000	.00000	.00000
15.000	4.000	6.676	5.772	.000	1.00000	.00000	.00000
25.000	4.000	6.636	5.720	.000	1.00000	.00000	.00000
35.000	4.000	6.633	5.674	.000	1.00000	.00000	.00000
45.000	4.000	6.672	5.635	.000	1.00000	.00000	.00000
50.000	4.000	6.703	5.630	.000	1.00000	.00000	.00000
55.000	4.000	6.732	5.620	.000	1.00000	.00000	.00000
60.000	4.000	6.747	5.603	.000	1.00000	.00000	.00000
62.000	4.000	6.746	5.593	.000	1.00000	.00000	.00000
63.000	4.000	6.743	5.587	.000	1.00000	.00000	.00000
64.000	4.000	6.739	5.580	.000	1.00000	.00000	.00000
66.000	4.000	6.727	5.564	.000	1.00000	.00000	.00000
68.500	4.000	6.703	5.540	.000	1.00000	.00000	.00000
70.000	4.000	6.684	5.523	.000	1.00000	.00000	.00000
72.000	4.000	6.653	5.498	.000	1.00000	.00000	.00000
73.000	4.000	6.636	5.483	.000	1.00000	.00000	.00000
74.000	4.000	6.617	5.468	.000	1.00000	.00000	.00000
84.000	4.000	6.380	5.296	.000	1.00000	.00000	.00000
94.000	4.000	6.117	5.137	.000	1.00000	.00000	.00000
104.000	4.000	5.887	4.980	.000	1.00000	.00000	.00000
114.000	4.000	5.696	4.835	.000	1.00000	.00000	.00000
124.000	4.000	5.531	4.707	.000	1.00000	.00000	.00000
134.000	4.000	5.358	4.585	.000	1.00000	.00000	.00000
137.000	4.000	5.300	4.573	.000	1.00000	.00000	.00000
.000	6.000	4.800	4.288	.000	1.00000	.00000	.00000
5.000	6.000	4.746	4.271	.000	1.00000	.00000	.00000
15.000	6.000	4.673	4.188	.000	1.00000	.00000	.00000
25.000	6.000	4.633	4.143	.000	1.00000	.00000	.00000
35.000	6.000	4.628	4.108	.000	1.00000	.00000	.00000
45.000	6.000	4.669	4.070	.000	1.00000	.00000	.00000
50.000	6.000	4.703	4.080	.000	1.00000	.00000	.00000
55.000	6.000	4.737	4.080	.000	1.00000	.00000	.00000
60.000	6.000	4.758	4.071	.000	1.00000	.00000	.00000
62.000	6.000	4.759	4.062	.000	1.00000	.00000	.00000
63.000	6.000	4.757	4.055	.000	1.00000	.00000	.00000
64.000	6.000	4.753	4.049	.000	1.00000	.00000	.00000
66.000	6.000	4.742	4.035	.000	1.00000	.00000	.00000
68.500	6.000	4.718	4.013	.000	1.00000	.00000	.00000
70.000	6.000	4.699	3.997	.000	1.00000	.00000	.00000
72.000	6.000	4.667	3.970	.000	1.00000	.00000	.00000
73.000	6.000	4.649	3.957	.000	1.00000	.00000	.00000

74.000	6.000	4.629	3.940	.000	1.00000	.00000	.00000
84.000	6.000	4.382	3.749	.000	1.00000	.00000	.00000
94.000	6.000	4.114	3.594	.000	1.00000	.00000	.00000
104.000	6.000	3.882	3.438	.000	1.00000	.00000	.00000
114.000	6.000	3.694	3.307	.000	1.00000	.00000	.00000
124.000	6.000	3.532	3.171	.000	1.00000	.00000	.00000
134.000	6.000	3.362	3.036	.000	1.00000	.00000	.00000
137.000	6.000	3.300	3.022	.000	1.00000	.00000	.00000
.000	8.000	2.800	2.672	.000	1.00000	.00000	.00000
5.000	8.000	2.740	2.648	.000	1.00000	.00000	.00000
15.000	8.000	2.669	2.547	.000	1.00000	.00000	.00000
25.000	8.000	2.628	2.513	.000	1.00000	.00000	.00000
35.000	8.000	2.622	2.493	.000	1.00000	.00000	.00000
45.000	8.000	2.665	2.478	.000	1.00000	.00000	.00000
50.000	8.000	2.704	2.504	.000	1.00000	.00000	.00000
55.000	8.000	2.745	2.546	.000	1.00000	.00000	.00000
60.000	8.000	2.774	2.547	.000	1.00000	.00000	.00000
62.000	8.000	2.777	2.527	.000	1.00000	.00000	.00000
63.000	8.000	2.777	2.523	.000	1.00000	.00000	.00000
64.000	8.000	2.774	2.516	.000	1.00000	.00000	.00000
66.000	8.000	2.764	2.510	.000	1.00000	.00000	.00000
68.500	8.000	2.740	2.497	.000	1.00000	.00000	.00000
70.000	8.000	2.720	2.478	.000	1.00000	.00000	.00000
72.000	8.000	2.687	2.454	.000	1.00000	.00000	.00000
73.000	8.000	2.667	2.435	.000	1.00000	.00000	.00000
74.000	8.000	2.647	2.423	.000	1.00000	.00000	.00000
84.000	8.000	2.384	2.195	.000	1.00000	.00000	.00000
94.000	8.000	2.108	2.018	.000	1.00000	.00000	.00000
104.000	8.000	1.876	1.851	.000	1.00000	.00000	.00000
114.000	8.000	1.690	1.768	.000	1.00000	.00000	.00000
124.000	8.000	1.532	1.612	.000	1.00000	.00000	.00000
134.000	8.000	1.369	1.458	.000	1.00000	.00000	.00000
137.000	8.000	1.300	1.427	.000	1.00000	.00000	.00000
.000	10.000	.800	1.033	.000	1.00000	.00000	.00000
5.000	10.000	.729	1.013	.000	1.00000	.00000	.00000
15.000	10.000	.664	.870	.000	1.00000	.00000	.00000
25.000	10.000	.621	.877	.000	1.00000	.00000	.00000
35.000	10.000	.613	.859	.000	1.00000	.00000	.00000
45.000	10.000	.658	.954	.000	1.00000	.00000	.00000
50.000	10.000	.703	.940	.000	1.00000	.00000	.00000
55.000	10.000	.755	1.148	.000	1.00000	.00000	.00000
60.000	10.000	.795	1.126	.000	1.00000	.00000	.00000
62.000	10.000	.802	1.096	.000	1.00000	.00000	.00000
63.000	10.000	.803	1.026	.000	1.00000	.00000	.00000
64.000	10.000	.802	1.027	.000	1.00000	.00000	.00000
66.000	10.000	.794	1.045	.000	1.00000	.00000	.00000
68.500	10.000	.770	1.100	.000	1.00000	.00000	.00000
70.000	10.000	.749	1.081	.000	1.00000	.00000	.00000
72.000	10.000	.713	.984	.000	1.00000	.00000	.00000
73.000	10.000	.692	1.033	.000	1.00000	.00000	.00000
74.000	10.000	.669	1.017	.000	1.00000	.00000	.00000

84.000	10.000	.386	.729	.000	1.00000	.00000	.00000
94.000	10.000	.100	.445	.000	1.00000	.00000	.00000
104.000	10.000	-.132	.302	.000	1.00000	.00000	.00000
114.000	10.000	-.315	.060	.000	1.00000	.00000	.00000
124.000	10.000	-.468	-.095	.000	1.00000	.00000	.00000
134.000	10.000	-.617	-.191	.000	1.00000	.00000	.00000
137.000	10.000	-.700	-.215	.000	1.00000	.00000	.00000
.000	12.000	-1.245	-.429	.000	.99980	.00010	.00010
5.000	12.000	-1.278	-.445	.000	.99980	.00010	.00010
15.000	12.000	-1.342	-.469	.000	.99980	.00010	.00010
25.000	12.000	-1.386	-.478	.000	.99970	.00020	.00010
35.000	12.000	-1.398	-.487	.000	.99970	.00020	.00010
45.000	12.000	-1.351	-.467	.000	.99970	.00020	.00010
50.000	12.000	-1.298	-.448	.000	.99970	.00020	.00010
55.000	12.000	-1.234	-.427	.000	.99980	.00010	.00010
60.000	12.000	-1.178	-.406	.000	.99980	.00010	.00010
62.000	12.000	-1.165	-.401	.000	.99980	.00020	.00010
63.000	12.000	-1.161	-.401	.000	.99980	.00010	.00010
64.000	12.000	-1.160	-.400	.000	.99980	.00020	.00010
66.000	12.000	-1.166	-.401	.000	.99970	.00020	.00010
68.500	12.000	-1.190	-.410	.000	.99980	.00020	.00010
70.000	12.000	-1.213	-.418	.000	.99980	.00010	.00010
72.000	12.000	-1.253	-.432	.000	.99970	.00020	.00010
73.000	12.000	-1.276	-.440	.000	.99970	.00020	.00010
74.000	12.000	-1.301	-.448	.000	.99970	.00020	.00010
84.000	12.000	-1.612	-.561	.000	.99970	.00010	.00020
94.000	12.000	-1.911	-.665	.000	.99960	.00000	.00030
104.000	12.000	-2.142	-.745	.000	.99940	.00020	.00050
114.000	12.000	-2.321	-.807	.000	.99930	.00010	.00060
124.000	12.000	-2.469	-.860	.000	.99930	.00000	.00070
134.000	12.000	-2.602	-.906	.000	.99920	.00000	.00080
137.000	12.000	-2.626	-.915	.000	.99910	.00000	.00090
.000	14.000	-3.271	-1.139	.000	.99830	.00000	.00170
5.000	14.000	-3.289	-1.145	.000	.99830	.00000	.00170
15.000	14.000	-3.348	-1.166	.000	.99820	.00000	.00180
25.000	14.000	-3.395	-1.182	.000	.99810	.00000	.00190
35.000	14.000	-3.411	-1.188	.000	.99810	.00000	.00190
45.000	14.000	-3.364	-1.171	.000	.99820	.00000	.00180
50.000	14.000	-3.302	-1.150	.000	.99830	.00000	.00170
55.000	14.000	-3.221	-1.122	.000	.99840	.00000	.00160
60.000	14.000	-3.143	-1.094	.000	.99850	.00000	.00150
62.000	14.000	-3.122	-1.087	.000	.99860	.00000	.00140
63.000	14.000	-3.115	-1.085	.000	.99860	.00000	.00140
64.000	14.000	-3.111	-1.083	.000	.99860	.00000	.00140
66.000	14.000	-3.113	-1.084	.000	.99860	.00000	.00140
68.500	14.000	-3.137	-1.092	.000	.99850	.00000	.00150
70.000	14.000	-3.162	-1.101	.000	.99850	.00000	.00150
72.000	14.000	-3.208	-1.117	.000	.99840	.00000	.00160
73.000	14.000	-3.234	-1.126	.000	.99840	.00000	.00160
74.000	14.000	-3.264	-1.137	.000	.99840	.00000	.00160
84.000	14.000	-3.612	-1.258	.000	.99780	.00000	.00220

94.000	14.000	-3.924	-1.367	.000	.99710	.00000	.00290
104.000	14.000	-4.154	-1.446	.000	.99660	.00000	.00340
114.000	14.000	-4.328	-1.507	.000	.99620	.00000	.00380
124.000	14.000	-4.471	-1.557	.000	.99580	.00000	.00420
134.000	14.000	-4.584	-1.596	.000	.99540	.00000	.00460
137.000	14.000	-4.595	-1.600	.000	.99540	.00000	.00460
.000	16.000	-5.288	-1.841	.000	.99300	.00000	.00700
5.000	16.000	-5.300	-1.846	.000	.99300	.00000	.00700
15.000	16.000	-5.355	-1.865	.000	.99280	.00000	.00720
25.000	16.000	-5.405	-1.882	.000	.99260	.00000	.00740
35.000	16.000	-5.426	-1.890	.000	.99250	.00000	.00750
45.000	16.000	-5.380	-1.873	.000	.99270	.00000	.00730
50.000	16.000	-5.308	-1.849	.000	.99300	.00000	.00700
55.000	16.000	-5.206	-1.813	.000	.99330	.00000	.00670
60.000	16.000	-5.097	-1.775	.000	.99380	.00000	.00620
62.000	16.000	-5.063	-1.763	.000	.99390	.00000	.00610
63.000	16.000	-5.051	-1.759	.000	.99390	.00000	.00610
64.000	16.000	-5.042	-1.756	.000	.99400	.00000	.00600
66.000	16.000	-5.039	-1.755	.000	.99400	.00000	.00600
68.500	16.000	-5.063	-1.763	.000	.99390	.00000	.00610
70.000	16.000	-5.092	-1.773	.000	.99380	.00000	.00620
72.000	16.000	-5.146	-1.792	.000	.99360	.00000	.00640
73.000	16.000	-5.179	-1.803	.000	.99350	.00000	.00650
74.000	16.000	-5.214	-1.816	.000	.99330	.00000	.00670
84.000	16.000	-5.613	-1.954	.000	.99170	.00000	.00830
94.000	16.000	-5.941	-2.069	.000	.99020	.00000	.00980
104.000	16.000	-6.168	-2.148	.000	.98900	.00000	.01100
114.000	16.000	-6.336	-2.206	.000	.98810	.00000	.01190
124.000	16.000	-6.472	-2.254	.000	.98730	.00000	.01270
134.000	16.000	-6.569	-2.288	.000	.98670	.00000	.01330
137.000	16.000	-6.577	-2.290	.000	.98670	.00000	.01330
.000	18.000	-7.301	-2.542	.000	.98190	.00000	.01810
5.000	18.000	-7.310	-2.546	.000	.98190	.00000	.01810
15.000	18.000	-7.362	-2.564	.000	.98150	.00000	.01850
25.000	18.000	-7.416	-2.582	.000	.98110	.00000	.01890
35.000	18.000	-7.444	-2.592	.000	.98090	.00000	.01910
45.000	18.000	-7.400	-2.577	.000	.98120	.00000	.01880
50.000	18.000	-7.318	-2.548	.000	.98180	.00000	.01820
55.000	18.000	-7.187	-2.503	.000	.98270	.00000	.01730
60.000	18.000	-7.032	-2.449	.000	.98380	.00000	.01620
62.000	18.000	-6.978	-2.430	.000	.98420	.00000	.01580
63.000	18.000	-6.957	-2.423	.000	.98430	.00000	.01570
64.000	18.000	-6.941	-2.417	.000	.98440	.00000	.01560
66.000	18.000	-6.928	-2.412	.000	.98450	.00000	.01550
68.500	18.000	-6.952	-2.421	.000	.98430	.00000	.01570
70.000	18.000	-6.989	-2.434	.000	.98410	.00000	.01590
72.000	18.000	-7.058	-2.458	.000	.98360	.00000	.01640
73.000	18.000	-7.100	-2.472	.000	.98330	.00000	.01670
74.000	18.000	-7.145	-2.488	.000	.98300	.00000	.01700
84.000	18.000	-7.615	-2.652	.000	.97960	.00000	.02040
94.000	18.000	-7.961	-2.772	.000	.97670	.00000	.02330

104.000	18.000	-8.184	-2.850	.000	.97480	.00000	.02520
114.000	18.000	-8.346	-2.906	.000	.97330	.00000	.02670
124.000	18.000	-8.474	-2.951	.000	.97210	.00000	.02790
134.000	18.000	-8.559	-2.980	.000	.97130	.00000	.02870
137.000	18.000	-8.565	-2.982	.000	.97120	.00000	.02880
.000	20.000	-9.311	-3.242	.000	.96340	.00000	.03660
5.000	20.000	-9.319	-3.245	.000	.96330	.00000	.03670
15.000	20.000	-9.370	-3.263	.000	.96270	.00000	.03730
25.000	20.000	-9.427	-3.283	.000	.96210	.00000	.03790
35.000	20.000	-9.463	-3.295	.000	.96170	.00000	.03830
45.000	20.000	-9.424	-3.282	.000	.96210	.00000	.03790
50.000	20.000	-9.329	-3.249	.000	.96320	.00000	.03680
55.000	20.000	-9.162	-3.190	.000	.96510	.00000	.03490
60.000	20.000	-8.938	-3.112	.000	.96750	.00000	.03250
62.000	20.000	-8.852	-3.082	.000	.96830	.00000	.03170
63.000	20.000	-8.815	-3.070	.000	.96870	.00000	.03130
64.000	20.000	-8.786	-3.059	.000	.96900	.00000	.03100
66.000	20.000	-8.755	-3.048	.000	.96930	.00010	.03060
68.500	20.000	-8.780	-3.056	.000	.96900	.00010	.03090
70.000	20.000	-8.829	-3.074	.000	.96860	.00000	.03140
72.000	20.000	-8.926	-3.108	.000	.96760	.00000	.03240
73.000	20.000	-8.984	-3.128	.000	.96700	.00000	.03300
74.000	20.000	-9.045	-3.150	.000	.96630	.00000	.03370
84.000	20.000	-9.616	-3.349	.000	.95990	.00000	.04010
94.000	20.000	-9.983	-3.476	.000	.95540	.00000	.04460
104.000	20.000	-10.201	-3.552	.000	.95260	.00000	.04740
114.000	20.000	-10.356	-3.606	.000	.95050	.00000	.04950
124.000	20.000	-10.477	-3.648	.000	.94890	.00000	.05110
134.000	20.000	-10.552	-3.674	.000	.94780	.00000	.05220
137.000	20.000	-10.557	-3.676	.000	.94780	.00000	.05220
.000	22.000	-11.319	-3.941	.000	.93660	.00000	.06340
5.000	22.000	-11.327	-3.944	.000	.93650	.00000	.06350
15.000	22.000	-11.377	-3.962	.000	.93570	.00000	.06430
25.000	22.000	-11.439	-3.983	.000	.93470	.00000	.06530
35.000	22.000	-11.482	-3.998	.000	.93400	.00000	.06600
45.000	22.000	-11.451	-3.988	.000	.93450	.00000	.06550
50.000	22.000	-11.342	-3.950	.000	.93620	.00000	.06380
55.000	22.000	-11.127	-3.875	.000	.93950	.00000	.06050
60.000	22.000	-10.797	-3.760	.000	.94440	.00000	.05560
62.000	22.000	-10.655	-3.706	.000	.94620	.00040	.05340
63.000	22.000	-10.594	-3.644	.000	.94600	.00300	.05100
64.000	22.000	-10.537	-3.491	.000	.94400	.01090	.04520
66.000	22.000	-10.461	-3.264	.000	.94060	.02210	.03730
68.500	22.000	-10.483	-3.231	.000	.93930	.02440	.03620
70.000	22.000	-10.567	-3.470	.000	.94280	.01280	.04440
72.000	22.000	-10.721	-3.670	.000	.94380	.00420	.05200
73.000	22.000	-10.807	-3.756	.000	.94380	.00070	.05550
74.000	22.000	-10.897	-3.794	.000	.94290	.00000	.05710
84.000	22.000	-11.615	-4.045	.000	.93190	.00000	.06810
94.000	22.000	-12.005	-4.180	.000	.92550	.00000	.07450
104.000	22.000	-12.218	-4.254	.000	.92180	.00000	.07820

114.000	22.000	-12.366	-4.306	.000	.91930	.00000	.08070
124.000	22.000	-12.480	-4.346	.000	.91720	.00000	.08280
134.000	22.000	-12.548	-4.369	.000	.91600	.00000	.08400
137.000	22.000	-12.552	-4.371	.000	.91590	.00000	.08410
.000	24.000	-13.325	-4.640	.000	.90150	.00000	.09850
5.000	24.000	-13.333	-4.643	.000	.90130	.00000	.09870
15.000	24.000	-13.383	-4.660	.000	.90030	.00000	.09970
25.000	24.000	-13.449	-4.683	.000	.89900	.00000	.10100
35.000	24.000	-13.501	-4.701	.000	.89800	.00000	.10200
45.000	24.000	-13.480	-4.694	.000	.89840	.00000	.10160
50.000	24.000	-13.356	-4.651	.000	.90090	.00000	.09910
55.000	24.000	-13.078	-4.554	.000	.90620	.00000	.09380
60.000	24.000	-12.588	-4.364	.000	.91460	.00170	.08370
62.000	24.000	-12.344	-4.009	.000	.91150	.02200	.06650
63.000	24.000	-12.206	-3.306	.000	.89490	.06640	.03870
64.000	24.000	-12.097	-2.618	.000	.87640	.10390	.01970
66.000	24.000	-11.975	-1.965	.000	.85830	.13320	.00850
68.500	24.000	-12.007	-1.912	.000	.85540	.13690	.00780
70.000	24.000	-12.098	-2.374	.000	.86820	.11700	.01480
72.000	24.000	-12.374	-3.333	.000	.89050	.06990	.03960
73.000	24.000	-12.531	-4.031	.000	.90680	.02570	.06750
74.000	24.000	-12.673	-4.402	.000	.91330	.00100	.08570
84.000	24.000	-13.608	-4.738	.000	.89590	.00000	.10410
94.000	24.000	-14.028	-4.885	.000	.88730	.00000	.11260
104.000	24.000	-14.235	-4.957	.000	.88300	.00000	.11700
114.000	24.000	-14.375	-5.006	.000	.88000	.00000	.11990
124.000	24.000	-14.484	-5.044	.000	.87770	.00000	.12230
134.000	24.000	-14.546	-5.065	.000	.87640	.00000	.12360
137.000	24.000	-14.550	-5.067	.000	.87630	.00000	.12370
.000	26.000	-15.330	-5.338	.000	.85900	.00000	.14100
5.000	26.000	-15.337	-5.340	.000	.85880	.00000	.14120
15.000	26.000	-15.389	-5.359	.000	.85770	.00000	.14230
25.000	26.000	-15.459	-5.383	.000	.85610	.00000	.14390
35.000	26.000	-15.518	-5.404	.000	.85470	.00000	.14530
45.000	26.000	-15.509	-5.400	.000	.85490	.00000	.14510
50.000	26.000	-15.369	-5.352	.000	.85810	.00000	.14190
55.000	26.000	-15.016	-5.223	.000	.86580	.00060	.13350
60.000	26.000	-14.271	-4.730	.000	.87430	.02210	.10360
62.000	26.000	-13.848	-3.012	.000	.82830	.14200	.02960
63.000	26.000	-13.762	-2.221	.000	.80130	.18650	.01210
64.000	26.000	-13.689	-1.779	.000	.78680	.20690	.00630
66.000	26.000	-13.606	-1.312	.000	.77140	.22600	.00250
68.500	26.000	-13.639	-1.294	.000	.76940	.22820	.00240
70.000	26.000	-13.744	-1.571	.000	.77630	.21940	.00430
72.000	26.000	-13.967	-2.394	.000	.80010	.18480	.01520
73.000	26.000	-14.119	-3.263	.000	.82760	.13510	.03730
74.000	26.000	-14.326	-4.839	.000	.87610	.01390	.11000
84.000	26.000	-15.589	-5.425	.000	.85290	.00040	.14670
94.000	26.000	-16.048	-5.588	.000	.84230	.00000	.15770
104.000	26.000	-16.251	-5.659	.000	.83750	.00000	.16250
114.000	26.000	-16.384	-5.705	.000	.83420	.00000	.16580

124.000	26.000	-16.488	-5.741	.000	.83170	.00000	.16830
134.000	26.000	-16.546	-5.762	.000	.83030	.00000	.16970
137.000	26.000	-16.550	-5.763	.000	.83020	.00000	.16980
.000	27.500	-16.831	-5.860	.000	.82330	.00000	.17660
5.000	27.500	-16.838	-5.863	.000	.82310	.00000	.17680
15.000	27.500	-16.892	-5.881	.000	.82180	.00000	.17810
25.000	27.500	-16.965	-5.907	.000	.82000	.00000	.17990
35.000	27.500	-17.028	-5.929	.000	.81840	.00000	.18150
45.000	27.500	-17.030	-5.930	.000	.81840	.00000	.18160
50.000	27.500	-16.871	-5.874	.000	.82230	.00010	.17760
55.000	27.500	-16.469	-5.654	.000	.82910	.00860	.16220
60.000	27.500	-15.406	-4.220	.000	.81510	.10840	.07650
62.000	27.500	-15.116	-2.312	.000	.75080	.23550	.01370
63.000	27.500	-15.013	-1.814	.000	.73470	.25860	.00670
64.000	27.500	-14.944	-1.450	.000	.72260	.27390	.00340
66.000	27.500	-14.881	-1.078	.000	.70990	.28860	.00140
68.500	27.500	-14.921	-1.062	.000	.70770	.29100	.00130
70.000	27.500	-15.014	-1.290	.000	.71320	.28440	.00240
72.000	27.500	-15.215	-1.979	.000	.73320	.25810	.00860
73.000	27.500	-15.335	-2.711	.000	.75810	.22000	.02180
74.000	27.500	-15.419	-4.353	.000	.81970	.09720	.08320
84.000	27.500	-17.065	-5.855	.000	.81420	.00960	.17620
94.000	27.500	-17.558	-6.114	.000	.80510	.00010	.19480
104.000	27.500	-17.761	-6.185	.000	.80000	.00000	.20000
114.000	27.500	-17.890	-6.229	.000	.79670	.00000	.20330
124.000	27.500	-17.991	-6.264	.000	.79410	.00000	.20580
134.000	27.500	-18.048	-6.284	.000	.79260	.00000	.20730
137.000	27.500	-18.052	-6.286	.000	.79250	.00000	.20740
.000	29.000	-18.330	-6.383	.000	.49770	.00000	.50230
5.000	29.000	-18.338	-6.386	.000	.49760	.00000	.50240
15.000	29.000	-18.393	-6.405	.000	.49660	.00000	.50340
25.000	29.000	-18.468	-6.431	.000	.49530	.00000	.50470
35.000	29.000	-18.535	-6.454	.000	.49420	.00000	.50580
45.000	29.000	-18.546	-6.458	.000	.49400	.00000	.50600
50.000	29.000	-18.368	-6.392	.000	.49690	.00030	.50280
55.000	29.000	-17.431	-5.652	.000	.50220	.03470	.46310
60.000	29.000	-15.589	-3.376	.000	.49070	.21390	.29540
62.000	29.000	-15.630	-2.443	.000	.46670	.33010	.20320
63.000	29.000	-15.571	-2.120	.000	.46060	.37050	.16880
64.000	29.000	-15.521	-1.896	.000	.45670	.39860	.14470
66.000	29.000	-15.465	-1.652	.000	.45250	.42890	.11850
68.500	29.000	-15.509	-1.635	.000	.45120	.43200	.11680
70.000	29.000	-15.596	-1.791	.000	.45270	.41390	.13340
72.000	29.000	-15.705	-2.206	.000	.45960	.36240	.17800
73.000	29.000	-15.626	-2.605	.000	.47070	.30930	.22000
74.000	29.000	-15.416	-3.264	.000	.49230	.22260	.28510
84.000	29.000	-18.122	-5.868	.000	.48970	.03510	.47530
94.000	29.000	-19.075	-6.640	.000	.48500	.00010	.51480
104.000	29.000	-19.266	-6.709	.000	.48200	.00000	.51800
114.000	29.000	-19.394	-6.753	.000	.47990	.00000	.52010
124.000	29.000	-19.493	-6.788	.000	.47830	.00000	.52170

134.000	29.000	-19.550	-6.808	.000	.47740	.00000	.52260
137.000	29.000	-19.554	-6.809	.000	.47730	.00000	.52270
.000	31.000	-20.313	-7.073	.000	.46550	.00000	.53450
5.000	31.000	-20.323	-7.077	.000	.46540	.00000	.53460
15.000	31.000	-20.392	-7.101	.000	.46430	.00000	.53570
25.000	31.000	-20.480	-7.131	.000	.46300	.00000	.53700
35.000	31.000	-20.563	-7.161	.000	.46170	.00000	.53830
45.000	31.000	-20.586	-7.168	.000	.46140	.00000	.53860
50.000	31.000	-20.189	-6.989	.000	.46640	.00280	.53080
55.000	31.000	-18.340	-5.283	.000	.46980	.08920	.44100
60.000	31.000	-16.431	-2.856	.000	.45780	.29660	.24560
62.000	31.000	-16.532	-2.371	.000	.44500	.35940	.19560
63.000	31.000	-16.525	-2.191	.000	.44140	.38220	.17650
64.000	31.000	-16.506	-2.060	.000	.43900	.39860	.16240
66.000	31.000	-16.478	-1.915	.000	.43660	.41670	.14670
68.500	31.000	-16.514	-1.900	.000	.43560	.41930	.14510
70.000	31.000	-16.575	-1.984	.000	.43610	.40970	.15420
72.000	31.000	-16.589	-2.212	.000	.44050	.38090	.17870
73.000	31.000	-16.428	-2.407	.000	.44800	.35260	.19940
74.000	31.000	-16.212	-2.668	.000	.45850	.31500	.22650
84.000	31.000	-19.373	-5.828	.000	.45850	.06840	.47310
94.000	31.000	-21.071	-7.328	.000	.45410	.00060	.54530
104.000	31.000	-21.298	-7.416	.000	.45100	.00000	.54900
114.000	31.000	-21.415	-7.457	.000	.44940	.00000	.55060
124.000	31.000	-21.510	-7.490	.000	.44800	.00000	.55200
134.000	31.000	-21.573	-7.512	.000	.44720	.00000	.55280
137.000	31.000	-21.576	-7.513	.000	.44710	.00000	.55290
.000	32.500	-21.799	-7.590	.000	.44400	.00000	.55600
5.000	32.500	-21.810	-7.594	.000	.44390	.00000	.55610
15.000	32.500	-21.888	-7.622	.000	.44280	.00000	.55720
25.000	32.500	-21.982	-7.654	.000	.44150	.00000	.55850
35.000	32.500	-22.072	-7.686	.000	.44030	.00000	.55970
45.000	32.500	-22.064	-7.683	.000	.44040	.00000	.55960
50.000	32.500	-21.334	-7.215	.000	.44590	.01350	.54060
55.000	32.500	-18.856	-4.596	.000	.44290	.16200	.39500
60.000	32.500	-17.338	-2.690	.000	.43490	.33620	.22880
62.000	32.500	-17.328	-2.313	.000	.42760	.38300	.18940
63.000	32.500	-17.333	-2.182	.000	.42490	.39960	.17540
64.000	32.500	-17.326	-2.084	.000	.42320	.41190	.16490
66.000	32.500	-17.303	-1.972	.000	.42150	.42570	.15280
68.500	32.500	-17.332	-1.956	.000	.42070	.42820	.15120
70.000	32.500	-17.373	-2.015	.000	.42100	.42150	.15750
72.000	32.500	-17.355	-2.178	.000	.42440	.40060	.17500
73.000	32.500	-17.232	-2.310	.000	.42940	.38140	.18910
74.000	32.500	-17.099	-2.490	.000	.43570	.35620	.20810
84.000	32.500	-20.155	-5.563	.000	.43610	.10600	.45790
94.000	32.500	-22.520	-7.810	.000	.43370	.00180	.56450
104.000	32.500	-22.806	-7.941	.000	.43060	.00000	.56940
114.000	32.500	-22.926	-7.983	.000	.42900	.00000	.57100
124.000	32.500	-23.022	-8.017	.000	.42780	.00000	.57220
134.000	32.500	-23.091	-8.040	.000	.42690	.00000	.57310

137.000	32.500	-23.094	-8.042	.000	.42690	.00000	.57310
.000	35.000	-24.275	-8.453	.000	.41240	.00000	.58760
5.000	35.000	-24.289	-8.458	.000	.41220	.00000	.58780
15.000	35.000	-24.377	-8.488	.000	.41120	.00000	.58880
25.000	35.000	-24.478	-8.524	.000	.41000	.00000	.59000
35.000	35.000	-24.562	-8.553	.000	.40900	.00000	.59100
45.000	35.000	-24.411	-8.497	.000	.41070	.00020	.58910
50.000	35.000	-22.711	-7.258	.000	.41920	.03840	.54240
55.000	35.000	-19.723	-3.917	.000	.41270	.24470	.34260
60.000	35.000	-18.733	-2.576	.000	.40640	.37660	.21700
62.000	35.000	-18.669	-2.278	.000	.40230	.41200	.18570
63.000	35.000	-18.653	-2.173	.000	.40080	.42480	.17450
64.000	35.000	-18.640	-2.094	.000	.39970	.43430	.16600
66.000	35.000	-18.615	-2.001	.000	.39850	.44550	.15600
68.500	35.000	-18.627	-1.984	.000	.39800	.44780	.15410
70.000	35.000	-18.641	-2.027	.000	.39850	.44270	.15880
72.000	35.000	-18.580	-2.152	.000	.40170	.42600	.17230
73.000	35.000	-18.497	-2.255	.000	.40490	.41180	.18330
74.000	35.000	-18.420	-2.387	.000	.40860	.39410	.19730
84.000	35.000	-21.222	-5.157	.000	.40800	.15900	.43300
94.000	35.000	-24.781	-8.536	.000	.40490	.00470	.59040
104.000	35.000	-25.296	-8.808	.000	.40070	.00000	.59930
114.000	35.000	-25.437	-8.858	.000	.39910	.00000	.60090
124.000	35.000	-25.535	-8.892	.000	.39800	.00000	.60200
134.000	35.000	-25.615	-8.920	.000	.39710	.00000	.60290
137.000	35.000	-25.619	-8.921	.000	.39710	.00000	.60290
.000	36.500	-25.765	-8.972	.000	.39550	.00000	.60450
5.000	36.500	-25.780	-8.977	.000	.39530	.00000	.60470
15.000	36.500	-25.872	-9.009	.000	.39430	.00000	.60570
25.000	36.500	-25.977	-9.046	.000	.39320	.00000	.60680
35.000	36.500	-26.048	-9.070	.000	.39250	.00000	.60750
45.000	36.500	-25.702	-8.923	.000	.39570	.00130	.60300
50.000	36.500	-23.081	-6.646	.000	.40150	.08340	.51510
55.000	36.500	-20.610	-3.644	.000	.39260	.28790	.31940
60.000	36.500	-19.611	-2.521	.000	.39060	.39800	.21140
62.000	36.500	-19.479	-2.255	.000	.38850	.42830	.18320
63.000	36.500	-19.441	-2.160	.000	.38760	.43940	.17310
64.000	36.500	-19.410	-2.088	.000	.38690	.44780	.16530
66.000	36.500	-19.366	-2.000	.000	.38620	.45790	.15590
68.500	36.500	-19.358	-1.982	.000	.38600	.46000	.15390
70.000	36.500	-19.358	-2.020	.000	.38660	.45530	.15800
72.000	36.500	-19.321	-2.133	.000	.38900	.44080	.17020
73.000	36.500	-19.291	-2.228	.000	.39100	.42860	.18030
74.000	36.500	-19.280	-2.358	.000	.39340	.41250	.19420
84.000	36.500	-21.826	-4.758	.000	.39100	.20250	.40650
94.000	36.500	-25.933	-8.787	.000	.38970	.01160	.59870
104.000	36.500	-26.795	-9.330	.000	.38460	.00000	.61530
114.000	36.500	-26.942	-9.382	.000	.38320	.00000	.61680
124.000	36.500	-27.043	-9.417	.000	.38210	.00000	.61790
134.000	36.500	-27.128	-9.446	.000	.38130	.00000	.61870
137.000	36.500	-27.132	-9.448	.000	.38120	.00000	.61880

.000	37.500	-26.761	-9.321	.000	.38500	.00000	.61500
5.000	37.500	-26.776	-9.327	.000	.38490	.00000	.61510
15.000	37.500	-26.868	-9.359	.000	.38390	.00000	.61610
25.000	37.500	-26.975	-9.396	.000	.38290	.00000	.61710
35.000	37.500	-27.053	-9.423	.000	.38210	.00000	.61790
45.000	37.500	-26.409	-9.079	.000	.38680	.00540	.60780
50.000	37.500	-23.361	-6.029	.000	.38670	.12920	.48410
55.000	37.500	-21.246	-3.538	.000	.38090	.30910	.31000
60.000	37.500	-20.187	-2.491	.000	.38110	.41070	.20830
62.000	37.500	-19.999	-2.242	.000	.38010	.43800	.18190
63.000	37.500	-19.935	-2.152	.000	.37970	.44810	.17220
64.000	37.500	-19.887	-2.082	.000	.37940	.45590	.16470
66.000	37.500	-19.825	-1.996	.000	.37900	.46550	.15550
68.500	37.500	-19.796	-1.977	.000	.37920	.46740	.15340
70.000	37.500	-19.788	-2.013	.000	.37980	.46290	.15730
72.000	37.500	-19.784	-2.120	.000	.38160	.44960	.16880
73.000	37.500	-19.801	-2.208	.000	.38260	.43910	.17820
74.000	37.500	-19.847	-2.342	.000	.38400	.42350	.19250
84.000	37.500	-22.247	-4.510	.000	.38040	.23080	.38880
94.000	37.500	-26.625	-8.614	.000	.37630	.03070	.59300
104.000	37.500	-27.799	-9.682	.000	.37470	.00000	.62530
114.000	37.500	-27.941	-9.733	.000	.37330	.00000	.62670
124.000	37.500	-28.048	-9.770	.000	.37230	.00000	.62770
134.000	37.500	-28.134	-9.800	.000	.37150	.00000	.62850
137.000	37.500	-28.138	-9.801	.000	.37140	.00000	.62860
.000	39.000	-28.260	-9.841	.000	.53160	.00000	.46840
5.000	39.000	-28.275	-9.846	.000	.53130	.00000	.46870
15.000	39.000	-28.368	-9.878	.000	.52920	.00000	.47080
25.000	39.000	-28.474	-9.915	.000	.52680	.00000	.47320
35.000	39.000	-28.553	-9.943	.000	.52500	.00000	.47500
45.000	39.000	-27.836	-9.587	.000	.53760	.01080	.45160
50.000	39.000	-24.691	-6.396	.000	.53600	.24840	.21560
55.000	39.000	-22.640	-3.867	.000	.51950	.42040	.06020
60.000	39.000	-21.551	-2.494	.000	.50990	.47300	.01710
62.000	39.000	-21.337	-2.113	.000	.50440	.48520	.01050
63.000	39.000	-21.263	-1.961	.000	.50180	.48980	.00840
64.000	39.000	-21.206	-1.838	.000	.49960	.49350	.00690
66.000	39.000	-21.134	-1.679	.000	.49680	.49790	.00530
68.500	39.000	-21.097	-1.638	.000	.49670	.49840	.00490
70.000	39.000	-21.090	-1.701	.000	.49890	.49560	.00550
72.000	39.000	-21.101	-1.885	.000	.50460	.48790	.00750
73.000	39.000	-21.134	-2.024	.000	.50820	.48260	.00920
74.000	39.000	-21.198	-2.190	.000	.51150	.47680	.01160
84.000	39.000	-23.601	-4.850	.000	.52020	.36920	.11060
94.000	39.000	-28.072	-9.324	.000	.52030	.04580	.43380
104.000	39.000	-29.291	-10.200	.000	.50870	.00000	.49130
114.000	39.000	-29.445	-10.253	.000	.50540	.00000	.49460
124.000	39.000	-29.553	-10.291	.000	.50310	.00000	.49690
134.000	39.000	-29.641	-10.321	.000	.50120	.00000	.49880
137.000	39.000	-29.646	-10.323	.000	.50110	.00000	.49890
.000	42.000	-31.257	-10.884	.000	.46780	.00000	.53220

5.000	42.000	-31.272	-10.889	.000	.46750	.00000	.53250
15.000	42.000	-31.366	-10.922	.000	.46560	.00000	.53440
25.000	42.000	-31.473	-10.959	.000	.46350	.00000	.53650
35.000	42.000	-31.555	-10.988	.000	.46190	.00000	.53810
45.000	42.000	-30.743	-10.550	.000	.47330	.01410	.51260
50.000	42.000	-27.340	-6.937	.000	.46690	.27670	.25650
55.000	42.000	-25.403	-4.451	.000	.45050	.46120	.08830
60.000	42.000	-24.076	-2.737	.000	.43930	.53830	.02240
62.000	42.000	-23.756	-2.169	.000	.43230	.55640	.01130
63.000	42.000	-23.632	-1.929	.000	.42900	.56300	.00800
64.000	42.000	-23.530	-1.728	.000	.42630	.56790	.00580
66.000	42.000	-23.391	-1.458	.000	.42270	.57380	.00350
68.500	42.000	-23.333	-1.385	.000	.42230	.57470	.00300
70.000	42.000	-23.348	-1.490	.000	.42480	.57150	.00370
72.000	42.000	-23.428	-1.792	.000	.43090	.56270	.00640
73.000	42.000	-23.504	-2.008	.000	.43480	.55610	.00900
74.000	42.000	-23.605	-2.263	.000	.43920	.54800	.01280
84.000	42.000	-26.383	-5.440	.000	.45070	.40150	.14770
94.000	42.000	-31.019	-10.274	.000	.45660	.04750	.49590
104.000	42.000	-32.291	-11.244	.000	.44770	.00000	.55230
114.000	42.000	-32.446	-11.298	.000	.44480	.00000	.55520
124.000	42.000	-32.555	-11.336	.000	.44270	.00000	.55730
134.000	42.000	-32.644	-11.367	.000	.44110	.00000	.55890
137.000	42.000	-32.649	-11.369	.000	.44100	.00000	.55900
.000	44.000	-33.253	-11.579	.000	.42990	.00000	.57010
5.000	44.000	-33.269	-11.585	.000	.42960	.00000	.57040
15.000	44.000	-33.366	-11.618	.000	.42780	.00000	.57220
25.000	44.000	-33.473	-11.656	.000	.42590	.00000	.57410
35.000	44.000	-33.559	-11.686	.000	.42430	.00000	.57570
45.000	44.000	-32.792	-11.229	.000	.43290	.01560	.55150
50.000	44.000	-29.243	-7.396	.000	.42510	.28330	.29170
55.000	44.000	-27.236	-4.849	.000	.41050	.47890	.11050
60.000	44.000	-25.697	-2.933	.000	.40080	.57180	.02740
62.000	44.000	-25.272	-2.222	.000	.39360	.59430	.01220
63.000	44.000	-25.094	-1.909	.000	.39020	.60210	.00780
64.000	44.000	-24.940	-1.642	.000	.38740	.60760	.00500
66.000	44.000	-24.718	-1.278	.000	.38400	.61370	.00230
68.500	44.000	-24.643	-1.177	.000	.38330	.61490	.00180
70.000	44.000	-24.697	-1.319	.000	.38550	.61200	.00260
72.000	44.000	-24.862	-1.725	.000	.39140	.60290	.00570
73.000	44.000	-24.979	-2.012	.000	.39560	.59530	.00910
74.000	44.000	-25.116	-2.344	.000	.40060	.58520	.01420
84.000	44.000	-28.301	-5.866	.000	.40930	.41370	.17700
94.000	44.000	-33.068	-10.957	.000	.41790	.04570	.53640
104.000	44.000	-34.300	-11.944	.000	.41140	.00000	.58860
114.000	44.000	-34.446	-11.995	.000	.40890	.00000	.59110
124.000	44.000	-34.555	-12.033	.000	.40700	.00000	.59300
134.000	44.000	-34.647	-12.064	.000	.40550	.00000	.59450
137.000	44.000	-34.652	-12.066	.000	.40540	.00000	.59460
.000	46.000	-35.248	-12.274	.000	.39550	.00000	.60450
5.000	46.000	-35.266	-12.280	.000	.39520	.00000	.60480

15.000	46.000	-35.365	-12.315	.000	.39350	.00000	.60650
25.000	46.000	-35.473	-12.352	.000	.39180	.00000	.60820
35.000	46.000	-35.562	-12.383	.000	.39040	.00000	.60960
45.000	46.000	-34.902	-11.965	.000	.39640	.01400	.58960
50.000	46.000	-31.249	-7.987	.000	.38830	.27480	.33680
55.000	46.000	-29.122	-5.334	.000	.37570	.48360	.14070
60.000	46.000	-27.303	-3.194	.000	.36820	.59680	.03510
62.000	46.000	-26.709	-2.289	.000	.36110	.62560	.01330
63.000	46.000	-26.443	-1.873	.000	.35780	.63490	.00730
64.000	46.000	-26.202	-1.510	.000	.35510	.64110	.00390
66.000	46.000	-25.838	-1.003	.000	.35200	.64690	.00110
68.500	46.000	-25.724	-.854	.000	.35120	.64810	.00070
70.000	46.000	-25.847	-1.054	.000	.35290	.64580	.00130
72.000	46.000	-26.177	-1.621	.000	.35810	.63710	.00480
73.000	46.000	-26.378	-2.018	.000	.36250	.62840	.00910
74.000	46.000	-26.592	-2.464	.000	.36770	.61580	.01650
84.000	46.000	-30.252	-6.404	.000	.37420	.40950	.21620
94.000	46.000	-35.188	-11.737	.000	.38370	.03800	.57830
104.000	46.000	-36.306	-12.642	.000	.37860	.00000	.62140
114.000	46.000	-36.446	-12.691	.000	.37640	.00000	.62360
124.000	46.000	-36.556	-12.729	.000	.37470	.00000	.62530
134.000	46.000	-36.650	-12.762	.000	.37330	.00000	.62670
137.000	46.000	-36.656	-12.764	.000	.37320	.00000	.62680
.000	47.500	-36.743	-12.795	.000	.37190	.00000	.62810
5.000	47.500	-36.764	-12.802	.000	.37160	.00000	.62840
15.000	47.500	-36.865	-12.837	.000	.37000	.00000	.63000
25.000	47.500	-36.973	-12.875	.000	.36840	.00000	.63160
35.000	47.500	-37.060	-12.905	.000	.36710	.00000	.63290
45.000	47.500	-36.558	-12.597	.000	.37160	.00900	.61940
50.000	47.500	-32.869	-8.579	.000	.36410	.25510	.38090
55.000	47.500	-30.605	-5.805	.000	.35270	.47450	.17270
60.000	47.500	-28.549	-3.487	.000	.34710	.60790	.04500
62.000	47.500	-27.759	-2.349	.000	.33980	.64590	.01430
63.000	47.500	-27.403	-1.805	.000	.33590	.65750	.00660
64.000	47.500	-27.085	-1.355	.000	.33330	.66390	.00280
66.000	47.500	-26.535	-.652	.000	.33020	.66950	.00030
68.500	47.500	-26.375	-.456	.000	.32950	67040	.00010
70.000	47.500	-26.570	-.710	.000	.33060	.66900	.00040
72.000	47.500	-27.105	-1.488	.000	.33550	.66080	.00370
73.000	47.500	-27.397	-1.996	.000	.34000	.65120	.00890
74.000	47.500	-27.705	-2.598	.000	.34610	.63460	.01930
84.000	47.500	-31.753	-6.955	.000	.35280	.38940	.25780
94.000	47.500	-36.842	-12.417	.000	.36100	.02780	.61120
104.000	47.500	-37.808	-13.165	.000	.35620	.00000	.64380
114.000	47.500	-37.947	-13.214	.000	.35420	.00000	.64580
124.000	47.500	-38.056	-13.252	.000	.35260	.00000	.64740
134.000	47.500	-38.153	-13.285	.000	.35130	.00000	.64870
137.000	47.500	-38.159	-13.288	.000	.35120	.00000	.64880
.000	50.000	-39.237	-13.663	.000	.33640	.00000	.66360
5.000	50.000	-39.261	-13.671	.000	.33610	.00000	.66390
15.000	50.000	-39.365	-13.707	.000	.33470	.00000	.66530

25.000	50.000	-39.473	-13.745	.000	.33330	.00000	.66670
35.000	50.000	-39.564	-13.777	.000	.33210	.00000	.66790
45.000	50.000	-39.279	-13.609	.000	.33450	.00400	.66150
50.000	50.000	-36.082	-10.007	.000	.32640	.19450	.47910
55.000	50.000	-33.271	-6.703	.000	.31690	.44440	.23870
60.000	50.000	-30.840	-4.425	.000	.31980	.59330	.08690
62.000	50.000	-29.724	-2.871	.000	.31160	.66260	.02580
63.000	50.000	-28.885	-1.765	.000	.30680	.68710	.00610
64.000	50.000	-28.014	-.622	.000	.30190	.69780	.00030
66.000	50.000	-27.171	.384	.000	.29910	.70090	.00000
68.500	50.000	-26.995	.574	.000	.29880	.70120	.00000
70.000	50.000	-27.217	.332	.000	.29920	.70080	.00000
72.000	50.000	-28.087	-.749	.000	.30290	.69670	.00050
73.000	50.000	-28.921	-1.980	.000	.31000	.68140	.00860
74.000	50.000	-29.757	-3.290	.000	.31880	.64300	.03820
84.000	50.000	-34.418	-8.091	.000	.32150	.33380	.34460
94.000	50.000	-39.636	-13.541	.000	.32600	.01510	.65890
104.000	50.000	-40.305	-14.035	.000	.32260	.00000	.67740
114.000	50.000	-40.450	-14.085	.000	.32080	.00000	.67920
124.000	50.000	-40.556	-14.122	.000	.31950	.00000	.68050
134.000	50.000	-40.657	-14.157	.000	.31820	.00000	.68180
137.000	50.000	-40.664	-14.160	.000	.31810	.00000	.68190
.000	52.000	-41.233	-14.358	.000	.31120	.00000	.68880
5.000	52.000	-41.260	-14.367	.000	.31090	.00000	.68910
15.000	52.000	-41.365	-14.404	.000	.30960	.00000	.69040
25.000	52.000	-41.473	-14.441	.000	.30840	.00000	.69160
35.000	52.000	-41.572	-14.476	.000	.30720	.00000	.69280
45.000	52.000	-41.378	-14.400	.000	.30930	.00040	.69020
50.000	52.000	-39.751	-13.204	.000	.31730	.03730	.64540
55.000	52.000	-36.061	-9.620	.000	.32280	.36960	.30760
60.000	52.000	-27.174	.004	.000	.30630	.69370	.00000
62.000	52.000	-26.110	1.424	.000	.29900	.70100	.00000
63.000	52.000	-27.029	1.538	.000	.28020	.71980	.00000
64.000	52.000	-27.694	1.347	.000	.27470	.72530	.00000
66.000	52.000	-27.616	1.625	.000	.27160	.72840	.00000
68.500	52.000	-27.505	1.742	.000	.27160	.72840	.00000
70.000	52.000	-27.633	1.595	.000	.27180	.72820	.00000
72.000	52.000	-27.723	1.293	.000	.27510	.72490	.00000
73.000	52.000	-27.122	1.500	.000	.27930	.72070	.00000
74.000	52.000	-25.762	1.522	.000	.30410	.69590	.00000
84.000	52.000	-37.427	-10.629	.000	.31450	.26820	.41720
94.000	52.000	-41.708	-14.451	.000	.30460	.00440	.69100
104.000	52.000	-42.348	-14.746	.000	.29820	.00000	.70180
114.000	52.000	-42.443	-14.779	.000	.29720	.00000	.70280
124.000	52.000	-42.558	-14.819	.000	.29590	.00000	.70410
134.000	52.000	-42.659	-14.854	.000	.29480	.00000	.70520
137.000	52.000	-42.667	-14.857	.000	.29470	.00000	.70530
.000	54.000	-43.231	-15.054	.000	.28850	.00000	.71150
5.000	54.000	-43.260	-15.064	.000	.28820	.00000	.71180
15.000	54.000	-43.365	-15.101	.000	.28710	.00000	.71290
25.000	54.000	-43.474	-15.139	.000	.28590	.00000	.71410

35.000	54.000	-43.570	-15.172	.000	.28490	.00000	.71510
45.000	54.000	-43.440	-15.128	.000	.28630	.00000	.71370
50.000	54.000	-42.299	-14.728	.000	.29880	.00010	.70120
55.000	54.000	-42.570	-14.822	.000	.29490	.00010	.70510
60.000	54.000	-43.857	-15.272	.000	.27990	.00000	.72010
62.000	54.000	-43.879	-15.279	.000	.27970	.00000	.72030
63.000	54.000	-26.670	2.561	.000	.26980	.73020	.00000
64.000	54.000	-28.714	3.000	.000	.23750	.76250	.00000
66.000	54.000	-28.689	3.000	.000	.23780	.76220	.00000
68.500	54.000	-28.677	3.000	.000	.23800	.76200	.00000
70.000	54.000	-28.684	3.000	.000	.23790	.76210	.00000
72.000	54.000	-28.515	3.000	.000	.24000	.76000	.00000
73.000	54.000	-27.914	2.549	.000	.25320	.74680	.00000
74.000	54.000	-44.010	-15.325	.000	.27830	.00000	.72170
84.000	54.000	-44.120	-15.363	.000	.27710	.00000	.72290
94.000	54.000	-44.159	-15.377	.000	.27670	.00000	.72330
104.000	54.000	-44.318	-15.433	.000	.27710	.00000	.72290
114.000	54.000	-44.451	-15.479	.000	.27580	.00000	.72420
124.000	54.000	-44.557	-15.516	.000	.27470	.00000	.72530
134.000	54.000	-44.660	-15.552	.000	.27370	.00000	.72630
137.000	54.000	-44.668	-15.555	.000	.27360	.00000	.72640

APPENDIX III: LIST OF PROGRAM

```
$DEBUG
      INCLUDE 'COMON.BLK'
C
C   INPUT INITIAL VALUE
C
   CALL INPT
   CALL SK
   T=0.0
1002  T=T+DT
C    NSTAT=0 NO CHANGE IN DISCHARGES Vs TIME
C    NSTAT=1 READ NEW DISCHARGES FROM DATA FILE IN EVERY TIME STEP
   IF(NSTAT.EQ.0.AND.T.EQ.DT)THEN
     CALL REDDAT(RSSW)
     CALL REDDAT(RSSN)
     CALL REDDAT(RSSA)
   ENDIF
   IF(NSTAT.EQ.1)THEN
C    NUMB=-1 SOURCE/SINK TERM IS THE SAME AS PREVIOUS TIME STEP
     READ(1,*)NUMB
     IF(NUMB.NE.-1)CALL REDDAT(RSSW)
     READ(1,*)NUMB
     IF(NUMB.NE.-1)CALL REDDAT(RSSN)
     READ(1,*)NUMB
     IF(NUMB.NE.-1)CALL REDDAT(RSSA)
   ENDIF
   DO 200 K=1,NROW
   DO 200 I=NCBEG(K),NCEND(K)
     SWOLD(I,K)=SW(I,K)
     SNOLD(I,K)=SW(I,K)
     HAOLD(I,K)=HA(I,K)
     SAOLD(I,K)=SW(I,K)
200  CONTINUE
   NDOB=NNODE*NPHASE
      IF(KFEV.EQ.0)GOTO 1003
   DO 1000 IT=1,MXIT
   write(*,*)IT
   DO 50 L=1,NDOB
   DO 50 LL=1,NDOB
   FJAC(L,LL)=0.0
   if(l.eq.ll)fjac(l,ll)=1.0
50   continue
   DO 51 L=1,NDOB
51   FVEC(L)=0.0
C    DO 52 K=1,NROW
C    DO 52 I=NCBEG(K),NCEND(K)
C      HCR=BETAAN(I,K)*HA(I,K)+BETANW(I,K)*HW(I,K)
```

```
C       HCR=HCR/(BETAAN(I,K)+BETANW(I,K))
C       IF(HN(I,K).GE.HCR)NOIL(I,K)=1
C52   CONTINUE

C     CALL SK(HW,HN,HA,NPHASE)
      NST=1
      CALL TRANS(NST)
      CALL VECT(NST)
      CALL FMAT(NST)
C
      NST=2
      CALL TRANS(NST)
      CALL VECT(NST)
      CALL FMAT(NST)
C
      IF(NPHASE.EQ.3)THEN
      NST=3
      CALL TRA
      CALL VECT(NST)
      CALL FMAT(NST)
      ENDIF
C     write(13,*)it
C     do 1313 l=1,ndob
C     write(13,*)l,fvec(l)
C1313  continue
C     close(13)
C*****************************************
      errf=0.
      do 11 iI=1,nDOB
       errf=errf+abs(fvec(iI))
11     continue
      if(errf.le.tolf)GOTO 1001
      do 12 iI=1,nDOB
       p(iI)=-fvec(iI)
12     continue
      call ludcmp(fjac,nDOB,MNRC,indx,d)
      call lubksb(fjac,nDOB,MNRC,indx,p)
      errHW=0.
      ERRHN=0.
      ERRHA=0.
      ND=1-NPHASE
     DO 13 K=1,NROW
     DO 13 I=NCBEG(K),NCEND(K)
       ND=ND+NPHASE
C        write(*,*)nd
       errHW=errHW+abs(p(ND))
       errHN=errHN+abs(p(ND+1))
       IF(NPHASE.EQ.3)errHA=errHA+abs(p(ND+2))
       IF(TYPEW(I,K).EQ.2)P(ND)=0.0
       HW(i,K)=HW(i,K)+p(ND)
       IF(TYPEN(I,K).EQ.2)P(ND+1)=0.0
```

```
      HN(i,K)=HN(i,K)+p(ND+1)
      IF(NPHASE.EQ.3)THEN
        IF(TYPEA(I,K).EQ.2)P(ND+2)=0.0
        HA(i,K)=HA(i,K)+p(ND+2)
      ENDIF
c     write(2,*)i,k,prn(i,k),sw(i,k),pcnw(i,k)
c     write(2,*)p(nd+1)
13    continue
c    close(2)
C     write(*,*)errf,errP,errS
    if(errHW.le.tolx.AND.ERRHN.LE.TOLX.AND.ERRHA.LE.TOLX)GOTO 1001
C*****************************************
    CALL SK

1000  CONTINUE
    WRITE(*,*)' NO CONVERGENCE !!!'
1001  write(*,'(" Time = ",f9.1)')T
    IF(INT(T/TPRN)*TPRN.EQ.T)THEN
      WRITE(5,321)T
321   FORMAT(/' ************TIME =',F9.1,'***************'/)
      fac1=1.
      fac2=1.
      TITLE=' WATER PRESSURE HEAD :'
      CALL OUTPT(HW,fac1,fac2,TITLE)
      fac1=1.
      fac2=1.
      TITLE=' NAPL PRESSURE HEAD :'
      CALL OUTPT(HN,fac1,fac2,TITLE)
      IF(NPHASE.EQ.3)THEN
        fac1=1.0
        fac2=1.0
        TITLE=' GAS PRESSURE HEAD  :'
        CALL OUTPT(HA,fac1,fac2,TITLE)
      ENDIF
    ENDIF
    IF(TMAX-T)1003,1003,1002
1003  STOP
    END
$DEBUG
    SUBROUTINE INPT
        INCLUDE 'COMON.BLK'
    CHARACTER*64 FIN,OUT1
        DIMENSION TYP(MNI,MNK),AF2(20),VVN2(20),TSRW2(20)
        &,TSNP2(20),PORS2(20),pmr2(20),zkzk(20),KMAT(MNI,MNK)

    WRITE(*,'(A\)')' INPUT FILE-NAME :'
    READ(*,'(A)')FIN
    OPEN(1,FILE=FIN,STATUS='OLD')
    WRITE(*,'(A\)')' OUTPUT FILE-NAME :'
    READ(*,'(A)')OUT1
    OPEN(5,FILE=OUT1,STATUS='UNKNOWN')
```

```
      OPEN(4,FILE='TEMP.DAT',STATUS='UNKNOWN')
      READ(1,170)TITLE
           WRITE(4,170)TITLE
           READ(1,170)TITLE
      READ(1,*)NROW,NCOL,MXIT,NSTAT,NPHASE,IRES,ITRN
      READ(1,170)TITLE
      READ(1,*)TSTR,DT,TMAX,TPRN,TOLF,TOLX
C          GAS COMPRESSIBILITY
C          COMPRESSIBLE   ICOM=0
C          INCOMPRESSIBLE ICOM=1
      IF(NPHASE.EQ.3)THEN
      READ(1,170)TITLE
      READ(1,*)ICOM
           ENDIF
c     WRITE(*,170)TITLE
c     WRITE(*,*)NROW,NCOL,DT,TMAX,TPRN,TOLF,TOLX,MXIT,NSTAT,NPHASE
      READ(1,170)TITLE
      DO K=1,NROW
        READ(1,*)NCBEG(K),NCEND(K)
c        WRITE(*,*)NCBEG(K),NCEND(K)
      ENDDO
      NNODE=0
      DO 175 K=2,NROW-1
      DO 175 I=NCBEG(K),NCEND(K)
        NNODE=NNODE+1
175   CONTINUE
C          PRESCRIBED HEAD  Negative numbers
C          PRESCRIBED FLOW  Positive numbers
C          Internal  Nodes  0
C
      CALL REDDAT(TYPEW)
      CALL REDDAT(TYPEN)
      IF(NPHASE.EQ.3)CALL REDDAT(TYPEA)
           TYWAXH=0.0
           TYWAXF=0.0
           TYNAXH=0.0
           TYNAXF=0.0
           TYAAXH=0.0
           TYAAXF=0.0
           DO I=1,NROW
           DO K=1,NCOL
           IF(TYPEW(I,K).LT.0.0)THEN
                IF(ABS(TYPEW(I,K).GT.TYWAXH)TYWAXH=TYPEW(I,K)
           ENDIF
           IF(TYPEW(I,K).GT.0.0)THEN
                IF(ABS(TYPEW(I,K).GT.TYWAXF)TYWAXF=TYPEW(I,K)
           ENDIF
           IF(TYPEN(I,K).LT.0.0)THEN
                IF(ABS(TYPEN(I,K).GT.TYNAXH)TYNAXH=TYPEN(I,K)
           ENDIF
           IF(TYPEN(I,K).GT.0.0)THEN
```

```
            IF(ABS(TYPEN(I,K).GT.TYNAXF)TYNAXF=TYPEN(I,K)
        ENDIF
        IF(NPHASE.EQ.3)THEN
        IF(TYPEA(I,K).LT.0.0)THEN
            IF(ABS(TYPEA(I,K).GT.TYAAXH)TYAAXH=TYPEA(I,K)
        ENDIF
        IF(TYPEA(I,K).GT.0.0)THEN
            IF(ABS(TYPEA(I,K).GT.TYAAXF)TYAAXF=TYPEA(I,K)
        ENDIF
        ENDIF

        ENDDO
        ENDDO
        NSCHW=TYWAXH
        NSCFW=TYWAXF
        NSCHN=TYNAXH
        NSCFN=TYNAXF
        NSCHA=TYWAXH
        NSCFA=TYWAXF
C   SCHADULE FOR PRESCRIBED HEAD FOR WATER
        DO IPE=1,NSCHW
        READ(1,*)IPHW
        DO IG=1,IPHW
        READ(1,*)TPHW(IG),PHW(IG)
        ENDDO
C       SCHADULE FOR PRESCRIBED HEAD FOR NAPL
        READ(1,*)IPHN
        DO IG=1,IPHN
        READ(1,*)TPHN(IG),PHN(IG)
        ENDDO
C       SCHADULE FOR PRESCRIBED HEAD FOR AIR
        IF(NPHASE.EQ.3)THEN
        READ(1,*)IPHA
        DO IG=1,IPHA
        READ(1,*)TPHA(IG),PHA(IG)
        ENDDO
        ENDIF
C
C   SCHADULE FOR PRESCRIBED FLOW FOR WATER
        READ(1,*)IPFW
        DO IG=1,IPFW
        READ(1,*)TPFW(IG),PFW(IG)
        ENDDO
C   SCHADULE FOR PRESCRIBED FLOW FOR NAPL
        READ(1,*)IPFN
        DO IG=1,IPFN
        READ(1,*)TPFN(IG),PFN(IG)
        ENDDO
C   SCHADULE FOR PRESCRIBED FLOW FOR AIR
        IF(NPHASE.EQ.3)THEN
        READ(1,*)IPFA
```

```
          DO IG=1,IPFA
          READ(1,*)TPFA(IG),PFA(IG)
          ENDDO
          ENDIF
C*********_____**********
      CALL REDDAT(X)
      CALL REDDAT(Z)
C*********_____**********
C     READ(1,'(A)')TITLE
C     READ(1,*)TTX,TTZ
C     DX=TTX/FLOAT(NCOL-1)
C     DZ=TTZ/FLOAT(NROW-1)
C     DO 134 K=1,NROW
C     DO 134 I=1,NCOL
C       X(I,K)=FLOAT(I-1)*DX
C       Z(I,K)=FLOAT(K-1)*DZ
C134  CONTINUE
C     DO 137 K=1,NROW
C       X(1,K)=0.0
C       X(NCOL,K)=1110.0
C137  CONTINUE
C     Z(1,2)=5.0
C     Z(NCOL,2)=5.0
C     DO K=3,NROW-1
C       Z(1,K)=Z(1,K-1)+DZ
C       Z(NCOL,K)=Z(NCOL,K-1)+DZ
C     ENDDO
C     Z(1,NROW)=Z(1,NROW-1)+5.0
C     Z(NCOL,NROW)=Z(NCOL,NROW-1)+5.0
C     DO 138 I=1,NCOL
C       Z(I,1)=0.0
C       Z(I,NROW)=Z(I,NROW-1)+5.0
C138  CONTINUE
C     X(2,1)=5.0
C     X(2,NROW)=5.0
C     DO I=3,NCOL-1
C       X(I,1)=X(I-1,1)+DX
C       X(I,NROW)=X(I-1,NROW)+DX
C     ENDDO
c     DO 129 K=1,NROW
c129      WRITE(11,'(14F7.2)')(X(I,K),I=1,14)
c     DO 131 K=1,NROW
c131      WRITE(11,'(14F7.2)')(Z(I,K),I=1,14)
c     close(11)
C*********_____**********
      DO 145 K=1,NROW
      DO 145 I=1,NCOL
      if(k.eq.nrow.or.i.eq.ncol)then
        sigma(i,k)=1.0
        goto 145
      endif
```

```
      sigma(i,K) =0.5*((x(i,k)-x(i+1,k+1))*(z(i+1,k)-z(i,k+1)) -
     *           (x(i+1,k)-x(i,k+1))*(z(i,k)-z(i+1,k+1)))
  145 CONTINUE
c     Computing length of nodes zls,zle,zln,zlw

c     South and North boundary - internal nodes
      do i=2,ncol-1
      zls(i) = 0.5*sqrt((x(i+1,1)-x(i-1,1))**2 +
     *           (z(i+1,1)-z(i-1,1))**2)

      zln(i) = 0.5*sqrt((x(i+1,Nrow)-x(i-1,Nrow))**2 +
     *           (z(i+1,Nrow)-z(i-1,Nrow))**2)
      end do

c     East and West boundary - internal nodes
          do j=2,Nrow-1
          m=ncol
      zle(j) = 0.5*sqrt((x(M,j+1)-x(M,j-1))**2 +
     *           (z(M,j+1)-z(M,j-1))**2)

      zlw(j) = 0.5*sqrt((x(1,j+1)-x(1,j-1))**2 +
     *           (z(1,j+1)-z(1,j-1))**2)
      end do

c     Corner (1,1)
      zl11 = 0.5*sqrt((x(1,2)-x(2,1))**2 +
     *           (z(1,2)-z(2,1))**2)

c     Corner (M,1)
          m=ncol
      zlM1 = 0.5*sqrt((x(M-1,1)-x(M,2))**2 +
     *           (z(M-1,1)-z(M,2))**2)

c     Corner (M,N)
      zlMN = 0.5*sqrt((x(M,Nrow-1)-x(M-1,Nrow))**2 +
     *           (z(M,Nrow-1)-z(M-1,Nrow))**2)

c     Corner (1,N)
      zl1N = 0.5*sqrt((x(2,Nrow)-x(1,Nrow-1))**2 +
     *           (z(2,Nrow)-z(1,Nrow-1))**2)

C
C
      READ(1,170)TITLE
      READ(1,*)RHOW,VMUW,RHON,VMUN,VMUA,betanw,betaan
c     READ(1,170)TITLE
c     READ(1,*)zx
c         do k=1,nrow
c         do i=1,ncol
c         perm(i,k)=0.0
c         enddo
```

```
c        enddo
C
     WRITE(*,'(A\)')' IS SOIL HOMOGENEOUS?'
     READ(*,'(A)')OUT1
     IF(OUT1.EQ.'Y'.OR.OUT1.EQ.'y')THEN
                    NMAT=1
       READ(1,170)TITLE
       READ(1,*)AF2(1),VVN2(1),TSRW2(1),TSNP2(1)
         &,PORS2(1),pmr2(1),zk
       DO 123 K=1,NROW
       DO 123 I=NCBEG(K),NCEND(K)
       N(I,K)=VVN2(1)
       ALPHA(I,K)=AF2(1)
       SRW(I,K)=TSRW2(1)
       PHI(I,K)=PORS2(1)
       SNMIN(I,K)=TSNP2(1)
                    perm(i,k)=pmr2(1)
            zkzk(1)=pmr2(1)*zk
123      CONTINUE
     ELSE
c                   READ(*,'(A\)')' NO. OF MATERIAL TYPES :'
c                   PRINT*, ' NO. OF MATERIAL TYPES :'
       READ(1,170)TITLE
                    READ(*,*)NMAT
                    DO LPN=1,NMAT
       READ(1,*)AF2(LPN),VVN2(LPN),TSRW2(LPN),TSNP2(LPN)
         &          ,PORS2(LPN),pmr2(LPN),zk
                    ENDDO
                    CALL REDDAT(TYP)
         DO K=1,NROW
         DO I=1,NCOL
         kmat(i,k)=typ(i,k)
         nfl=kmat(i,k)
         alpha(i,k)=af2(nfl)
         n(i,k)=vvn2(nfl)
         srw(i,k)=tsrw2(nfl)
         snmin(i,k)=tsnp2(nfl)
         phi(i,k)=pors2(nfl)
         enddo
         do i=ncbeg(k),ncend(k)
         nfl=kmat(i,k)
         perm(i,k)=pmr2(nfl)
         zkzk(nfl)=pmr2(nfl)*zk
         enddo
         enddo
     ENDIF
     READ(1,170)TITLE
C        INITIAL CONDITION FOR WATER AND NAPL
C        PRESSURE HEAD FROM BILINEAR INTERPOLATION = 0
C        NONUNIFORM WATER PRESSURE DISRIBUTION   IFW = 1
C        NO NAPL CONDITION IFN = 1
```

```
C       NONUNIFORM NAPL PRESSURE DISTRIBUTION IFN = 2
        READ(1,*)IFW,IFN
        IF(IFW.EQ.0)THEN
    READ(1,170)TITLE
        READ(1,*)WP1,WP2
        ENDIF
        IF(IFW.EQ.1)CALL REDDAT(HW)
        IF(IFN.EQ.0)THEN
    READ(1,170)TITLE
        READ(1,*)OP1,OP2
        ENDIF
        IF(IFN.EQ.2)CALL REDDAT(HN)
C**************** MODIFIED FOR EXAMPLE 2 - MOFAT ********
C     CALL REDDAT(HW)
C     CALL REDDAT(HN)
C     CALL REDDAT(HA)
c     DO 10 I=1,12
c     DO 10 K=1,9
c     READ(1,*)HW(I,K),Ha(I,K),Hn(I,K)
c     HW(I,K)=HW(I,K)*100.
c     HN(I,K)=HN(I,K)*100.
c     HA(I,K)=HA(I,K)*100.
c10   CONTINUE
    TITLE=' Hw'
    CALL OUTPT(HW,1.0,1.0,TITLE)
    TITLE=' Hn'
    CALL OUTPT(HN,1.0,1.0,TITLE)
    TITLE=' Ha'
    CALL OUTPT(HA,1.0,1.0,TITLE)
C*********************************************
c     CALL REDDAT(PERM)
        do k=1,nrow
        doi=1,ncol
        gammaw(i,k)=0.0
        gamman(i,k)=0.0
        gammaa(i,k)=0.0
        enddo
        enddo
ccccc
        icn=1
        idim=1
        imcor=0
        jinf=0
        tinf=0.0
        tfact=1.03
        tmxg=0.0
ccccc
        irun=1
        ifemc=1
        kfemc=0
        irad=0
```

```
      ioil=0
      iair=0
      nzj=1
      if(nphase.ne.1)ioil=1
      if(nphase.eq.3)iair=1
      write(4,370)irun,ires,irad,ioil,iair,itrn,idim,ifemc,kfemc
370   format(I5)
380   format(7e10.4)
      mtx=9000
      kequl=0
      isolve=1
      itpnt1=0
      write(4,370)mtx,mxit,NMAT,icn,nrow,ncol,kequl,imcor,isolve,itpnt1
      nbeg=-10
      nend=500
   do k=1,nrow
      mlkj=ncend(k)-ncbeg(k)+1
      if(ncbeg(k).gt.nbeg)nbeg=ncbeg(k)
      if(ncend(k).lt.nend)nend=ncend(k)
      if(mlkj.eq.ncol)nkj=k
      enddo
      write(4,380)(z(nbeg,il),il=1,nrow)
   write(4,380)(x(il,nkj),il=1,ncol)
      write(4,'(i5,f5.1)')jinf,tinf
      dtmx=dt*10.0
      WRITE(4,'(E10.4)')tstr,dt,tmax,dtmx,tfact,tprn
      visow=Vmun/Vmuw
      rhow=rhon/rhow
   write(4,'(e10.4)')visow,rhow,betaan,betanw
      th=1.0
      uwf=1.0
      REG1=-1.0
      write(4,'(e10.4)')th,tolf,tolx,uwf
      IF(IRES.EQ.0)THEN
      WRITE(4,370)IFW,IFN
      IF(IFW.EQ.0)WRITE(4,'(E10.4)')WP1,WP2,REG1
      if(ifn.eq.0)write(4,'(E10.4)')oP1,oP2,REG1
      endif
   IF(IFW.EQ.1)THEN
      if(nrow.ge.ncol)write(4,380)((hw(i,k),i=1,ncol),k=1,nrow)
      if(ncol.gt.nrow)write(4,380)((hw(i,k),k=1,nrow),i=1,ncol)
      endif
      IF(IFn.EQ.1)THEN
      if(nrow.ge.ncol)write(4,380)((hn(i,k),i=1,ncol),k=1,nrow)
      if(ncol.gt.nrow)write(4,380)((hn(i,k),k=1,nrow),i=1,ncol)
      endif
      do kfn=1,nmat
      write(4,380)pmr2(kfn),zkzk(kfn),pors2(kfn),tsrw2(kfn)
      &,tsnp2(kfn),af2(kfn),vvn2(kfn)
      enddo
      if(nmat.gt.1)then
```

```
          imat=2
          write(4,'(i5)')imat
          if(nrow.ge.ncol)write(4,380)((kmat(i,k),i=1,ncol),k=1,nrow)
          if(ncol.gt.nrow)write(4,380)((kmat(i,k),k=1,nrow),i=1,ncol)
          endif
          IF(IOIL.EQ.1.AND.IAIR.EQ.1)WRITE(4,'(i5,e10.4)')icom,tmxg
c         CALL REDDAT(GAMMAW)
c         CALL REDDAT(GAMMAN)
c         IF(NPHASE.EQ.3)CALL REDDAT(GAMMAA)
C     DO 93 K=1,NROW
C     DO 93 I=NCBEG(K),NCEND(K)
C       QW(I,K)=QW(I,K)*DX(I)
C       QN(I,K)=QN(I,K)*DX(I)
C93   CONTINUE
170   FORMAT(A64)
      RETURN
      END
C*************************************************************************
      SUBROUTINE REDDAT(EXA)
C
      PARAMETER (MNI=20, MNK=20)
      DIMENSION EXA(MNI,MNK),UPS(6),IRW(6),ICL(6)
      CHARACTER*64 TITLE
      COMMON/MND/ NROW,NCOL,NNODE,NCBEG(MNK),NCEND(MNK),NPHASE,DT
      READ(1,180)TITLE
C     KPRN=1 PRINT INITAL VALUE IN OUTPUT FILE
      READ(1,*)DEFALT,FAC1,FAC2,KPRN
      DO 150 K=1,NROW
      DO 150 I=1,ncol
      EXA(I,K)=DEFALT*FAC1*FAC2
150   CONTINUE
      DO 40 I=1,10000
      READ(1,*)(IRW(K),ICL(K),UPS(K),K=1,6)
c     WRITE(2,'(6(2I3,f9.3))')(IRW(K),ICL(K),UPS(K),K=1,6)
      DO 40 KJ=1,6
       IF(IRW(KJ).EQ.0)GO TO 50
       EXA(IRW(KJ),ICL(KJ))=UPS(KJ)*FAC1*FAC2
40    CONTINUE
50     IF(KPRN.EQ.1)CALL OUTPT(EXA,fac1,fac2,TITLE)
180   FORMAT(A64)
      RETURN
      END
SUBROUTINE OUTPT(EXA,fac1,fac2,TITLE)
       PARAMETER (MNI=20, MNK=20)
       DIMENSION EXA(MNI,MNK),WRT(MNI)
       COMMON/GEO/ X(MNI,MNK),Z(MNI,MNK),SIGMA(MNI,MNK)
       COMMON/MND/ NROW,NCOL,NNODE,NCBEG(MNK),NCEND(MNK),NPHASE,DT
       CHARACTER*64 TITLE
       WRITE(5,'(64A)')TITLE
       DO 70 K=NROW,1,-1
       DO 80 I=1,NCOL
```

```
80     WRT(I)=0.0
       DO 90 I=NCBEG(K),NCEND(K)
90     WRT(I)=EXA(I,K)/fac1/fac2
       WRITE(5,73)(WRT(IC),IC=1,NCOL)
       DO 70 I=NCBEG(K),NCEND(K)
       WRITE(7,'(3G15.3)')X(I,K),Z(I,K),WRT(I)
70     CONTINUE
       WRITE(5,'(/)')
73     FORMAT(22(1X,F9.3))
       RETURN
       END
SUBROUTINE FMAT(NST)
          INCLUDE 'COMON.BLK'
      LANDA=1.17E-6
      RHA0=0.00112
      RAC=0.0
      NDOB=NNODE*NPHASE
          kn=nrow
          m=ncol
C
      DO 100 K=2,NROW-1
      DO 100 I=NCBEG(K)+1,NCEND(K)-1
          IF(NST.EQ.1)ITY=TYPEW(I,K)
          IF(NST.EQ.2)ITY=TYPEN(I,K)
          IF(NST.EQ.3)ITY=TYPEA(I,K)
      IF(ITY.EQ.2)GOTO 100
      if(nst.eq.3.and.sa(i,k).LE.1.E-4)goto 100
c     if(nst.eq.2.and.hn(i,k).eq.0.0)goto 100
      NC=0
      DO 300 II=1,K-1
300   NC=NC+(NCEND(II)-NCBEG(II)+1)
      NN=NC+(I-NCBEG(K)+1)
      NL=NN-1
      NR=NN+1
      ND=NC-NCEND(K-1)+I
      NU=NC+(NCEND(K)-NCBEG(K)+1)+(I-NCBEG(K+1)+1)
      NDW=ND-1
      NDE=ND+1
      NUW=NU-1
      NUE=NU+1
      NO=NN*NPHASE-NPHASE+NST
      LT=NST-NPHASE
C
      VN=(SIGMA(I,K)+SIGMA(I-1,K)+SIGMA(I-1,K-1)+SIGMA(I,K-1))/4.0
C
      IF(NST.EQ.3)THEN
        RHOX=1.0
        RHY=RHOA(I,K)
        RHOL=LANDA*HAOLD(I,K)+RHA0+RAC
      ELSE
        IF(NST.EQ.1)RHOX=RHOW
```

```
                IF(NST.EQ.2)RHOX=RHON
          RHY=1.0
          RHOL=1.0
        ENDIF
            rpd=rhy*phi(i,k)/dt
            xn=n(i,k)
            emi=1.0-1./xn
            IF (NPHASE.EQ.1.AND.NST.EQ.1)THEN
            hAW=HA(I,K)-hW(i,k)
            if(hAW.le.epsi)then
                    ch=0.0
                    goto 23
            endif
            swbar=1.0/((1.0+(ALphA(i,k)*HAW)**XN)**EMI)
            ch1=(1.-srw(i,k))*(xn-1.)*alpha(i,k)**xn
            chww=ch1*swbar**(1+(xn/(xn-1.)))*HAW**(xn-1.)
            if(chww.gt.1.0)chww=1.0
            chww=chww*rpd
            chnn=0.0
            chaa=0.0
            ENDIF
            IF (NPHASE.NE.1.AND.NST.EQ.1)THEN
            HNW=HN(I,K)-HW(I,K)
            SWBAR=1.0/((1.+(ALPHA(I,K)*BETANW*HNW)**XN)**EMI)
            CH1=(XN-1.)*(SWBAR**((EMI+1.)/EMI))
            CHWW=CH1*(ALPHA(I,K)*BETANW)**XN*HNW**(XN-1.)
            if(chWW.gt.1.0)chWW=1.0
            chww=chww*rpd
            CHWN=-CHWW
            ENDIF
            IF (NPHASE.NE.1.AND.NST.EQ.2)THEN
            HAN=HA(I,K)-HN(I,K)
            SWT=1./((1.+(ALPHA(I,K)*BETAAN*HAN)**XN)**EMI)
            CH1=(XN-1.)*(SWT**((EMI+1.)/EMI))
            CH2=CH1*(ALPHA(I,K)*BETANW)**XN*HAW**(XN-1.)
            CHNN=CH2+CHWN
            if(chNN.gt.1.0)chNN=1.0
            chnn=chnn*rpd
            chww=0.0
            chaa=0.0
            ENDIF
            CHNW=CHWN
c           IF (NPHASE.EQ.3.AND.NST.EQ.3)THEN
C
C
      if(i.eq.1.and.k.ne.1.and.k.ne.nrow)then
      csx = +0.5*(z(2,k)-z(1,k-1))*
     *   (kx(1,k-1)*(z(1,k)-z(2,k-1))/(2.*sigma(1,k-1))-
     *    zkxy(1,k-1)*(x(1,k)-x(2,k-1))/(2.*sigma(1,k-1)))
      csy =  -0.5*(x(2,k)-x(1,k-1))*
     *   (zkxy(1,k-1)*(z(1,k)-z(2,k-1))/(2.*sigma(1,k-1))-
```

```
*     kz(1,k-1)*(x(1,k)-x(2,k-1))/(2.*sigma(1,k-1)))
      CS=(csx + csy)/zlw(k)
      fjac(no,(nd*nphase-lt))=CS
C
C
      csex = -0.5*(z(2,k)-z(1,k-1))*
*     (kx(1,k-1)*(z(2,k)-z(1,k-1))/(2.*sigma(1,k-1))-
*      zkxy(1,k-1)*(x(2,k)-x(1,k-1))/(2.*sigma(1,k-1)))
      csey =  +0.5*(x(2,k)-x(1,k-1))*
*     (zkxy(1,k-1)*(z(2,k)-z(1,k-1))/(2.*sigma(1,k-1))-
*      kz(1,k-1)*(x(2,k)-x(1,k-1))/(2.*sigma(1,k-1)))
      CSE=(csex + csey)/zlw(k)
      FJAC(NO,(NDE*NPHASE-LT)) =CSE
C
C
       cex = -0.5*(z(1,k+1)-z(2,k))*
*     (kx(1,k)*(z(2,k+1)-z(1,k))/(2.*sigma(1,k))-
*      zkxy(1,k)*(x(2,k+1)-x(1,k))/(2.*sigma(1,k)))
*        -0.5*(z(2,k)-z(1,k-1))*
*     (kx(1,k-1)*(z(1,k)-z(2,k-1))/(2.*sigma(1,k-1))-
*      zkxy(1,k-1)*(x(1,k)-x(2,k-1))/(2.*sigma(1,k-1)))
       cey = +0.5*(x(1,k+1)-x(2,k))*
*     (zkxy(1,k)*(z(2,k+1)-z(1,k))/(2.*sigma(1,k))-
*      kz(1,k)*(x(2,k+1)-x(1,k))/(2.*sigma(1,k)))
*        +0.5*(x(2,k)-x(1,k-1))*
*     (zkxy(1,k-1)*(z(1,k)-z(2,k-1))/(2.*sigma(1,k-1))-
*      kz(1,k-1)*(x(1,k)-x(2,k-1))/(2.*sigma(1,k-1)))

      ce =(cex + cey)/zlw(k)
      FJAC(NO,(NR*NPHASE-LT))=CE
C
C
       cnx = +0.5*(z(1,k+1)-z(2,k))*
*     (kx(1,k)*(z(2,k+1)-z(1,k))/(2.*sigma(1,k))-
*      zkxy(1,k)*(x(2,k+1)-x(1,k))/(2.*sigma(1,k)))
       cny = -0.5*(x(1,k+1)-x(2,k))*
*     (zkxy(1,k)*(z(2,k+1)-z(1,k))/(2.*sigma(1,k))-
*      kz(1,k)*(x(2,k+1)-x(1,k))/(2.*sigma(1,k)))

      CN=(cnx + cny)/zlw(k)
      FJAC(NO,(NU*NPHASE-LT))=CN
C
C
      cnex = -0.5*(z(1,k+1)-z(2,k))*
*     (kx(1,k)*(z(1,k+1)-z(2,k))/(2.*sigma(1,k))-
*      zkxy(1,k)*(x(1,k+1)-x(2,k))/(2.*sigma(1,k)))
      cney = +0.5*(x(1,k+1)-x(2,k))*
*     (zkxy(1,k)*(z(1,k+1)-z(2,k))/(2.*sigma(1,k))-
*      kz(1,k)*(x(1,k+1)-x(2,k))/(2.*sigma(1,k)))
      CNE=(cnex + cney)/zlw(k)
      FJAC(NO,(NUE*NPHASE-LT))=CNE
```

```
C
C
      cc = -(ce + cne + cn + cs +cse-chww-chnn-chaa)
      FJAC(NO,(NN*NPHASE-LT))=CC
C
C
            goto 100
      endif

      if(k.eq.1.and.i.ne.ncbeg(k).and.i.ne.ncend(k))then

       cwx = +0.5*(z(i,2)-z(i-1,1))*
     *  (-kx(i-1,1)*(z(i-1,2)-z(i,1))/(2.*sigma(i-1,1))+
     *    zkxy(i-1,1)*(x(i-1,2)-x(i,1))/(2.*sigma(i-1,1)))

c     group related to approximation of term
c     ny*(kxy du/dx + kyy du/dy)

      cwy = -0.5*(x(i,2)-x(i-1,1))*
     *  (-zkxy(i-1,1)*(z(i-1,2)-z(i,1))/(2.*sigma(i-1,1))+
     *    kz(i-1,1)*(x(i-1,2)-x(i,1))/(2.*sigma(i-1,1)))

      cw =(cwx + cwy)/zls(i)
      FJAC(NO,(NL*NPHASE-LT))=CW
C
C
      cex = -0.5*(z(i,2)-z(i+1,1))*
     * ( kx(i,1)*(z(i+1,2)-z(i,1))/(2.*sigma(i,1))-
     • zkxy(i,1)*(x(i+1,2)-x(i,1))/(2.*sigma(i,1)))

      cey = +0.5*(x(i,2)-x(i+1,1))*
     • ( zkxy(i,1)*(z(i+1,2)-z(i,1))/(2.*sigma(i,1))-
     * kz(i,1)*(x(i+1,2)-x(i,1))/(2.*sigma(i,1)))

      ce=(cex + cey)/zls(i)
      FJAC(NO,(NR*NPHASE-LT))=CE
C
C
      cnwx = +0.5*(z(i,2)-z(i-1,1))*
     * (-kx(i-1,1)*(z(i,2)-z(i-1,1))/(2.*sigma(i-1,1))+
     *   zkxy(i-1,1)*(x(i,2)-x(i-1,1))/(2.*sigma(i-1,1)))

      cnwy = -0.5*(x(i,2)-x(i-1,1))*
     * (-zkxy(i-1,1)*(z(i,2)-z(i-1,1))/(2.*sigma(i-1,1))+
     *   kz(i-1,1)*(x(i,2)-x(i-1,1))/(2.*sigma(i-1,1)))

      cnw =(cnwx + cnwy)/zls(i)
      FJAC(NO,(NUW*NPHASE-LT))=CNW
C
C
      cnx = -0.5*(z(i,2)-z(i+1,1))*
```

```
     * (- kx(i,1)*(z(i+1,2)-z(i,1))/(2.*sigma(i,1))+
     * zkxy(i,1)*(x(i+1,2)-x(i,1))/(2.*sigma(i,1)))
     *    + 0.5*(z(i,2)-z(i-1,1))*
     * (kx(i-1,1)*(z(i-1,2)-z(i,1))/(2.*sigma(i-1,1))
     * -zkxy(i-1,1)*(x(i-1,2)-x(i,1))/(2.*sigma(i-1,1)))

      cny = +0.5*(x(i,2)-x(i+1,1))*
     * ( -zkxy(i,1)*(z(i+1,2)-z(i,1))/(2.*sigma(i,1))+
     * kz(i,1)*(x(i+1,2)-x(i,1))/(2.*sigma(i,1)))
     *    - 0.5*(x(i,2)-x(i-1,1))*
     * (zkxy(i-1,1)*(z(i-1,2)-z(i,1))/(2.*sigma(i-1,1))
     * -kz(i-1,1)*(x(i-1,2)-x(i,1))/(2.*sigma(i-1,1)))

      cn =(cnx + cny)/zls(i)
      FJAC(NO,(NU*NPHASE-LT))=CN
C
C
      cnex = -0.5*(z(i,2)-z(i+1,1))*
     * ( kx(i,1)*(z(i,2)-z(i+1,1))/(2.*sigma(i,1))-
     * zkxy(i,1)*(x(i,2)-x(i+1,1))/(2.*sigma(i,1)))

      cney = +0.5*(x(i,2)-x(i+1,1))*
     * ( zkxy(i,1)*(z(i,2)-z(i+1,1))/(2.*sigma(i,1))-
     * kz(i,1)*(x(i,2)-x(i+1,1))/(2.*sigma(i,1)))

      cne =(cnex + cney)/zls(i)
      FJAC(NO,(NUE*NPHASE-LT))=CNE
C
C
      cc = -(ce + cne + cn + cnw + cw-chww-chnn-chaa)
      FJAC(NO,(NN*NPHASE-LT))=CC
C
C
           goto 100
      endif

      if(k.eq.nrow.and.i.ne.1.and.i.ne.ncend(k))then

       cswx = +0.5*(z(i-1,kn)-z(i,kn-1))*
     *  (-kx(i-1,kn-1)*(z(i-1,kn)-z(i,kn-1))/(2.*sigma(i-1,kn-1))+
     *    zkxy(i-1,kn-1)*(x(i-1,kn)-x(i,kn-1))/(2.*sigma(i-1,kn-1)))

       cswy = -0.5*(x(i-1,kn)-x(i,kn-1))*
     *  (-zkxy(i-1,kn-1)*(z(i-1,kn)-z(i,kn-1))/(2.*sigma(i-1,kn-1))+
     *    kz(i-1,kn-1)*(x(i-1,kn)-x(i,kn-1))/(2.*sigma(i-1,kn-1)))

       csw =(cswx + cswy)/zln(i)
      FJAC(NO,(NDW*NPHASE-LT))=CSW
C
C
       csx = -0.5*(z(i-1,kn)-z(i,kn-1))*
```

```
     * (-kx(i-1,kn-1)*(z(i,kn)-z(i-1,kn-1))/(2.*sigma(i-1,kn-1))+
     *  zkxy(i-1,kn-1)*(x(i,kn)-x(i-1,kn-1))/(2.*sigma(i-1,kn-1)))
     *    +0.5*(z(i+1,kn)-z(i,kn-1))*
     * (kx(i,kn-1)*(z(i,kn)-z(i+1,kn-1))/(2.*sigma(i,kn-1))-
     *  zkxy(i,kn-1)*(x(i,kn)-x(i+1,kn-1))/(2.*sigma(i,kn-1)))

      csy = +0.5*(x(i-1,kn)-x(i,kn-1))*
     * (-zkxy(i-1,kn-1)*(z(i,kn)-z(i-1,kn-1))/(2.*sigma(i-1,kn-1))+
     *  kz(i-1,kn-1)*(x(i,kn)-x(i-1,kn-1))/(2.*sigma(i-1,kn-1)))
     *    -0.5*(x(i+1,kn)-x(i,kn-1))*
     * (zkxy(i,kn-1)*(z(i,kn)-z(i+1,kn-1))/(2.*sigma(i,kn-1))-
     *  kz(i,kn-1)*(x(i,kn)-x(i+1,kn-1))/(2.*sigma(i,kn-1)))

      cs =(csx + csy)/zln(i)
     FJAC(NO,(ND*NPHASE-LT))=CS
C
C
      csex = +0.5*(z(i+1,kn)-z(i,kn-1))*
     * (-kx(i,kn-1)*(z(i+1,kn)-z(i,kn-1))/(2.*sigma(i,kn-1))+
     *  zkxy(i,kn-1)*(x(i+1,kn)-x(i,kn-1))/(2.*sigma(i,kn-1)))

      csey = -0.5*(x(i+1,kn)-x(i,kn-1))*
     * (-zkxy(i,kn-1)*(z(i+1,kn)-z(i,kn-1))/(2.*sigma(i,kn-1))+
     *  kz(i,kn-1)*(x(i+1,kn)-x(i,kn-1))/(2.*sigma(i,kn-1)))

      cse =(csex + csey)/zln(i)
     FJAC(NO,(NDE*NPHASE-LT))=CSE
C
C
      cwx = +0.5*(z(i-1,kn)-z(i,kn-1))*
     * (-kx(i-1,kn-1)*(z(i,kn)-z(i-1,kn-1))/(2.*sigma(i-1,kn-1))+
     *  zkxy(i-1,kn-1)*(x(i,kn)-x(i-1,kn-1))/(2.*sigma(i-1,kn-1)))

      cwy = -0.5*(x(i-1,kn)-x(i,kn-1))*
     * (-zkxy(i-1,kn-1)*(z(i,kn)-z(i-1,kn-1))/(2.*sigma(i-1,kn-1))+
     *  kz(i-1,kn-1)*(x(i,kn)-x(i-1,kn-1))/(2.*sigma(i-1,kn-1)))

      cw =(cwx + cwy)/zln(i)
     FJAC(NO,(NL*NPHASE-LT))=CW
C
C
      cex =  -0.5*(z(i+1,kn)-z(i,kn-1))*
     * (kx(i,kn-1)*(z(i,kn)-z(i+1,kn-1))/(2.*sigma(i,kn-1))-
     *  zkxy(i,kn-1)*(x(i,kn)-x(i+1,kn-1))/(2.*sigma(i,kn-1)))

c     group related to approximation of term
c     ny*(kxy du/dx + kyy du/dy)

      cey =  +0.5*(x(i+1,kn)-x(i,kn-1))*
     * (zkxy(i,kn-1)*(z(i,kn)-z(i+1,kn-1))/(2.*sigma(i,kn-1))-
     *  kz(i,kn-1)*(x(i,kn)-x(i+1,kn-1))/(2.*sigma(i,kn-1)))
```

```
      ce =(cex + cey)/zln(i)
      FJAC(NO,(NR*NPHASE-LT))=CE
C
C
      cc = - (cw + csw +cs + cse +ce-chww-chnn-chaa)
      FJAC(NO,(NN*NPHASE-LT))=CC

      goto 100
      endif

      if(i.eq.ncend(k).and.k.ne.1.and.k.ne.nrow)then

      cswx = -0.5*(z(M-1,k)-z(M,k-1))*
     * (kx(M-1,k-1)*(z(M-1,k)-z(M,k-1))/(2.*sigma(M-1,k-1))-
     *  zkxy(M-1,k-1)*(x(M-1,k)-x(M,k-1))/(2.*sigma(M-1,k-1)))

      cswy = +0.5*(x(M-1,k)-x(M,k-1))*
     * (zkxy(M-1,k-1)*(z(M-1,k)-z(M,k-1))/(2.*sigma(M-1,k-1))-
     *  kz(M-1,k-1)*(x(M-1,k)-x(M,k-1))/(2.*sigma(M-1,k-1)))

      csw =(cswx + cswy)/zle(k)
      FJAC(NO,(NDW*NPHASE-LT))=csw
C
      csx = +0.5*(z(M-1,k)-z(M,k-1))*
     * (kx(M-1,k-1)*(z(M,k)-z(M-1,k-1))/(2.*sigma(M-1,k-1))-
     *  zkxy(M-1,k-1)*(x(M,k)-x(M-1,k-1))/(2.*sigma(M-1,k-1)))

      csy = -0.5*(x(M-1,k)-x(M,k-1))*
     * (zkxy(M-1,k-1)*(z(M,k)-z(M-1,k-1))/(2.*sigma(M-1,k-1))-
     *  kz(M-1,k-1)*(x(M,k)-x(M-1,k-1))/(2.*sigma(M-1,k-1)))

      cs =(csx + csy)/zle(k)
      FJAC(NO,(ND*NPHASE-LT))=CS
C
      cwx = +0.5*(z(M-1,k)-z(M,k-1))*
     * (-kx(M-1,k-1)*(z(M,k)-z(M-1,k-1))/(2.*sigma(M-1,k-1))+
     *   zkxy(M-1,k-1)*(x(M,k)-x(M-1,k-1))/(2.*sigma(M-1,k-1)))
     *    +0.5*(z(M,k+1)-z(M-1,k))*
     * (-kx(M-1,k)*(z(M-1,k+1)-z(M,k))/(2.*sigma(M-1,k))+
     *   zkxy(M-1,k)*(x(M-1,k+1)-x(M,k))/(2.*sigma(M-1,k)))

      cwy = -0.5*(x(M-1,k)-x(M,k-1))*
     * (-zkxy(M-1,k-1)*(z(M,k)-z(M-1,k-1))/(2.*sigma(M-1,k-1))+
     *   kz(M-1,k-1)*(x(M,k)-x(M-1,k-1))/(2.*sigma(M-1,k-1)))
     *    -0.5*(x(M,k+1)-x(M-1,k))*
     * (-zkxy(M-1,k)*(z(M-1,k+1)-z(M,k))/(2.*sigma(M-1,k))+
     *   kz(M-1,k)*(x(M-1,k+1)-x(M,k))/(2.*sigma(M-1,k)))

      cw =(cwx + cwy)/zle(k)
      FJAC(NO,(NL*NPHASE-LT))=CW
```

```
C
      cnwx = +0.5*(z(M,k+1)-z(M-1,k))*
     * (-kx(M-1,k)*(z(M,k+1)-z(M-1,k))/(2*sigma(M-1,k))+
     *   zkxy(M-1,k)*(x(M,k+1)-x(M-1,k))/(2*sigma(M-1,k)))

      cnwy = -0.5*(x(M,k+1)-x(M-1,k))*
     * (-zkxy(M-1,k)*(z(M,k+1)-z(M-1,k))/(2*sigma(M-1,k))+
     *   kz(M-1,k)*(x(M,k+1)-x(M-1,k))/(2*sigma(M-1,k)))

      cnw =(cnwx + cnwy)/zle(k)
      FJAC(NO,(NUW*NPHASE-LT))=CNW
C
      cnx = +0.5*(z(M,k+1)-z(M-1,k))*
     * (kx(M-1,k)*(z(M-1,k+1)-z(M,k))/(2*sigma(M-1,k))-
     *  zkxy(M-1,k)*(x(M-1,k+1)-x(M,k))/(2*sigma(M-1,k)))

      cny = -0.5*(x(M,k+1)-x(M-1,k))*
     * (zkxy(M-1,k)*(z(M-1,k+1)-z(M,k))/(2*sigma(M-1,k))-
     *  kz(M-1,k)*(x(M-1,k+1)-x(M,k))/(2*sigma(M-1,k)))

      cn =(cnx + cny)/zle(k)
      FJAC(NO,(NU*NPHASE-LT))=CN
C
      cc = -(cn + cnw + cw + csw + cs-chww-chnn-chaa)
      FJAC(NO,(NN*NPHASE-LT))=CC

      goto 100
      endif

      if(k.eq.1.and.i.eq.ncbeg(1))then
C
      cey = +0.5*(x(1,2)-x(2,1))*
     * (zkxy(1,1)*(z(2,2)-z(1,1))/(2.*sigma(1,1))-
     *  kz(1,1)*(x(2,2)-x(1,1))/(2.*sigma(1,1)))

      ce =(cex + cey)/zl11
      FJAC(NO,(NR*NPHASE-LT))=CE
C
      cnx = +0.5*(z(1,2)-z(2,1))*
     * (kx(1,1)*(z(2,2)-z(1,1))/(2.*sigma(1,1))-
     *  zkxy(1,1)*(x(2,2)-x(1,1))/(2.*sigma(1,1)))

      cny = -0.5*(x(1,2)-x(2,1))*
     * (zkxy(1,1)*(z(2,2)-z(1,1))/(2.*sigma(1,1))-
     *  kz(1,1)*(x(2,2)-x(1,1))/(2.*sigma(1,1)))

      cn =(cnx + cny)/zl11
      FJAC(NO,(NU*NPHASE-LT))=CN
C
      cnex = -0.5*(z(1,2)-z(2,1))*
     * (kx(1,1)*(z(1,2)-z(2,1))/(2.*sigma(1,1))-
```

```
     *  zkxy(1,1)*(x(1,2)-x(2,1))/(2.*sigma(1,1)))

      cney = +0.5*(x(1,2)-x(2,1))*
     * (zkxy(1,1)*(z(1,2)-z(2,1))/(2.*sigma(1,1))-
     *  kz(1,1)*(x(1,2)-x(2,1))/(2.*sigma(1,1)))

      cne =(cnex + cney)/zl11
     FJAC(NO,(NUE*NPHASE-LT))=CNE
C
      cc = -(ce+cne+cn-chww-chnn-chaa)
     FJAC(NO,(NN*NPHASE-LT))=CC

     goto 100
     endif

     if(k.eq.1.and.i.eq.ncend(1))then
C
      cwx = -0.5*(z(M,2)-z(M-1,1))*
     *  (kx(M-1,1)*(z(M-1,2)-z(M,1))/(2.*sigma(M-1,1))-
     *   zkxy(M-1,1)*(x(M-1,2)-x(M,1))/(2.*sigma(M-1,1)))

      cwy = +0.5*(x(M,2)-x(M-1,1))*
     *  (zkxy(M-1,1)*(z(M-1,2)-z(M,1))/(2.*sigma(M-1,1))-
     *   kz(M-1,1)*(x(M-1,2)-x(M,1))/(2.*sigma(M-1,1)))

     cw =(cwx + cwy)/zlM1
     FJAC(NO,(NL*NPHASE-LT))=CW
C
      cnwx = -0.5*(z(M,2)-z(M-1,1))*
     *  (kx(M-1,1)*(z(M,2)-z(M-1,1))/(2.*sigma(M-1,1))-
     *   zkxy(M-1,1)*(x(M,2)-x(M-1,1))/(2.*sigma(M-1,1)))

c    group related to approximation of term
c    ny*(kxy du/dx + kyy du/dy)
     cnwy = +0.5*(x(M,2)-x(M-1,1))*
     *  (zkxy(M-1,1)*(z(M,2)-z(M-1,1))/(2.*sigma(M-1,1))-
     *   kz(M-1,1)*(x(M,2)-x(M-1,1))/(2.*sigma(M-1,1)))

     cnw =(cnwx + cnwy)/zlM1
     FJAC(NO,(NUW*NPHASE-LT))=CNW
C
      cnx = +0.5*(z(M,2)-z(M-1,1))*
     *  (kx(M-1,1)*(z(M-1,2)-z(M,1))/(2.*sigma(M-1,1))-
     *   zkxy(M-1,1)*(x(M-1,2)-x(M,1))/(2.*sigma(M-1,1)))

      cny = -0.5*(x(M,2)-x(M-1,1))*
     *  (zkxy(M-1,1)*(z(M-1,2)-z(M,1))/(2.*sigma(M-1,1))-
     *   kz(M-1,1)*(x(M-1,2)-x(M,1))/(2.*sigma(M-1,1)))

     cn =(cnx + cny)/zlM1
     FJAC(NO,(NU*NPHASE-LT))=CN
```

```
C
      cc = -(cn+cnw+cw-chww-chnn-chaa)
      FJAC(NO,(NN*NPHASE-LT))=CC

      goto 100
      endif

      if(k.eq.nrow.and.i.eq.ncbeg(k))then
C
      csx = +0.5*(z(2,kn)-z(1,kn-1))*
     * (kx(1,kn-1)*(z(1,kn)-z(2,kn-1))/(2.*sigma(1,kn-1))-
     *  zkxy(1,kn-1)*(x(1,kn)-x(2,kn-1))/(2.*sigma(1,kn-1)))

      csy = -0.5*(x(2,kn)-x(1,kn-1))*
     * (zkxy(1,kn-1)*(z(1,kn)-z(2,kn-1))/(2.*sigma(1,kn-1))-
     *  kz(1,kn-1)*(x(1,kn)-x(2,kn-1))/(2.*sigma(1,kn-1)))

       cs =(csx + csy)/zl1N
          FJAC(NO,(NDE*NPHASE-LT))=CS
C
      csex = -0.5*(z(2,kn)-z(1,kn-1))*
     * (kx(1,kn-1)*(z(2,kn)-z(1,kn-1))/(2.*sigma(1,kn-1))-
     *  zkxy(1,kn-1)*(x(2,kn)-x(1,kn-1))/(2.*sigma(1,kn-1)))

      csey = +0.5*(x(2,kn)-x(1,kn-1))*
     * (zkxy(1,kn-1)*(z(2,kn)-z(1,kn-1))/(2.*sigma(1,kn-1))-
     *  kz(1,kn-1)*(x(2,kn)-x(1,kn-1))/(2.*sigma(1,kn-1)))

       cse =(csex + csey)/zl1N
      FJAC(NO,(NDE*NPHASE-LT))=CSE
C
      cex = -0.5*(z(2,kn)-z(1,kn-1))*
     * (kx(1,kn-1)*(z(1,kn)-z(2,kn-1))/(2.*sigma(1,kn-1))-
     *  zkxy(1,kn-1)*(x(1,kn)-x(2,kn-1))/(2.*sigma(1,kn-1)))

      cey = +0.5*(x(2,kn)-x(1,kn-1))*
     * (zkxy(1,kn-1)*(z(1,kn)-z(2,kn-1))/(2.*sigma(1,kn-1))-
     *  kz(1,kn-1)*(x(1,kn)-x(2,kn-1))/(2.*sigma(1,kn-1)))

       ce =(cex + cey)/zl1N
      FJAC(NO,(NR*NPHASE-LT))=CE
C
       cc = -(cs+cse+ce-chww-chnn-chaa)
      FJAC(NO,(NN*NPHASE-LT))=CC

      goto 100
      endif

      if(k.eq.nrow.and.i.eq.ncend(k))then

      cswx = -0.5*(z(M-1,kn)-z(M,kn-1))*
```

```
     * (kx(M-1,kn-1)*(z(M-1,kn)-z(M,kn-1))
     * /(2.*sigma(M-1,kn-1))-
     *  zkxy(M-1,kn-1)*(x(M-1,kn)-x(M,kn-1))
     * /(2.*sigma(M-1,kn-1)))

      cswy = +0.5*(x(M-1,kn)-x(M,kn-1))*
     * (zkxy(M-1,kn-1)*(z(M-1,kn)-z(M,kn-1))
     * /(2.*sigma(M-1,kn-1))-
     *  kz(M-1,kn-1)*(x(M-1,kn)-x(M,kn-1))
     * /(2.*sigma(M-1,kn-1)))

      csw =(cswx + cswy)/zlMN
      FJAC(NO,(NDW*NPHASE-LT))=CSW
C
      csx = +0.5*(z(M-1,kn)-z(M,kn-1))*
     * (kx(M-1,kn-1)*(z(M,kn)-z(M-1,kn-1))
     * /(2.*sigma(M-1,kn-1))-
     *  zkxy(M-1,kn-1)*(x(M,kn)-x(M-1,kn-1))
     * /(2.*sigma(M-1,kn-1)))

      csy = -0.5*(x(M-1,kn)-x(M,kn-1))*
     * (zkxy(M-1,kn-1)*(z(M,kn)-z(M-1,kn-1))
     * /(2.*sigma(M-1,kn-1))-
     *  kz(M-1,kn-1)*(x(M,kn)-x(M-1,kn-1))
     * /(2.*sigma(M-1,kn-1)))

      cs =(csx + csy)/zlMN
      FJAC(NO,(ND*NPHASE-LT))=CS
C
      cwx = -0.5*(z(M-1,kn)-z(M,kn-1))*
     * (kx(M-1,kn-1)*(z(M,kn)-z(M-1,kn-1))
     */(2.*sigma(M-1,kn-1))-
     *  zkxy(M-1,kn-1)*(x(M,kn)-x(M-1,kn-1))
     */(2.*sigma(M-1,kn-1)))

      cwy = +0.5*(x(M-1,kn)-x(M,kn-1))*
     * (zkxy(M-1,kn-1)*(z(M,kn)-z(M-1,kn-1))
     * /(2.*sigma(M-1,kn-1))-
     *  kz(M-1,kn-1)*(x(M,kn)-x(M-1,kn-1))
     * /(2.*sigma(M-1,kn-1)))

      cw =(cwx + cwy)/zlMN
      FJAC(NO,(NL*NPHASE-LT))=CW
C
      cc = -(cw+csw+cs-chww-chnn-chaa)
      FJAC(NO,(NN*NPHASE-LT))=CC

      goto 100
      endif
C
c
```

```
      cswxx =
     *      -(z(i,k-1)-z(i-1,k))
     *      *(KX(i-1,k-1)/(2.d0*sigma(i-1,k-1)))*(z(i,k-1)-z(i-1,k))
c
      cswxy =
     *      +(z(i,k-1)-z(i-1,k))
     *      *(ZKXY(i-1,k-1)/(2.d0*sigma(i-1,k-1)))*(x(i,k-1)-x(i-1,k))
c
      cswyx =
     *      +(x(i,k-1)-x(i-1,k))
     *      *(ZKXY(i-1,k-1)/(2.d0*sigma(i-1,k-1)))*(z(i,k-1)-z(i-1,k))
c
      cswyy =
     *      -(x(i,k-1)-x(i-1,k))
     *      *(Kz(i-1,k-1)/(2.d0*sigma(i-1,k-1)))*(x(i,k-1)-x(i-1,k))

      csw=0.5*(cswxx+cswxy+cswyx+cswyy)/VN
      FJAC(NO,(NDW*NPHASE-LT))=CSW
C
c
        csxx =
     *  +(z(i,k-1)-z(i-1,k))
     *  *(KX(i-1,k-1)/(2.d0*sigma(i-1,k-1)))*(z(i-1,k-1)-z(i,k))
     *  -(Z(i+1,k)-Z(i,k-1))
     *  *(KX(i,k-1)/(2.d0*sigma(i,k-1)))*(z(i+1,k-1)-z(i,k))
c
        csxy =
     *  -(z(i,k-1)-z(i-1,k))
     *  *(ZKXY(i-1,k-1)/(2.d0*sigma(i-1,k-1)))*(x(i-1,k-1)-x(i,k))
     *  +(z(i+1,k)-z(i,k-1))
     *  *(ZKXY(i,k-1)/(2.d0*sigma(i,k-1)))*(x(i+1,k-1)-x(i,k))
c
        csyx =
     *  -(x(i,k-1)-x(i-1,k))
     *  *(ZKXY(i-1,k-1)/(2.d0*sigma(i-1,k-1)))*(z(i-1,k-1)-z(i,k))
     *  +(x(i+1,k)-x(i,k-1))
     *  *(ZKXY(i,k-1)/(2.d0*sigma(i,k-1)))*(z(i+1,k-1)-z(i,k))
c
        csyy =
     *  +(x(i,k-1)-x(i-1,k))
     *  *(Kz(i-1,k-1)/(2.d0*sigma(i-1,k-1)))*(x(i-1,k-1)-x(i,k))
     *  -(x(i+1,k)-x(i,k-1))
     *  *(Kz(i,k-1)/(2.d0*sigma(i,k-1)))*(x(i+1,k-1)-x(i,k))

      cs=0.5*(csxx+csxy+csyx+csyy)/VN
      FJAC(NO,(ND*NPHASE-LT))=CS
C
C
      csexx =
     *      + (z(i+1,k)-z(i,k-1))
     *      *(KX(i,k-1)/(2.d0*sigma(i,k-1)))*(z(i,k-1)-z(i+1,k))
```

```
c
      csexy =
     *      -(z(i+1,k)-z(i,k-1))
     *      *(ZKXY(i,k-1)/(2.d0*sigma(i,k-1)))*(x(i,k-1)-x(i+1,k))
c
      cseyx =
     *      -(x(i+1,k)-x(i,k-1))
     *      *(ZKXY(i,k-1)/(2.d0*sigma(i,k-1)))*(z(i,k-1)-z(i+1,k))
c
      cseyy =
     *      + (x(i+1,k)-x(i,k-1))
     *      *(Kz(i,k-1)/(2.d0*sigma(i,k-1)))*(x(i,k-1)-x(i+1,k))

      cse=0.5*(csexx+csexy+cseyx+cseyy)/VN
      FJAC(NO,(NDE*NPHASE-LT))=CSE
C
C
      cwxx =
     *  -(z(i-1,k)-z(i,k+1))
     *  *(KX(i-1,k)/(2.d0*sigma(i-1,k)))*(z(i,k)-z(i-1,k+1))
     *  -(z(i,k-1)-z(i-1,k))
     *  *(KX(i-1,k-1)/(2.d0*sigma(i-1,k-1)))*(z(i-1,k-1)-z(i,K))
c
      cwxy =
     *  + (z(i-1,k)-z(i,k+1))
     *  *(ZKXY(i-1,k)/(2.d0*sigma(i-1,k)))*(x(i,k)-x(i-1,k+1))
     *  + (z(i,k-1)-z(i-1,k))
     *  *(ZKXY(i-1,k-1)/(2.d0*sigma(i-1,k-1)))*(x(i-1,k-1)-x(i,k))
c
      cwyx =
     *  +(x(i-1,k)-x(i,k+1))
     *  *(ZKXY(i-1,k)/(2.d0*sigma(i-1,k)))*(z(i,k)-z(i-1,k+1))
     *  +(x(i,k-1)-x(i-1,k))
     *  *(ZKXY(i-1,k-1)/(2.d0*sigma(i-1,k-1)))*(z(i-1,k-1)-z(i,k))
c
      cwyy =
     *  -(x(i-1,k)-x(i,k+1))
     *  *(Kz(i-1,k)/(2.d0*sigma(i-1,k)))*(x(i,k)-x(i-1,k+1))
     *  -(x(i,k-1)-x(i-1,k))
     *  *(Kz(i-1,k-1)/(2.d0*sigma(i-1,k-1)))*(x(i-1,k-1)-x(i,k))

      cw=0.5*(cwxx+cwxy+cwyx+cwyy)/VN
      FJAC(NO,(NL*NPHASE-LT))=CW
C
C
      cexx =
     *  + (z(i,k+1)-z(i+1,k))
     *  *(kx(i,k)/(2.d0*sigma(i,k)))*(z(i,k)-z(i+1,k+1))
     *  +(z(i+1,k)-z(i,k-1))
     *  *(kx(i,k-1)/(2.d0*sigma(i,k-1)))*(z(i+1,k-1)-z(i,k))
c
```

```
      cexy =
     *  -(z(i,k+1)-z(i+1,k))
     *  *(ZKXY(i,k)/(2.d0*sigma(i,k)))*(x(i,k)-x(i+1,k+1))
     *  -(z(i+1,k)-z(i,k-1))
     *  *(ZKXY(i,k-1)/(2.d0*sigma(i,k-1)))*(x(i+1,k-1)-x(i,k))
c
      ceyx =
     *  -(x(i,k+1)-x(i+1,k))
     *  *(ZKXY(i,k)/(2.d0*sigma(i,k)))*(z(i,k)-z(i+1,k+1))
     *  -(x(i+1,k)-x(i,k-1))
     *  *(ZKXY(i,k-1)/(2.d0*sigma(i,k-1)))*(z(i+1,k-1)-z(i,k))
c
      ceyy =
     *  +(x(i,k+1)-x(i+1,k))
     *  *(kz(i,k)/(2.d0*sigma(i,k)))*(x(i,k)-x(i+1,k+1))
     *  +(x(i+1,k)-x(i,k-1))
     *  *(kz(i,k-1)/(2.d0*sigma(i,k-1)))*(x(i+1,k-1)-x(i,k))

     ce=0.5*(cexx+cexy+ceyx+ceyy)/VN
     FJAC(NO,(NR*NPHASE-LT))=CE
C
C
     cnwxx =
     *       -(z(i-1,k)-z(i,k+1))
     *       *(KX(i-1,k)/(2.d0*sigma(i-1,k)))*(z(i-1,k)-z(i,k+1))
c
     cnwxy =
     *       +(z(i-1,k)-z(i,k+1))
     *       *(ZKXY(i-1,k)/(2.d0*sigma(i-1,k)))*(x(i-1,k)-x(i,k+1))
c
     cnwyx =
     *       +(x(i-1,k)-x(i,k+1))
     *       *(ZKXY(i-1,k)/(2.d0*sigma(i-1,k)))*(z(i-1,k)-z(i,k+1))
c
     cnwyy =
     *       -(x(i-1,k)-x(i,k+1))
     *       *(Kz(i-1,k)/(2.d0*sigma(i-1,k)))*(x(i-1,k)-x(i,k+1))

     cnw=0.5*(cnwxx+cnwxy+cnwyx+cnwyy)/VN
     FJAC(NO,(NUW*NPHASE-LT))=CNW
C
C
      cnxx =
     *  -(z(i,k+1)-z(i+1,k))
     *  *(KX(i,k)/(2.d0*sigma(i,k)))*(z(i,k)-z(i+1,k+1))
     *  +(z(i-1,k)-z(i,k+1))
     *  *(KX(i-1,k)/(2.d0*sigma(i-1,k)))*(z(i,k)-z(i-1,k+1))
c
      cnxy =
     *  +(z(i,k+1)-z(i+1,k))
     *  *(ZKXY(i,k)/(2.d0*sigma(i,k)))*(x(i,k)-x(i+1,k+1))
```

```
     *   -(z(i-1,k)-z(i,k+1))
     *   *(ZKXY(i-1,k)/(2.d0*sigma(i-1,k)))*(x(i,k)-x(i-1,k+1))
c
        cnyx =
     *   +(x(i,k+1)-x(i+1,k))
     *   *(ZKXY(i,k)/(2.d0*sigma(i,k)))*(z(i,k)-z(i+1,k+1))
     *   -(x(i-1,k)-x(i,k+1))
     *   *(ZKXY(i-1,k)/(2.d0*sigma(i-1,k)))*(z(i,k)-z(i-1,k+1))
c
        cnyy =
     *   -(x(i,k+1)-x(i+1,k))
     *   *(Kz(i,k)/(2.d0*sigma(i,k)))*(x(i,k)-x(i+1,k+1))
     *   +(x(i-1,k)-x(i,k+1))
     *   *(Kz(i-1,k)/(2.d0*sigma(i-1,k)))*(x(i,k)-x(i-1,k+1))

     cn=0.5*(cnxx+cnxy+cnyx+cnyy)/VN
     FJAC(NO,(NU*NPHASE-LT))=CN
C
C
     cnexx = + (z(i,k+1)-z(i+1,k))
     *       *(kx(i,K)/(2.d0*sigma(i,k)))*(z(i+1,k)-z(i,k+1))
c
     cnexy = -(z(i,k+1)-z(i+1,k))
     *       *(ZKXY(i,k)/(2.d0*sigma(i,k)))*(x(i+1,k)-x(i,k+1))
c
     cneyx = -(x(i,k+1)-x(i+1,k))
     *       *(ZKXY(i,k)/(2.d0*sigma(i,k)))*(z(i+1,k)-z(i,k+1))
c
     cneyy = + (x(i,k+1)-x(i+1,k))
     *       *(kz(i,k)/(2.d0*sigma(i,k)))*(x(i+1,k)-x(i,k+1))

     cne=0.5*(cnexx+cnexy+cneyx+cneyy)/VN
     FJAC(NO,(NUE*NPHASE-LT))=CNE
C
C
23    cc = - ( ce + cne + cn + cnw +cw + csw + cs + cse
    &-chww-chnn-chaa)
     FJAC(NO,(NN*NPHASE-LT))=CC
C
C
100   CONTINUE

C     WRITE(*,*)NNODE,NDOB
c     DO 200 L=1,NDOB
c     WRITE(13,'(280E10.2)')(FJAC(L,JL),JL=1,NDOB)
c200  CONTINUE
c     CLOSE(13)
c     PAUSE

     RETURN
     END
```

```
      SUBROUTINE lubksb(a,n,np,indx,b)
          INTEGER n,np,indx(nP)
          REAL a(np,np),b(nP)
          INTEGER i,ii,j,ll
          REAL sum
          ii=0
          do 12 i=1,n
           ll=indx(i)
           sum=b(ll)
           b(ll)=b(i)
           if (ii.ne.0)then
            do 11 j=ii,i-1
             sum=sum-a(i,j)*b(j)
     11      continue
           else if (sum.ne.0.) then
            ii=i
           endif
           b(i)=sum
     12    continue
          do 14 i=n,1,-1
           sum=b(i)
           do 13 j=i+1,n
            sum=sum-a(i,j)*b(j)
     13     continue
           b(i)=sum/a(i,i)
     14    continue
          return
          END
      C  (C) Copr. 1986-92 Numerical Recipes Software +-.
      SUBROUTINE ludcmp(a,n,np,indx,d)
          INTEGER n,np,indx(n),NMAX
          REAL d,a(np,np),TINY
          PARAMETER (NMAX=500,TINY=1.0e-20)
          INTEGER i,imax,j,k
          DOUBLE PRECISION aamax,dum,sum,vv(NMAX)
      c    write(*,*)n,np,a(6,6)
          d=1.
          do 12 i=1,n
           aamax=0.
           do 11 j=1,n
            if (abs(a(i,j)).gt.aamax) aamax=abs(a(i,j))
     11     continue
      C     write(*,*)I,aamax
           if (aamax.eq.0.) pause 'singular matrix in ludcmp'
           vv(i)=1./aamax
     12    continue
          do 19 j=1,n
           do 14 i=1,j-1
            sum=a(i,j)
            do 13 k=1,i-1
             sum=sum-a(i,k)*a(k,j)
```

```
13      continue
        a(i,j)=sum
14     continue
       aamax=0.
       do 16 i=j,n
        sum=a(i,j)
        do 15 k=1,j-1
         sum=sum-a(i,k)*a(k,j)
15      continue
        a(i,j)=sum
        dum=vv(i)*abs(sum)
        if (dum.ge.aamax) then
         imax=i
         aamax=dum
        endif
16     continue
       if (j.ne.imax)then
        do 17 k=1,n
         dum=a(imax,k)
         a(imax,k)=a(j,k)
         a(j,k)=dum
17      continue
        d=-d
        vv(imax)=vv(j)
       endif
       indx(j)=imax
       if(a(j,j).eq.0.)a(j,j)=TINY
       if(j.ne.n)then
        dum=1./a(j,j)
        do 18 i=j+1,n
         a(i,j)=a(i,j)*dum
18      continue
       endif
19    continue
      return
      END
C  (C) Copr. 1986-92 Numerical Recipes Software +-.
$debug
      SUBROUTINE SK
           INCLUDE 'COMON.BLK'
           PARAMETER(SSMM=1.0E-6)
C
      DO 100 K=1,NROW
      DO 100 I=NCBEG(K),NCEND(K)
      VM=1.-1./N(I,K)
      VMINV=1./VM
C     NOIL = 0 : THERE IS NO SIGNIFICANT NAPL IN THE CELL
C     NOIL = 1 : THERE IS NAPL IN THE CELL
      hcr=(betaan(i,k)*ha(i,k)+betanw(i,k)*hw(i,k))
     &/(betaan(i,k)+betanw(i,k))
      if(hn(i,k).gt.hcr.or.noil(i,k).eq.1)noil(i,k)=1
```

```
      IF(NOIL(I,K).EQ.0)THEN
        if(sn(i,k).lt.ssmm)sn(i,k)=ssmm
        HAW=HA(I,K)-HW(I,K)
        IF(HAW.LT.ssmm)THEN
                        swbar=1.0
                        sw(i,k)=1.0
                        stbar=1.0
                        krw(i,k)=1.0
                        goto 100
                ENDIF
        SWBAR=(1.0+(ALPHA(I,K)*HAW)**N(I,K))**(-VM)
        SW(I,K)=SWBAR*(1-SRW(I,K))+SRW(I,K)
        IF(SW(I,K).GT.1.0)SW(I,K)=1.0-SN(I,K)
        SA(I,K)=1.-SW(I,K)-SN(I,K)
        KRN(I,K)=SSMM
        swbar=(sw(i,k)-srw(i,k))/(1.-srw(i,k))
        STBAR=SWBAR
      ENDIF
      IF(NOIL(I,K).EQ.1)THEN
        HNW=(HN(I,K)-HW(I,K))
        HAN=(HA(I,K)-HN(I,K))
        IF(HNW.LT.ssmm)HNW=ssmm
        IF(HAN.LT.ssmm)HAN=ssmm
        SWBAR=(1.0+(ALPHA(I,K)*BETANW(I,K)*HNW)**N(I,K))**(-VM)
        STBAR=(1.0+(ALPHA(I,K)*BETAAN(I,K)*HAN)**N(I,K))**(-VM)
        if(swbar.ge.(1.-srw(i,k)))stbar=swbar
        SW(I,K)=SWBAR*(1.-SRW(I,K))+SRW(I,K)
        SN(I,K)=STBAR*(1.-SRW(I,K))+SRW(I,K)-SW(I,K)
        IF((SN(I,K)+SW(I,K)).GT.1.0)THEN
          IF(SW(I,K).GT.SN(I,K))THEN
            SN(I,K)=ssmm
            SW(I,K)=1.-SN(I,K)
          ENDIF
          IF(SN(I,K).GT.SW(I,K))THEN
            SW(I,K)=SRW(I,K)
            SN(I,K)=1.-SW(I,K)
          ENDIF
          IF(SN(I,K).EQ.SW(I,K))THEN
            SW(I,K)=0.5
            SN(I,K)=0.5
          ENDIF
        ENDIF
        SA(I,K)=1.-SW(I,K)-SN(I,K)
        stbar=(sn(i,k)+sw(i,k)-srw(i,k))/(1.-srw(i,k))
        swbar=(sw(i,k)-srw(i,k))/(1-srw(i,k))
      ENDIF
      KRW(I,K)=SQRT(SWBAR)*(1.-(1.-SWBAR**VMINV)**VM)**2
      IF(NOIL(I,K).EQ.0)GOTO 102
      KRN(I,K)=SQRT(STBAR-SWBAR)*((1.-SWBAR**VMINV)**VM
     &-(1.-STBAR**VMINV)**VM)**2
  102 KRA(I,K)=SQRT(1-STBAR)*(1.-STBAR)**(2.*VM)
```

```
100  CONTINUE
     RETURN
     END
SUBROUTINE TRA
          INCLUDE 'COMON.BLK'
     LANDA=1.17E-6
     RHA0=0.00112
     RAC=0.0
     DO 100 K=1,NROW
     DO 100 I=NCBEG(K),NCEND(K)
     RHOA(I,K)=LANDA*HA(I,K)+RHA0+RAC
     KX(I,K)=PERM(I,K)*RHOA(I,K)*VMUA/vmuw*KRA(I,K)
     KZ(I,K)=KX(I,K)*ZX
     IF(TYPEA(I,K).EQ.-3)THEN
       KX(I,K)=0.0
       KZ(I,K)=0.0
     ENDIF
100  CONTINUE
          do k=1,nrow-1
          do i=1,ncol-1
     kx(i,k)=0.25*(kx(i,k)+kx(i+1,k)+kx(i+1,k+1)+kx(i,k+1))
          kz(i,k)=0.25*(kz(i,k)+kz(i+1,k)+kz(i+1,k+1)+kz(i,k+1))
          zkxy(i,k)=(kx(i,k)+kz(i,k))/2.0
          enddo
          enddo
     RETURN
     END
$DEBUG
     SUBROUTINE TRANS(NST)
          include 'comon.blk'
          IF(NST.EQ.1)rvisc=1.0
          IF(NST.EQ.2)rvisc=vmun/vmun
     DO 100 K=1,NROW
     DO 100 I=NCBEG(K),NCEND(K)
          IF(NST.EQ.1)ITY=TYPEW(I,K)
          IF(NST.EQ.2)ITY=TYPEN(I,K)
          IF(NST.EQ.1)RK=KRW(I,K)
          IF(NST.EQ.2)RK=KRN(I,K)
     KX(I,K)=PERM(I,K)*RK*rvisc
     KZ(I,K)=KX(I,K)*ZX
     IF(ITY.EQ.-3)THEN
       KX(I,K)=0.0
       KZ(I,K)=0.0
     ENDIF
100  CONTINUE
          do k=1,nrow-1
          do i=1,ncol-1
     kx(i,k)=0.25*(kx(i,k)+kx(i+1,k)+kx(i+1,k+1)+kx(i,k+1))
          kz(i,k)=0.25*(kz(i,k)+kz(i+1,k)+kz(i+1,k+1)+kz(i,k+1))
          zkxy(i,k)=(kx(i,k)+kz(i,k))/2.0
          enddo
```

```
      enddo
    RETURN
    END
 SUBROUTINE VECT(HED,PERMX,PERMZ,RHOW,RHO,SAT,SATOLD,RSS,NST)
    PARAMETER (MNI=20,MNK=20,MNRC=1200)

    COMMON/GEO/ X(MNI,MNK),Z(MNI,MNK),SIGMA(MNI,MNK)
    COMMON/MND/ NROW,NCOL,NNODE,NCBEG(MNK),NCEND(MNK),NPHASE,DT
    COMMON/HOL/ HWOLD(MNI,MNK),HNOLD(MNI,MNK),HAOLD(MNI,MNK)
   &,RHOA(MNI,MNK)
    COMMON/PRP/ ALPHA(MNI,MNK),N(MNI,MNK),BETANW(MNI,MNK),SRW(MNI,MNK)
   &,BETAAN(MNI,MNK),SNMIN(MNI,MNK),PHI(MNI,MNK)
    COMMON/ATR/ FJAC(MNRC,MNRC),FVEC(MNRC)
    REAL*4 HED(MNI,MNK),PERMX(MNI,MNK),PERMZ(MNI,MNK),SAT(MNI,MNK)
   &,SATOLD(MNI,MNK),RSS(MNI,MNK),N
C
    LANDA=1.17E-6
    RHA0=0.00112
    RAC=0.0
    KM=-(NPHASE-NST)
    DO 100 K=1,NROW
    DO 100 I=NCBEG(K),NCEND(K)
    f11=0.0
    f12=0.0
    f13=0.0
    f14=0.0
    f21=0.0
    f22=0.0
    f23=0.0
    f24=0.0
    if(nst.eq.3.and.sat(i,k).eq.0.0)goto 100
    if(nst.eq.2.and.hed(i,k).eq.0.0)goto 100
    KM=KM+NPHASE
C
    if(k.eq.1)goto 31
    if(i.eq.1)goto 31
    IF(NST.EQ.3)RHO=RHOA(I-1,K-1)
    F11=(HED(I,K)-HED(I-1,K-1))*(X(I-1,K)-X(I,K-1))
    F11=F11-(HED(I-1,K)-HED(I,K-1))*(X(I,K)-X(I-1,K-1))
    F11=PERMZ(I-1,K-1)*(F11/(2.0)+RHO/RHOW*SIGMA(I-1,K-1))
    F11=(X(I-1,K)-X(I,K-1))/2.0*F11
C
31   if(k.eq.nrow)goto 32
    if(i.eq.ncend(k))goto 32
    IF(NST.EQ.3)RHO=RHOA(I,K)
    F12=(HED(I+1,K+1)-HED(I,K))*(X(I,K+1)-X(I+1,K))
    F12=F12-(HED(I,K+1)-HED(I+1,K))*(X(I+1,K+1)-X(I,K))
    F12=PERMZ(I,K)*(F12/(2.0)+RHO/RHOW*SIGMA(I,K))
    F12=(X(I,K+1)-X(I+1,K))/2.0*F12
C
32   if(k.eq.1)goto 33
```

```
      if(i.eq.ncend(k))goto 33
      IF(NST.EQ.3)RHO=RHOA(I,K-1)
      F13=(HED(I+1,K)-HED(I,K-1))*(X(I,K)-X(I+1,K-1))
      F13=F13-(HED(I,K)-HED(I+1,K-1))*(X(I+1,K)-X(I,K-1))
      F13=PERMZ(I,K-1)*(F13/(2.0)+RHO/RHOW*SIGMA(I,K-1))
      F13=(X(I+1,K)-X(I,K-1))/2.0*F13
33    if(k.eq.nrow)goto 34
      if(i.eq.1)goto 34
      IF(NST.EQ.3)RHO=RHOA(I-1,K)
      F14=(HED(I,K+1)-HED(I-1,K))*(X(I-1,K+1)-X(I,K))
      F14=F14-(HED(I-1,K+1)-HED(I,K))*(X(I,K+1)-X(I-1,K))
      F14=PERMZ(I-1,K)*(F14/(2.0)+RHO/RHOW*SIGMA(I-1,K))
      F14=(X(I,K+1)-X(I-1,K))/2.0*F14
34    if(k.eq.1)goto 35
      if(i.eq.1)goto 35
      F21=(HED(I,K)-HED(I-1,K-1))*(Z(I-1,K)-Z(I,K-1))
      F21=F21-(HED(I-1,K)-HED(I,K-1))*(Z(I,K)-Z(I-1,K-1))
      F21=(Z(I-1,K)-Z(I,K-1))*PERMX(I-1,K-1)*F21/4.0
35    if(k.eq.nrow)goto 36
      if(i.eq.ncend(k))goto 36
      F22=(HED(I+1,K+1)-HED(I,K))*(Z(I,K+1)-Z(I+1,K))
      F22=F22-(HED(I,K+1)-HED(I+1,K))*(Z(I+1,K+1)-Z(I,K))
      F22=(Z(I,K+1)-Z(I+1,K))*PERMX(I,K)*F22/4.0
36    if(i.eq.ncend(k))goto 37
      if(k.eq.1)goto 37
      F23=(HED(I+1,K)-HED(I,K-1))*(Z(I,K)-Z(I+1,K-1))
      F23=F23-(HED(I,K)-HED(I+1,K-1))*(Z(I+1,K)-Z(I,K-1))
      F23=(Z(I+1,K)-Z(I,K-1))*PERMX(I,K-1)*F23/4.0
C
      if(k.eq.nrow)goto 37
      if(i.eq.1)goto 37
      F24=(HED(I,K+1)-HED(I-1,K))*(Z(I-1,K+1)-Z(I,K))
      F24=F24-(HED(I-1,K+1)-HED(I,K))*(Z(I,K+1)-Z(I-1,K))
      F24=(Z(I,K+1)-Z(I-1,K))*PERMX(I-1,K)*F24/4.0
C
37    if(k.eq.1.and.i.ge.2.and.i.le.ncol-1)then
      DX=(X(I+1,k)-X(I-1,k))**2
      DZ=(Z(I+1,k)-Z(I-1,k))**2
      vn=SQRT(DX+DZ)/2.0
      goto 39
      endif
      if(i.eq.ncol.and.k.ge.2.and.k.le.nrow-1)then
      DX=(X(Ncend(k),k+1)-X(Ncend(k),k-1))**2
      DZ=(Z(Ncend(k),k+1)-Z(Ncend(k),k-1))**2
      vn=SQRT(DX+DZ)/2.0
      goto 39
      endif
      if(k.eq.nrow.and.i.ge.ncbeg(k)+1.and.i.le.ncend(k)-1)then
      DX=(X(I+1,k)-X(I-1,k))**2
      DZ=(Z(I+1,k)-Z(I-1,k))**2
      vn=SQRT(DX+DZ)/2.0
```

```
      goto 39
      endif
      if(i.eq.1.and.k.ge.2.and.k.le.nrow-1)then
      DX=(X(i,k+1)-X(i,k-1))**2
      DZ=(Z(i,k+1)-Z(i,k-1))**2
      vn=SQRT(DX+DZ)/2.0
      goto 39
      endif
      if(i.eq.1.and.k.eq.1)then
      DX=(X(2,1)-X(1,2))**2
      DZ=(Z(2,1)-Z(2,1))**2
      vn=SQRT(DX+DZ)/2.0
      goto 39
      endif
      if(i.eq.ncend(k).and.k.eq.1)then
      DX=(X(i,2)-X(i-1,1))**2
      DZ=(Z(i,2)-Z(i-1,1))**2
      vn=SQRT(DX+DZ)/2.0
      goto 39
      endif
      if(i.eq.ncend(k).and.k.eq.nrow)then
      DX=(X(i-1,NROW)-X(i,NROW-1))**2
      DZ=(Z(i-1,NROW)-Z(i,NROW-1))**2
      vn=SQRT(DX+DZ)/2.0
      goto 39
      endif
      if(i.eq.1.and.k.eq.nrow)then
      DX=(X(i,NROW-1)-X(i+1,NROW))**2
      DZ=(Z(i,NROW-1)-Z(i+1,NROW))**2
      vn=SQRT(DX+DZ)/2.0
      goto 39
      endif
      VN=(SIGMA(I,K)+SIGMA(I-1,K)+SIGMA(I-1,K-1)+SIGMA(I,K-1))/4.0
39    FVEC(KM)=(F11+F12+F13+F14+F21+F22+F23+F24)/VN
      IF(NST.EQ.3)THEN
        RHOX=1.0
        RHY=RHOA(I,K)
        RHOL=LANDA*HAOLD(I,K)+RHA0+RAC
      ELSE
        RHOX=RHO
        RHY=1.0
        RHOL=1.0
      ENDIF
      FVEC(KM)=FVEC(KM)+RSS(I,K)/RHOX-(RHY*SAT(I,K)-RHOL*SATOLD(I,K))
     &*PHI(I,K)/DT
      if(nst.eq.2)write(*,*)sat(i,k),satold(i,k)
      if(nst.eq.2)pause
100   CONTINUE
      RETURN
      END
```

COMON.BLK

```
PARAMETER (MNI=20,MNK=20,MNRC=1200,EPSI=1.0E-6)

    COMMON/GEO/ X(MNI,MNK),Z(MNI,MNK),SIGMA(MNI,MNK)
    COMMON/MND/ NROW,NCOL,NNODE,NCBEG(MNK),NCEND(MNK),NPHASE,DT
    COMMON/KRS/ KRW(MNI,MNK),KRN(MNI,MNK),KRA(MNI,MNK),SW(MNI,MNK)
   &,SN(MNI,MNK),SA(MNI,MNK)
    COMMON/PRP/ ALPHA(MNI,MNK),N(MNI,MNK),BETANW,SRW(MNI,MNK)
   &,BETAAN,SNMIN(MNI,MNK),PHI(MNI,MNK),ZX,KX(MNI,MNK)
   &,KZ(MNI,MNK)
    COMMON/PHY/ PERM(MNI,MNK),RHOW,VMUW,RHON,VMUN,VMUA
    COMMON/OLD/ SWOLD(MNI,MNK),SNOLD(MNI,MNK),SAOLD(MNI,MNK)
    COMMON/HOL/ HWOLD(MNI,MNK),HNOLD(MNI,MNK),HAOLD(MNI,MNK)
   &,RHOA(MNI,MNK)
    COMMON/TYP/TYPEW(MNI,MNK),TYPEN(MNI,MNK),TYPEA(MNI,MNK)
   &,NOIL(MNI,MNK)
    COMMON/HHD/ HW(MNI,MNK),HN(MNI,MNK),HA(MNI,MNK),RSSW(MNI,MNK)
   &,RSSN(MNI,MNK),RSSA(MNI,MNK),P(MNRC),FJAC(MNRC,MNRC),FVEC(MNRC)
        &,indx(mnrc)
    common/kxy/zkxy(mni,mnk)
    REAL KX,KZ,KRW,KRN,KRA,N
          COMMON/TOL/ TMAX,TPRN,TOLF,TOLX,MXIT,NSTAT,G
    common/psi/ GAMMAW(MNI,MNK),GAMMAN(MNI,MNK),GAMMAA(MNI,MNK)
          common/zlw/ zl1n,zlmn,zlm1,zl11,zlw(mnk),zle(mnk)
         *,zln(mni),zls(mni)
          COMMON /AFP/ tphw(5),phw(5),tphn(5),phn(5),tpha(5),pha(5)
         *,tpfw(5),pfw(5),tpfn(5),pfn(5),tpfa(5),pfa(5)
    CHARACTER*64 TITLE
```